Development of a fully integrated Lab-o-a-Chip for amphetamine detection in sewage

Juan Gallardo Gonzalez

N°d'ordre NNT : xxx

THESE de DOCTORAT DE L'UNIVERSITE DE LYON
opérée au sein de
l'Université Claude Bernard Lyon 1

Ecole Doctorale N° 206
Ecole Doctorale de Chimie

Spécialité de doctorat :
Discipline : Chimie

Soutenue publiquement 17/10/2018, par :
Juan Gallardo González

Développement d'un laboratoire sur puce pour la détection des amphétamines dans les égouts

Devant le jury composé de :

JAFFREZIC-RENAULT, Nicole	Directrice de recherche du CNRS	Présidente
MARTY, Jean Louis	Directeur de recherche Univ. Perpignan	Rapporteur
KORRI YOUSSOUFI, Hafsa	Directrice de recherche ICMMO	Rapporteur
BAUSELLS ROIGE, Joan	Directeur de recherche CNM (Espagne)	Examinateur
ANASTHASE, Raphaël	Directeur R&D, Biotray	Examinateur
LEONARD, Didier	Professeur des Universités, UCBL	Examinateur
ERRACHID EL SALHI, Abdelhamid	Professeur des Universités, UCBL	Directeur de thèse
ZINE, Nadia	Maître de conférences, UCBL	Co-directrice de thèse

UNIVERSITE CLAUDE BERNARD - LYON 1

Président de l'Université	**M. le Professeur Frédéric FLEURY**
Président du Conseil Académique	M. le Professeur Hamda BEN HADID
Vice-président du Conseil d'Administration	M. le Professeur Didier REVEL
Vice-président du Conseil Formation et Vie Universitaire	M. le Professeur Philippe CHEVALIER
Vice-président de la Commission Recherche	M. Fabrice VALLÉE
Directrice Générale des Services	Mme Dominique MARCHAND

COMPOSANTES SANTE

Faculté de Médecine Lyon Est – Claude Bernard	Directeur : M. le Professeur G.RODE
Faculté de Médecine et de Maïeutique Lyon Sud – Charles Mérieux	Directeur : Mme la Professeure C. BURILLON
Faculté d'Odontologie	Directeur : M. le Professeur D. BOURGEOIS
Institut des Sciences Pharmaceutiques et Biologiques	Directeur : Mme la Professeure C. VINCIGUERRA
Institut des Sciences et Techniques de la Réadaptation	Directeur : M. X. PERROT
Département de formation et Centre de Recherche en Biologie Humaine	Directeur : Mme la Professeure A-M. SCHOTT

COMPOSANTES ET DEPARTEMENTS DE SCIENCES ET TECHNOLOGIE

Faculté des Sciences et Technologies	Directeur : M. F. DE MARCHI
Département Biologie	Directeur : M. le Professeur F. THEVENARD
Département Chimie Biochimie	Directeur : Mme C. FELIX
Département GEP	Directeur : M. Hassan HAMMOURI
Département Informatique	Directeur : M. le Professeur S. AKKOUCHE
Département Mathématiques	Directeur : M. le Professeur G. TOMANOV
Département Mécanique	Directeur : M. le Professeur H. BEN HADID
Département Physique	Directeur : M. le Professeur J-C PLENET
UFR Sciences et Techniques des Activités Physiques et Sportives	Directeur : M. Y.VANPOULLE
Observatoire des Sciences de l'Univers de Lyon	Directeur : M. B. GUIDERDONI
Polytech Lyon	Directeur : M. le Professeur E.PERRIN
Ecole Supérieure de Chimie Physique Electronique	Directeur : M. G. PIGNAULT
Institut Universitaire de Technologie de Lyon 1	Directeur : M. le Professeur C. VITON
Ecole Supérieure du Professorat et de l'Education	Directeur : M. le Professeur A. MOUGNIOTTE
Institut de Science Financière et d'Assurances	Directeur : M. N. LEBOISNE

TITRE en français : **Développent d'un laboratoire sur puce pour la détection des amphétamines dans les égouts.**

Ce travail de thèse est consacré au développement d'un dispositif autarcique pour le contrôle des amphétamines dans les égouts. Il a été conçu dans le cadre du projet européen MicroMole pour aider la police scientifique à résoudre des scènes concernant la localisation des laboratoires clandestins d'amphétamines et produits dérivés. Il est composé de trois volets : le premier volet est dédié au développement de deux générations de capteurs potentiométriques sélectifs à l'amphétamine en utilisant le ionophore commercial dibenzo-18-crown-6 éther dans un premier temps puis le ion-pair complexe [amphetamine-H]$^{+}$[3,3'-Co(1,2-$C_2B_9H_{11})_2]^{-}$ synthétisé comme sites actifs pour la reconnaissance sélective d'amphétamine. Le deuxième volet est consacré au développement d'un système microfluidique passif permettant de contrôler le flux d'échantillon arrivant à la partie sensible du capteur en utilisant des micro-filtres et micro-mélangeurs. Le troisième et dernier volet est dédié à la conception et fabrication d'un système autonome d'échantillonnage miniaturisé pour le stockage des échantillons dans les égouts lors des enquêtes menées par la police scientifique correspondant à la localisation de laboratoires clandestins d'amphétamines.

TITRE en anglais : **Development of a fully integrated Lab-o-a-Chip for amphetamine detection in sewage.**

The work in this thesis is devoted to the development of an autarkic device for real-time monitoring of amphetamines in sewage. It has been developed within the EU project Micromole to help Law Enforcement Agents (LEA) to solve forensic scenarios related to the production of amphetamines and amphetamines-type stimulants (ATS). It is composed of three main sections. The first section is devoted to the development of two generation of potentiometric sensors for the detection of amphetamines using first, the commercial ionophore dibenzo-18-crown-6 ether, then the synthetized ion-pair complex [amphetamine-H]$^{+}$[3,3'-Co(1,2-$C_2B_9H_{11})_2]^{-}$ as active sites for amphetamine recognition. The second section is dedicated to the fabrication of a passive microfluidic system integrated into a Lab-on-a-Chip to protect the sensor from harsh environment through the control of the sample amount reaching the sensor. For this purpose, the microfluidic system formed a combination of passive micromixers, microfilters and microchannels. The final section was devoted to the development of an autarkic sample storage unit to help LEA to store spontaneous samples during forensic investigations related to the clandestine production of amphetamines in illegal laboratories.

DISCIPLINE: **Electroanalytical chemistry and micro-nanotechnology**

MOTS-CLES en français: **Laboratoire sur puce ; µISE ; amphétamine ; potentiométrie ; spectroscopie d'impédance ; analyse des égouts.**

MOTS-CLES en anglais : **Lab-on-a-Chip**, **µISE ; amphetamine ; potentiometry ; electrochemical impedance spectroscopy ; sewage analysis.**

INTITULE ET ADRESSE DE L'U.F.R. OU DU LABORATOIRE : **ISA- Institut des Sciences analytiques. Département LSA-Laboratoire des Sciences Analytiques. Université Claude Bernard Lyon 1, 5 Rue de la Doua, 69100, Villeurbanne, CEDEX, France.**

A mi familia, a ti

Ten siempre a Itaca en tu mente.
Llegar allí es tu destino.
Mas no apresures nunca el viaje.
Mejor que dure muchos años
y atracar, viejo ya, en la isla,
enriquecido de cuanto ganaste en el camino
sin aguantar a que Itaca te enriquezca.

C.P Cavafis. Itaca. 1911

Acknowledgments

La vida da muchas vueltas. Nunca me imaginé el momento en el que me encontraría sentado, delante del ordenador y escribiendo los agradecimientos de mi tesis. Si me hubieran preguntado hace 12 años si quería ser doctor, seguramente hubiera dicho sí con firmeza, aunque los que me conocen bien, saben que la relación con el título de doctor al que me presento defendiendo esta memoria es escasa, o nula. Sin embargo, aquí me hallo, escribiendo las últimas líneas de este trabajo. Y es que, "mi tesis" no es solo mía. Yo soy la cara visible de todas aquellas personas cuya contribución ha hecho posible en mayor o menor medida que hoy presente "mi tesis" para optar al título de Doctor en Química. A tod@s vosotr@s, ¡GRACIAS!

En primer lugar, me gustaría agradecer a mis directores de tesis, Nadia y Errachid, por haberme dado la oportunidad de disfrutar realmente de la ciencia durante estos últimos tres años. Mención especial merece su dedicación, la constante motivación en los momentos difíciles, así como las horas empeñadas en la discusión y corrección de este trabajo.

Un grand merci à toute les personnes de l'ISA avec qui j'ai partagé cette aventure et qui ont participé de près ou de loin à ce projet : Mme Bonhomme Anne, Mme Jaffrezic-Renault Nicole, Mr. Marote Pedro, Mr. Dupont Stéphane, Mr. Pages Christophe, Mme Jose Catherine, Mme Deregnaucourt Maryline, Mr. Tantangelo David, Mme. Canehan Mai, à toute la « team » ISATOPE pour faire de l'ISA un endroit plus convivial ainsi qu'à l'ensemble du service technique. Une pensée également pour tous et toutes les étudiants/es qui sont passés par notre équipe et qui ont contribué à l'avancement du groupe ainsi qu'à la société BioTray avec qui on a passé des journées en faisant les design 3D des systèmes microfluidiques.

Une partie de mes pensées est également réservée à mes plus proches collègues avec qui j'ai passé les heures à rigoler et boire du café : Mr Universe Mickey, Mr. Palacio Bonet Fran, Mme Lagouanelle Florence, Mme Hangouet Marie, et bien évidement Mr Baraket Abdoullatif pour m'avoir appris autant de choses dans l'aspect scientifique et personnel et enfin Mr Boudjaoui Selim, Boudjidji avec qui j'ai passé les meilleurs et pire moments au labo pendent ces trois ans.

Gracias infinitas a mi familia por haberme guiado en mi vida personal y profesional. Durante toda esta trayectoria, ha sido y sigue siendo duro encontrarse a miles de kilómetros de casa pero aun así, vuestro continuo apoyo y vuestro calor ha servido para que hoy sea la persona que soy. Nunca dejare de agradecéroslo.

Y finalmente, te quiero agradecer a ti Ana, mi compañera de vida y de viaje, por cerrar los ojos junto a mí y descubrir la belleza del mundo a mi lado. Si alguien es responsable de que haya llegado hasta aquí, esa eres tú. ¡GRACIAS!

Table of contents

Acronyms

AM:	Additive manufacturing
APAAN:	alfa-fenylacetoacetonitril
ASE:	Amphetamine-selective microelectrode
ATS:	Amphetamine-type stimulants
BKA:	German Forensic Police
BMK:	Benzyl methyl ketone
CE:	Counter electrode
CNM:	Centro nacional de microelectronica
CV:	Cyclic voltammetry
DB18C6:	Dibenzo-18-crown-6 ether
DB24C8:	Dibenzo-24-crown-8 ether
DBP:	Di-butyl phthalate
DOP:	Di-octyl phthalate
DOS:	Di-octyl sebacate
DPIA:	Di-phenylisopropyl amine
DRIE:	Deep reactive ion etching
EIS:	Electrochemical impedance spectroscopy
Emf:	Electromotrive force
FIM:	Fixed interference method
FTIR:	Fourier Transform Infrared spectroscopy
GC-MS:	Gas chromatography and mass spectrometry
HPLC:	High performance liquid chromatography

ICP: Inductively coupled plasma

KWB: Berlin Center of Competence for water

LEA: Law Enforcement Agents

LOC: Lab-on-a-Chip

MCDDA: Monitoring Center for Drug and Drug Addiction

MDMA: Methylenedioxy-methamphetamine

NFA: N-formyl amphetamine

NMR: Nuclear magnetic resonance

o-NPOE: o-nitrophenyloctyl ether

PANI: Polyaniline

PCB: Printed circuit board

PDMS: Poly(dimethylsiloxane)

PECVD: Plasma enhanced chemical vapor deposition

PPy: Polypyrrole

PSU: Polysulfone

PVC: poly (vinyl chloride)

PVD: Physical vapor deposition

RE: Reference electrode

RIE: Reactive ion etching

SCE: Saturated calomel electrode

SELEX: Systematic evolution of ligands by exponential enrichment

SL: Stereolithography

SPI: Serial periphery interface

SSM:	Separate solution method
TOP:	Tri-octyl phosphate
UNDOC:	United Nation Office on Drug and Crime
WE:	Working electrode

General Introduction

Drug matters has appeared high on the political agenda of developed countries since 1990s. In Europe, over one million seizures of illicit drugs are reported annually. Most of these are small quantities of drugs confiscated from users, however, multi-kilogram consignments of drugs seized from traffickers and producers account for most of the total quantity of drugs seized. Cannabis is the most commonly confiscated drug, accounting for over 70 % of seizures in Europe. Cocaine ranks second overall (9 %), followed by synthetic drugs, mostly, amphetamines and amphetamine-type stimulants (ATS) (7 %) [1].

Although European Union got a step further in the last decade by implementing a rigorous action plan against synthetic drug consumption, statistics shows that trafficking and production has seen a steady increase in Member States [2]. Even if the production of amphetamine and methylenedioxy-methamphetamine (MDMA, also known as ecstasy) remains concentrated in Europe, manufacture of MDMA has spread to varying degrees to other parts of the world, notably North and South America, South Africa, Oceania and Asia. This is reflected in an apparent reduction in the export of MDMA from the European Union, to North America in particular. Moreover, the number of illicit laboratories that produces amphetamine and ATS keep raising despite the efforts of European Police Agencies. Most of those illicit laboratories are located in East Europe and although, some amphetamine is produced in 'kitchen-like' laboratories, it is likely that the vast majority is manufactured in middling to large, sometimes 'industrial size' facilities.

In average, it is estimated that 8 L of liquid waste are generated per Kg of amphetamine synthetized in common illicit laboratories. It means that after every drug synthesis a post-production waste handle must be carried out. When accessible, this waste is poured directly to the sewer network. In that cases, it is easy to track the location of any suspected illicit laboratory by monitoring the wastewater quality nearby. In this context, the project MicroMole founded by the European Union's Horizon 2020 research and innovation program was born in 2015 to help law enforcement agencies (LEA) to track synthetic-drugs (mostly amphetamine and ATS) clandestine laboratories through the monitoring of wastewater. The project main objective was to develop an autarkic device that enables the continuous analysis of wastewater searching for markers related to the synthesis of amphetamines in suspected areas and to link this later to an automated sampler that store the evidences when those markers are found in the wastewater background.

Illicit drug monitoring has been commonly performed through conventional analytical methods that are widely spread over the scientific community as they are reliable, highly accurate and sophisticated. Nevertheless, they are methodical and complex, time consuming, expensive and require highly qualified

personal. Therefore, the development of novel technologies that are faster, low-cost, easy-to-handle and enable to perform real-time analysis in situ are very sought lately. Moreover, the need of working in such as harsh and inaccessible environment as sewage, implies the use of miniaturized, robust, and low-power-consumption devices what suppose a great challenge that needs of innovation. The use of chemical sensors has been presented as an attractive alternative in a broad range of applications for the analysis of illicit drugs samples. Consequently, amphetamine-selective microsensors together with microfluidics will be the basis of the work that is about to be presented in this manuscript.

This thesis is composed of four chapters, with the first dedicated to a general bibliography, the second to the development of two all-solid-state amphetamine-selective microelectrdes, the third to the implementation of a passive microfluidic Lab-on-a-Chip (LOC) for the continuous monitoring of water flow and a final chapter dedicated to the development of an autarkic sample storage device.

In the first chapter of this manuscript, a general bibliography is given, beginning with the general problem linked to the use and production of narcotics and the contribution of the project MicroMole to help LEA solving forensic scenarios. A description of the state-of-the-art of amphetamine sensors is provided followed by a background to the applied principles and components used in the construction of potentiometric sensors. The current state-of-the-art of microfluidic LOC for water monitoring is also discussed as well as an overview of silicon technology. The first chapter ends up with an outline of 3D printing technologies.

The second chapter is dedicated to the fabrication of two generation of ion-selective electrodes (ISE) for the detection of amphetamine. In a first stage, a miniaturized all-solid-state amphetamine ISE was described based on the use of dibenzo-18-crown-6 ether as amphetamine ionophore incorporated to a PVC-type polymeric membrane deposited on to platinum substrate. A second version was fabricating using a synthetized ion-pair complex, $[\text{amphetamine-H}]^{+}[3,3'\text{-Co}(1,2\text{-closo-}C_2B_9H_{11})_2]^{-}$, as the active site for amphetamine recognition. The aim of developing a second generation, was to improve the sensor's selectivity and lifetime. In addition, it integrated both working, auxiliary and reference electrodes in a single miniaturized device what made the sensor to be more adapted for real applications.

The third chapter is dedicated to the fabrication of a passive microfluidic Lab-on-a-Chip (LOC) to perform real-time potentiometric measurements in a water stream. The LOC consisted of two parts: a PDMS microfluidic structure and fully integrated ammonium-selective microelectrode. The aim of this device was to develop a passive microfluidic system to protect the sensitive part of the sensor when performing potentiometric measurements in a dynamic flow of water and that do not need from external input of energy to actuate. The microfluidic device that contained passive micromixers, microfilters, microchannels and a detection microchamber was evaluated in laboratory under a stream of tap water

and also under wastewater in a municipal sewer network in Berlin to assess its implementations within the Micromole project.

The final chapter is dedicated to the fabrication of an automated sampler that was installed in the sewer network and enabled to store up to three samples of 2 mL each when triggered by an external alarm. The device was fabricated using 3D printing technologies and comprised two manifolds made on polycarbonate-like polymer. The main body contained three electrovalves, one piezoelectric micropump and three independent microchannels that end up in the second manifold containing three reservoirs. The main objective of this sample-storage unit was to store wastewater samples when the chemical sensors have detected the presence of suspicious markers related to the synthesis of amphetamines in the wastewater background. Therefore, it will help LEA to store evidences of clandestine laboratories activities.

References

[1] EMCDDA, European Drug Report 2017: Trends and Developments, 2017. doi:10.2810/88175.

[2] T. Hague, Amphetamine-Type Stimulants in the European Union 1998-2007, (2007).

Chapter 1

General bibliography

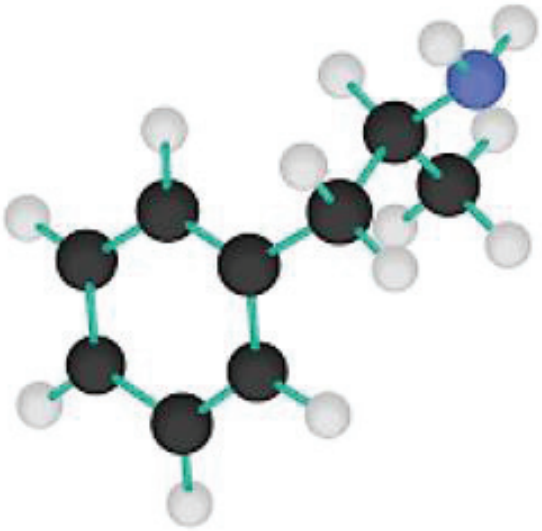

1. The social problem of narcotics.

Nowadays, illicit drugs are considered one of the major concerns for developed countries due to the potential of bringing about all types of health problems. Although cannabis and cocaine are by far the most used narcotics, amphetamine and amphetamine-type stimulants (ATS) like methylenedioxy-methamphetamine (MDMA) are becoming more and more popular. While, worldwide, MDMA is probably the most widely used synthetic stimulant, in Europe it is amphetamine, mostly in the form of the sulfate salt, that has historically been, and remains, the most produced, trafficked and used synthetic stimulant. Amphetamine, therefore, may be neatly viewed as a 'European drug' [1]. The United Nations Office on Drugs and Crime (UNODC) reports that the number of seizures increased from 93 tons in 2010 to 191 tons in 2015, of which amphetamines accounted for 61-80% annually [2]. In addition, the production capacity in laboratories has increased from 5-8 Kg per batch to 30-40 Kg in the Netherlands and Belgium, thanks to the usage of industrial equipment. Moreover, it was also found that the largest numbers of laboratories seizures are located in Poland, The Netherlands and Germany as it can be seen in **Fig. 1.**

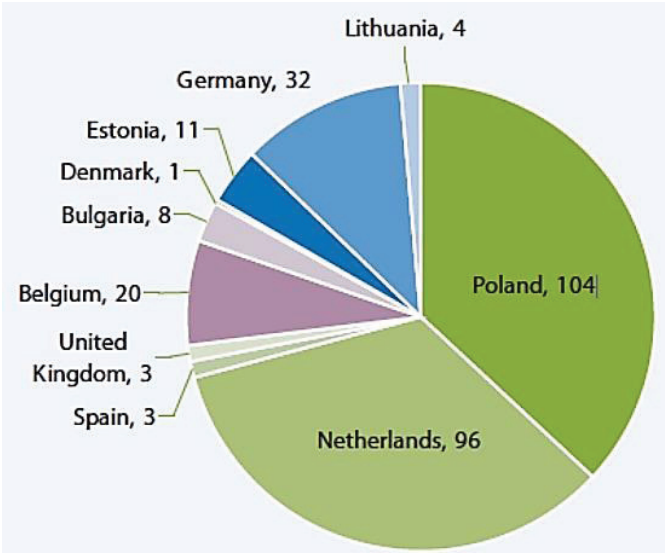

Figure 1. Illicit amphetamine laboratories seizures by European countries of origin in the last decade [3].

Paradoxically, amphetamine has attracted much less attention in the European and global media, in policy circles and in academia than other drugs such as cannabis, cocaine or heroin. Even the closely related methamphetamine often seems to get more attention, although, compared with amphetamine, its production and use are much less prevalent in Europe. As a result, comparatively less information and analysis is available on amphetamine than on many other substances. The last report from the European Monitoring Centre for Drug and Drug Addiction (MCDDA) estimated that about 1.3 and 2.1 million people consumed amphetamine and MDMA respectively, in the last year [4] what represents highly profitable 'business opportunities' for organised crime. Therefore, it is not only the health problems

related to drug use that are a matter of concern but also the black economy that it generates has become alarming. The estimated annual value of the retail market for amphetamine in Europe is about EUR 1.8 billion according to the MCDDA, which means that 76 tonnes of amphetamine were consumed in 2016 [5]. Although some amphetamine is produced in 'kitchen-type' laboratories (see **Fig. 2)** set up by chemistry students to supply a group of local friends, it is likely that the vast majority is manufactured in middling to large, sometimes 'industrial size', facilities [6]. In this case, production and wholesale trafficking are in the hands of criminal organisations, some of which are able to operate throughout Europe, and even beyond, and which reap the corresponding profits. The decrease in the number of amphetamine production facilities dismantled in Europe in recent years does not necessarily make for comforting news, as forensic intelligence suggests that there is an increase in the production capacity of the facilities seized in key producer countries.

Figure 2. Amphetamine powder in a clandestine facility at Calandsoog, the Netherlands, dismantled in 2011 [6].

Furthermore, ATS production implies a threat even to non-consumers. Firefighters continuously report cases of explosions and fire in clandestine ATS (or precursors) laboratories, caused by the lack of full knowledge of the synthesis process. Additionally, the conversion laboratories, in which pre-precursor compound like alfa-fenylacetoacetonitrile (APAAN) are converted to benzyl methyl ketone (BMK) with concentrated mineral acids, besides their intrinsic danger, impose a significant threat to the public sewage system and the environment by dumping of big quantities of highly acidic waste into the public sewer system.

2. What is the aim of the MicroMole project?

Every drug synthesis involves post-production waste handling. In the case of ATS, laboratories generate a huge amount of liquid waste. For instance, for the production of each kilogram of amphetamine sulfate it has been estimated that 8 L of wastes are produced [7,8]. The personnel of illicit laboratories located at facilities with access to a sewage system often dispose of this waste by pouring it to the sewage system directly. Moreover, this waste comprises organic solvents, inorganic compounds and acidic/basic residues, which pose a considerable strain on the environment and wastewater treatment processes. The presence of these substances in the sewage would constitute specific marker to account for the location of illicit drug production laboratory on a given area, making the sewage system a very attractive place for chemicals monitoring and tracking of illegal manufacturing of ATS.

In this context, the main objective of the MicroMole project founded by the European Union's Horizon 2020 research and innovation program with No 653626 has been to design and develop an automated sensor system for the sewer networking for tracking synthetic drugs laboratories and to support criminal investigations of clandestine production (see **Fig. 3**) of amphetamine and its precursors [9]. The sensor system was designed for the continuous examination of wastewater flow, and the device was able to collect wastewater in internal small tanks, so a forensic laboratory could further corroborate the findings of the sensor and use such samples as supporting evidence for criminal prosecution. Moreover, the system should keep track of the location and place where each sample was taken, as well as to provide enough information about the chemical sample for its usage as legal evidence.

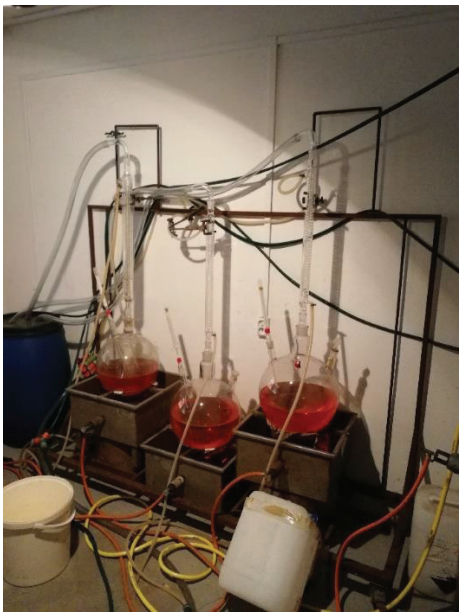

Figure 3. Seized amphetamine laboratory in Czech Republic by Europol and moved to the Forensic Police Training Center in Legionowo, Poland for training purposes. Photo taken by Juan Gallardo-Gonzalez during a Micromole meeting.

The sophisticated device contained a specialized robot for deployment, installation and extraction of the miniaturized sensors within the sewage system in a safe and unnoticed way. Depending on the low enforcement agents (LEAs) strategy one or a set of sensors must be placed within the sewer network near to a suspected area. Manual installation of such sensor system could be difficult or impossible in some cases where the locations are unreachable. Therefore, the MicroMole device must be adapted to sewage inspection and repair technology for quickly, securely and unnoticed placing up to six MicroMole rings devices in a single robot run within the sewage system and for their extraction, without incurring damages to the sewage system. The rings installed by the robot contained both physical and chemical sensors so that pH, electrical conductivity (EC) and byproducts derived from the synthesis of amphetamines included in the wastewater stream can be monitored in continuous with a reduced probability of false-positive alarms. Moreover, low-power consumption was mandatory when designing the device as it must operate for long periods of time (up to two weeks) without the need of an external intervention.

3. Illegal production of amphetamines. The Leuckart synthesis.

Amphetamine, (±)-1-phenylpropan-2-amine, one of the oldest synthetic stimulant was first synthetized in 1887 following the Leuckart method according to several authors [10,11]. This methods consist on the conversion of certain ketones and aldehydes to the corresponding amines by heating with excess of ammonium formate, and was described firstly by Leuckart in 1885 [12]. Since 1990s, the synthesis of amphetamine by the Leuckart method is most commonly performed illegally [13] and is accompanied by varying levels of impurities in the final product, depending on the quality of the starting materials, route of synthesis, reaction conditions, extent of purification of the final product and, above all, on the skills of the clandestine chemist [14–17]. According to the Europol Leuckart synthesis is the most frequently used method in Europe despite its low yield [18]. However, it is arguably the easiest method to learn and put into practice. In this context, the production of amphetamine sulfate is a multistep process involving the precursor BMK, also known as 1-phenyl-2-propanone (P2P) or as phenylacetone whose commercialization is banned all over the world and therefore, it can only be purchased in the dark net. The first step comprises the formation of N-formylamphetamine (NFA) from the reaction at high temperature between BMK and ammonium formate as shown in **Fig. 4**. Subsequently, the conversion of NFA into amphetamine base takes place by acid hydrolysis of NFA using HCl, then reaction of amphetamine chloride with NaOH. The oil-like liquid obtained that contains the amphetamine base is finally crystalized with H_2SO_4 to obtain amphetamine sulfate as final product. The efficiency of the process (yield) remains between 60 and 70% depending on the reaction conditions, distillation equipment, etc. what means that for every litre of BMK, 700-800g of amphetamine sulfate can be obtained.

During the synthesis of amphetamine with Leuckart method, nearly 8.7 L of wastes are produced being water the main component resulting from the water-vapour distillations performed at every step. However, a very important amount of organic waste is produced; between 0.7 and 0.8 L per kilogram of final product. In that organic waste, BMK, NFA and amphetamine are the main components however, other byproducts such as di(β-phenylisopropyl) amine (DPIA) can also be found.

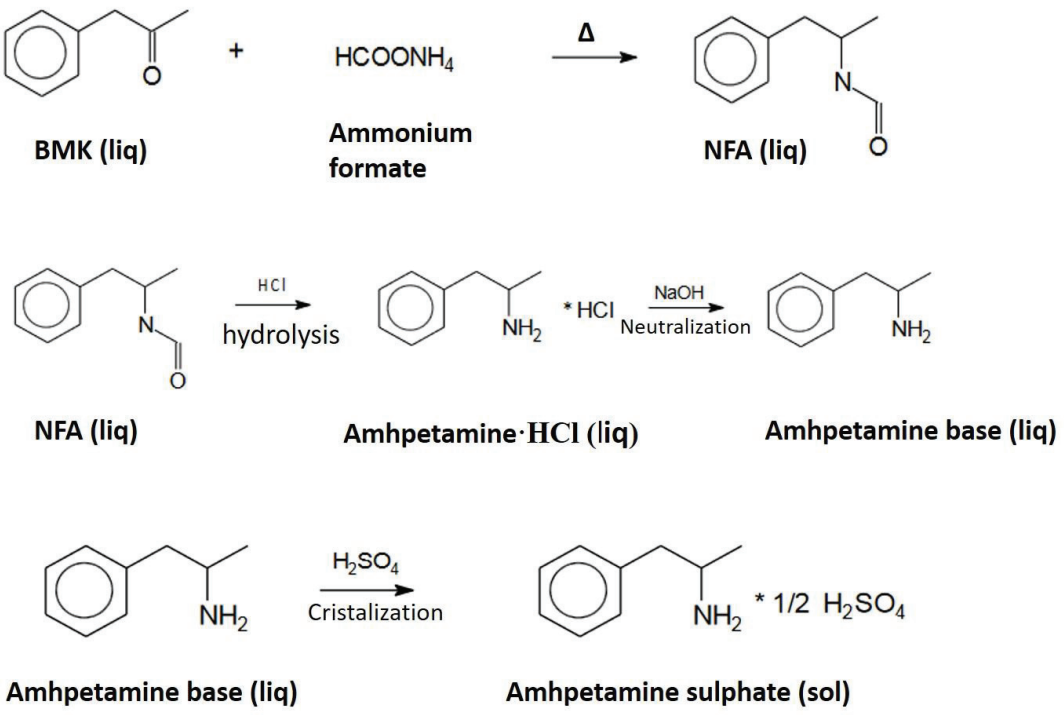

Figure 4. Schema illustrating the **s**teps involved during the synthesis of amphetamine sulfate following the Leuckart method.

4. The current state of ATS detection and the need of innovation.

Collecting information concerning illicit-drug use plays a vital role in not only helping law enforcement agencies in prevention and fight against criminal organizations, but also to estimate drug production and consumption. At present, chemical analysis is widely used to complement epidemiology studies of population traditionally carried out in surveys. Particularly, the chemical analysis of wastewater is a powerful tool to monitor the pattern and trends of illicit drug consumption in a community [19][20]. However, as in the case of amphetamine and its derivatives most analytical techniques used to analyze wastewater samples and detect the illicit compounds are based on ex-situ studies like colorimetric measurements, capillary electrophoresis and especially chromatographic analyses coupled with mass spectrometry techniques [21–23]. Many researchers have assessed drug concentration in a close community analysing sewage samples. Among them, several have been focused on the ATS control in

wastewater to provide a reliable profile of drug consumption both among large and small communities [24–26]. One of the latest studies in sewage epidemiology carried out by Zuccato et al. using SPE and HPLC-MS/MS showed the profile of drug consumption in several Italian school populations. They found that ATS concentration can arise up to 0.2g/day 1000 people depending on the school and season [27]. Although conventional analytical methods are spread over the scientific community as they are reliable, highly accurate and sophisticated, they present a major drawback as they are methodical and complex, time consuming, expensive and require highly qualified personal. Therefore, the development of novel technologies that are faster, low-cost, easy-to-handle and enable to perform real-time analysis in-situ have hugely grown during the past decades. The use of chemical sensors has been presented as an attractive alternative in a broad range of applications.

4.1. Amphetamine sensors. The state-of-the-art.

In the literature, amphetamine and ATS sensors have been scarcely reported as most of narcotics-based samples are controlled in certified laboratories using conventional analytical methods. However, some studies can be found especially in the area of colorimetric measurements and some potentiometric.

4.1.1. Colorimetric sensors for amphetamine and ATS detection.

Commonly, colorimetric methods are extensively used as they are very useful when information of the type "negative or positive" is required. In this context, a miniaturized optical sensor has been described by Gerhard J. Mohr et *al*. in 2001 as the first solid-state sensor developed to perform qualitative analysis of amphetamine [28]. In their work, authors used a synthetized azo dye 4-[4-(4-trifluoroacetylphenylazo)-1-naphthylazo]-N,N-dioctylaniline, as the sensitive part of a poly(vinyl chloride)-type (PVC) polymeric membrane. The recognition process is based on a reversible chemical reaction between the dye's trifluoroacetyl group and the amino group of amphetamine. The chromoreactand was embedded in a thin layer of plasticised PVC and exposed to aqueous solutions containing amphetamine. After exposure to amphetamine, the layer is further analysed by UV-vis spectrophotometry. Before interaction with amphetamine the dye is present in the layer in the blue trifluoroacetyl form. On interaction with the amino group of amphetamine, a hemiaminal is formed giving a deep red colour. The sensor presented a limit of detection (LOD) of 0.1 mM. Nevertheless, it presents a great drawback since common interferences such as methamphetamine and simples aliphatic amines also provide positive alarm.

As a combination of colorimetric and fluorimetric assays, another optical sensor has been reported as a sensor for drug abuse [29]. The DETECHIP® has been presented as an all-in-one spot test device for laboratory and potential field use. It is a mix-and-measure platform providing a lasting colour and fluorescent signal for the rapid detection of commonly abused plant-derived and synthetic drugs. The device contains a simple 12 column x 5 row blank table. Fourteen dyes were initially tested against each

drug for noticeable colour or fluorescent changes. This selection was narrowed to five dyes based on their selectivity for drugs of abuse and adulterants, easy-to-see colour and fluorescence changes, and easy handling and disposal. Each dye is casted on the appropriate wells of a 96-well optical bottom plate. Two different buffers are used, one for control and another to dilute the sample to be analysed. Thus, the analyte gets in contact with the dye casted previously and its colour and fluorescence are registered and contrasted to the reference samples using a portable short-wavelength UV lamp. Authors stated that results obtained regarding the great selectivity of the proposed sensor suggests that changes in colour and fluorescence are most likely based on intermolecular interactions between dyes and drugs, rather than chemical reactions which are functional group specific.

4.1.2. Amphetamine sensors for quantitative analysis.

The two first ion-selective electrodes (ISE) for amphetamine detection were reported in 1989 by Saad S. M. Hassan et *al* [32]. In their work, they described the development of a liquid-membrane sensor based on dibenzo-18-crown-6 ether (DB18C6) and dibenzo-24-crown-8 ether (DB24C8) as the active component for amphetamonium cation recognition. The crown ethers were incorporated to a 1,2-dichloroethane solvent membrane to fabricate two neutral-ionophore-based liquid-membrane ISEs. Both electrodes exhibited stable near-Nemstian response over the range 10^{-2}-10^{-5} M of amphetamonium cation with a slope in the range of 55-58 mV/decade of concentration. The working pH range was found to be 3-7, the response time varied from 30 to 50 s and the lower limit of detection was 3 ppm approximately. The selectivity toward amphetamonium cation was reasonably high relative to some common inorganic cations and alkaloids as well as some amines structurally related to amphetamine being the DB18C6-based electrode between 2 to 14 times more selective for amphetamine in the presence of possible interfering compounds than its homologous DB24C8-based electrode. Even if far to be a real application due to the big size of the electrodes and liquid-state membrane, this work supposed a step further in the literature of amphetamine-selective electrodes as it was the first work that created a reliable but low-cost device for the rapid quantification of amphetamine separating thus from conventional analytical methods.

Subsequently, many authors have reported on the use of ionophores for cation and anion recognition using potentiometric sensors as electroanalytical devices. Such is the case of using α- cyclodextrins (α-CD) as potentiometric sensors for chiral molecules including aryl groups [33]. Here, authors investigated the feasibility of using per-octylated α-CD as a sensing ionophore for monosubstituted arylammonium salts and its ability of discriminating between enantiomers using PVC-type polymeric membrane. As a result, the sensor was proven to provide very stable Nernstian response and to be able to differentiate between the enantiomers (-) and (+) ephedrine presenting a good coefficient of selectivity.

The same authors published a second work three year later in which the study was extended to the examination of some α, β, and γ cyclodextrines to establish their selective binding to a large range of onium cations [34]. They found several CDs to be excellent ionophores for a variety of ions of vital importance in clinical, pharmaceutical and forensic analysis. As an example, amphetamonium cation was successfully quantified using a partially octylated α-CD included in a PVC-type membrane using o-NPOE as plasticizer and tetrakis ([3,5-bis(trifluoromethyl)phenyl] borate) as ion exchanger. In this case, the ISEs described provided a sub-Nernstian slope of 50 mV/ decade of concentration and a LOD of $2.5 \cdot 10^{-4}$ M. However, no study of selectivity in the presence of interferences was reported.

In parallel to ionophores, aptamers have been extensively described as highly selective entities for molecule recognition in electrochemical sensors [35–40]. Aptamers are ribonucleic acid (RNA) or single strand deoxyribonucleic acid (ssDNA) sequences. Depending on their three dimensional structure, they are able to bind specifically to various targets such as organic and inorganic molecules, peptides, proteins or even complete cells. Aptamers could be obtained through a consecutive process which is called Systematic Evolution of Ligands by EXponential enrichment (SELEX). They can be modified for immobilization and labelled with some reporter molecules, without changing their affinity to the target. Authors reported on a specific ssDNA aptamer for the detection of methamphetamine the "aptaMETH" obtained through SELEX process [41]. They fabricated a methamphetamine-selective electrode by drop-cast of the aptaMETH previously diluted in a solution of Tris-HCL buffer. The sensor response to methamphetamine was followed through electrochemical impedance spectroscopy (EIS). However, EIS was performed only to validate the SELEX fabrication process through Nyquist plot before and after aptaMETH-modified electrode incubation in one non-specified concentration of methamphetamine. Thus, neither calibration data nor selectivity study were reported.

Recently, a disposable screen printed sensor for the electrochemical detection of methamphetamine in undiluted saliva has been reported [30]. Authors used a commercially available screen-printed carbon electrode coated with polypropylene thermoplastic matrix that contained cellulose fibres, abaca and N,N′-(1,4-phenylene)-dibenzenesulfonamide as a mediator for the detection of methamphetamine in saliva. The oxidized mediator reacts with methamphetamine to give an electrochemically active adduct which undergo electrochemical reduction. Galvanostatic oxidation in combination with a double square wave reduction technique resulted in detection of methamphetamine in undiluted saliva with a response time of 55 s and lower detection limit of 400 ng/mL. Once again, the selectivity presents the major drawback of this application as the mechanism of reaction described for the oxide-reduction of the N,N′-(1,4-phenylene)-dibenzenesulfonamide/methamphetamine adduct has been reported by Adams and Schowalter to also serve for primary and secondary amines what may cause competition troubles when analysing saliva [31].

5. Ionophores for potentiometric sensors

Over the past 40 years, the application of carrier-based ISEs has evolved to a well-established routine analytical technique. It was estimated that in the United States about 200 million clinical assays of K^+ are made every year with valinomycin-based ISEs which is one of the most established ionophores (see **Fig. 5**) for potassium recognition as nonactin is for NH_4^+ [42].

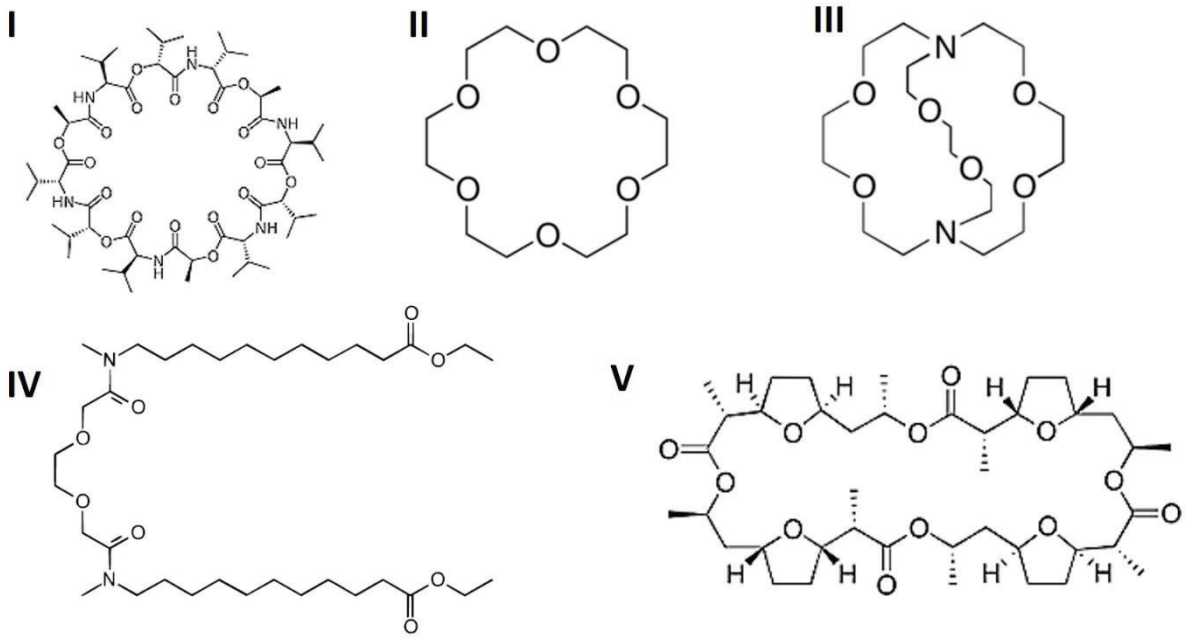

Figure 5. Chemical structures of first relevant ion carriers: **I**, valinomycin, **II**, 18-crown-6 ether, **III** cryptand [2,2,2]. All of them have been described as ionophores for K^+ complexation. **IV**, was the first lipophilic uncharged ion carrier reported as Ca^{2+} ligand. **V**, nonactin is a natural antibiotic which acts as ligand of NH_4^+.

One of the key components of these types of bio/chemical sensors are lipophilic complexing agents capable of reversibly binding ions. They are usually called ionophores or ion carriers. The latter name reflects the fact that these compounds also catalyse ion transport across hydrophobic membranes. The essential part of a carrier-based ISE is the ion-sensitive polymeric membrane, physically a water-immiscible polymer of high viscosity that is commonly made of a mixture of PVC and a plasticizer. A part from PVC and plasticizers, membranes contains various electroactive constituents: commonly the ionophore and a lipophilic salt that serves as ion-exchanger. Sensitivity and selectivity are essential characteristics to evaluate the performance of an ISE. They respond to the activity of the target ion and usually cover a large sensitivity range. Its selectivity is related to the equilibrium constant of the exchange reaction of primary and interfering ions between the polymeric membrane and the media to be analysed. It strongly depends on the ratio of complex formation constants of these ions with the ionophore in the membrane phase.

Ionophores are in their uncomplexed form, either charged or electrically neutral. The first neutral ionophores used in ISE membranes were antibiotics [43]. They were followed by a large number of natural and synthetic, mainly uncharged carriers for cations and some less for anion. After the discovery that some antibiotics induce ion transport in mitochondria, it was shown that the phenomenon is mainly due to the selective formation of complexes between these compounds and certain cations [44,45]. The introduction of the first neutral-carrier based ISE demonstrated that these antibiotics induce in vitro selectivities similar to those observed in vivo. Afterwards, the first macrocyclic polyethers and macroheterobicyclic compounds where synthetized [46] showing to acted as complexing agents for alkali and alkali-earth metal ions.

An important contribution to the development of modern ISEs came from Shatkay and co-workers [47] and Ross, [48] who published the first solvent polymeric membranes in Analytical Chemistry and Science journals respectively in 1967. The later, a Ca^{2+}-selective electrode with a lipophilic organophosphoric acid as the most prominent finding in this line of research is still relevant. PVC was quickly widely accepted and, even though the use of various other polymer matrices has been reported, it still remains the standard matrix for carrier-based ISEs.

Consequently, the basic theory of the response of potentiometric ISEs was developed many decades ago [49].

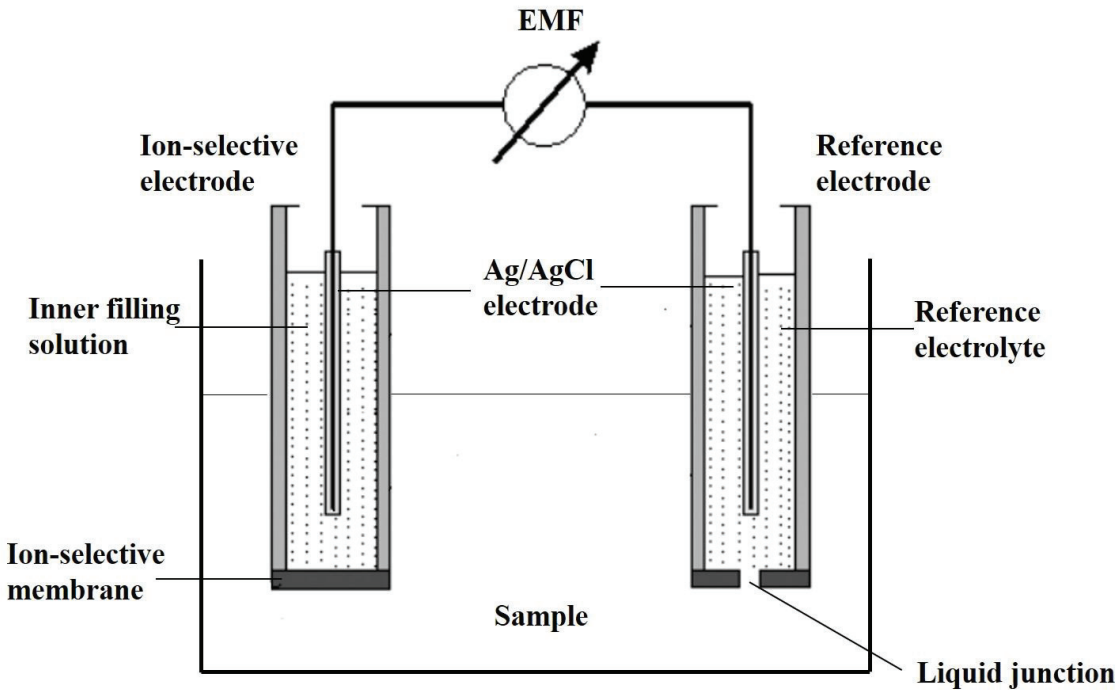

Figure 6. Schematic diagram of a classic liquid-membrane ISE measuring circuit and cell assembly.

ISEs membranes are typically investigated under zero-current conditions in a classic galvanic cell (see **Fig. 6**) such as the following:

Ag ⎪AgCl⎪ reference electrolyte (KCl sat.) **::** sample solution ⎪⎪ ion-selective membrane ⎪⎪ internal filling solution ⎪AgCl ⎪ Ag

The electromotive force (emf) across this cell is the sum of all individual potential contributions. Many of these are sample-independent, and therefore, the measured emf can usually be described as:

$$Emf = E_{const} + E_J + E_M \quad (1)$$

where E_M is the membrane potential and E_j is the liquid junction potential at the sample/bridge electrolyte interface, which can be kept reasonably small and constant under well-defined conditions. Thus, it is common to divide the E_M into two separate potential contributions, namely the phase boundary potentials at both interfaces and the diffusion potential within the ion-selective membrane. For ion-selective electrodes, the membrane internal diffusion potential is zero or constant if no ion concentration gradients occur. This is often the case for membranes that show Nernstian response. Therefore, for the sake of simplicity, diffusion potentials are treated as constant. Consequently, we can stablish;

$$E_M = E_{const} + E_{PB} \quad (2)$$

Where E_{PB} is the phase boundary potential at the membrane-sample interface which can be derived from basic thermodynamic considerations. First the electrochemical potential, $\mu(aq)$, is formulated for the aqueous phase

$$\mu(aq) = \mu^0(aq) + RTln\, a_I(aq) + zF\Phi\,(aq) \quad (3)$$

and for the contacting polymeric membrane,

$$\mu(mem) = \mu^0(mem) + RTln\, a_I(mem) + zF\Phi\,(mem) \quad (4)$$

where μ is the chemical potential (μ^0 under standard conditions), z is the valence and a_I the activity of the uncomplexed ion I, Φ is the electrical potential, and R, T and F are the universal gas constant, the absolute temperature and the Faraday constant respectively. It is now assumed that the interfacial ion transfers and complexation processes are relatively fast and that, therefore, equilibrium holds at the interface so that the electrochemical potentials for both phases are equal. This leads to a simple expression for the phase boundary potential:

$$E_{PB} = \Delta\Phi = \frac{\mu^0(mem) - \mu^0(aq)}{zF} + \frac{RT}{zF}\ln\frac{a_I(aq)}{a_I(mem)} \quad (5)$$

By combining equations 2 and 5 one obtains:

$$E_M = E_{const} + E_{PB} = E_{const} - \frac{\mu^0(mem) - \mu^0(aq)}{zF} - \frac{RT}{zF}\ln a_I(mem) + \frac{RT}{zF}\ln a_I(aq) \qquad (6)$$

Apparently, a simple function of the phase boundary potential based on sample ion activities is expected if the activity of the primary ion in the membrane, a_I(mem), is not significantly altered by the sample. Such is the case of solid-contact PVC-type polymeric membranes [50]. Consequently, the condition establishing a_I(mem) = constant, together with all other sample-independent potential contribution can be included in a new term for the standard potential, E^0 and equation 6 can be reduced into the well-known Nernst equation;

$$E_M = E^0 + \frac{RT}{zF}\ln a_I(aq) \qquad (7)$$

Accordingly, we can affirm that the either the composition and the thickness of the polymeric layer being in contact with the transducer must be kept constant in order to obtain a reproducible Nernstian response, otherwise, changes in electrode preparation would affect E^0 and therefore the final E observed. In the practice, some unconventionalities from the theory commonly appear as parameters such as ionophore lixiviation from the polymeric membrane, limited hydrophobicity of the plasticizer or permselectivity to counterions among others play a key role on the deviation from a Nernstian response [42,49].

On the other hand, selectivity is clearly one of the most important characteristics of an ISE as it often determines whether a final application as the detection of a desired ion in the presence of a complex matrix is possible or not. A theoretically thorough selectivity description allows researchers to identify the key parameters for optimizing the performance of potentiometric sensors, e.g., by adjusting weighing parameters such as absolute membrane concentrations or choosing different plasticizers or polymeric matrices.

From an experimental point of view, all selectivity considerations have been based on the semiempirical Nicolskii-Eisenman equation [51]. Although several authors have reported on a new and more rigorous model for the description of mixed ion response of solvent polymeric membrane based on the phase boundary potential [51–53], the Nicolskii coefficient of selectivity is still in relevance nowadays keeping in mind that the model is limited to the comparison of ions with the same charge [49]. Thus, according to the Nicolskii-Eisenman equation and under ideal conditions, the activity term in the Nernst equation is replaced by a sum of selectivity-dependent activities, as follows;

$$E = E_I^0 + \frac{RT}{z_I F}\ln(a_I(IJ) + K_{IJ}^{Pot} a_j(IJ)^{z_I/z_j}) \quad (8)$$

where a_I(IJ) and a_J(IJ) are the activities of the target ion, I, and the interference ion J in the mixed sample respectively having both the same charge, z. For extremely selective electrodes, the Nicolskii coefficient K_{IJ}^{pot}, is very small and the potential E, observed is mostly dependant of a_I(I) as in the case of ion-pair complex that will be discuss later.

For experimental convenience, two approaches are usually used in order to obtain the potentiometric coefficient K_{IJ}^{pot}: the separate solution method (SSM) and the fixed interference method (FIM) [52]. The SSM compare the calibration curve obtained for two different solutions; one for the primary ion and another for the interference ion. In such a case, the K_{IJ}^{pot}, comparing both responses is rearranged as:

$$K_{IJ}^{Pot} = \frac{a_I(I)}{a_J(J)^{z_I/z_J}} \quad (9)$$

Using the FIM, the calibration curve is obtained by titration of the primary ion in the presence of a fixed background of interference. Therefore, the calculation of the K_{IJ}^{pot}, can be obtained as follows:

$$K_{IJ}^{Pot} = \exp\{\frac{(E_J^0 - E_I^0)z_I F}{RT}\} \quad (10)$$

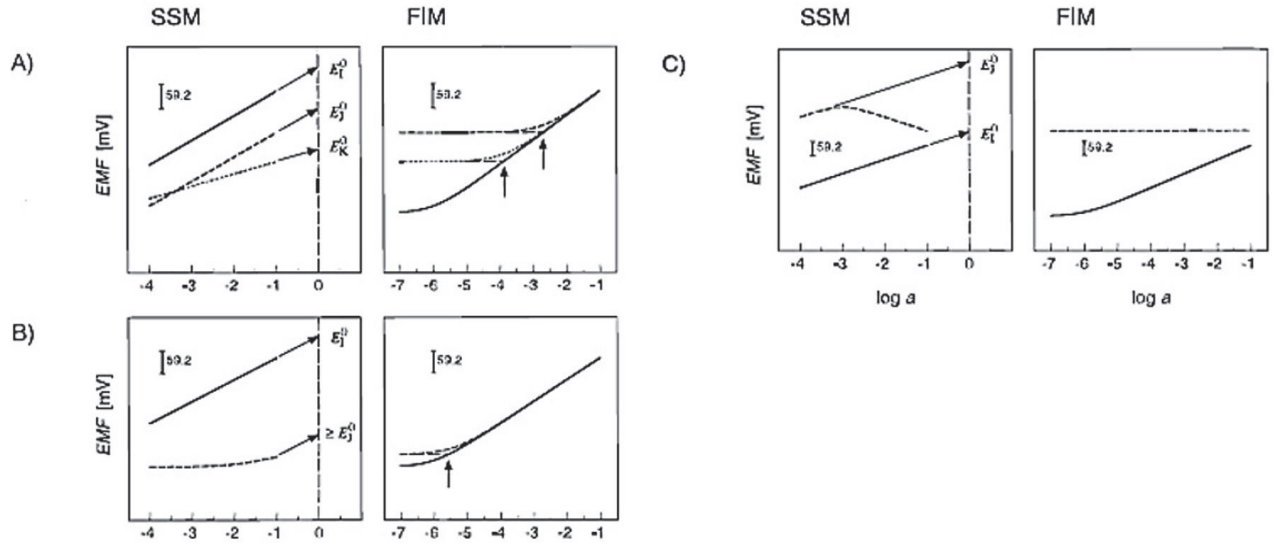

Figure 7. Representation of the separate solution method (SSM, left) and fixed interference method (FIM, right) under (A) ideal and (B, C) nonideal conditions. Solid lines, response to primary ion; dashed and dotted lines, monovalent and divalent interfering ions, respectively. With SSM, the selectivity coefficient is determined from the E^0 values, which can be obtained from extrapolation to log a = 0. In the case of the FIM, information about the electrode slope for the response of the interfering ion should be obtained in additional experiments. The experiment

can be mainly biased by (B) the lower or (C) the upper detection limit. For situation (B), only a maximum selectivity coefficient can be reported; the highest possible activity of the interfering ion should be used [52].

6. Ion-pair complexes for potentiometric sensors.

Ion-pair complexes have been denominated as ion exchangers whose selectivity toward a primary ion is greater in comparison to neutral ionophores who associate with ions in a more non-specific way. Therefore, they are also known as charged ion-carriers or charged ionophores [54]. Among the first ion exchangers were potassium salts of the tetraphenylboric acid derivatives (lipophilic anions) and also salts of tetraalkylammonium, tetraalkylphosphonium and tetraalkylarsonium (lipophilic cations) [55]. Generally speaking, common ion exchangers are lipophilic salts with acid/base properties that dissociate in the polymeric membrane in a more or less degree depending on their chemical characteristics. Thus, for a classic ion exchanger, the potassium tetraphenylborate i.e., the products of the dissociation are a lipophilic anion, $[B(C_6H_5)_4]^-$, and a hydrophilic cation, K^+. The lipophilicity of the former is vital as it prevents significant leak (lixiviation) of the salt from the membrane to the aqueous phase. However, the hydrophilicity of the latter can vary within a broad range since it can be of inorganic or of organic nature. Nevertheless, it is capable to cross the interface and distribute reversibly between the two phases: membrane and aqueous phase. Due to the macroscopic electroneutrality, the total number of hydrophilic ions in a membrane is equivalent to the total number of ion-exchanger sites, regardless of the dissociation degree.

Ideally, the presence of ion-exchanger (anionic i.e.) sites in a membrane prevents from co-extraction of other aqueous electrolytes, in other words, from ions of the same charge (anions) penetration. That is why ion-exchangers are also called ionic additives. The ability of ion exchangers to prevent from co-extraction is also called Donnan exclusion [55]. Basically, the Donnan exclusion principle states that as long as the ion-exchanger concentration in the membrane is high enough (between 0.001 and 0.01 M), the concentration of the interference ion is not too high (below 1M) and the partition coefficient solution/membrane for the complex is low (favouring therefore its presence in the membrane phase) the Donnan exclusion holds and therefore, the charge-transfer across the membrane/solution interface is due to ion-exchange processes. However, it has been observed that the selectivity of conventional ion-exchange-based ISEs is very low as the interaction with the ions is governed by electrostatic forces only and this interaction is sufficient weak.

Contrary to ion exchangers, ion-pair complexes (charged ionophores) associate ions in a more complex form than a simple electrostatic interaction as most of authors coincide [46,49,54,56]. This interaction is much stronger and more selective than in the case of ion-exchangers. From the formal point of view, these differences are quantified by the respective ion-to-ionophore association constants which strongly depend on both the ion's and ionophore's hydrophobic interactions. It is not possible to define a

threshold value of the association constant in such a way that lipophilic species with association constants below the threshold value are ion exchangers and those above the threshold are charged ionophores. In this sense, there is no way to set a formal difference between ion-exchangers and charged ionophores. However, some studies have proven [57–59] that the difference in association constants between ion exchangers and charged ionophores is about several orders of magnitude. So that, we can state that depending on the selectivity needed toward the primary ion from the application point of view, an ion exchanger can be classified as charged ionophore and vice versa. Consequently, for low hydrophilic anions such as thiocyanates or perchlorates, a purely cationic ion-exchanger will be highly selective enough while for alkali or alkali-earth metal cations which are highly hydrophilic, a purer ion carrier-based membrane (supported with an ion-exchanger if needed) will be required to discriminate between the cationic species.

In the context of charged ionophores many publications have reported on the use of ion-pair complexes as recognition sites in the field of potentiometric sensors. Some examples are the use of calcium bis[4-(1,1,3,3-tetramethyl butyl)phenyl]phosphate for Ca^{2+} detection [60], surfactant determination [61–63], fluorous-bulk ion-pair for the alkali and alkali-earth recognition [64] or even for the detection of drugs in pharmaceutical analysis [65,66].

So far, ion-pair complex-based ISEs did not describe any application for biological markers. Instead, they focused on inorganic cations and several organics anions. It was then that A.I Stoica et *al.* were pioneers in publishing a paper that opened the doors to the ion-pair complex formation with a large range of nitrogenous organic bases [67]. By using the metallocarborane cobalt bis(dicarbollide) anion and its properties when isolated with organic bases of the type $[R\text{-}NH]^+$ two novel ion-pair were synthetized and incorporated into PVC-type potentiometric sensors for the detection of isoniazide and pyrazinamide in the application of tuberculosis drug analysis. They demonstrated that very stable ion-pair complex of the type $[cation\text{-}NH]^{n+}n[3,3\text{-}Co(1,2\text{-}C_2B_9H_{11})_2]^-$ can be easily isolated between the metallocarborane cobalt bis(dicarbollide) anion and almost any protonable amine group. Moreover, the cobalt bis(dicarbollide)-amine-ion-pair-complexes-based ISEs reported excellent hydrophobicity and great selectivity. Since most biological molecules present amine groups in their structure, these find marked a step further in the field of bio/chemical sensors [68].

The cobalt bis(dicarbollide) anion $[3',3\text{-}Co\text{-}(1,2\text{-}C_2B_9H_{11})_2]^-$ was very soon established as an ideal hydrophobic anion for extractions through ion-pair mechanism, as it has been reported many decades ago [69], and recently as ionophores in ion-pair complexes-based ISEs [67,70,71].

Cobalt bis(dicarbollide) anion (see **Fig. 8**) (called from now $\mathbf{1}^-$) belongs to a class of low nucleophilic and low coordinating anions [72,73]. The molecular size of this ion is relatively large. The terminal

hydrogens in **1**$^{-}$**,** have a hydric character. Along with charge delocalization over the surface, this is apparently the main cause of the high degree of dissociation of the very strong free conjugate acids, and the unique hydrophobicity of all cobalt bis(dicarbollide) derivatives. A characteristic feature of the bis-icosahedral cobalt bis(dicarbollide) is the good solubility of its free conjugate acids and most of their salts in medium polarity solvents like ethers, nitro-solvents, halogenated solvents, etc, to which they can be extracted from an aqueous phase. The salts with bulky cations are sparingly soluble in water [74]. More importantly, **1**$^{-}$ is able to self-assemble through $C_{cluster}$–H···H–B dihydrogen bonds, and to be non-covalently bonded to the plasticizer through $C_{cluster}$–H···O hydrogen bonds. Moreover, it can have weak B–H···H–N dihydrogen bonds isolated with protonated amino compounds [75]. Cobalt bis(dicarbollide) anion **1**$^{-}$ has also been used as doping agent on intelligent membranes for ion capture [76]. In the field of solid-contact ISEs, cobalt bis(dicarbolide) anion was reported as doping agent on polypyrrole solid-contact layers. The resulting Ppy polymer doped with **1**$^{-}$ showed enhanced thermal stability and a dramatic enhancement of its overoxidation threshold what demonstrated to greatly improve the electrical characteristics of transducers [71,77–82].

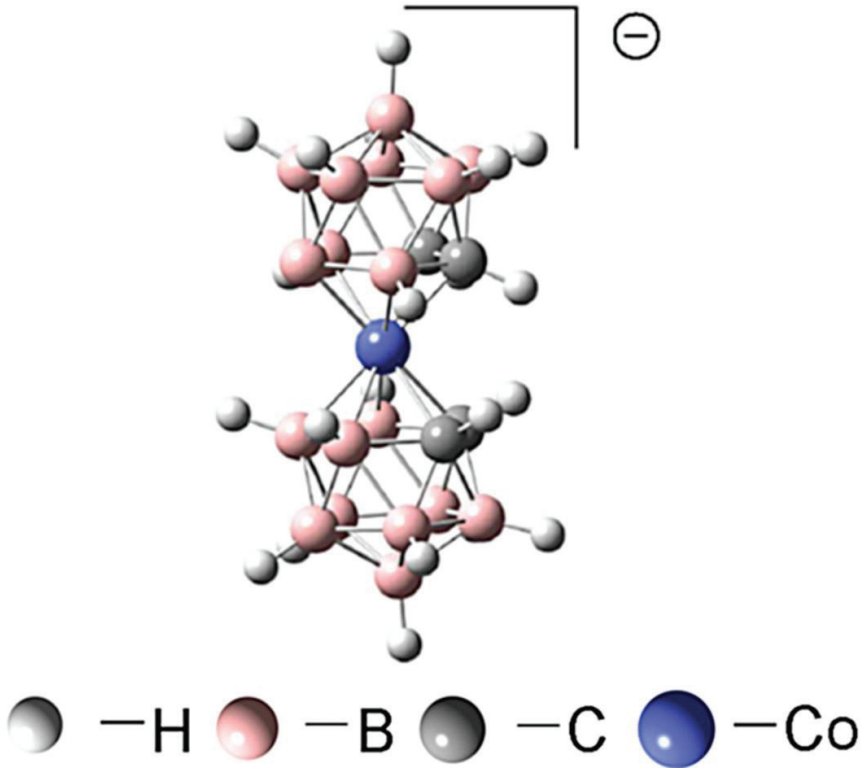

Figure 8. Chemical structure of Cobalt bis(dicarbollide) anion, $[3,3\text{-}Co(1,2\text{-}C_2B_9H_{11})_2]^-$ [68].

All these excellent properties have been extensively studied and reported in many reviews and monograms mostly in the field of organic synthesis and liquid-liquid extraction. However, the capability of ion-pair complex formation of the type $[cation\text{-}NH]^{n+}n[3,3\text{-}Co(1,2\text{-}C_2B_9H_{11})_2]^-$ and its use as charged ion-carrier (charged ionophores) for potentiometric sensors has been slightly explored [67,70,71,83].

This strategy enables to incorporate the primary ion, I, to the polymeric membrane enhancing the sensor's performance and selectivity through the formation of its corresponding ion-pair complex with the only requirement that I, presents a protonable amine, I-NH_3^+. Moreover, one can transform almost any potential interfering amine-compound of the same family into a primary ion by the isolation of the corresponding ion-pair complex and its incorporation to another sensor.

7. Plasticizers.

Polymeric membranes used in ISEs are usually based on a matrix containing about 33% of PVC and 66% of a plasticizer that is slightly altered by the introduction of ionophores in a small amount from 1 to 7%. The plasticizer plays the role of membrane solvent. It is presented in a highly viscous form at room temperature and it ensures the mobility of constituents through the polymeric membrane. Thus, without the inclusion of a plasticizer, the mobility of ions and ionophores would be extremely hindered as the PVC glass transition temperature , T_g, is between 85 to 120 °C and ISEs applications occur mostly at room temperature [84,85]. Plasticizers used in PVC membranes are non-volatile organic liquids compatible with PVC. These are mostly esters (see **Fig. 9**), like carboxylic acid esters or phosphorous and phosphonic acid esters, and also some ethers, in first place, o-nitrophenyloctyl ether.

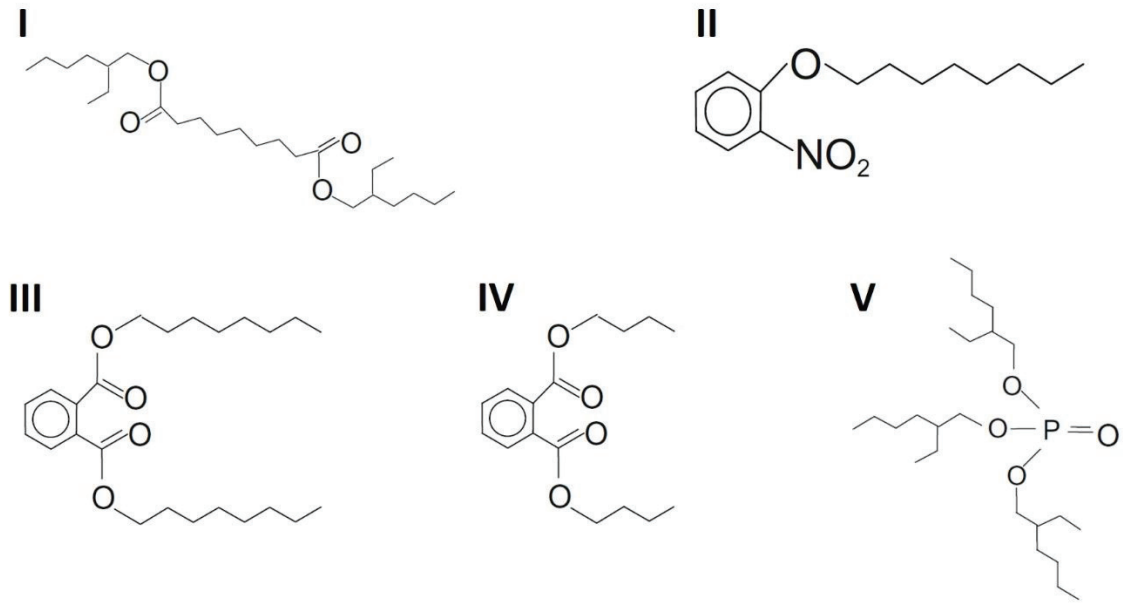

Figure 9. Structures of some plasticizers used in PVC-type membranes. **I**, di-octyl sebacate (DOS). **II**, o-nitrophenyloctly ether (o-NPOE). **III**, di-octyl phthalate (DOP). **IV**, di-butyl phthalate (DBP). **V**, tri-octyl phosphate (TOP).

In general, the basic requirements for an adequate plasticizer are given by at least four criteria [86][87]. On one hand a plasticizer must exhibit sufficient lipophilicity, no crystallization in the membrane phase

and no exudation in order to guarantee a good membrane performance. On the other hand, an optimisation of the selectivities should be assessed for each application. The point is that the potentiometric selectivity can be achieved if the target analyte is more likely to transfer from the aqueous solution phase to the polymeric membrane than other ions present in the sample. In principle, in terms of energy, a transfer from a polar phase (aqueous solution) to a low-polar phase (membrane) is unfavourable for any charged species. However, the energy loss is especially large for a divalent ion. Morf and Simon considered this issue using the Born equation for the energy of the transfer of charged species from vacuum to a phase with a dielectric constant, ε [88]. Assuming I^{z+} ions in aqueous solution, $[IL]^{z+}$ complexes with L, being a neutral ionophore, who then distributes between the two phases, they obtained the below relation for the partition coefficient between the aqueous and membrane phase:

$$\log k_{IL} \sim \frac{z_{IL}^2}{r_{IL}}\left(\frac{1}{78.5} - \frac{1}{\varepsilon}\right) \tag{10}$$

where k_{IL} is the so-called partition coefficient between the phases, z_{IL} is the electrical charge of the ionophore-ion complex, r_{IL}, the ion-ligand radius, 78.5 the dielectric constant of water and ε the dielectric constant of the plasticizer. Therefore, it is observed that the lower the value of ε is, the less the affinity of the species to the membrane. Moreover, as the electrical charge appears in the second power, the effect is more pronounced for divalent ions. Thus, low-polar plasticizers are especially unfavourable for divalent ions and therefore are more suitable for monovalent ions, while ISEs for divalent ions require membranes with polar plasticizers generally.

8. Solid-contact ISEs. The role of conducting polymers.

It is difficult to scale-down conventional ISEs where internal solution and internal electrode are commonly used. This hinders the ISE application in small volumes which would be especially advantageous for the analysis of clinical, biological and even environmental samples. The solid-contact ISEs comprise of an electronically conducting substrate covered with a transducer layer and a sensitive membrane on the top of the transducer layer. Elimination of the classic inner filling solution and replacement thereof with a solid contact appears a purely technical task. However, solving this task encounters fundamental problems. From the practical point of view, these problems result in insufficient long-term stability (lifetime) of the ISE potentials and in poor piece-to-piece reproducibility [54].

Conducting polymers (CP) appear very promising for the stabilization of the solid-contact ISEs' potentials. Most of the conducting polymers are p-type semiconductors when oxidized and doped with anions to maintain the macroscopic electroneutrality. There are, however, also n-type CPs doped with cations. Thus, the doping/de-doping reaction is coupled with oxidation/reduction of the polymer. In this way, CPs work as transducers from ionic to electronic conductivity. Moreover, as the polymer shape

can be often controlled the adhesion of the sensitive membrane can be enhanced by its casting into a porous CP that indirectly improves the mechanical contact of the sensitive layer with the transducer surfaces, commonly noble metals. Most popular CPs used in solid-contact ISEs are polythiophenes: polytrioctylthiophene (POT), polyethylenedioxythiophene (PEDOT), polyaniline (PANI), and polypyrrole (PPy). All these CPs belong to the p-type semiconductors.

It is worth mentioning that the electrochemical properties of this CP can be altered by changing the doping ion who compensate the polymer's electrical charge. Such is the case, of using the above mentioned metallocarborane anion, $[3,3\text{-}Co(1,2\text{-}C_2B_9H_{11})_2]^-$, as doping anion in Ppy conductive polymers (see **Fig. 10**) [71,77–83,89].

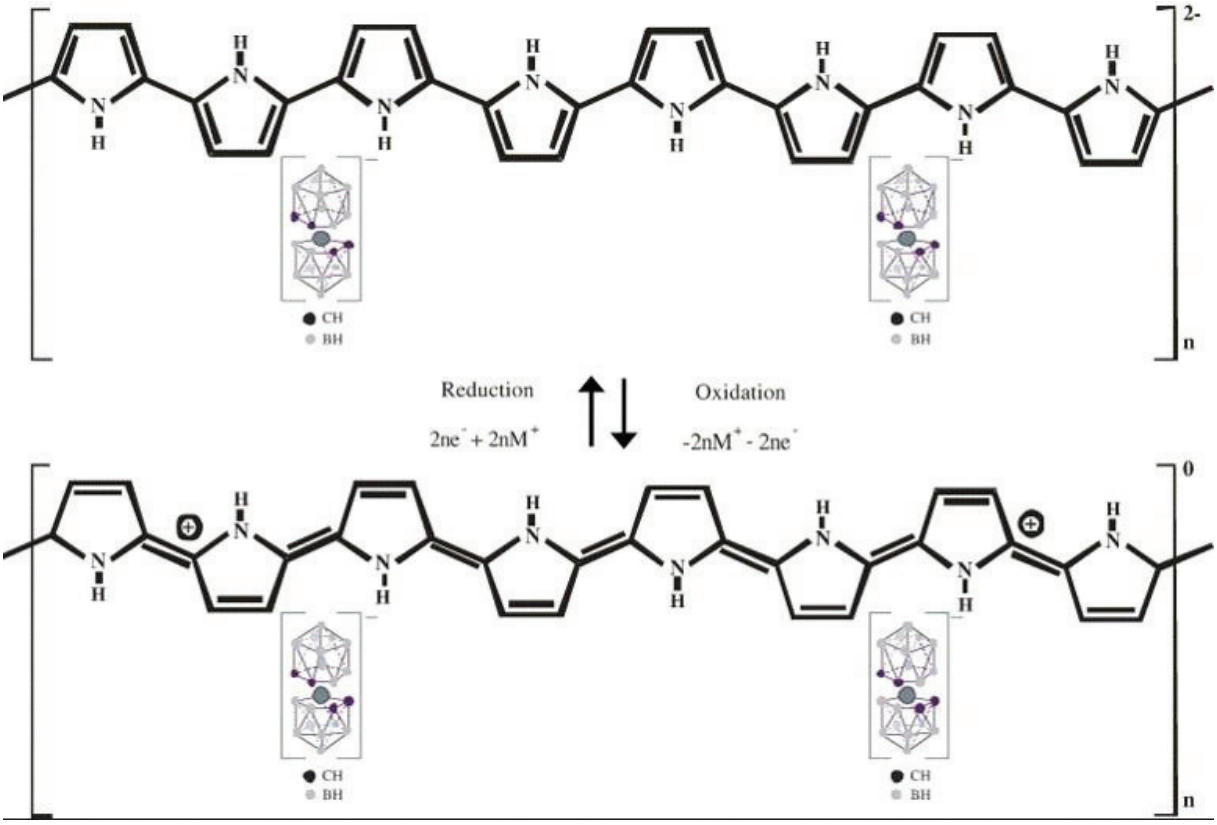

Figure 10. Illustration of charge delocalization in Ppy-COSANE polymer [90].

9. Microfluidic Lab-on-a-Chip for water analysis. The state-of-the-art.

Waste discharges from industrial, agriculture, animal and human activities have hugely increased since the worldwide population and global economy grow [91]. Accordingly, wastewater quality assessment has become an essential tool for environmental monitoring on the last decades. Yet, sewage monitoring is not only helpful to improve wastewater quality from an environmental point of view, but also to perform epidemiology studies in communities. In this context, most of extended analytical techniques

reported to analyze wastewater are sample-based studies like spectroscopic measurements and especially capillary electrophoresis and chromatographic analyses coupled with mass spectrometry techniques (HPLC and GC/GC-MS) [24,27,92–97]. Although these techniques are highly selective and sensitive, they are still limited by the high costs and also they are time consuming. Moreover, this sophisticate equipment cannot provide results at real time neither to be used for in-situ analysis.

Microfluidic lab-on-a-chip (LOC) platforms have been extensively studied due to their possibility of replacing a fully equipped conventional laboratory. In general, advantages of these LOC sensing systems include: compactness, low sample consumption, low-cost production, better overall process control, real-time analysis and a fast response. Great efforts have been devoted in downscaling the instrumentation and an increase of the number of microfluidic LOC that enable rapid analysis of water quality in general have been reported in the last decade [98–103].

Lately, the identification of biological contaminants has been extensively studied as several authors pointed out the presence of antibiotic-resistant bacteria in wastewater as a consequence of antibacterial drug consumption by population [92,94,95]. O. Schwartz and M. Bercovici, presented a microfluidic assay for continuous and quantitative detection of bacteria in water. The work involved the integration of high concentration labelled antimicrobial peptides within microfluidic channel, aiming to achieve limit of detection as low as 105 cfu/mL and yield 4 bacteria in 2 min using isotachophoresis (ITP) and electrophoresis as analytical techniques [104]. In 2013, Z. Wang et al. [105] reported on the rapid detection and quantification of *Escherichia coli* (*E. Coli*) using a glass microfluidic device (see **Fig. 11** (**I** and **II**)). It contained planar micromixer used for mixing bacterial cells with tagging molecules and a preconcentrator that consisted of two microchannels connected through a ~25 μm-thick polydimethylsiloxane (PDMS) membrane. Nanochannels were created in the PDMS membrane by electric breakdown using high electric shock and bacterial cells were preconcentrated by the exclusion-enrichment effect. Subsequently, a gradient of bacteria concentration is created at the PDMS interface and resulting transfer through this later is controlled by measuring the fluorescence of tagged samples at the preconcentration chamber. Almost one year later, in 2014, J. Jing et al. [106] presented a smartphone-based portable microfluidic sensor for preconcentrated bacteria detection using electrochemical impedance spectroscopy (EIS) (see **Fig. 11** (**III, IV, V** and **VI**)). The device contained a multi-stage filtering platform that enabled to preconcentrate bacterial cells in a 10 μm pore-size filter that remained wet. This later is in contact with an array of interdigitated electrodes where the EIS measurements are performed. Using this configuration, authors were able to achieve a limit of detection of 10 cells/mL.

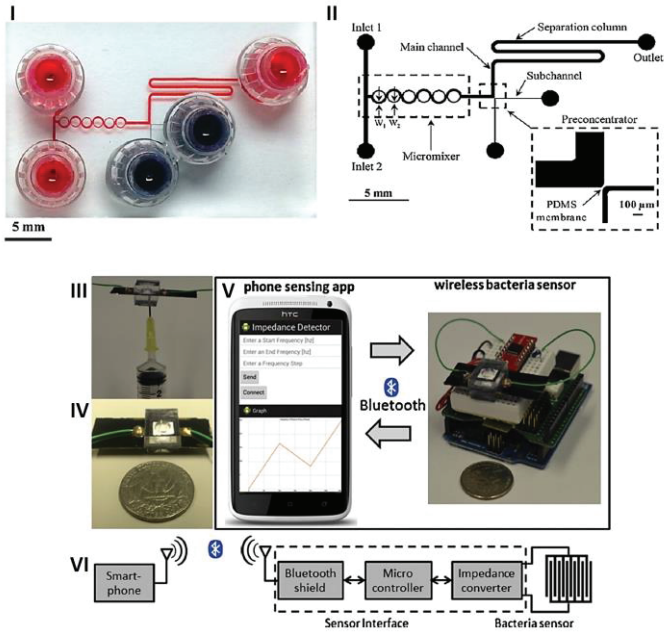

Figure 11. Photograph of the microdevice (**I**) and schematic diagram (**II**) of integrated micro/nanofluidic device for E. Coli detection reported by Z. Wang et al [105]**.** Wireless mobile phone bacteria sensing system reported by J. Jing et al. [106]. (**III**) Picture showing syringe injection of testing liquid into the sensor package; (**IV**) close view of the EIS bacteria sensor package; (**V**) picture showing communication scheme between smartphone sensing app and wireless bacteria sensor; (**VI**) diagram of wireless sensing system.

Non-biological compounds such as pesticides [107], heavy metals [108], inorganic compounds[109] or phenols [110] have also attracted many researchers' attention. In 2010, D. Slater et al. [111] reported the development of a fully autonomous phosphate analyzer based on a microfluidic LOC to determine the total phosphorous (TP) concentration for wastewater quality assessment (see **Fig. 12** (**I**)). The analyzer contained all the required chemical storage, pumping and electronic components to carry out a complete phosphate assay. The function of the microfluidic LOC was to mix the sample, blank or phosphate standard with the reagent chosen to react with phosphate groups and to present the samples in the chamber of analyses where absorbance measurements are carried out. In the same context of TP analyzers, D. Geon et al. [112] have recently published a miniature and single-device LOC. Here, the device consisted of integrated mixing and pretreatment chambers and was based on photocatalytic reaction for phosphorous detection in a time interval of 20 minutes (see **Fig. 12** (**II**)). The instrumentation's size was highly minimized and its performance was comparable to conventional TP analyzers achieving a LOD of 0.1 ppm.

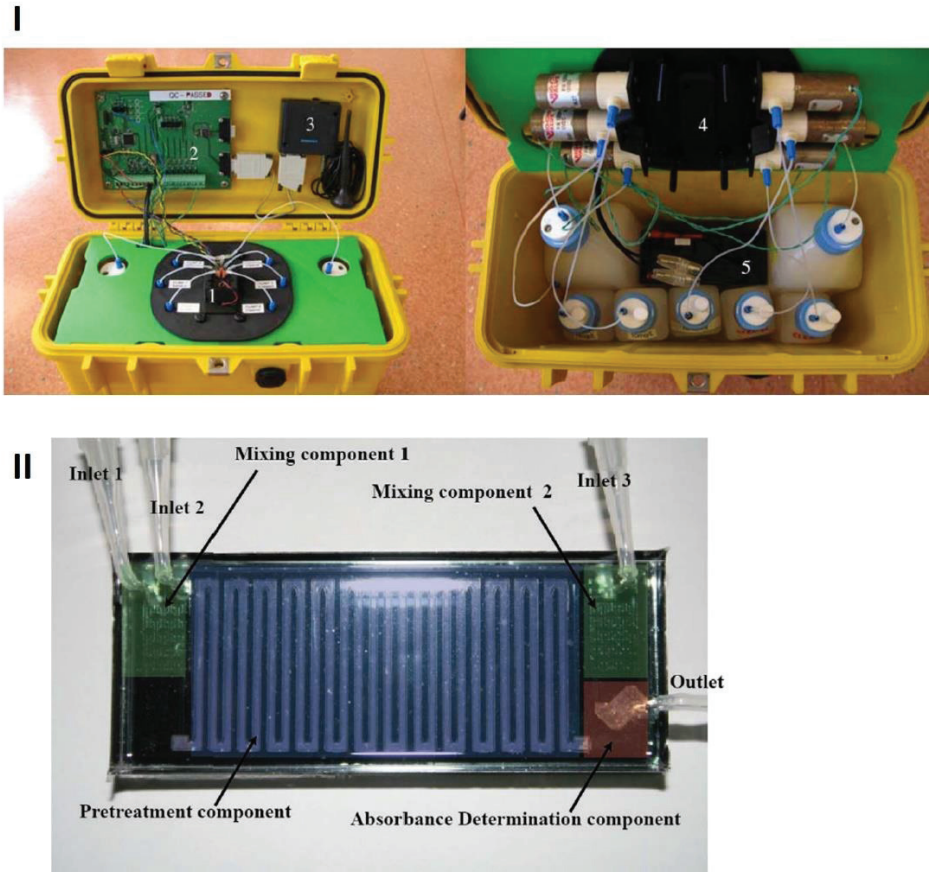

Figure 12. In (**I**) the total-phosphorous analyzer developed by D. Slater et al. in 2010 is shown [111]. It contained the microfluidic LOC (1) integrated in a suitcase with all electronic components needed for a phosphorous assay, such as PCB (2), GSM modem (3), pump (4) and battery (5). In (**II**) the single-device and miniature LOC for total-phosphorous analysis reported by D. Geon et al. eight years later, in 2018 [112].

The content of ammonia in water was also measured using a colorimetric sensor that integrated a microfluidic system [113]. Authors used the Berthelot reaction for ammonia detection. The experimental setup consisted in a micromixer that put in contact ammonia-containing samples with indophenol blue reagent and the samples absorbance was measured at the outlet of the system. The device showed linear range between 0-1 ppm. However, the presence of nitrogenous species in water meant an issue regarding the selectivity of the sensor proposed.

Similarly, a microfluidic multisensorial LOC that was able to operate in all natural waters has been reported [114]. It used colorimetric measurements to assess nitrate and nitrite concentration with a limit of detection of 0.02 μM for both inorganic anions. The device was deployed in an estuarine environment and was able to monitor the content of nitrate and nitrite in continuous with the ease of using a single device.

Passive microfluidic LOC are devices machined with microfabrication techniques that provide the possibility to analyse, separate, concentrate, manipulate, and detect markers of interest with a better sensitivity, throughput, easier than classical or conventional methods and what is more important, they do not need from an external input of energy to make the fluid circulate through the system itself. Therefore, the dynamic flow is created naturally by means of capillary forces, diffusion or pressure drop which depend directly on the geometry of the microfluidic device [100]. These features make passive microfluidic LOC very interesting from an efficiency point of view as they can be more miniaturized than usually, use very low power consumption, are easy-to-prepare, inexpensive and can be mass produced.

The most basic example of passive microfluidic LOC are paper-based microfluidic devices. They have been extensively reported in the literature as disposable sensors for the detection of heavy metals in water samples [115]. A more sophisticated approach was reported by B. M. Jayawardane et al. [116] in 2015. In their work, they developed a gas-diffusion microfluidic paper-based analytical device for the determination of ammonia in wastewater samples. The device presented a filter paper with hydrophobic zones embedded in NaOH and hydrophilic zone embedded with the acid−base indicators 3-nitrophenol or bromothymol blue. Thus, when the sample was introduced into the sodium hydroxide impregnated sample zone the quantitative conversion of the ammonium ion to molecular ammonia took place and the gas diffused across the hydrophobic microporous Teflon membrane to the zone containing the acid−base indicators. The change in indicator colour was measured using a desktop scanner for ammonia quantification. A LOD of 0.8 mg/L was achieved (see **Fig. 13** (**I**)).

P. B. Lillehoj et al. [117] reported on a phone-based electrochemical detection of *Plasmodium falciparum* histidine-rich protein 2 (*Pf*HRP2), an important biomarker for malaria using a passive microfluidic system. The sensor consisted of an embedded circuit for signal processing and data analysis, and disposable microfluidic chips for fluidic handling and biosensing. The microfluidic system based on PDMS was sealed onto a glass substrate including the microelectrodes. The microfluidic device contained a micromixer and a capillary pump to make the sample flow through the system without the need of external energy input. Serpentine-like microchannels were in contact with the microelectrodes where amperometric measurements were carried out. Finally, the signal was processed using a mobile phone (see **Fig. 13** (**II**)).

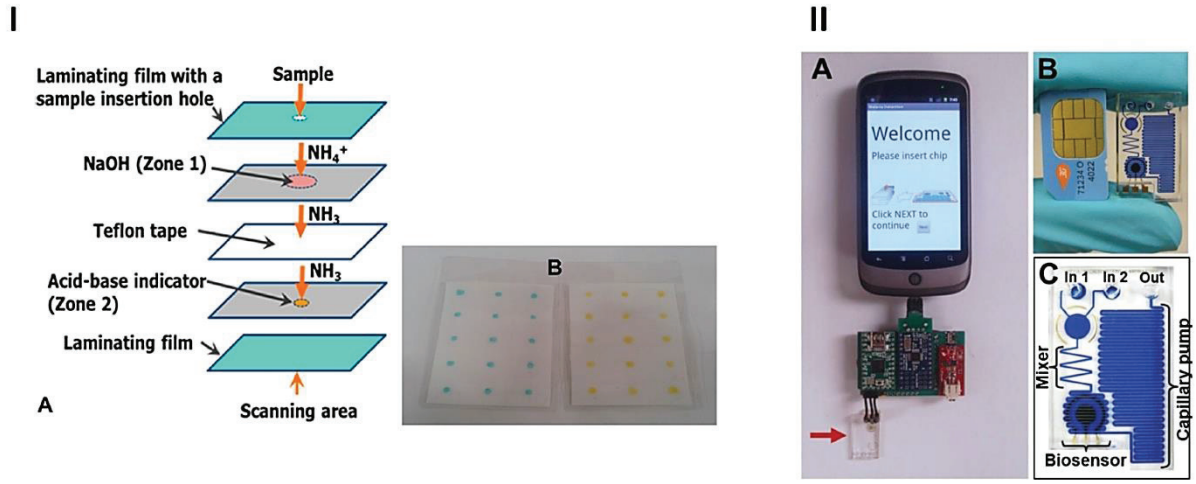

Figure 13. In (**I**) the paper-based gas-diffusion analytical device reported by B. M. Jayawardane et al. is shown [116]. In (**II**) the phone-based electrochemical LOC presented by P. B. Lillehoj et al. is shown [117].

9.1. Silicon technology.

Commonly, the fabrication of these microfluidic devices requires the patterning of the microfluidic element desired onto glass or silicon (Si) substrates. The microfabrication process of microfluidic devices and its surface chemistry for both glass and Si have been extensively studied and the first reports dated from the 90s [118,119]. The most popular fabrication methods for developing microfluidics are etching techniques such as wet etching [119][120], dry etching [118][121], reactive ion etching (RIE) [122] or inductively coupled plasma (ICP) etching [123]. One of the most used methods by the microfluidic community is known as deep reactive ion etching (DRIE) [124]. It is commonly preferred over the above mentioned methods, since DRIE conditions are well optimized for etching these multilayer systems [125–127]. Also, DRIE has been reported to provide good definition of the side walls to depths of hundreds of nanometres.

9.2. PDMS-based microfluidics. The replica-molding technology.

Soft lithography represents a non-photolithographic strategy based on self-assembly and replica molding for carrying out micro- and nanofabrication. It provides a convenient, effective, and low-cost method for the formation and manufacturing of micro- and nanostructures. As indicate by its name, the replica molding technique is used to obtain the positive-shaped structure from a negative-shaped mold. Normally, the microfluidic features desired are etched in a Si master using the microfabrication techniques described in Section 5.1. A liquid polymer is poured onto the master and the replica structure is obtained by peeling-off the future solid polymer from the Si master [128,129]. PDMS is the most used polymer for developing microfluidic structures as it is a transparent elastomer, non-toxic, gas permeable, and is liquid-based at room temperature [130]. Accordingly, the value of replica molding is as a

replication method: it allows duplication of three-dimensional topologies (see **Fig. 14**) in a single step and it also enables faithful duplication of complex structures in the master in multiple copies with nanometre resolution in a simple, reliable, and inexpensive way.

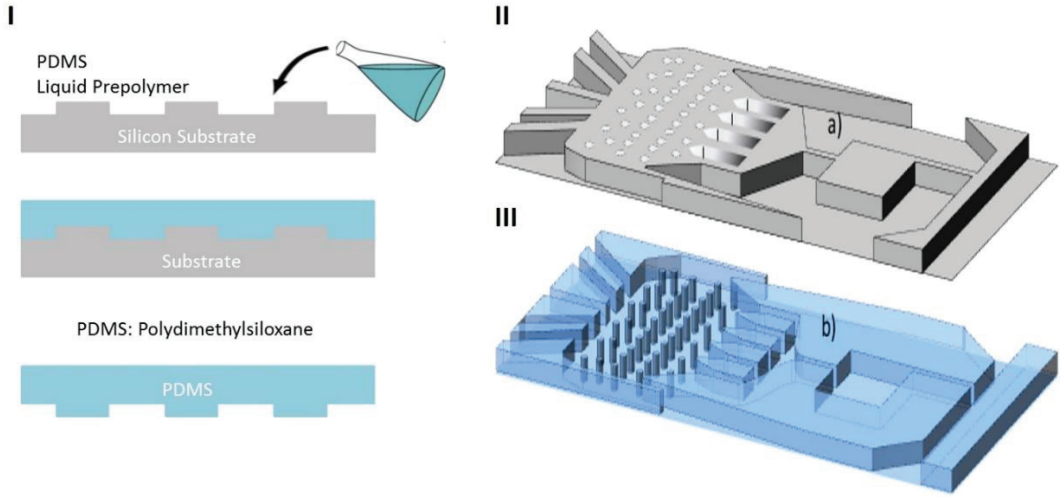

Figure 14. In (**I**), schematic diagram of replica molding technique. In (**II**), Si master with negative features. In (**III**), PDMS-replica structure with positive microfluidic features.

9.3. PDMS-Si activated bonding.

PDMS microfluidic structures can be bonded irreversibly to flat surfaces. Thus, it is common to create enclosed microfluidic devices by bonding of the microfluidic structure to a Si or glass slide. Due to the presence of O-Si-O groups in both PDMS and Si substrate (made of SiO_2 on its surface), it is easy to create a covalent bond between both surfaces through previous -Si-O conversion to -Si-OH activated groups (See **Fig. 15**) [131]. This activation process is commonly achieved using a source of controlled plasma oxygen [129,132–135], while oxidant solution KOH/piranha has also been reported for the same purpose [136].

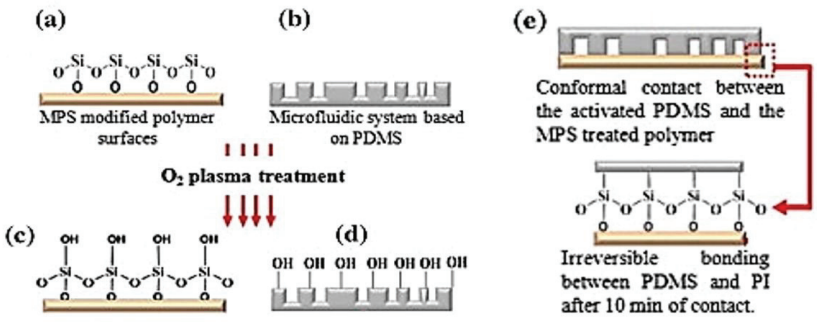

Figure 15. The scheme illustrates the bonding process between the Si and a PDMS microfluidic system with: (a) Si substrate, (b) PDMS microfluidic system, (c) and (d) surface hydroxylation by O_2 plasma treatment onto both

PDMS and Si treated surfaces, (e) conformal contact between the activated PDMS and the Si substrate with Si–O–Si bonding formation [133].

10. Additive manufacturing processes. The 3D printing.

Additive manufacturing (AM) commonly known as 3D printing; is the process of joining materials to make objects from 3D model data, usually layer upon layer [137]. Unlike conventional manufacturing techniques such as machining and stamping to fabricate products by removing materials from a bulky metal, additive manufacturing creates the final shape by adding materials. It has the ability to make efficient use of raw materials (usually polymers) and produce minimal waste while reaching satisfactory geometric accuracy [138,139]. Using additive manufacturing, a design in the form of a computerized 3D solid model can be directly transformed to a finished product without the use of additional fixtures and cutting tools. This opens up the possibility of producing parts with complex geometry that are difficult to obtain using material removal processes.

The development of AM technology started in the 1980s and one of the first publications in the scientific community was reported by J. P. Kruth in 1991 [140]. From there, AM processes have hugely evolved and many different methods are used nowadays.

In its simplest form, a 3D-printing process can be summarized in the steps described below [137]:

- conceptualisation and computer aided design (CAD) as shown in **Fig. 16**. It represents the AM first step and comprises the 3D design of a geometry using a specialized software for that purpose.
- 3D CAD model conversion to STL file. This step involves the 3D draw conversion into the so-called Standard Tessellation Language (STL). Thus, STL represent the standard file format for most of AM processes. STL file creation process mainly converts the continuous geometry in the CAD file into a header, small triangles, or coordinates triplet list of x, y, and z coordinates and the normal vector to the triangles [141].
- transfer to AM machine and file manipulation. Here, the 3D printer is connected to the personal computer and the STL is read and executed.
- AM printing. This step involves the execution of the 3D printing process.
- Removal and clean up. Here, the final piece is removed from the 3D printer and cleaned up. This step is very important specially when microstructures are fabricated to avoid the presence remaining material that can damage the piece.
- Post processing. This step is needed when photopolymers i.e. are used. Once the printing process has ended, an UV bath is given to the piece to end up the polymerization process.
- application.

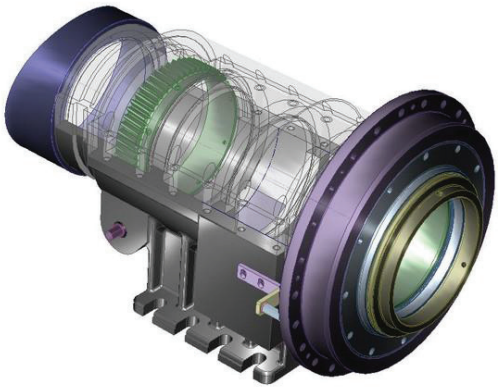

Figure 16. CAD 3D showing part of a mechanic piece. 3D model designed using software SpaceClaim®. Image taken from http://www.directindustry.es/prod/spaceclaim/product-40180-352254.html

In the last two decades, the vast majority of microfluidic systems have been built in PDMS as it was extensively described in Section 5. 3D-printing has recently attracted attention as a way to fabricate microfluidic systems due to its automated, assembly-free 3D fabrication, rapidly decreasing costs, and fast-improving resolution and throughput. Resins with properties approaching those of PDMS are being developed [142] (see **Fig. 17)**. In this context, several authors have classified the AM processes into three categories according to the physical state of the printing process: liquid based, solid based and powder based [137,140,143–145].

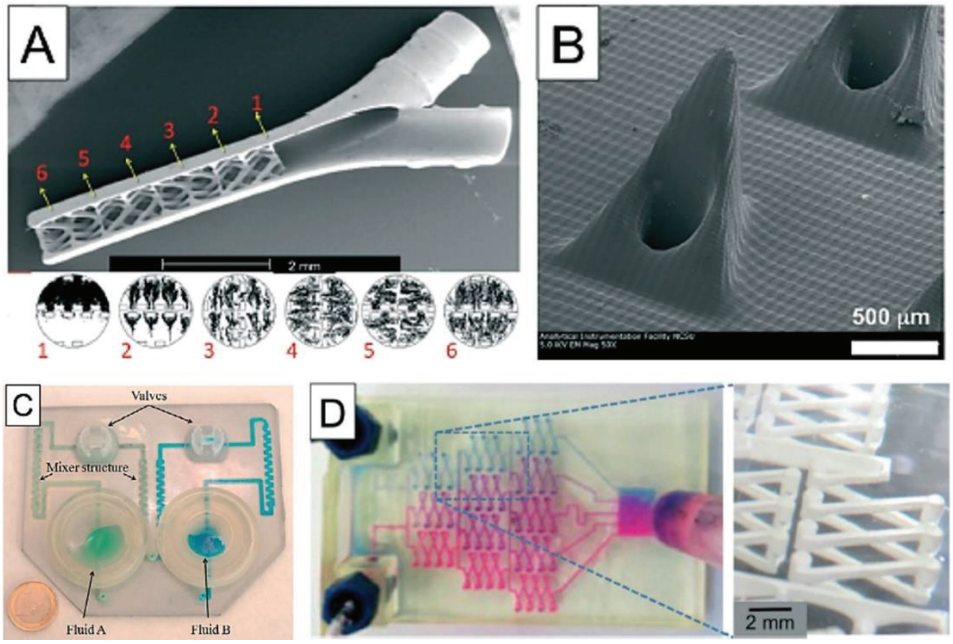

Figure 17. SEM micrographs of (**A**) one of the first microfluidic device (micro-mixer) and (**B**) hollow micro-needles printed by stereolithograpy. In (**C**), a fluid mixer and homogenizer printed with Objet Eden 250 using the Full Cure 720 resin by PolyJet technology. In (**D**), a complex microfluidic mixer and gradient generator printed with a commercial desktop stereolithography system. Images taken from reference [142].

10.1. Liquid-based AM processes.

Concerning liquid-based methods, three sub-categories can be found regarding the technology involved in the manufacturing process: fused deposition modeling (FDM), stereolithograpy (SL) and polyjet.

Fused deposition modeling (FDM) is an additive manufacturing process in which a liquid thermoplastic material is extruded from a movable FDM head and then deposited in ultra-thin layers onto a substrate as illustrated in **Fig. 18** (**I**). The material is heated to 1 °C above its melting point so that it solidifies almost immediately after extrusion and cold welds to the previous layers [146]. The materials used have been expanded to include wax, metals, and ceramics. However, polycarbonate (PC), acrylonitrile butadiene styrene (ABS), polyphenylsulfone (PPSF), PC-ABS blends, and PC-ISO which is a medical grade PC are most used materials. Although this technique is not expensive and does not require post-processing treatment, a major drawback is found as the resolution on the z axis is very low compared to other additive manufacturing methods. Therefore, if a smooth surface is required, a finishing process is essential what is time-consuming.Stereolithography (SL) uses a photosensitive monomer resin and a UV laser to build parts one layer at a time [146–148] (see **Fig. 18** (**III**)). On each layer, the laser beam installed in a x, y and z movable head traces the cross-section of the part on the surface of the liquid resin to solidify the pattern. Afterwards, the platform where the piece is growing is lowered in order to coat the part thoroughly. It is then raised to a level such that an edge wipes the resin, leaving exactly one layer of resin above the part. The part is then lowered by one layer and left until the liquid has settled to ensure an even surface before the next layer is built. SL is a well stablished technology over the manufacturing industry as it reduces the time for a prototype to be produced as well as it gets good surface finish. However, this technique is limited by the size of the piece to be produced who usually does not exceed 60 cm^3. Also, materials used in SL are limited compared to other AM processes.

Polyjet is a AM method that uses inkjet technologies to manufacture physical models [149,150] (see **Fig. 18** (**II**)). The inkjet head moves in the x and y axes depositing a photopolymer which is cured by ultraviolet lamps after each layer is finished. The layer thickness achieved in this process is 16 μm, so the produced parts have a high resolution. However, the parts produced by this process are weaker than others like SL. A gel-type polymer is used for supporting the overhang features and after the process is finished this material is water jetted. With this process, parts of multiple colors can be built.

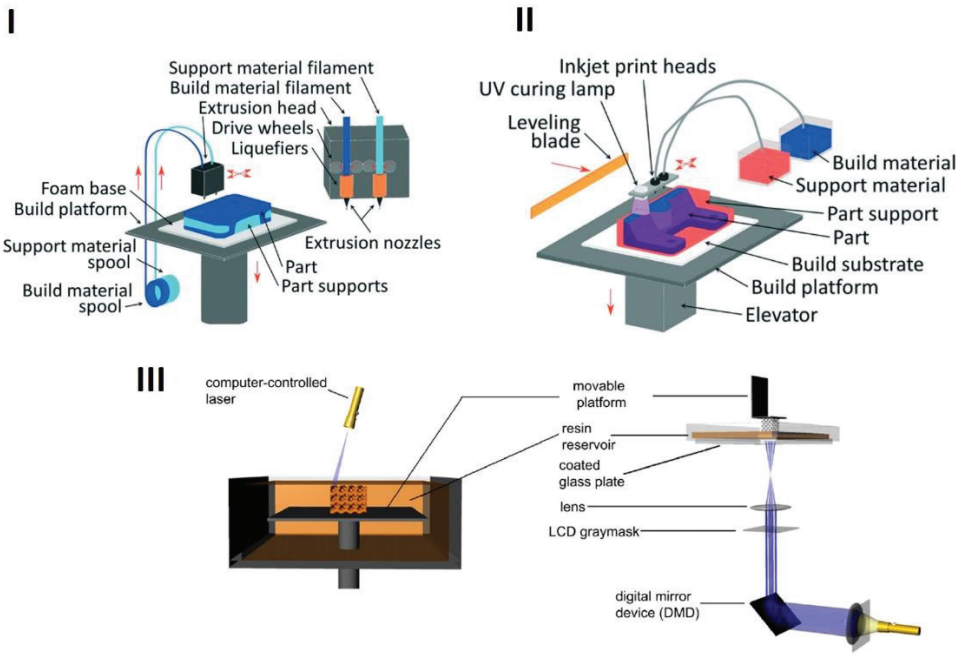

Figure 18. Schematic illustration of (**I**) fused deposition modeling [142], (**II**) polyjet [142] and (**III**) stereolithography [147].

10.2. Solid-based AM processes.

Only one AM process has been classified as solid-based printing method; the laminated object manufacturing (LOM) technique. Here, adhesive-coated sheet materials are used. The process combines additive and subtractive techniques to build a piece layer by layer as shown in **Fig. 19**. The layers are bonded together by pressure and heat application and using a thermal adhesive coating. A CO_2 laser cuts the material to the shape of each layer given the information of the 3D model from the CAD and STL file. The advantages of this process are the low cost, no post processing and supporting structures are required, no deformation or phase change during the process, and the possibility of building large parts. The disadvantages are that the fabrication material is subtracted thus wasting it, low surface definition, the material is directional dependent for machinability and mechanical properties, and complex internal cavities are very difficult to be built. This process can be used for models with papers, composites, and metals [151,152].

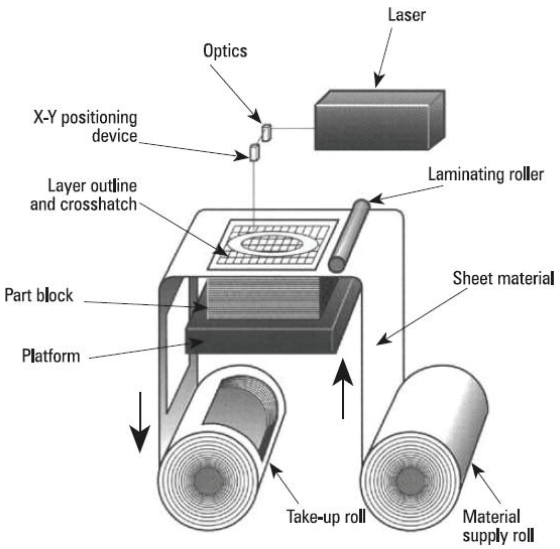

Figure 19. Schematic functioning of LOM additive manufacturing process [152].

10.3. Powder-based AM processes.

Powder-based AM processes are subdivided into two subcategories depending on the physical transformation involved during the manufacturing process: melting and binding.

Selective laser sintering (SLS) (see **Fig. 20** (**I**)) is included into the melting subcategory as it uses high power laser to fuse small particles of the build material (polymers, metals, ceramics, glass, or any material that can be pulverized) [153–155]. The laser fused the powder at a specific location for each layer specified by the design. The particles lie loosely in a bed, which is controlled by a piston, that is lowered the same amount of the layer thickness each time a layer is finished. No post curing is required, and the build time is fast. However, SLS operation is complicated as many build variables need to be decided. Moreover, the surface finish achieved with SLS is not as good as that obtained from SL.

Electron beam melting (EBM) together with laser engineered net shaping (LENS) are AM processes similar to SLS. However, in both EBM and LENS is a high voltage electron laser beam that melts the powder. The processes (see **Fig. 20** (**II**)) take place in high vacuum chambers to avoid oxidation issues because it is intended for building metal parts. LENS method enables to produce parts of a wide variety combination of metals (see **Fig. 20** (**III**)). Other than this, the processes are very similar to SLS. One of the future uses of these processes is the manufacturing in outer space since it is all done in a high vacuum chamber [156,157]. A major drawback is the danger it presents the handling of metallic powder from a health point of view.

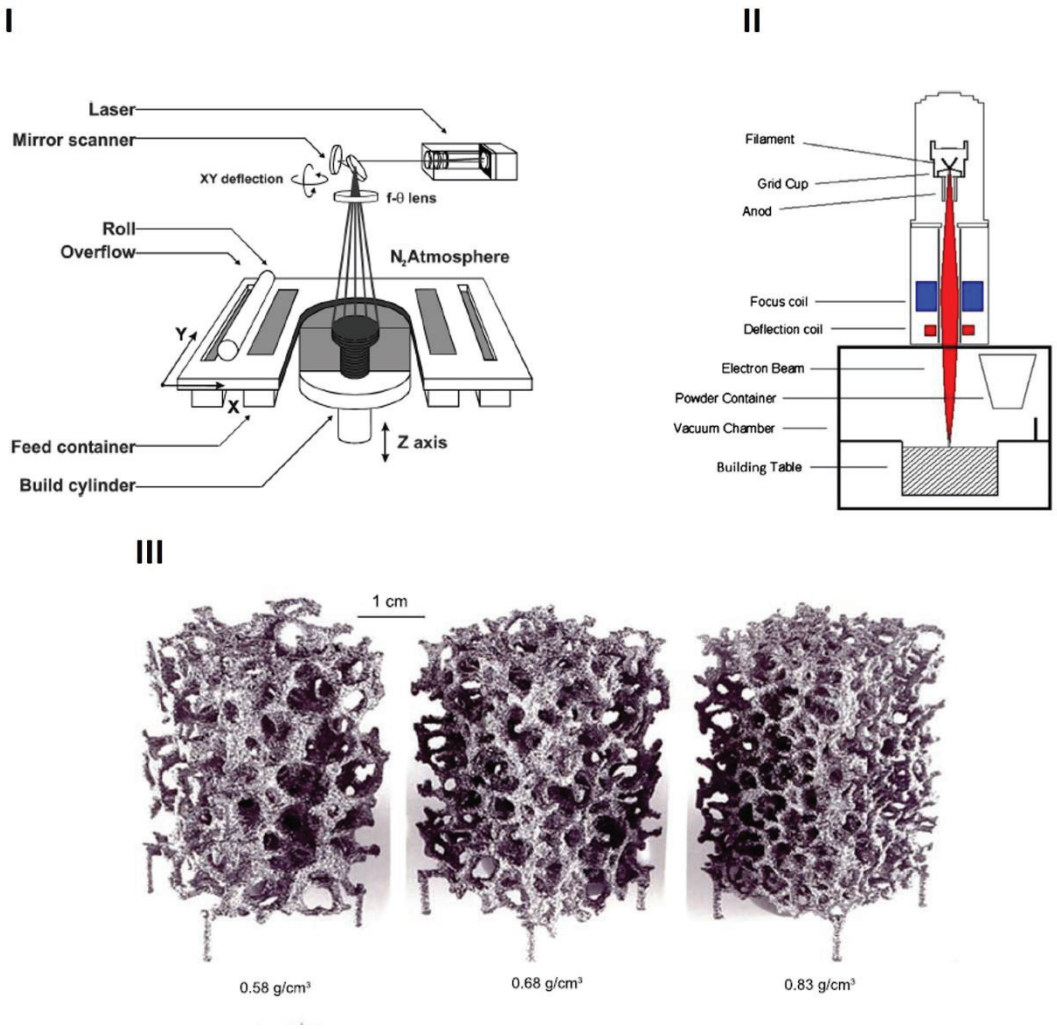

Figure 20. Schematic functioning of (**I**) SLS [154] and (**II**) EBM [157] processes. In (**III**) EBM-fabricated foams of Ti-6Al-4V with different densities are shown [156].

Three-dimensional printing (3DP) [158] belongs to the binding subcategory. Here, the functioning principle is the deposition of powdered material on a substrate that are selectively joined using a binder sprayed through a nozzle. The material is first stabilized through misting with water droplets to avoid excessive disturbance when it is hit by the binder. Following the sequential application of layers, the unbound powder is removed. 3DP is probably the fastest of all AM processes. However, there are some limitations such as rough surface finish, size limitation, and high cost.

11. References.

[1] European Monitoring Centre for Drugs and Drug Addiction, European Drug Report 2016: Trends and Developments, Publication Office of the European Union, Luxembourg, 2016. doi:10.2810/88175.

[2] O. on D. and C. United Nations, World Drug Report.Market analysis of sythetic drugs. Amphetamine-type stimulants new psychoactive substances., (2017). https://www.unodc.org/wdr2017/field/WDR_2017_presentation_lauch_version.pdf.

[3] United Nations Office on Drugs and Crime, Amphetamines and Ecstasy - 2011 Global ATS Assessment, 2011. http://www.unodc.org/documents/ATS/ATS_Global_Assessment_2011.pdf.

[4] EMCDDA, European Drug Report 2017: Trends and Developments, 2017. doi:10.2810/88175.

[5] European Monitoring Centre for Drugs and Drug Addiction and Europol, EU drug markets report. In-depth analysis, EMCDDA-Europol Joint publications, Publications Office of the European Union, Luxembourg, 2016. doi:10.2810/219411.

[6] EMCDDA, EMCDDA – Europol joint publications: Amphetamine, 2011. doi:10.2810/49525.

[7] T. Hague, Amphetamine-Type Stimulants in the European Union 1998-2007, (2007).

[8] EMCDDA, Wastewater analysis and drugs: a European multi-city study, (2016) 1–5. doi:http://www.emcdda.europa.eu/topics/pods/waste-water-analysis.

[9] MicroMole©, sewage monitoring system for tracking synthetic drugs laboratories, (2015). http://micromole.eu.

[10] R. Adams, W.E. Bachmann, J.R. Johnson, H.R. Snyder, T.L. Jacobs, M.S. Newman, The Leuckart Reaction. Organic Reactions, 1949.

[11] M. Nevešćanin, S.B. Stević, S. Petrović, V. Vajs, Analysis of amphetamines illegally produced in Serbia, J. Serbian Chem. Soc. 73 (2008) 691–701. doi:10.2298/JSC0807691N.

[12] R. Leuckart, Ueber eine neue Bildungeweiae von Tribensylemin, Berichte Der Dtsch. Chem. Gesellschaft. 154 (1885) 72–75.

[13] M. Bohn, G. Bohn, G. Blaschke, Synthesis markers in illegally manufactured 3,4-methylenedioxyamphetamine and 3,4-methylenedioxymethamphetamine, Int. J. Legal Med. 106 (1993) 19–23. doi:10.1007/BF01225019.

[14] F. Palhol, S. Boyer, N. Naulet, M. Chabrillat, Impurity profiling of seized MDMA tablets by capillary gas chromatography, Anal. Bioanal. Chem. 374 (2002) 274–281. doi:10.1007/s00216-002-1477-6.

[15] D. Blachut, K. Wojtasiewicz, Z. Czarnocki, Identification and synthesis of some contaminants present in 4-methoxyamphetamine (PMA) prepared by the Leuckart method, Forensic Sci. Int. 127 (2002) 45–62. doi:10.1016/S0379-0738(02)00121-4.

[16] V. Kunalan, N.N. Daéid, W.J. Kerr, H.A.S. Buchanan, A.R. McPherson, Characterization of route specific impurities found in methamphetamine synthesized by the Leuckart and reductive amination methods, Anal. Chem. 81 (2009) 7342–7348. doi:10.1021/ac9005588.

[17] M. Lambrechts, K.E. Rasmussen, Leuckart-specific impurities in amphetamine and methamphetamine seized in Norway, Bull. Narc. 36 (1984) 47–57. doi:10.1016/S0021-9673(01)87855-9.

[18] Europol, Europoly synthetic dug production equipment cataloge, (2010).

[19] European Monitoring Centre for Drugs and Drug Addiction, Assesing ilicit drugs in wastewater: advances in wastwater-based drug epidemiology, Publication Office of the European Union, Luxembourg, 2016. doi:10.2810/017397.

[20] S. Castiglioni, K. V. Thomas, B. Kasprzyk-Hordern, L. Vandam, P. Griffiths, Testing wastewater to detect illicit drugs: State of the art, potential and research needs, Sci. Total Environ. 487 (2014) 613–620.

[21] N. Schaefer, B. Peters, P. Schmidt, A.H. Ewald, Development and validation of two LC-MS/MS methods for the detection and quantification of amphetamines, designer amphetamines, benzoylecgonine, benzodiazepines, opiates, and opioids in urine using turbulent flow chromatography, Anal. Bioanal. Chem. 405 (2013) 247–258. doi:10.1007/s00216-012-6458-9.

[22] O. on D. and C. United Nations, Amphetamine, Methamphetamine and Their Ring-Substituted Analogues in Seized Materials, 2006. https://www.unodc.org/pdf/scientific/stnar34.pdf.

[23] J. Sun, X. Xu, C. Wang, T. You, Analysis of amphetamines in urine with liquid-liquid extraction by capillary electrophoresis with simultaneous electrochemical and electrochemiluminescence detection., Electrophoresis. 29 (2008) 3999–4007.

[24] Z. Xu, P. Du, K. Li, T. Gao, Z. Wang, X. Fu, X. Li, Tracing methamphetamine and amphetamine sources in wastewater and receiving waters via concentration and enantiomeric profiling, Sci. Total Environ. 601–602 (2017) 159–166. doi:https://doi.org/10.1016/j.scitotenv.2017.05.045.

[25] I. Senta, I. Krizman, M. Ahel, S. Terzic, Multiresidual analysis of emerging amphetamine-like

psychoactive substances in wastewater and river water, J. Chromatogr. A. 1425 (2015) 204–212. doi:https://doi.org/10.1016/j.chroma.2015.11.043.

[26] T.H. Boles, M.J.M. Wells, Analysis of amphetamine and methamphetamine in municipal wastewater influent and effluent using weak cation-exchange SPE and LC-MS/MS, Electrophoresis. 37 (2016) 3101–3108. doi:10.1002/elps.201600271.

[27] E. Zuccato, E. Gracia-Lor, N.I. Rousis, A. Parabiaghi, I. Senta, F. Riva, S. Castiglioni, Illicit drug consumption in school populations measured by wastewater analysis, Drug Alcohol Depend. 178 (2017) 285–290. doi:https://doi.org/10.1016/j.drugalcdep.2017.05.030.

[28] G.J. Mohr, M. Wenzel, F. Lehmann, P. Czerney, A chromoreactand for optical sensing of amphetamines, Anal. Bioanal. Chem. 374 (2002) 399–402. doi:10.1007/s00216-002-1519-0.

[29] R.M. Burks, S.E. Pacquette, M.A. Guericke, M. V. Wilson, D.J. Symonsbergen, K.A. Lucas, A.E. Holmes, DETECHIP®: A sensor for drugs of abuse, J. Forensic Sci. 55 (2010) 723–727. doi:10.1111/j.1556-4029.2010.01323.x.

[30] C.A. Bartlett, S. Taylor, C. Fernandez, C. Wanklyn, D. Burton, E. Enston, A. Raniczkowska, M. Black, L. Murphy, Disposable screen printed sensor for the electrochemical detection of methamphetamine in undiluted saliva, Chem. Cent. J. 10 (2016) 1–9. doi:10.1186/s13065-016-0147-2.

[31] R. Adams, K.A. Schowalter, Quinone Imides. X. Addition of Amines to p-Quinonedibenzenesulfonimide, J. Am. Chem. Soc. 74 (1952) 2597–2602. doi:10.1021/ja01130a039.

[32] S.S.M.H. J, E.M. Elnemma, H. Saad S M, E. Eman M, Amphetamine Selective Electrodes Based on Dibenzo- 18-crown-6 and Dibenzo-24-crown-8 Liquid Membranes, Anal. Chem. (1989) 2189–2192.

[33] R. Kataky, P.S. Bates, D. Parker, Functionalized α-cyclodextrins as potentiometric chiral sensors, Analyst. 117 (1992) 1313. doi:10.1039/an9921701313.

[34] R. Kataky, D. Parker, P.M. Kelly, Potentiometric, enantioselective sensors for alkyl and aryl ammonium ions of pharmaceutical significance, based on lipophilic cyclodextrins, Scand. J. Clin. Lab. Invest. 55 (1995) 409–419. doi:10.3109/00365519509104980.

[35] H. Zhang, L. Zhou, Z. Zhu, C. Yang, Recent Progress in Aptamer-Based Functional Probes for

Bioanalysis and Biomedicine, Chem. - A Eur. J. 22 (2016) 9886–9900. doi:10.1002/chem.201503543.

[36] A. Hayat, J.L. Marty, Aptamer based electrochemical sensors for emerging environmental pollutants, Front. Chem. 2 (2014) 41. doi:10.3389/fchem.2014.00041.

[37] B. Jiang, F. Li, C. Yang, J. Xie, Y. Xiang, R. Yuan, Aptamer pseudoknot-functionalized electronic sensor for reagentless and single-step detection of immunoglobulin e in human serum, Anal. Chem. 87 (2015) 3094–3098. doi:10.1021/acs.analchem.5b00041.

[38] K. Sefah, J.A. Phillips, X. Xiong, L. Meng, D. Van Simaeys, H. Chen, J. Martin, W. Tan, Nucleic acid aptamers for biosensors and bio-analytical applications, Analyst. 134 (2009) 1765–1775. doi:10.1039/B905609M.

[39] J.R. Kanwar, J.S. Shankaranarayanan, S. Gurudevan, R.K. Kanwar, Aptamer-based therapeutics of the past, present and future: from the perspective of eye-related diseases, Drug Discov. Today. 19 (2014) 1309–1321. doi:10.1016/j.drudis.2014.02.009.

[40] Q. Shi, Y. Shi, Y. Pan, Z. Yue, H. Zhang, C. Yi, Colorimetric and bare eye determination of urinary methylamphetamine based on the use of aptamers and the salt-induced aggregation of unmodified gold nanoparticles, Microchim. Acta. 182 (2014) 505–511.

[41] M. Ebrahimi, M. Johari-Ahar, H. Hamzeiy, J. Barar, O. Mashinchian, Y. Omidi, Electrochemical impedance spectroscopic sensing of methamphetamine by a specific aptamer, BioImpacts. 2 (2012) 91–95. doi:10.5681/bi.2012.013.

[42] G. Dimeski, T. Badrick, A.S. John, Ion Selective Electrodes (ISEs) and interferences-A review, Anal. Lett. 411 (2010) 309–317. doi:10.1016/j.cca.2009.12.005.

[43] L.A.R. Pioda, V. Stankova, W. Simon, Highly Selective Potassium Ion Responsive Liquid-Membrane Electrode, Anal. Lett. 2 (1969) 665–674. doi:10.1080/00032716908051343.

[44] D. Ammann, W.E. Morf, P. Anker, P.C. Meier, E. Pretsch, W. Simon, Neutral Carrier Based Ion-Selective Electrodes, in: J.D.R. THOMAS (Ed.), Ion-Selective Electrode Rev., Elsevier, 1983: pp. 3–92. doi:https://doi.org/10.1016/B978-0-08-031492-1.50005-X.

[45] C. Moore, B.C. Pressman, Mechanism of action of valinomycin on mitochondria, Biochem. Biophys. Res. Commun. 15 (1964) 562–567. doi:https://doi.org/10.1016/0006-291X(64)90505-4.

[46] P. Bühlmann, E. Pretsch, E. Bakker, Carrier-based ion-selective electrodes and bulk optodes. 2. Ionophores for potentiometric and optical sensors, Chem. Rev. 98 (1998) 1593–1688. doi:cr970113+ [pii].

[47] A. Shatkay, Ion specific membranes as electrodes in determination of activity of calcium, Anal. Chem. 39 (1967) 1057.

[48] J.W. Ross, Calcium-selective electrodes with liquid ion exchanger, Science (80-.). 156 (1967) 1378–1379.

[49] E. Bakker, P. Bühlmann, E. Pretsch, Carrier-Based Ion-Selective Electrodes and Bulk Optodes. 1. General Characteristics, Chem. Rev. 97 (1997) 3083–3132.

[50] B. Philippe, Y. Setsuko, T. Koji, U. Kayoko, N. Seiichi, U. Yoshio, Studies on the phase boundaries and the significance of ionic sites of liquid membrane ion- selective electrodes, Electroanalysis. 7 (1995) 811–816. doi:10.1002/elan.1140070905.

[51] Y. Umezawa, CRC handbook of ion-selective electrodes: Selectivity coefficients., 1990.

[52] E. Bakker, E. Pretsch, P. Bühlmann, Selectivity of Potentiometric Ion Sensors, Anal. Chem. 72 (2000) 1127–1133.

[53] F. Deyhimi, A method for the determination of potentiometric selectivity coefficients of ion selective electrodes in the presence of several interfering ions, Talanta. 50 (1999) 1129–1134. doi:https://doi.org/10.1016/S0039-9140(99)00194-0.

[54] K.N. Mikhelson, Lecture Notes in Chemistry 81. Ion-Selective Electrodes, 2013. doi:10.1007/978-3-319-10410-2.

[55] C.J. Coetzee, H. Freiser, Anion-responsive electrodes based on ion association extraction systems, Anal. Chem. 40 (1968) 2071. doi:10.1021/ac60269a036.

[56] H. Freiser, Ion-selective electrodes in analytical chemistry, Springer Science & Business Media, 2012.

[57] V. V. Egorov, P. L. Lyaskovski, I. V. Il'inchik, S. V. Vera, V. A. Nazarov, Estimation of Ion-Pairing Constants in Plasticized Poly(vinyl chloride) Membranes Using Segmented Sandwich Membranes Technique, Electroanalysis. 21 (n.d.) 2061–2070. doi:10.1002/elan.200904639.

[58] M.A. Peshkova, A.I. Korobeynikov, K.N. Mikhelson, Estimation of ion-site association

constants in ion-selective electrode membranes by modified segmented sandwich membrane method, Electrochim. Acta. 53 (2008) 5819–5826. doi:https://doi.org/10.1016/j.electacta.2008.03.030.

[59] M. Konstantin N., Numeric Simulation of Ion- Site Association Effects in Ion- Selective Electrode Response, Electroanalysis. 15 (2003) 1236–1243. doi:10.1002/elan.200302804.

[60] T. Lindfors, A. Ivaska, Calcium-selective electrode based on polyaniline functionalized with bis[4-(1,1,3,3-tetramethylbutyl)phenyl]phosphate, Anal. Chim. Acta. 437 (2001) 171–182. doi:https://doi.org/10.1016/S0003-2670(01)00996-5.

[61] K. Vitras, J. Kalous, Determination of some ampholytic and cationic surfactants by potentiometric titrations based on ion-pair formation, Anal. Chim. Acta Elsevier Sci. Publ. B.V. 177 (1985) 219–223.

[62] R. Matesic-Puac, M. Sak-Bosnar, M. Bilic, B.S. Grabaric, Potentiometric determination of anionic surfactants using a new ion-pair-based all-solid-state surfactant sensitive electrode, Sensors Actuators, B Chem. 106 (2005) 221–228. doi:10.1016/j.snb.2004.08.001.

[63] H.M. Abu Shawish, S.M. Saadeh, A.R. Al-Dalou, N.A. Ghalwa, A.A.A. Assi, Optimization of tramadol-PVC membrane electrodes using miscellaneous plasticizers and ion-pair complexes, Mater. Sci. Eng. C. 31 (2011) 300–306. doi:10.1016/j.msec.2010.09.014.

[64] P.G. Boswell, P. Bühlmann, Fluorous bulk membranes for potentiometric sensors with wide selectivity ranges: Observation of exceptionally strong ion pair formation, J. Am. Chem. Soc. 127 (2005) 8958–8959. doi:10.1021/ja052403a.

[65] M. Shamsipur, F. Jalali, S. Ershad, Preparation of a diclofenac potentiometric sensor and its application to pharmaceutical analysis and to drug recovery from biological fluids, J. Pharm. Biomed. Anal. 37 (2005) 943–947. doi:10.1016/j.jpba.2004.07.051.

[66] J.A. Ortuño, V. Ródenas, M.S. Garcia, M.I. Albero, C. Sánchez-Pedreño, A new tiapride selective electrode and its clinical application, Sensors. 7 (2007) 400–409. doi:10.3390/s7030400.

[67] A.-I. Stoica, C. Vinas, F. Teixidor, Application of the cobaltabisdicarbollide anion to the development of ion selective PVC membrane electrodes for tuberculosis drug analysis, Chem. Commun. (2008) 6492–6494. doi:10.1039/B813285B.

[68] Y. Marcus, A. K.SenGupta, J.A. Marinsky, Ion Exchange and Solvent Extraction: A Series of Advances, Volume 17, 2005. doi:10.1016/S0304-386X(02)00007-5.

[69] J. Rais, P. Selucký, M. Kyrš, Extraction of alkali metals into nitrobenzene in the presence of univalent polyhedral borate anions, J. Inorg. Nucl. Chem. 38 (1976) 1376–1378. doi:https://doi.org/10.1016/0022-1902(76)80156-X.

[70] A.-I. Stoica, C. Vinas, F. Teixidor, Cobaltabisdicarbollide anion receptor for enantiomer-selective membrane electrodes, Chem. Commun. (2009) 4988–4990. doi:10.1039/B910645F.

[71] A. Saini, J. Gallardo-Gonzalez, A. Baraket, I. Fuentes, C. Viñas, N. Zine, J. Bausells, F. Teixidor, A. Errachid, A novel potentiometric microsensor for real-time detection of Irgarol using the ion-pair complex [Irgarol-H]+[Co(C2B9H11)2]−, Sensors Actuators, B Chem. 268 (2018) 164–169. doi:10.1016/j.snb.2018.04.070.

[72] C.A. Reed, Carboranes: A New Class of Weakly Coordinating Anions for Strong Electrophiles, Oxidants, and Superacids, Acc. Chem. Res. 31 (1998) 133–139. doi:10.1021/ar970230r.

[73] S.H. Strauss, The search for larger and more weakly coordinating anions, Chem. Rev. 93 (1993) 927–942. doi:10.1021/cr00019a005.

[74] I.B. Sivaev, V.I. Bregadze, Chemistry of cobalt bis (dicarbollides). A review, Collect. Czechoslov. Chem. Commun. 64 (1999) 783–805. doi:10.1135/cccc19990783.

[75] J. Plesek, K. Base, F. Mares, F. Hanousek, S. Hermanek, Potential Uses Of Metallocarborane Sadnwich Anions For Analysis, Characterization And Isolation Of Various Cations and Organic Bases, Collect. Czech. Chem. Commun. 49 (1983) 2776–2789.

[76] C. Masalles, F. Teixidor, S. Borrós, C. Viñas, Cobaltabisdicarbollide anion [Co(C2B9H11)2]-as doping agent on intelligent membranes for ion capture, J. Organomet. Chem. 657 (2002) 239–246. doi:10.1016/S0022-328X(02)01432-8.

[77] O.A. Biloivan, S.V. Dzyadevych, A.V. El'skaya, N. Jaffrezic-Renault, N. Zine, J. Bausells, J. Samitier, A. Errachid, Development of bi-enzyme microbiosensor based on solid-contact ion-selective microelectrodes for protein detection, Sensors Actuators B Chem. 123 (2007) 1096–1100.

[78] O.A. Biloivan, S.V. Verevka, S.V. Dzyadevych, N. Zine, J. Bausells, J. Samitier, A. Errachid, Protein detection based on microelectrodes with the PPy[3,3-Co(1,2-C2B9H11)]2 solid contact

and immobilized proteinases: Preliminary investigations, Mater. Sci. Eng. C. 26 (2006) 574–577.

[79] I.A. Marques de Oliveira, M. Pla-Roca, L. Escriche, J. Casabó, N. Zine, J. Bausells, F. Teixidor, E. Crespo, A. Errachid, J. Samitier, Novel all-solid-state copper(II) microelectrode based on a dithiomacrocycle as a neutral carrier, Electrochim. Acta. 51 (2006) 5070–5074.

[80] I.A. Marques de Oliveira, D. Risco, F. Vocanson, E. Crespo, F. Teixidor, N. Zine, J. Bausells, J. Samitier, A. Errachid, Sodium ion sensitive microelectrode based on a p-tert-butylcalix[4]arene ethyl ester, Sensors Actuators B Chem. 130 (2008) 295–299.

[81] N. Zine, J. Bausells, F. Vocanson, R. Lamartine, Z. Asfari, F. Teixidor, E. Crespo, I.A.M. de Oliveira, J. Samitier, A. Errachid, Potassium-ion selective solid contact microelectrode based on a novel 1,3-(di-4-oxabutanol)-calix[4]arene-crown-5 neutral carrier, Electrochim. Acta. 51 (2006) 5075–5079.

[82] N. Zine, J. Bausells, A. Ivorra, J. Aguiló, M. Zabala, F. Teixidor, C. Masalles, C. Viñas, A. Errachid, Hydrogen-selective microelectrodes based on silicon needles, Sensors Actuators B Chem. 91 (2003) 76–82.

[83] J. Gallardo-González, A. Baraket, S. Boudjaoui, A. Streklas, F. Teixidor, N. Zine, J. Bausells, A. Errachid, A Highly Sensitive Potentiometric Amphetamine Microsensor Based on All-Solid-State Membrane Using a New Ion-Par Complex , Proc. Eurosensors Conf. Paris 2017. 1 (2017) 2–5. doi:10.3390/proceedings1040481.

[84] E. Malinowska, L. Gawart, P. Parzuchowski, G. Rokicki, Z. Brzózka, Novel approach of immobilization of calix[4]arene type ionophore in ‘self-plasticized’ polymeric membrane, Anal. Chim. Acta. 421 (2000) 93–101. doi:https://doi.org/10.1016/S0003-2670(00)00999-5.

[85] G.J. Moody, B. Saad, J.D.R. Thomas, Glass transition temperatures of poly(vinyl chloride) and polyacrylate materials and calcium ion-selective electrode properties, Analyst. 112 (1987) 1143–1147. doi:10.1039/AN9871201143.

[86] M. De los A. Arada Pérez, L. Marín Pérez, J. Calvo Quintana, M. Yazdani-Pedram, Influence of different plasticizers on the response of chemical sensors based on polymeric membranes for nitrate ion determination, Sensors Actuators B Chem. 89 (2003) 262–268.

[87] R. Eugster, T. Rosatzin, B. Rusterholz, B. Aebersold, U. Pedrazza, D. Rüegg, A. Schmid, U.E. Spichiger, W. Simon, Plasticizers for liquid polymeric membranes of ion-selective chemical sensors, Anal. Chim. Acta. 289 (1994) 1–13. doi:10.1016/0003-2670(94)80001-4.

[88] M.W. E., S. W., Abschätzung der Alkali- und Erdalkali-Ionenselektivität von elektrisch neutralen träger-antibiotica (<carrier- antibiotica>) und modellverbindungen, Helv. Chim. Acta. 54 (2018) 2683–2704. doi:10.1002/hlca.19710540832.

[89] M. C., B. S., V. C., T. F., Are Low-Coordinating Anions of Interest as Doping Agents in Organic Conducting Polymers?, Adv. Mater. 12 (2000) 1199–1202. doi:10.1002/1521-4095(200008)12:16<1199::AID-ADMA1199>3.0.CO;2-W.

[90] N. Zine, J. Bausells, F. Teixidor, C. Viñas, C. Masalles, J. Samitier, A. Errachid, All-solid-state hydrogen sensing microelectrodes based on novel PPy[3,3′-Co(1,2-C2B9H11)2] as a solid internal contact, Mater. Sci. Eng. C. 26 (2006) 399–404. doi:https://doi.org/10.1016/j.msec.2005.10.073.

[91] H. Wang, D.W. Juma, H. Wang, F. Li, Impacts of population growth and economic development on water quality of a lake : Case study of Lake Victoria Kenya water., Environ. Sci. Pollut. Res. 21 (2014) 5737–5746. doi:10.1007/s11356-014-2524-5.

[92] L. Rizzo, C. Manaia, C. Merlin, T. Schwartz, C. Dagot, M.C. Ploy, I. Michael, D. Fatta-kassinos, Urban wastewater treatment plants as hotspots for antibiotic resistant bacteria and genes spread into the environment : A review, Sci. Total Environ. 447 (2013) 345–360. doi:10.1016/j.scitotenv.2013.01.032.

[93] B. Petrie, R. Barden, B. Kasprzyk-hordern, A review on emerging contaminants in wastewaters and the environment : Current knowledge , understudied areas and recommendations for future monitoring, Water Res. 72 (2015) 3–27. doi:10.1016/j.watres.2014.08.053.

[94] L. He, G. Ying, Y. Liu, H. Su, J. Chen, S. Liu, J. Zhao, Discharge of swine wastes risks water quality and food safety : Antibiotics and antibiotic resistance genes from swine sources to the receiving environments, Environ. Int. 92–93 (2016) 210–219. doi:10.1016/j.envint.2016.03.023.

[95] B.P. Bougnom, L.J. V Piddock, Wastewater for Urban Agriculture: A Significant Factor in Dissemination of Antibiotic Resistance, Environ. Sci. Technol. 51 (2017) 5863–5864.

[96] A.K. Awasthi, X. Zeng, J. Li, Environmental pollution of electronic waste recycling in India : A critical review, Environ. Pollut. 211 (2016) 259–270. doi:10.1016/j.envpol.2015.11.027.

[97] S. Castiglioni, K. V Thomas, B. Kasprzyk-hordern, L. Vandam, P. Grif, Testing wastewater to detect illicit drugs :, Sci. Total Environ. 487 (2014) 613–620. doi:10.1016/j.scitotenv.2013.10.034.

[98] O. Korostynska, A. Mason, A.I. Al-shamma, Smart Sensors for Real-Time Water Quality Monitoring, 4 (2013) 1–24. doi:10.1007/978-3-642-37006-9.

[99] A.J. Wade, E.J. Palmer-Felgate, S.J. Halliday, R.A. Skeffington, M. Loewenthal, H.P. Jarvie, M.J. Bowes, G.M. Greenway, S.J. Haswell, I.M. Bell, E. Joly, A. Fallatah, C. Neal, R.J. Williams, E. Gozzard, J.R. Newman, From existing in situ , high-resolution measurement technologies to lab-on-a-chip - the future of water quality monitoring?, Hydrol. Earth Syst. Sci. Discuss. 9 (2012) 6457–6506. doi:10.5194/hessd-9-6457-2012.

[100] Q. Zhang, M. Zhang, L. Djeghlaf, J. Bataille, J. Gamby, A. Pallandre, Logic digital fluidic in miniaturized functional devices : Perspective to the next generation of microfluidic lab-on-chips, Electrophoresis. 38 (2017) 953–976. doi:10.1002/elps.201600429.

[101] D. Gabriel, M. Baeza, R. Pol, C. Francisco, Trends in Analytical Chemistry Micro fluidic lab-on-a-chip platforms for environmental monitoring, Trends Anal. Chem. 95 (2017) 62–68. doi:10.1016/j.trac.2017.08.001.

[102] E.M. Carstea, J. Bridgeman, A. Baker, D.M. Reynolds, Fluorescence spectroscopy for wastewater monitoring : A review, Water Res. 95 (2016) 205–219. doi:10.1016/j.watres.2016.03.021.

[103] A. Jang, Z. Zou, K.K. Lee, C.H. Ahn, P.L. Bishop, State-of-the-art lab chip sensors for environmental water monitoring, Meas. Sci. Technol. 22 (2011) (18pp). doi:10.1088/0957-0233/22/3/032001.

[104] O. Schwartz, M. Bercovici, Microfluidic assay for continuous bacteria detection using antimicrobial peptides and isotachophoresis, Anal. Chem. 86 (2014) 10106–10113. doi:10.1021/ac5017776.

[105] Z. Wang, T. Han, T.J. Jeon, S. Park, S.M. Kim, Rapid detection and quantification of bacteria using an integrated micro/nanofluidic device, Sensors Actuators, B Chem. 178 (2013) 683–688. doi:10.1016/j.snb.2013.01.017.

[106] J. Jiang, X. Wang, R. Chao, Y. Ren, C. Hu, Z. Xu, G.L. Liu, Smartphone based portable bacteria pre-concentrating microfluidic sensor and impedance sensing system, Sensors Actuators, B Chem. 193 (2014) 653–659. doi:10.1016/j.snb.2013.11.103.

[107] S. Nurani, H. Abdul, W. Lau, Detection of contaminants in water supply : A review on state-of-the-art monitoring technologies and their applications, Sensors Actuators B. Chem. 255 (2017)

2657–2689. doi:10.1016/j.snb.2017.09.078.

[108] J.P. Lafleur, S. Senkbeil, T.G. Jensen, J.P. Kutter, Gold nanoparticle-based optical microfluidic sensors for analysis of environmental pollutants, Lab Chip. 12 (2012) 4651. doi:10.1039/c2lc40543a.

[109] J.-N. Wang, A Microfluidic Long-Period Fiber Grating Sensor Platform for Chloride Ion Concentration Measurement, Sensors. 11 (2011) 8550–8568. doi:10.3390/s110908550.

[110] A. Manz, M. Arundell, P.D. Whalley, A. Manz, Indirect fluorescence detection of phenolic compounds by capillary electrophoresis on a glass device by capillary electrophoresis on a glass device, (2017). doi:10.1007/s002160000460.

[111] C. Slater, J. Cleary, K. Lau, D. Snakenborg, B. Corcoran, J.P. Kutter, D. Diamond, Validation of a fully autonomous phosphate analyser based on a microfluidic lab-on-a-chip, (2010) 1811–1818. doi:10.2166/wst.2010.069.

[112] D. Geon, D. Jung, S. Ho, Lab-on-a-chip based total-phosphorus analysis device utilizing a photocatalytic reaction, Solid State Electron. 140 (2018) 100–108. doi:10.1016/j.sse.2017.10.026.

[113] A. Daridon, M. Sequeira, G. Pennarun-Thomas, H. Dirac, J.P. Krog, P. Gravesen, J. Lichtenberg, D. Diamond, E. Verpoorte, N.F. De Rooij, Chemical sensing using an integrated microfluidic system based on the Berthelot reaction, Sensors Actuators, B Chem. 76 (2001) 235–243. doi:10.1016/S0925-4005(01)00573-1.

[114] A.D. Beaton, C.L. Cardwell, R.S. Thomas, V.J. Sieben, E.M. Waugh, P.J. Statham, M.C. Mowlem, H. Morgan, Lab-on-Chip Measurement of Nitrate and Nitrite for In Situ Analysis of Natural Waters, Environ. Sci. Technol. 46 (2012) 9548–9556. doi:10.1021/es300419u.

[115] Y. Lin, D. Gritsenko, S. Feng, Y.C. Teh, X. Lu, J. Xu, Detection of heavy metal by paper-based microfluidics, Biosens. Bioelectron. 83 (2016) 256–266. doi:10.1016/j.bios.2016.04.061.

[116] B.M. Jayawardane, I.D. McKelvie, S.D. Kolev, Development of a gas-diffusion microfluidic paper-based analytical device (μPAD) for the determination of ammonia in wastewater samples, Anal. Chem. 87 (2015) 4621–4626. doi:10.1021/acs.analchem.5b00125.

[117] P.B. Lillehoj, M.-C. Huang, N. Truong, C.-M. Ho, Rapid electrochemical detection on a mobile phone, Lab Chip. 13 (2013) 2950. doi:10.1039/c3lc50306b.

[118] J. Bhardwaj, H. Ashraf, A. McQuarrie, Dry Silicon Etching for MEMS, Int. Symp. Microstruct. Microfabr. Syst. (1997) 118–130. doi:10.1017/CBO9781107415324.004.

[119] H. Linde, Wet Silicon Etching with Aqueous Amine Gallates, J. Electrochem. Soc. 139 (1992) 1170. doi:10.1149/1.2069360.

[120] T. Corman, P. Enoksson, G. Stemme, Deep wet etching of borosilicate glass using an anodically bonded silicon substrate as mask, J. Micromechanics Microengineering. 8 (1998) 84–87. doi:10.1088/0960-1317/8/2/010.

[121] J.H. Park, N.E. Lee, J. Lee, J.S. Park, H.D. Park, Deep dry etching of borosilicate glass using SF6and SF6/Ar inductively coupled plasmas, Microelectron. Eng. 82 (2005) 119–128. doi:10.1016/j.mee.2005.07.006.

[122] S. Tachi, K. Tsujimoto, S. Okudaira, Low-temperature reactive ion etching and microwave plasma etching of silicon, Appl. Phys. Lett. 52 (1988) 616–618. doi:10.1063/1.99382.

[123] T.E.F.M. Standaert, M. Schaepkens, N.R. Rueger, P.G.M. Sebel, G.S. Oehrlein, J.M. Cook, High density fluorocarbon etching of silicon in an inductively coupled plasma: Mechanism of etching through a thick steady state fluorocarbon layer, J. Vac. Sci. Technol. A Vacuum, Surfaces, Film. 16 (1998) 239–249. doi:10.1116/1.580978.

[124] E.H. Klaassen, K. Petersen, J.M. Noworolski, J. Logan, N.I. Maluf, J. Brown, C. Storment, W. McCulley, G.T.A. Kovacs, Silicon fusion bonding and deep reactive ion etching: a new technology for microstructures, Sensors Actuators A Phys. 52 (1996) 132–139. doi:10.1016/0924-4247(96)80138-5.

[125] E. Prats-alfonso, X. Sisquella, N. Zine, G. Gabriel, A. Guimerà, F.J. Campo, R. Villa, A.H. Eisenberg, M. Mrksich, Cancer Prognostics by Direct Detection of p53-Antibodies on Gold Surfaces by Impedance Measurements, Small. 8 (2012) 2106–2115. doi:10.1002/smll.201102724.

[126] C.A. Mills, J.G. Fernandez, E. Martinez, M. Funes, E. Engel, A. Errachid, J. Planell, J. Samitier, Directional Alignment of MG63 Cells on Polymer Surfaces Containing Point Microstructures, Small. 3 (2007) 871–879. doi:10.1002/smll.200600683.

[127] D. Caballero, J. Samitier, J. Bausells, A. Errachid, Direct Patterning of Anti-Human Serum Albumin Antibodies on Aldehyde-Terminated Silicon Nitride Surfaces for HSA Protein Detection, Small. 5 (2009) 1531–1534. doi:10.1002/smll.200801735.

[128] G.M. Whitesides, E. Ostuni, X. Jiang, D.E. Ingber, Soft Lithography in Biology and Biochemistry., Annu. Rev. Biomed. Eng. 3 (2001) 335–73. doi:10.1146/annurev.bioeng.3.1.335.

[129] Y. Xia, G.M. Whitesides, Soft Lithography, Angew. Chemie Int. Ed. 37 (1998) 550–575. doi:10.1002/(SICI)1521-3773(19980316)37:5<550::AID-ANIE550>3.0.CO;2-G.

[130] T.C. Merkel, V.I. Bondar, K. Nagai, B.D. Freeman, I. Pinnau, Gas sorption, diffusion, and permeation in poly(dimethylsiloxane), J. Polym. Sci. Part B Polym. Phys. 38 (2000) 415–434. doi:10.1002/(SICI)1099-0488(20000201)38:3<415::AID-POLB8>3.0.CO;2-Z.

[131] K.C. Tang, E. Liao, W.L. Ong, J.D.S. Wong, A. Agarwal, R. Nagarajan, L. Yobas, Evaluation of bonding between oxygen plasma treated polydimethyl siloxane and passivated silicon, J. Phys. Conf. Ser. 34 (2006) 155–161. doi:10.1088/1742-6596/34/1/026.

[132] D.C. Duffy, J.C. McDonald, O.J.A. Schueller, G.M. Whitesides, Rapid prototyping of microfluidic systems in poly(dimethylsiloxane), Anal. Chem. 70 (1998) 4974–4984. doi:10.1021/ac980656z.

[133] A. Baraket, N. Zine, M. Lee, J. Bausells, N. Jaffrezic-renault, F. Bessueille, N. Yaakoubi, A. Errachid, Development of a flexible microfluidic system based on a simple and reproducible sealing process between polymers and poly (dimethylsiloxane), Microelectron. Eng. 111 (2013) 332–338. doi:10.1016/j.mee.2013.02.059.

[134] M. Lee, M.J. Lopez-Martinez, A. Baraket, N. Zine, J. Esteve, J.A. Plaza, N. Jaffrezic-Renault, A. Errachid, Polymer micromixers bonded to thermoplastic films combining soft-lithography with plasma and aptes treatment processes, J. Polym. Sci. Part A Polym. Chem. 51 (2013) 59–70. doi:10.1002/pola.26387.

[135] A. Baraket, M. Lee, N. Zine, N. Yaakoubi, J. Bausells, A. Errachid, A flexible electrochemical micro lab-on-chip : application to the detection of interleukin-10, Microchim. Acta. 183 (2016) 2155–2162. doi:10.1007/s00604-016-1847-y.

[136] D. Maji, S.K. Lahiri, S. Das, Study of hydrophilicity and stability of chemically modified PDMS surface using piranha and KOH solution, Surf. Interface Anal. 44 (2012) 62–69. doi:10.1002/sia.3770.

[137] S.H. Huang, P. Liu, A. Mokasdar, L. Hou, Additive manufacturing and its societal impact: A literature review, Int. J. Adv. Manuf. Technol. 67 (2013) 1191–1203. doi:10.1007/s00170-012-4558-5.

[138] J.U. Pucci, B.R. Christophe, J.A. Sisti, E.S. Connolly, Three-dimensional printing: technologies, applications, and limitations in neurosurgery, Biotechnol. Adv. 35 (2017) 521–529. doi:10.1016/j.biotechadv.2017.05.007.

[139] J.Y. Lee, J. An, C.K. Chua, Fundamentals and applications of 3D printing for novel materials, Appl. Mater. Today. 7 (2017) 120–133. doi:10.1016/j.apmt.2017.02.004.

[140] J.P. Kruth, Material Incress Manufacturing by Rapid Prototyping Techniques, CIRP Ann. 40 (1991) 603–614. doi:https://doi.org/10.1016/S0007-8506(07)61136-6.

[141] I. Catalin, I. Daniela, S. Alin, From CAD model to 3D print via "STL" file format, Fiability Durab. (2010) 73–80.

[142] N. Bhattacharjee, A. Urrios, S. Kang, A. Folch, The upcoming 3D-printing revolution in microfluidics, Lab Chip. 16 (2016) 1720–1742. doi:10.1039/C6LC00163G.

[143] K. V. Wong, A. Hernandez, A Review of Additive Manufacturing, ISRN Mech. Eng. 2012 (2012) 1–10. doi:10.5402/2012/208760.

[144] I. Gibson, D. Rosen, B. Stucker, Additive Manufacturing Technologies: 3D Printing, Rapid Prototyping, and Direct Digital Manufacturing, (2014) 193–198. https://books.google.com/books?id=OPGbBQAAQBAJ.

[145] T.D. Ngo, A. Kashani, G. Imbalzano, K.T.Q. Nguyen, D. Hui, Additive manufacturing (3D printing): A review of materials, methods, applications and challenges, Compos. Part B Eng. 143 (2018) 172–196. doi:10.1016/j.compositesb.2018.02.012.

[146] O.A. Mohamed, S.H. Masood, J.L. Bhowmik, Optimization of fused deposition modeling process parameters: a review of current research and future prospects, Adv. Manuf. 3 (2015) 42–53. doi:10.1007/s40436-014-0097-7.

[147] F.P.W. Melchels, J. Feijen, D.W. Grijpma, A review on stereolithography and its applications in biomedical engineering, Biomaterials. 31 (2010) 6121–6130. doi:10.1016/j.biomaterials.2010.04.050.

[148] C. Hull, StereoLithography: Plastic prototypes from CAD data without tooling, Mod. Cast. 78 (1988) 38.

[149] R. Singh, Process capability study of polyjet printing for plastic components, Evol. Ecol. 25 (2011) 1011–1015. doi:10.1007/s12206-011-0203-8.

[150] R. Vdovin, T. Tomilina, V. Smelov, M. Laktionova, Implementation of the Additive PolyJet Technology to the Development and Fabricating the Samples of the Acoustic Metamaterials, Procedia Eng. 176 (2017) 595–599. doi:10.1016/j.proeng.2017.02.302.

[151] W. Wang, J.G. Conley, H.W. Stoll, Rapid tooling for sand casting using laminated object manufacturing process, Rapid Prototyp. J. 5 (1999) 134–141. doi:10.1108/13552549910278964.

[152] J. Park, M.J. Tari, H.T. Hahn, Characterization of the laminated object manufacturing (LOM) process, Rapid Prototyp. J. 6 (2000) 36–50. doi:10.1108/13552540010309868.

[153] E.O. Olakanmi, R.F. Cochrane, K.W. Dalgarno, A review on selective laser sintering/melting (SLS/SLM) of aluminium alloy powders: Processing, microstructure, and properties, Prog. Mater. Sci. 74 (2015) 401–477. doi:10.1016/j.pmatsci.2015.03.002.

[154] J.M. Williams, A. Adewunmi, R.M. Schek, C.L. Flanagan, P.H. Krebsbach, S.E. Feinberg, S.J. Hollister, S. Das, Bone tissue engineering using polycaprolactone scaffolds fabricated via selective laser sintering, Biomaterials. 26 (2005) 4817–4827. doi:10.1016/j.biomaterials.2004.11.057.

[155] J. Kruth, P. Mercelis, J. Van Vaerenbergh, L. Froyen, M. Rombouts, Binding mechanisms in selective laser sintering and selective laser melting, Rapid Prototyp. J. 11 (2005) 26–36. doi:10.1108/13552540510573365.

[156] L.E. Murr, S.M. Gaytan, D.A. Ramirez, E. Martinez, J. Hernandez, K.N. Amato, P.W. Shindo, F.R. Medina, R.B. Wicker, Metal Fabrication by Additive Manufacturing Using Laser and Electron Beam Melting Technologies, J. Mater. Sci. Technol. 28 (2012) 1–14. doi:10.1016/S1005-0302(12)60016-4.

[157] X. Gong, T. Anderson, K. Chou, Review on powder - based electron beam additive manufacturing technology, Manuf. Rev. 1 (2014) 1–9. doi:10.1051/mfreview/2014001.

[158] B. Utela, D. Storti, R. Anderson, M. Ganter, A review of process development steps for new material systems in three dimensional printing (3DP), J. Manuf. Process. 10 (2008) 96–104. doi:10.1016/j.jmapro.2009.03.002.

Chapter 2:

All-Solid-State Amphetamine-Selective Microelectrodes

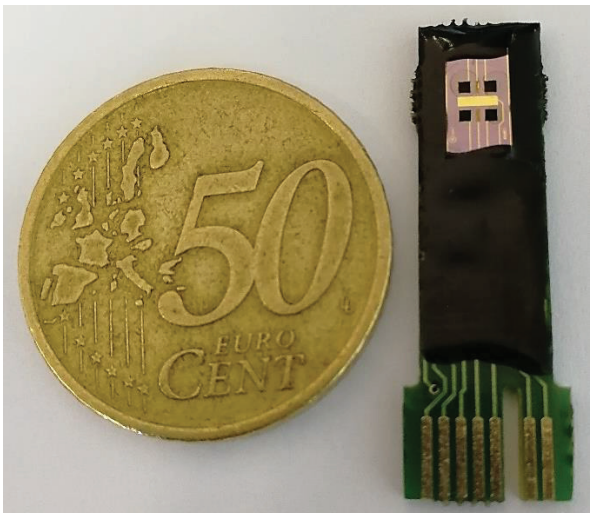

1. Objectives

The aim of this chapter was to report on the development of two generations of all-solid state ion-selective microelectrodes (ISEs) for amphetamine detection. The sensors must have fulfilled some requirements so that it can be used for sewage applications in a near future, namely: to be as much miniaturized as possible, to provide reliable data, to be easy-to-handle, inexpensive and to be able to perform real-time detection of amphetamine in-situ.

In a first stage, an amphetamine-selective microelectrode was fabricated using the commercially available amphetamine ionophore, dibenzo-18-crown-6 ether (DB18C6). It was used as the sensitive element of a polymeric membrane deposited onto polypyrrole-modified platinum microelectrodes. The composition of the polymeric membrane was optimized through the evaluation of different plasticizers and different ionophore concentrations and the sensors' performance was assessed by potentiometric measurements.

Next, a second generation of the previously developed amphetamine-selective microsensor was fabricated. In this case, a novel ion-pair complex, the [amphetamine-H]$^{+}$[3,3'-Co(1,2-*closo*-$C_2B_9H_{11})_2$]$^{-}$ was synthetized and incorporated to the polymeric membrane to replace the commercial amphetamine-ionophore DB18C6 as the sensitive part of the sensor. The aim of using this novel ion-pair complex was to improve the general sensor's performance. Moreover, the transducer used in the second version integrated the elements needed to perform potentiometric measurements using a miniaturized single device.

2. Introduction

Collecting information concerning illicit-drug use plays a vital role in not only helping law enforcement agencies in prevention and fight against criminal organizations, but also to estimate drug production and consumption. The analysis of wastewater has served for many epidemiology study both in the field of environmental, medical and drug analysis. However, as in the case of amphetamine and its derivatives most techniques used to analyze wastewater samples and detect the illicit compounds are based on conventional analytical methods that commonly are expensive, time-consuming, must be carried out in external laboratories and need for qualified personal [1]. Therefore, in the literature, amphetamine and ATS sensors have been scarcely reported. In this context, there is a need of innovation to develop miniaturized devices that are faster, low-cost, easy-to-handle and enable to perform real-time analysis on site.

As it was described in deep in Chapter 1, Section 4.1.2, the two first ISEs reported in the literature for amphetamine detection were published in 1989 [2]. Here, authors presented two macroelectrode made of liquid membrane of 1,2-dichloroethane that incorporated two crown ethers as amphetamine ionophore dibenzo-18-crown-6 ether (DB18C6) and dibenzo-24-crown-8 ether (DB24C8) respectively. Even if their work supposed a step further on the field of amphetamine sensors at that period, the ISEs reported are far to be used for real applications as they are big and used liquid-state membranes. To solve this problem, in a first stage, we have developed a miniaturized and all-solid-state version of the ISE reported by Saad S. M. Hassan et al., using the ionophore DB18C6. It was incorporated to a PVC-type polymeric membrane that was then deposited onto a polypyrrole-modified platinum microelectrode [3].

3. Sensitive Potentiometric Determination of Amphetamine with an All-Solid-State Ion-Selective Microelectrode.

3.1. Microelectrodes fabrication.

Platinum (Pt) microelectrodes were used in this study. The microelectronics fabrication process for the planar microelectrodes was performed at the Centro Nacional de Microelectrónica (CNM) in Barcelona, Spain. The fabrication of metal microelectrodes on silicon has only two photolithographic steps. The starting material is P-type <100> silicon 100 mm diameter wafers with a nominal thickness of 525 µm. The process starts with a thermal oxidation process to grow a thick oxide layer (0.8 µm). A first photoresist layer is then applied and patterned on the wafer surface. A double metal layer (50 nm Ti plus 150 nm Pt) is deposited and then patterned by the so-called lift-off technique. The next step consists on the deposition of two layers of SiO_2 and Si_3N_4, acting as a passivation layer. The second photolithographic process is performed to open the passivation on the active Pt microelectrodes and on

the soldering pads. After etching the passivation layer, the wafer was diced into individual transducers as shown in **Fig. 1 (I)**. The chips were mounted to a specially designed printed circuit board (PCB), then wire-bonded in the usual manner and finally insulated using an epoxy resin (see **Fig. 1 (II** and **III**)). Afterwards, Pt microelectrodes were cleaned by soft-scrubbing the surface with HF 1% (w/w) and finally put in contact with a source of UV-plasma in order to remove the organic traces. At this stage, the transducer was ready for electrochemical measurements (see **Fig. 1** (**V**)).

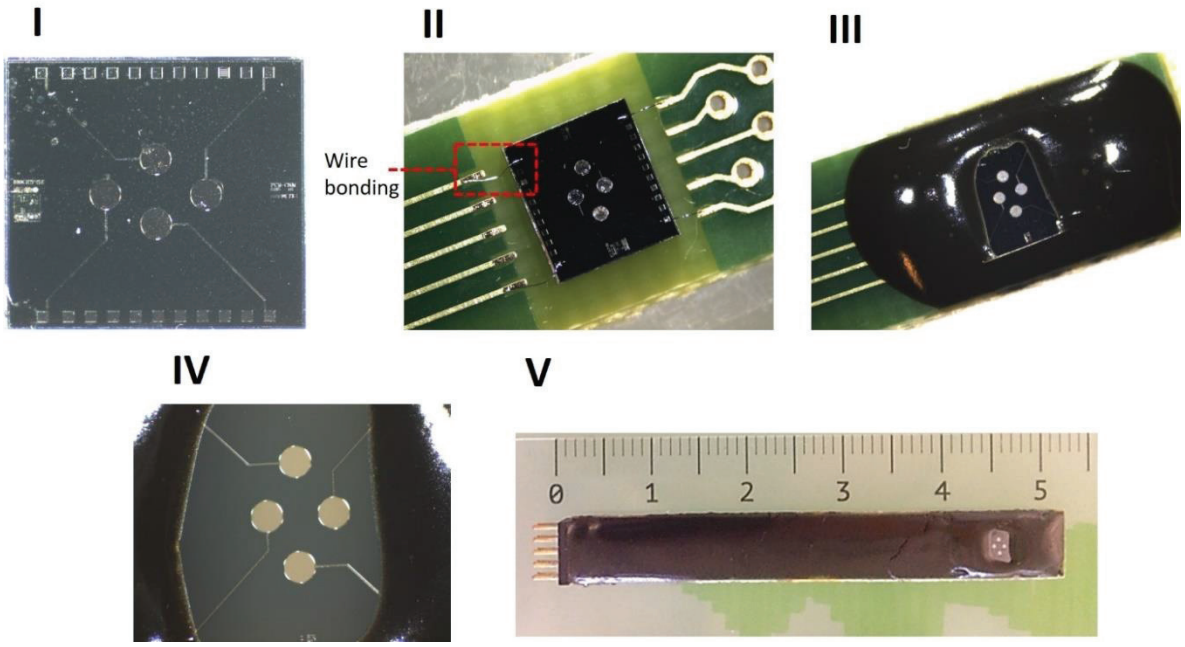

Figure 1. Microelectrodes preparation stages: **I,** micrograph of the transducer holding four bare Pt microelectrodes. **II** the transducer was wire-bonded to a PCB. **III**, the electrical connections have been isolated using an epoxy resin. **IV**, bare Pt microelectrodes after cleaning procedure. **V**, final device.

3.2. Microelectrodes characterisation.

In order to validate the microelectrode manufacturing process, Pt microelectrodes were characterized by cyclic voltammetry (CV). All the electrochemical measurements were carried out using a multichannel potentiostat (Biologic-EC-Lab VMP3) analyser and a three-electrode electrochemical cell based on a saturated-calomel reference electrode (SCE), platinum-wire auxiliary electrode and working microelectrode made of platinum substrate. Measurements were made in redox probe $K_3[Fe(CN)_6]/K_4[Fe(CN)_6]$ 5mM in phosphate buffer saline solution (PBS, pH 7.4). For the CV, the potential was scanned from -0.2 to 0.6 at a scan rate of 100 mV/s. Although **Fig. 2** only shows the results obtained for one Pt microelectrode, all four working microelectrodes were characterized simultaneously using a multichannel potentiostat. Note that the redox peaks observed at E = 0.12 and 0.27 V as well as the symmetry of the intensity current peaks at I = ± 1.5 µA are uniform and stable over the cycles. This

confirm the normal behavior of the redox reaction; $Fe^{2+} \leftrightarrow Fe^{3+} + e^-$, at the Pt interface what validates the good microelectrodes manufacturing process.

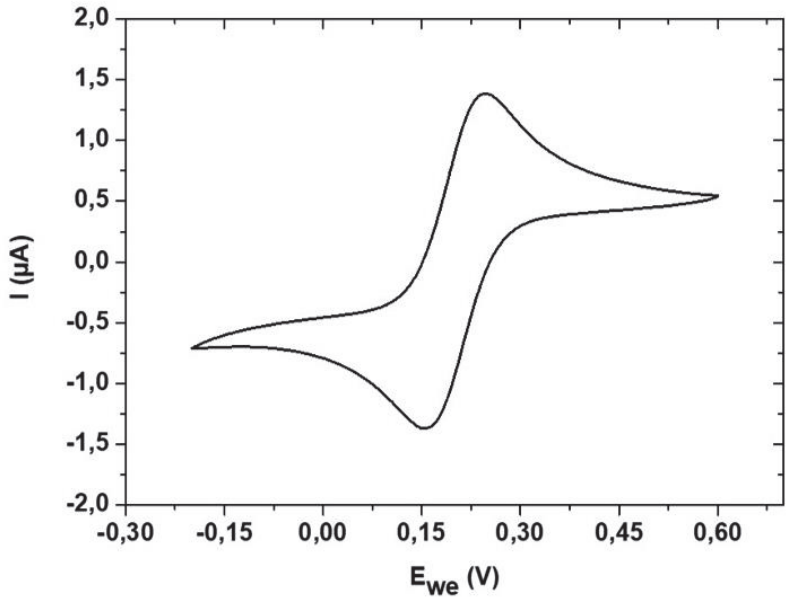

Figure 2. Cyclic voltammogram of bare platinum microelectrode in redox probe $K_3[Fe(CN)_6]/K_4[Fe(CN)_6]$ 5mM in phosphate buffer solution. Potential scanned from -0.2 to 0.6 V vs SCE at scan rate of 100 mV/s.

3.3. Deposition of PPyCOSANE as solid-contact layer.

$[3,3'\text{-}Co(1,2\text{-}C_2B_9H_{11})_2]^-$ anion was purchased from Katchem in the Cs salt form as Cesium Cosane ($Cs[3,3'\text{-}Co(1,2\text{-}C_2B_9H_{11})_2]$) and Pyrrole was obtained from Sigma & Aldrich. The solution for the electropolymerization was made of 0.035M $Cs[3,3'\text{-}Co(1,2\text{-}C_2B_9H_{11})_2]$ and 0.1 M pyrrole in acetonitrile with 1 wt.% in water. The electrochemical polymerization of pyrrole doped with $[3,3'\text{-}Co(1,2\text{-}C_2B_9H_{11})_2]^-$ anion was carried on by applying 10 potential sweep cycles between -0.6 V and 1.2 V, at a scan rate of 100 mV/s by means of CV (**Fig. 3).** We obtained a homogeneous layer of PpyCOSANE as shown in **Fig. 4 (II)**. After polymerization, the micro-electrodes were rinsed with water and dried under nitrogen before electrochemical measurements.

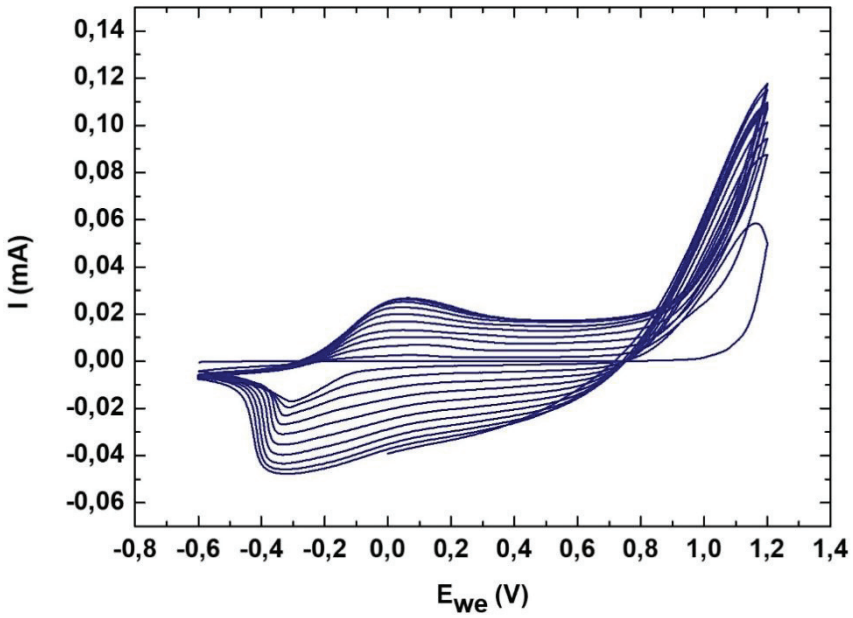

Figure 3. Cyclic voltammogram obtained for the electrochemical polymerization of the PpyCOSANE solid-contact layer.

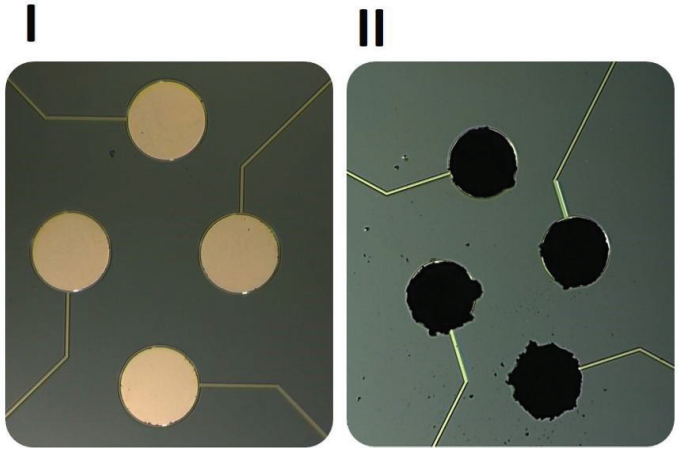

Figure 4. Micrographs of **I**, bare Pt microelectrodes and **II**, PpyCOSANE-modified microelectrodes.

As it was mentioned in Chapter 1 Section 8, conducting polymers appear very promising for the stabilization of the solid-contact ISEs potentials as they enhance the electrochemical characteristics of the transducing system [4]. Polypyrrole doped with cobalt bis(dicarbollide) anion was grown onto platinum substrate to improve the mechanical and electrical contact between the polymeric membrane and the microelectrode surface as it was described previously in several works [5–13]. When a monomer of pyrrole is oxidized after the application of an anodic potential (E ≈ -0.2 V), it creates a cation radical, $py^{+\bullet}$. This cation radical $py^{+\bullet}$, having a greater unpaired electron density in the α-position dimerizes, resulting in the formation of the dihydromer dication. Subsequently the dimer gets transformed into a

delocalized dimer cation radical $[py\text{-}py]^{+\bullet}$ as the anodic potential continues the scanning and so the propagation step occurs. The positive charges formed are localised in bipolaron states stabilized by resonance in the conjugated polymer chain [14]. Charge neutrality is achieved by the introduction [3,3'-$Co(1,2\text{-}C_2B_9H_{11})_2]^-$ anion and finally the PpyCOSANE layer is deposited on the microelectrode surface.

3.4. Characterisation of the PpyCOSANE modified electrodes.

The good functionalization of Pt microelectrodes with PpyCOSANE layer was evaluated by CV and EIS. The CV was carried out as it has been described in Section 3.2 for the characterization of bare microelectrodes. All measurements were made in redox probe $K_3[Fe(CN)_6]/K_4[Fe(CN)_6]$ 5mM in phosphate buffer saline solution (PBS, pH 7.4). For the CV, the potential was scanned from -0.2 to 0.6 at a scan rate of 100 mV/s. For the EIS measurments, the potential applied vs saturated calomel electrode was, E vs SCE = -0.2 V and frequencies scanned from 200 KHz to 100 mHz. Sinus amplitude = 75 mV.

Fig. 5 (I) and **(II)** show the cyclic voltammograms and Nyquist plot of platinum microelectrode respectively, before and after electrochemical functionalization with the PPyCOSANE solid and conductive layer. It can be seen from the cyclic voltammogram how redox peaks have increased in terms of intensity current. The Nyquist plot also have shown a decrease of the electrochemical impedance. Therefore, the high conductivity of the PpyCOSANE layer deposited onto the Pt microelectrode was confirmed.

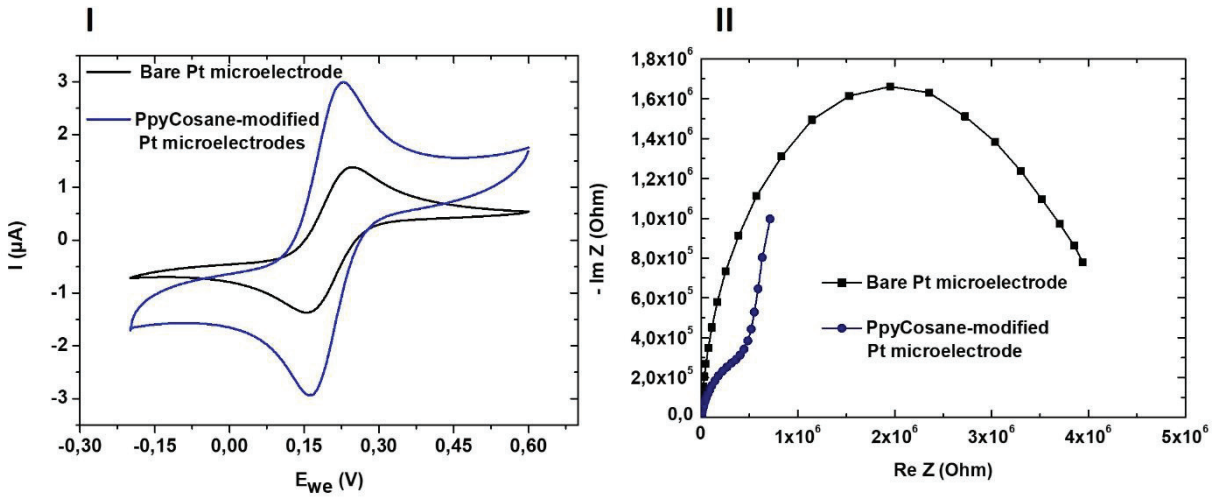

Figure 5. Cyclic voltammogram (**I**) and Nyquist diagram (**II**) of bare platinum microelectrode and PpyCOSANE-modified microelectrode in redox probe $K_3[Fe(CN)_6]/K_4[Fe(CN)_6]$ 5mM in phosphate buffer solution.

3.5. The sensitive membrane.

The sensitive membrane is presented as the key component to obtain an all-solid-state amphetamine-selective microelectrode that provides a good performance. In this context, the four constituents of any

sensitive membrane in classic ISEs are the plasticizer who plays the role of solvent, the ionophore who acts as selective ion carrier, the ion-exchanger that prevents the counter-ions to penetrate the membrane as well as favour the ionic transport across the interface membrane/solution and PVC which is commonly used as the polymeric matrix. The percentage of each component in the membrane has been extensively studied [4,15–19] and it is usually based on a matrix containing about 26-33% of PVC, 62-66% of plasticizer, 0-7% of ion-exchanger and 1-7% of ionophore. Five PVC-type membranes were prepared using four different plasticizers; di-butyl phthalate (DBP), di-octyl phthalate (DOP), di-octyl sebacate (DOS) and tri-octyl phosphate (TOP) and two concentrations of ionophore DB18C6. Four membrane were made of 1 wt.% of DB18C6, 30 wt.% of PVC, 63 wt.% of plasticizer and 6 wt.% of sodium tetraphenylborate (Na-TPB) as ion exchanger. The fifth one was made of 5 wt.% of DB18C6, 26 wt.% of PVC, 63 wt.% of DBP and 6 wt.% of Na-TPB to test the impact of higher amount of ionophore to the sensor's response. **Table 1** summarizes the composition of the five membranes prepared. The mixtures were dissolved in 1.5 ml of THF. Afterwards, the polymeric membrane was drop-cast onto the PPyCOSANE- modified Pt microelectrode. Then the device was left overnight for total solvent evaporation. **Fig. 6** shows micrographs of the three steps involved in the preparation of the amphetamine-selective microelectrode.

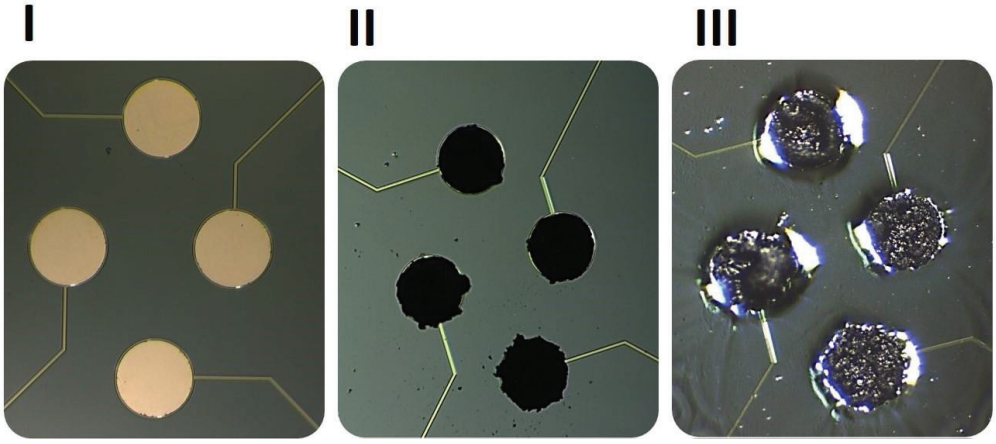

Figure 6. Micrographs of **I**, bare Pt microelectrodes, **II**, PPyCOSANE-modified microelectrodes and **III**, microelectrodes coated with one of the amphetamine-sensitive membrane.

Table 1. Membrane composition of different ASEs prepared expressed in wt.%.

ASE	Polymeric membrane (30%)	Plasticizer (63%)	Ion exchanger (6%)	Ionophore (1%)
1	Poly (vinyl chloride)	Di-octyl phthalate	Sodium tetraphenylborate	Dibenzo-18-crown 6-ether

2	Poly (vinyl chloride)	Di-octyl sebacate	Sodium tetraphenylborate	Dibenzo-18-crown 6-ether
3	Poly (vinyl chloride)	Tri-octyl phosphate	Sodium tetraphenylborate	Dibenzo-18-crown 6-ether
4	Poly (vinyl chloride)	Di-butyl phthalate	Sodium tetraphenylborate	Dibenzo-18-crown 6-ether
ASE	Polymeric membrane (26%)	Plasticizer (63%)	Ion exchanger (6%)	Ionophore (5%)
5	Poly (vinyl chloride)	Di-butyl phthalate	Sodium tetraphenylborate	Dibenzo-18-crown 6-ether

Fig. 7 shows the monographs of the ASE1, ASE2, ASE3 and ASE4 prepared with the four different plasticizers used.

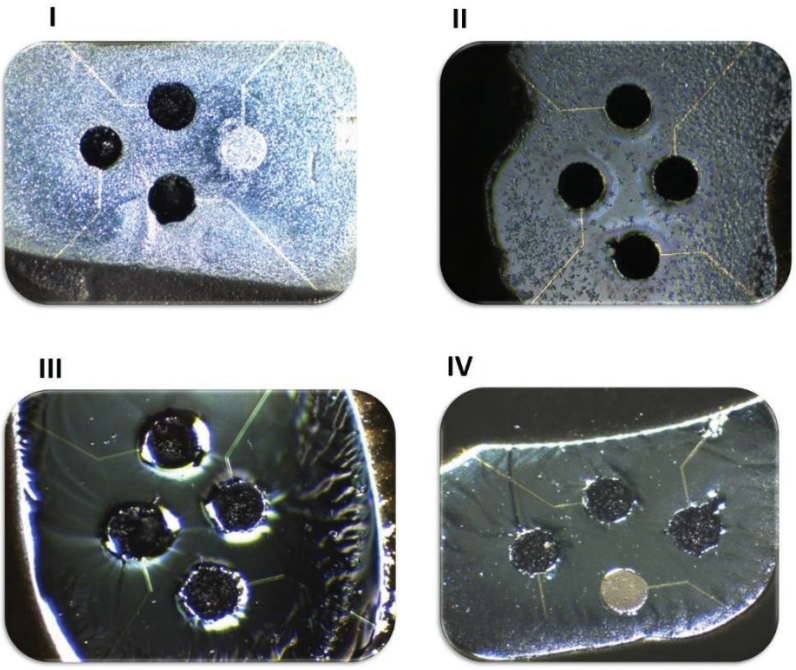

Figure 7. Monographs of four ASEs prepared with the four different plasticizers: **I**, di-octyl phthalate, **II**, di-octyl sebacate, **III**, tri-octyl phosphate and **IV**, di-butyl phthalate.

In **Fig. 7** it is demonstrated how different a polymeric membrane looks when only the plasticizer was changed. In the top-left monograph where DOP was used, a quite rigid and porous membrane was obtained. The top-right monograph shows one of the ASEs prepared with DOS. A crystallization phenomenon is observed. As a result, the membrane may behave as an inflexible glass-like membrane and so hindering the ionic flux. This membrane provided an instable potential when performing the calibration of the sensor. Membrane based on TOP is shown in the down-left monograph. We can

observe that it presents a very homogeneous but fluid shape. Finally, the fourth membrane prepared, was based on DBP and it is shown in the down-right monograph. There, one can observe that it is also highly homogeneous and keeps the finest ratio fluidity/rigidity of the four plasticizer tested.

The results obtained confirmed that plasticizers play an important role in the behaviour of polymeric membranes. It is well-known that for a plasticizer to be adequate it should gather certain properties such as having high lipophilicity, high molecular weight, being compatible with other membrane components and consequently to provide stability. Additionally, a high value of dielectric constant of the membrane is vital for a good potentiometric response and it is very influenced by the plasticizer nature as it was discussed in Chapter 1, Section 7 [20][11]. On the contrary, a lack of compatibility between the plasticizers and the other membrane constituents may drive to highly rigid membranes which hinder the ionic movement across the interface solution/membrane

3.6. Potentiometric measurements and sensor calibration.

All measurements were carried out at room temperature using a multichannel homemade-data-acquisition system set up in which the four microelectrodes included in one device were connected at the same time and were controlled by a personal computer. Measurements were made relative to a SCE reference electrode (Radiometer SAS) and under magnetic stirring (see **Fig. 8**). Calibration curves were obtained by adding successive aliquots of amphetamine sulphate solutions prepared with a concentration range from 10^{-5} to 10^{-1} M to 25 mL of deionised water. Thus, amphetamine concentration was increased in the medium from 10^{-7} to 10^{-3} M following the generalized standard addition method (GSAM) [21]. Variations in the electromotive force (emf) were recorded after signal stabilization and the value was plotted as a function of the logarithm of the activity of amphetamine following the Nernst approach (see equation 7 in Chapter 1, Section 5). Calibration curves were obtained for all the five ASEs prepared with different membrane composition of plasticizers and ionophore.

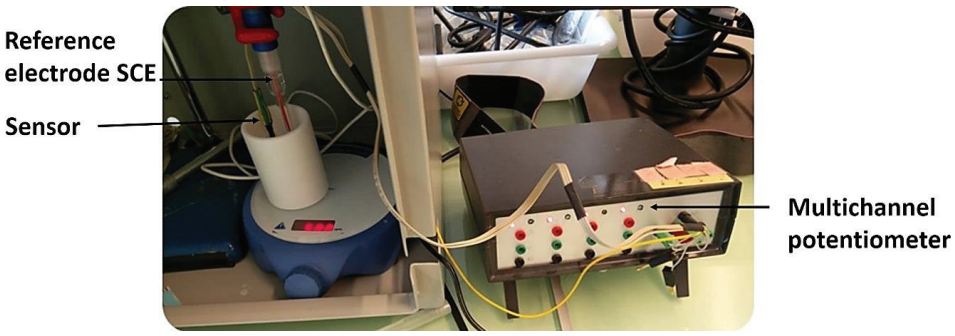

Figure 8. Electrochemical cell operating simultaneously with four ASEs. The device is controlled through a homemade multichannel potentiometer.

Fig. 9 shows the dynamic response obtained for the four ASEs prepared with different plasticizers. Potentiometric measurements were carried out following the GSAM for amphetamine detection. The first conclusion one can obtain when observing the plots is that the external electrical noise, which is different from one day to another, affects the absolute emf signal obtained. Moreover, although we envisioned to control the thickness and homogeneity of membranes by casting 10 µL of the mixture along all the ASEs prepared, it is actually far to be controlled as the membrane reticulates differently from one plasticizer to another and even in a same device from one microelectrode to another. Nevertheless, for a same device, the fact of having four microelectrodes measuring simultaneously enables to faster interpret the repeatability of the preparation. In our case, it is worth mentioning that in most cases three over four electrodes included in a device present exactly the same behaviour as we can see some overlapped plots. Membrane based on DOS (**Fig. 9 (II)**) did not reach a stable signal and so was discarded. DOP and DBP presenting similar chemical structures but with different alkyl chain length, eight and four carbons respectively, have been found to be the best choice in our case.

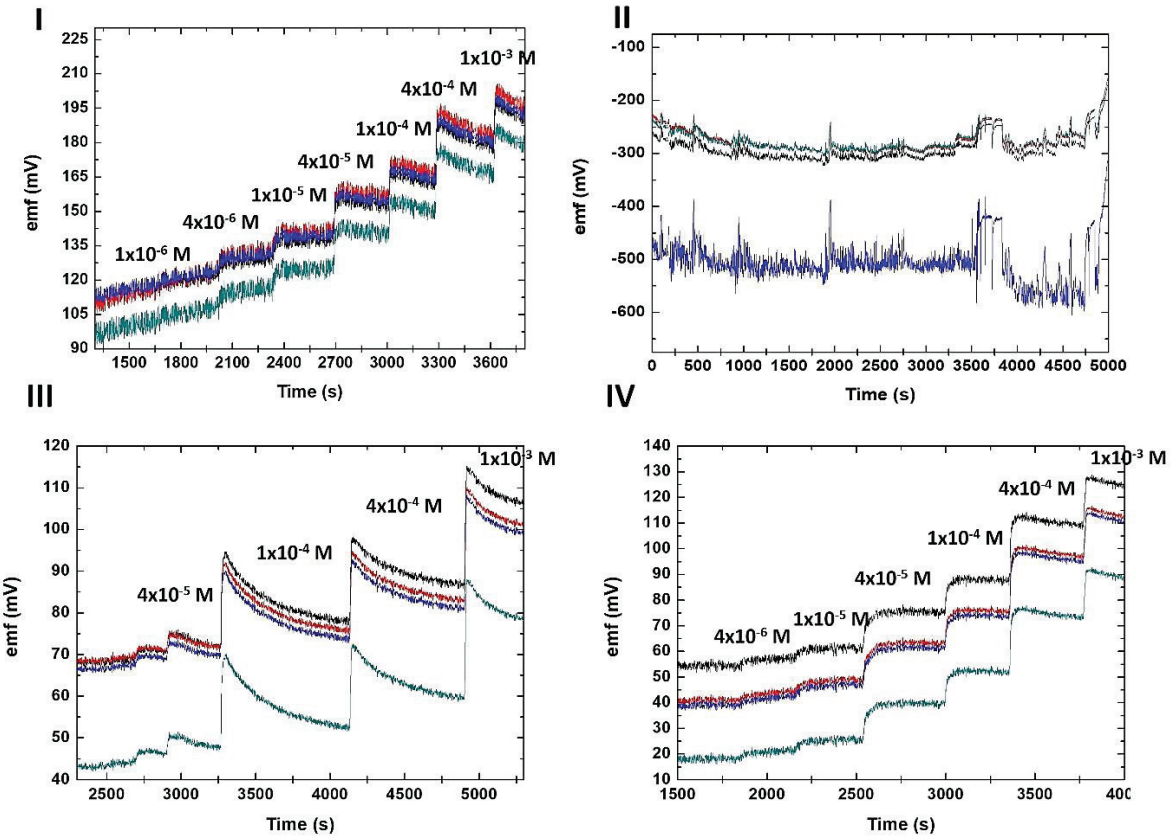

Figure 9. Dynamic response obtained through potentiometric measurements of ASEs prepared with different plasticizers **I** DOP, **II** DOS, **III** TOP and **IV** DBP for amphetamine detection following the GSAM in a concentration range of 10^{-7} M to 10^{-3} M of amphetamine sulphate.

One more amphetamine-selective electrode (ASE5) was prepared in which the amount of ionophore was increased up to 5 wt.% and using DBP as plasticizer since it provided the best response. The results obtained for the calibration of the five ASEs prepared are summarized in **Table 2** and their characteristic response curves are shown in **Fig. 10.**

Table 2. Comparison of the characteristic responses of different ASEs developed

Parameter	ASE1	ASE2	ASE3	ASE4	ASE5
Slope (mV/decade)	29	NA	30	32	53
Lower limit of detection (M)	$4 \cdot 10^{-6}$	NA	$4 \cdot 10^{-5}$	$8 \cdot 10^{-6}$	$4 \cdot 10^{-5}$
Linear range (M)	$4 \cdot 10^{-6}$ to $1 \cdot 10^{-3}$	NA	$4 \cdot 10^{-5}$ to $1 \cdot 10^{-3}$	$2 \cdot 10^{-5}$ to $1 \cdot 10^{-3}$	$3 \cdot 10^{-5}$ to $1 \cdot 10^{-3}$
Useful pH range	NA[1]	NA	NA	NA	1.5 to 8.5
Time of response	12-16 s	NA	12-16 s	12-16 s	12-16 s

[1]Not available.

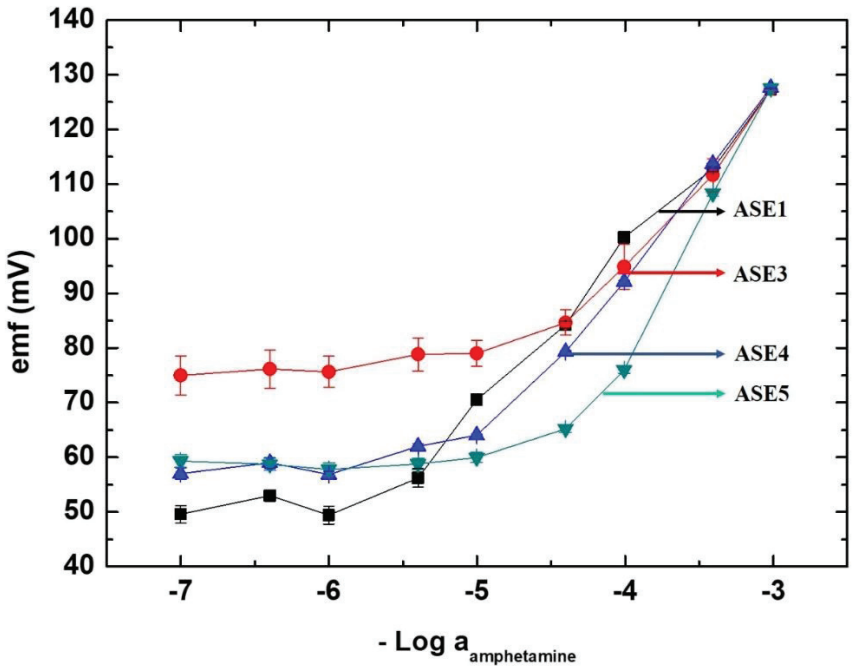

Figure 10. Potentiometric response of amphetamine-selective microelectrodes prepared with different membrane composition and plasticizers.

ASE1 and ASE4 provided similar sub-Nernstian response in which the slope varies from 29 to 32 mV/decade concentration of amphetamine. The limit of detection was calculated as the crossing point between the two linear segments forming the calibration curves. Very low limit of detection in the range of µM have been obtained. ASE1 and ASE4 having a composition of DOP + 1 wt.% DB18C6 and DBP + 1 wt.% DB18C6 respectively, show the lowest limit of detection around 10^{-6} M concentration of

amphetamine. ASE3 also presents sub-Nernstian response with a slope of 30 mV/decade and a limit of detection about $4 \cdot 10^{-5}$ M (about ten times higher comparing to sensors ASE1 and ASE4). ASE2 was discarded as previously mentioned.

As it can be seen from the results mentioned above, ASE4 based on di-butyl phthalate as plasticizer (and 1 wt.% of ionophore) provided the more stable response and lowest limit of detection regarding all four plasticizer tested. However, a slope of 32 mV/decade is far from the theoretical Nernstian value of 59 mV/decade expected for a monovalent cation such as amphetamine in the protonated form. Thus, an additional membrane for ASE5 was prepared based on DBP as plasticizer in which the amount of ionophore was increased up to 5 wt.% (di-butyl phthalate + 5 wt.% dibenzo-18-crown 6-ether). In this case, best response was found. ASE5 provided a near-Nernstian slope of 53 mV/decade of concentration much closer to the theoretical value of 59 mV/decade. The limit of detection for this ASE5 was found to be $4 \cdot 10^{-5}$ M.

Another parameter very sought when developing ISEs is the time of response. Commonly, the time needed for the electrode to achieve a 95% of full response (t_{95}) is the parameter stablished to evaluate an ISEs' time of response. As shown in **Fig. 11**, the time of response observed in ASE5 in the linear range of its potentiometric response, was 15 s approx. what is much faster than the response time observed in conventional liquid-membrane-based amphetamine sensors (see **Table 3**).

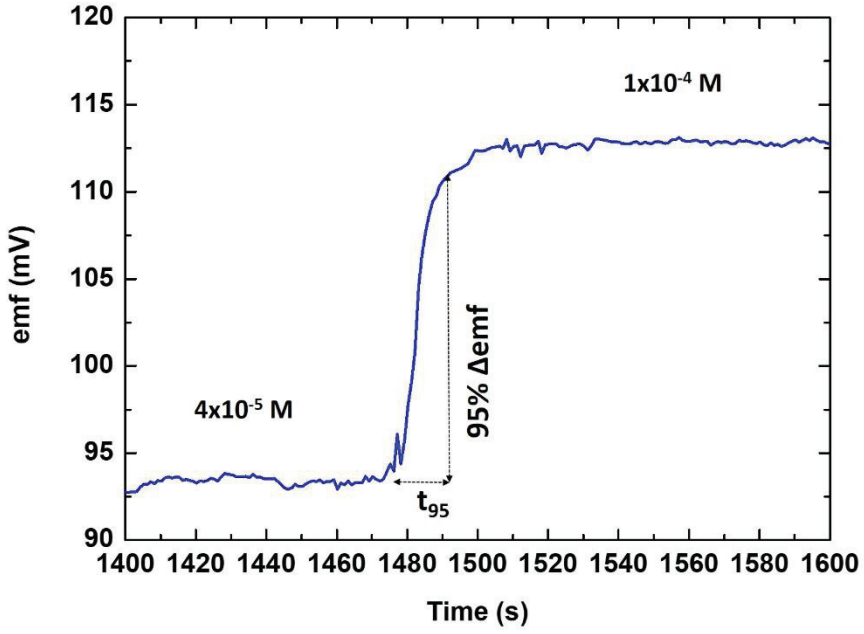

Figure 11. Time of response, t_{95}, obtained in the linear range during the calibration of ASE5.

The time of response in ISEs is governed by the diffusion of the ionic species across the polymeric membrane who is directly dependant to its thickness. Nevertheless, the membrane constituents are also

extremely important as they promote or hinder the ionic mobility inside the membrane itself that is why it is extremely important to optimized the membrane composition.

In **Table 3** results obtained for ASE5 are compared to the ionophore-based amphetamine sensors found in literature. It can be observed how lower limit of detection is achieved compared to the α-cyclodextrins-based sensor. A similar response is observed when the ionophore dibenzo-18-crown 6-ether is used in a 1,2-dichloroethane liquid-membrane sensor. However, much faster response is marked in the case of ASE5.

Table 3. Comparison of ASE5 with ionophore-based amphetamine sensors reported in the literature until then.

Parameter	ASE5	α-Cyclodextrins-based amphetamine sensor [22]	Dibenzo-18-crown 6-ether amphetamine sensor in liquid membranes [2]
Slope (mV/decade)	53	50	58
Lower limit of detection (M)	$4.0 \cdot 10^{-5}$	$2.5 \cdot 10^{-4}$	$8.0 \cdot 10^{-6}$
Lower limit of linear range (M)	$4.0 \cdot 10^{-5}$	NA[1]	$1.0 \cdot 10^{-5}$
Useful pH range	1.5 to 8.5	NA	3.0 to 7.0
Time of full response (s)	12-16	NA	30-50

[1]Not available.

3.7. Cross-selectivity study.

ASE5 was used to perform the selectivity study as it showed the best performance among the five ASEs prepared. For this purpose, several amino compounds as epinephrine, phenylalanine, caffeine and N-formyl amphetamine (**Fig. 12**) related structurally to amphetamine and three common monovalent cations, K^+, Na^+ and NH_4^+ were chosen for the cross-selectivity study. Experimentally, the setup used for the cross-selectivity study was similar to that carried out for the sensor's calibration. However, in this case a fixed background of any interference in deionized water was used as initial solution. The concentration of the interference was fixed at 1 mM as it is slightly lower than the highest concentration one can obtain for amphetamine according to its solubility in water, 1.7 mg/mL. Therefore, we can assess the sensor's performance in high concentration of interferences. Consequently, coefficients of selectivity, $log\ K_{IJ}^{Pot}$, were obtained by titration of amphetamine sulfate standard solutions from 10^{-5} to 10^{-1} M into a 25 ml of 1mM solution of any interference as described in the fixed interference method [23]. Results are summarized in **Table 4**.

Table 4. Selectivity of ASE5 against possible interfering substances. Potentiometric coefficient of selectivity, *log* K_{IJ}^{Pot}.

Interference	*Log* K_{IJ}^{Pot}	
	ASE5	Dibenzo-18-crown 6-ether amphetamine sensor in liquid membranes [2]
None	-	
(±)-epinephrine bitartrate salt	-1.36	- 3.22
dl-phenylalanine	-1.39	-3.33
Caffeine	-1.40	-3.58
K^+	-1.15	-
Na^+	-1.40	-
NH_4^+	-1.39	-
N-formyl amphetamine	-1.39	-

To determine the K_{IJ}^{Pot}, the emf values obtained were plotted vs the logarithm of the activity of the different analytes. The intersection of the extrapolation of the two linear parts of the plot indicate the value of the analyte activity that was used to calculate the potentiometric coefficient of selectivity K_{IJ}^{Pot}, from the Nikolsky-Eisenman equation (see equation 7 in Chapter 1, Section 4.2) [23]. The results obtained showed that ASE5 was not more selective to epinephrine, caffeine and phenylalanine than the liquid-membrane sensor reported by Saad et al what is presented as a drawback of all-solid-state ISE generally. This might be due to the fact that including components to the membrane such as plasticizers and PVC hinders the interaction ionophore/amphetamine when compared to the liquid membrane that only contained the ionophore and the solvent dichloromethane. Nevertheless, the results confirm the good selectivity of ASE5 toward amphetamine in the presence of the interferences evaluated. The values obtained for the *log* K_{IJ}^{Pot}, (between -1.40 and -1.15) show that the response toward both amino/amide compounds and common inorganic cations is low and so no important interferences were observed.

Crown ethers are molecules in which the host cavity is very sensitive not only to the cation guest size but also the nature, position of the substituents and number of hydrogen atoms available in the cation for hydrogen bonding. Such an interaction can destabilize the cation guest complexation into the host cavity by steric repulsion of the substituents or stabilize it by hydrophobic/hydrophilic and dipole-dipole bonding [17][24]. Dibenzo-18-crown 6-ether having an inner cavity negatively polarized whose radius is ~1.45 Å can host selectively the R-NH_3^+ cationic group of amphetamine with a radius of 1.43 Å

[25][2]. The three hydrogens are interacting with 6 oxygens (ratio 2:1) by hydrogen bonding. It allows the $-NH_3^+$ to be hosted in the middle of the crown ether cavity and the rest of the alkyl chain remains outside, stabilizing the interaction by hydrophobic bonding with the components of the lipophilic membrane. From inorganic cations tested, K^+ appears to be the most interfering one. Taking into account that K^+ and amphetamine in the protonated form are monovalent cations, it can be explained by the ion-size fitting inside the crown ether cavity. One can expect that K^+ presenting an ionic radius of 1.32 Å may interact more with the crown ether cavity than Na^+ whose ionic radius is smaller (1.02 Å). In the case of NH_4^+ (with similar ionic radius than $-NH_3^+$ in amphetamine), the presence of four hydrogen fitting into the cavity breaks the symmetry and provokes that complexation ratio varies from 2:1which leads to a less effective interaction.

In the case of phenylalanine, which presents similar structure to amphetamine, the presence of a carboxylic group in the molecule affects not only the protonation of the amino group but also avoids its complexation with the cavity of the crown ether due to hindrance effects. Something similar occurs with N-formyl amphetamine in which the presence of a secondary amide hinders the interaction with DB18C6. In the case of epinephrine, the presence of a secondary amine group hinders the complexation inside the ether cavity. However, due to the presence of hydroxyl groups, hydrogen bonding may occur. Caffeine has been also studied since it is one of the most used adulterants to decrease drugs purity [26]. Caffeine structure presents great differences comparing to amphetamine and so less interaction with the membrane is expected.

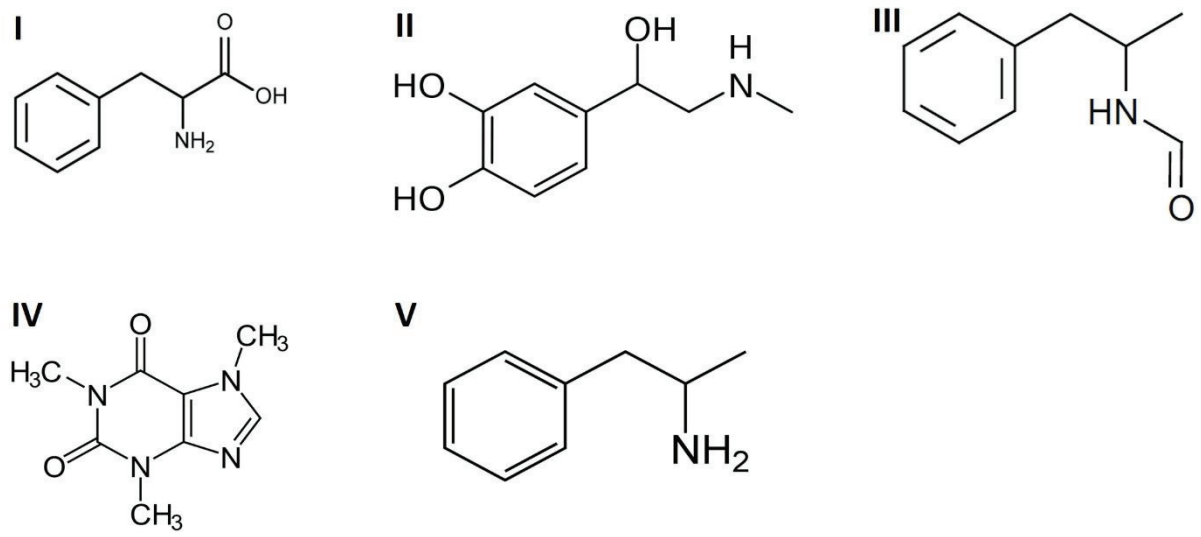

Figure 12. Chemical structures of **I**, phenylalanine, **II**, epinephrine, **III**, N-formyl amphetamine, **IV**, caffeine and **V**, amphetamine.

3.8. Sensor's lifetime.

The lifetime of ASE5 was also evaluated. For this purpose, the sensor was used for one week every day then it was stored for three months. Afterwards, the ASE5 was calibrated one more time following the GSAM. The results (see **Fig. 13**) showed a decreased in terms of sensitivity with a slope of 42 mV/decade of amphetamine concentration. Moreover, the LOD was increased up to 5 x 10^{-5} M. The worsening of the sensor is likely to be due to the lixiviation of the ionophore from the membrane to the aqueous phase as an important decrease of sensitivity is observed after three months.

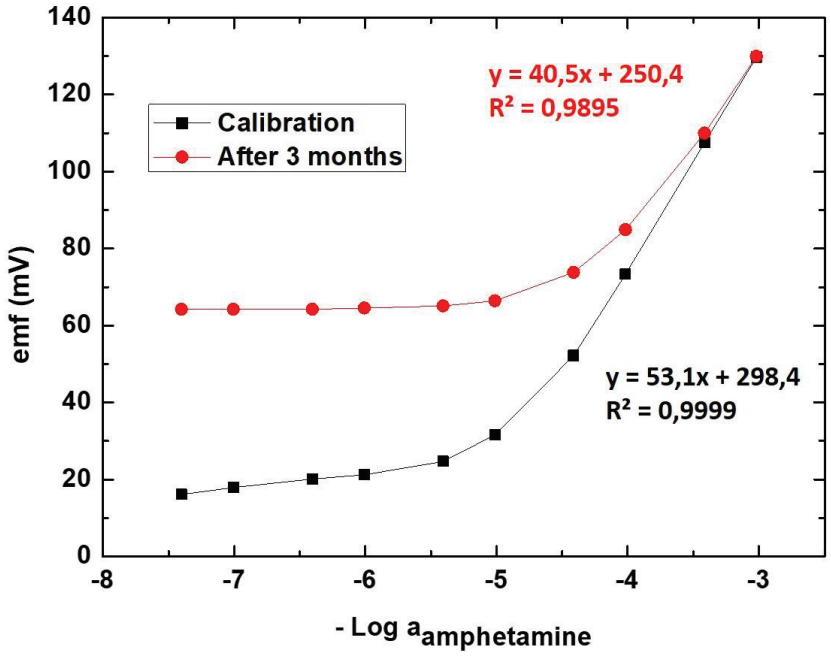

Figure 13. Potentiometric response of ASE5 over a period of three months.

3.9. Influence of pH on the sensor's response.

The pH working interval was also measured. For this purpose, a 25 m L solution of amphetamine sulfate at 1 mM concentration was prepared in deionized water (initial pH = 5.5). Subsequently the pH was decreased to 1.5 by adding small aliquots of HCl 1M (250 µL). A this point, the emf was recorded and the pH of the solution was increased with small amounts of NaOH 1M in order to obtain approximately a reading per unit of pH from 1.50 to 12.5 (pH-meter: Mettler Toledo FE20/EL20). Also for this study, ASE5 was used as it showed the best performance among the five ASEs prepared.

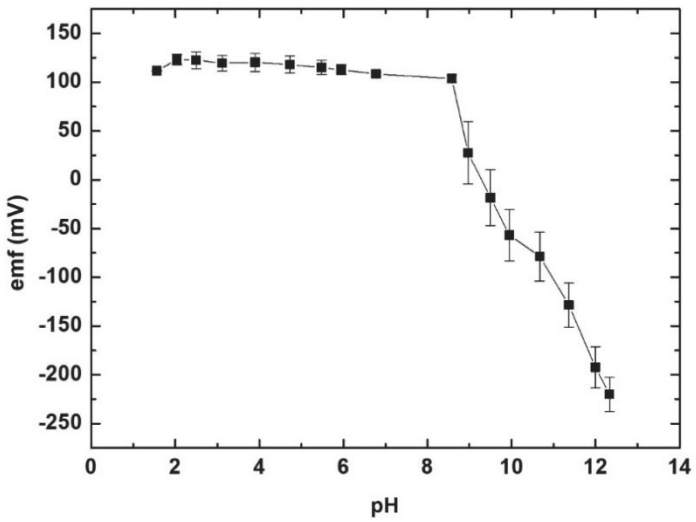

Figure 14. Reilley diagram showing the effect of pH on the emf of the amphetamine-selective electrode ASE5.

The emf observed remains constant for a pH between 1.50 and 8.50 as the potential at the working electrode varies approximately 10 mV for seven decade of H^+ concentration as shown in **Fig. 14.** This is negligible when compared to the 59mV variation per decade of amphetamine concentration in the sensor's linear range. Contrarily, beyond pH = 8.5 the amphetamonium cation starts deprotonating and so the emf changes drastically as the concentration of amphetamine in the neutral form increases.

4. A highly selective potentiometric amphetamine microsensor based on all-solid-state membrane using a new ion-pair complex, [3,3'-Co(1,2-*closo*-$C_2B_9H_{11})_2]^-$ $[C_9H_{13}NH]^+$.

4.1. Introduction

In the previous section, the first generation of all-solid-state amphetamine selective microelectrode was presented. The advantages of the reported sensor were its miniaturized feature as well as its solid state. These two characteristics made the sensor to be useful under real conditions, i.e in sewage. Moreover, as the components that constituted the sensitive membrane are commercially available it was easy to prepare and therefore, it can be mass produced. However, it has been observed that after three months, the sensors' sensitivity decreased by a 20%. In addition, the needs of an external reference electrode suppose a drawback as analysis cannot be carried out using a single device. Moreover, an improvement on the selectivity would be needed when working in such as harsh environment as sewage where the matrix is plenty of interfering compounds.

In order to solve this drawbacks, a new generation of all-solid-state amphetamine selective microelectrode was developed using a novel ionophore synthetized as the active site for amphetamine recognition: the ion pair complex [amphetamine-H]$^+$[3,3'-Co(1,2-$C_2B_9H_{11})_2]^-$. Several transducers containing an array of working, reference and counter microelectrodes were also fabricated in order to choose the best device for the fabrication of the amphetamine sensor. Consequently, the aim of this section was to present an innovative solution for the preparation of a more performant all-solid-state amphetamine-selective microelectrode that finally fulfil the requirements needed to be used in a final application.

4.2. Microelectrodes fabrication

Various geometries of transducer (see **Fig. 15** (**I**), (**II**), (**III**) and (**IV**)) have been fabricated using silicon technology. All of them included the integration of gold working microelectrode, gold counter microelectrode and silver/silver chloride reference microelectrode in a single device. In **I**, the transducer presents four gold WEs, one gold CE and two Ag/AgCl REs. In **II**, the transducer presents two gold WEs, one gold CE and two Ag/AgCl REs. In **III**, the transducer presents one gold WE, one gold CE and one Ag/AgCl RE. Finally, the fourth transducer, **IV**, presents one gold WE, one gold CE and one Ag/AgCl RE with different sizes and disposition in comparison to transducer **III**.

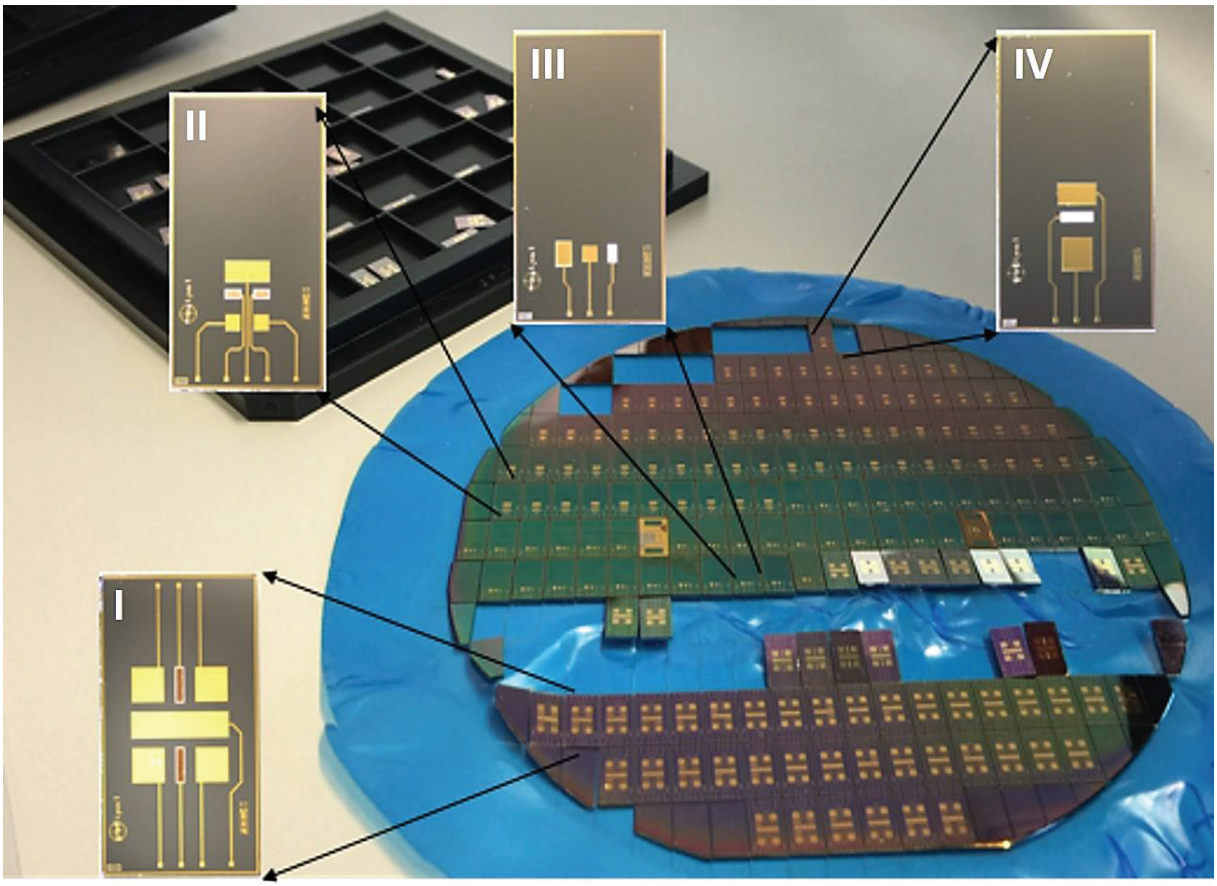

Figure 15. Image of the wafer containing 203 devices with different configuration of transducers.

The transducer fabrication was carried out at the "Centro Nacional de Microelectrónica" in Barcelona. The process starts by growing a silicon dioxide layer of 800 nm thickness using thermal oxidation to isolate the metallic microelectrodes from the silicon substrate. Afterward, gold microelectrodes were fabricated by physical vapor deposition (PVD) of a tri-layer of Ti (50 nm), Ni (50 nm), and Au (200 nm). The Ti layer ensures good adhesion to the SiO_2 and the Ni layer avoids intermixing of Ti and Au. The geometry of the microelectrodes was defined by photolithography and wet chemical etching. Silver for the reference electrodes was deposited by PVD as a bilayer of Ti (15 nm) and Ag (150 nm), and patterned by photolithography and lift-off. A dielectric passivation layer was deposited over the microelectrodes by plasma enhanced chemical vapor deposition (PECVD) of SiO_2 (400 nm) plus Si_3N_4 (400 nm). The passivation was removed then from the active microelectrode areas and the microelectrodes' pads by photolithography and dry reactive ion etching (DRIE).

Afterwards, the transducer was glued to a printed circuit board (PCB) using an epoxy resin (Ep-Tek H70E-2LC, from Epoxy Technology). All microelectrodes' pads were wire-bonded (using Kulicke and Sofa equipment 4523A) to the gold tracks of PCB and then the electrical connections were insulated using the same epoxy resin (Ep-Tek H70E-2LC). Afterwards, microelectrodes were cleaned by soft-

scrubbing the surface with acetone, then ethanol and finally put in contact with a source of UV-plasma in order to remove the organic traces. At this stage, the transducer was ready for electrochemical measurements (see **Fig. 16** for illustration of device fabrication steps).

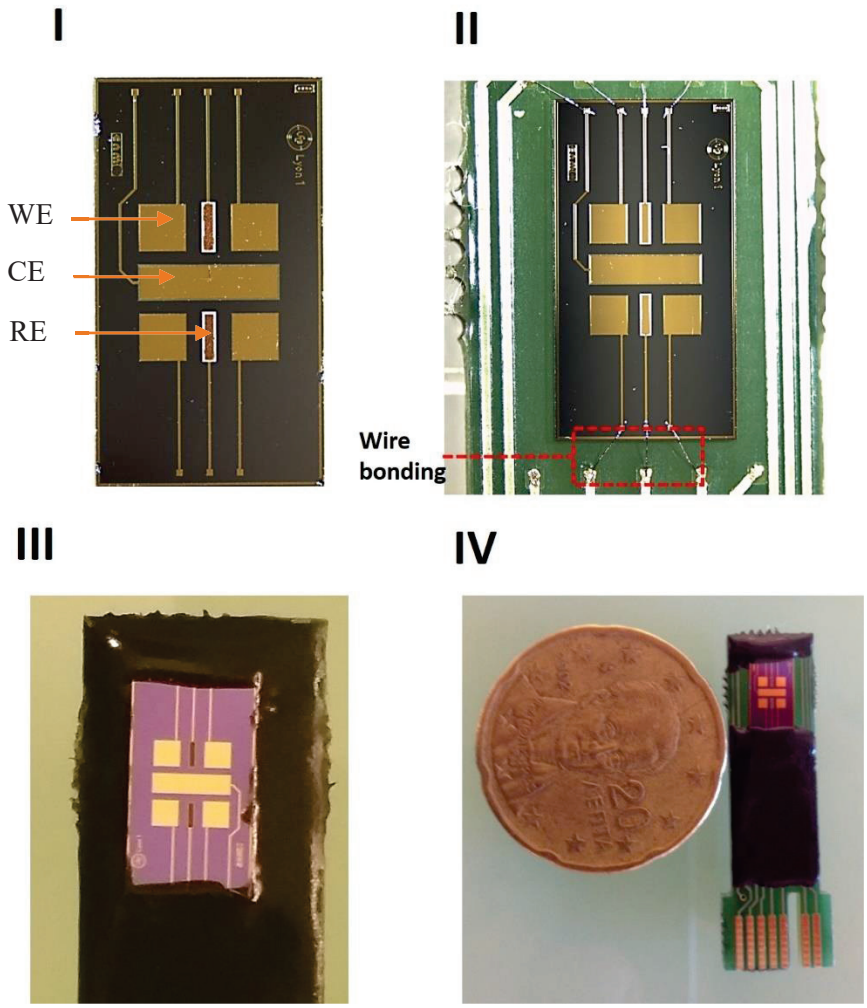

Figure 16. Microelectrodes preparation stages. In **I,** micrograph of the transducer holding four gold WE, one gold CE and two Ag/AgCl RE. In **II** the transducer was wire-bonded to a PCB. In **III**, the electrical connections have been isolated using an epoxy resin. In **IV**, final device ready for electrochemical measurements.

As mentioned previously, four different microelectrodes configurations were manufactured (the layouts are shown in **Fig. 17)** in order to evaluate the impact of the electrode's dimensions and arrangement to the electrochemical signal.

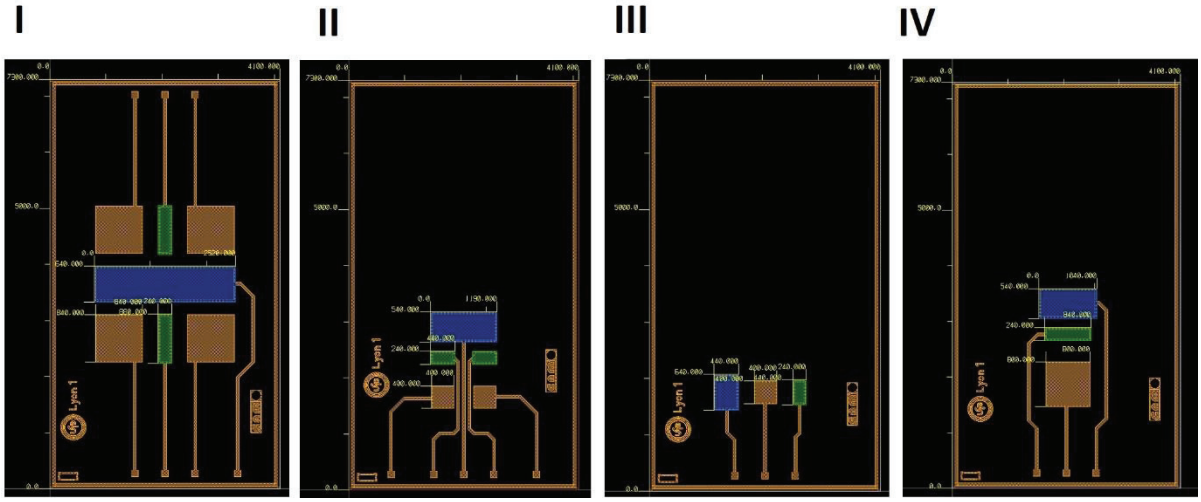

Figure 17. Layouts of different transducers fabricated. In all configuration, the brown microelectrodes represent the WEs, the blue microelectrode represents the CE and the green microelectrodes represent the RE

4.3. Microelectrodes characterization.

In order to evaluate the microelectrodes manufacturing process, all the devices fabricated were characterized by CV as previously described in Section .3.2. Measurements were made in redox probe $K_3[Fe(CN)_6]/K_4[Fe(CN)_6]$ 5mM in phosphate buffer saline solution (PBS, pH 7.4). For the CV, the potential was scanned from -0.2 to 0.6 V vs Ag/AgCl internal reference microelectrode at a scan rate of 100 mV/s using a single-device electrochemical cell. The cyclic voltammograms obtained were compared in **Fig. 18**.

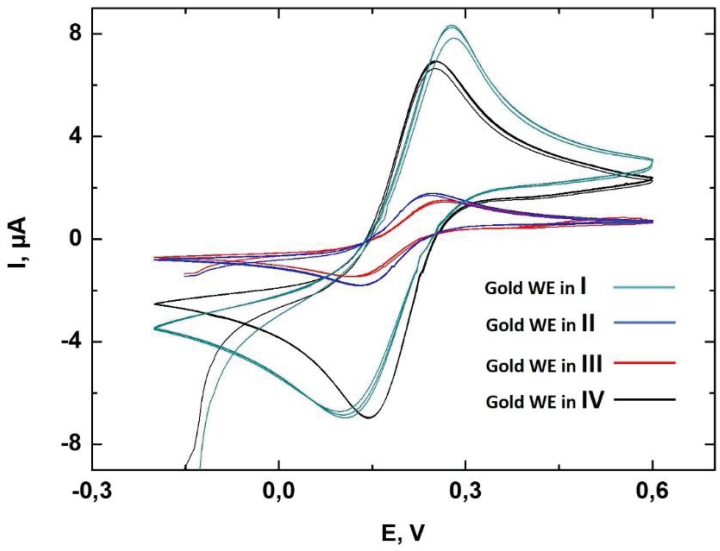

Figure 18. Cyclic voltammogram of gold WE of different transducers manufactured. Measurements carried out in redox probe $K_3[Fe(CN)_6]/K_4[Fe(CN)_6]$ 5mM in phosphate buffer solution.

Gold working microelectrodes in transducer **II** and **III**, presenting the same dimensions (0.16 mm^2) showed similar cyclic voltammogram. Moreover, as they are the smallest among the four configurations, the intensity current values obtained are substantially lower when compared to **I** and **IV**. Likewise, gold working microelectrodes in transducers **I** and **IV** present the same sizes (0.64 mm^2). They are four time bigger than WEs in **II** and **III**. This is furthermore confirmed through the CV plot in which the intensity current values obtained for the Fe^{2+}/Fe^{3+} redox peaks are ± 8 µA and ±2 µA for **I**, **IV** and **II**, **III** respectively. According to the results obtained, the transducer **I** was chosen for the fabrication of the amphetamine-selective microelectrode as it presents the more intense signal. Moreover, it enables to perform four measurements simultaneously.

4.4. Electrochemical deposition of PPyCOSANE as a solid-contact layer

A conducting solid contact layer has been generated by growing electrochemically PPyCOSANE as described previously in Section 3.3. This time, only four potential sweep cycles were applied during the electrochemical polymerization process in order to obtain a thinner layer. The microelectrodes were characterised before and after PPyCOSANE modification by CV. For this purpose, measurements were made in redox probe $K_3[Fe(CN)_6]/K_4[Fe(CN)_6]$ 5mM in phosphate buffer solution and the potential was scanned from -0.2 to 0.6 V vs internal Ag/AgCl at scan rate of 100mV/s. **Fig. 19** shows device before and after surface modification with the PPyCOSANE as well as cyclic voltammogram that confirmed the increase of microelectrode's conductivity.

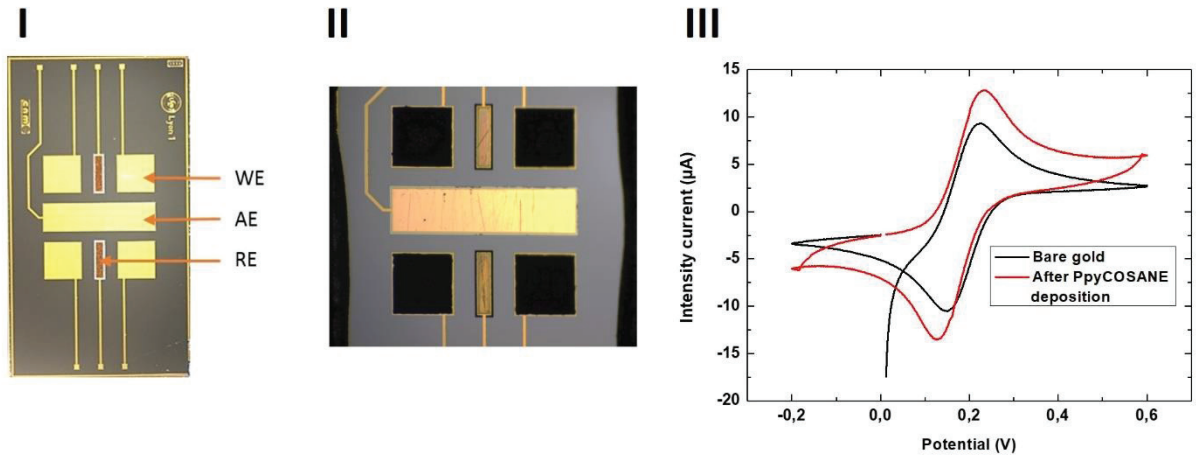

Figure 19. Micrographs of **I**, bare gold WEs and **II**, PpyCOSANE-modified WEs. In **III,** cyclic voltammogram of gold microelectrode in redox probe $K_3[Fe(CN)_6]/K_4[Fe(CN)_6]$ 5mM in phosphate buffer solution.

4.5. Synthesis and characterization of the ion-pair complex [3,3'-Co(1,2 -$C_2B_9H_{11})_2]^-$ $[C_9H_{13}NH]^+$.

The ion-pair complex [amphetamine-H]$^+$ [3,3'-Co(1,2-$C_2B_9H_{11})_2]^-$ was synthetized in the laboratory by ion-exchange procedure. For this purpose, Cs[3,3'-Co(1,2-$C_2B_9H_{11})_2$] (300 mg, 0.657 mmol) was extracted with H_2SO_4 1 M (15 mL) and diethyl ether (20 mL). Afterwards, the organic layer was shaken three times with H_2SO_4 1 M (15 mL 3x). Then, the diethyl ether was evaporated and the residue was diluted with water to generate 0.05 M solution of H[3,3'-Co(1,2-$C_2B_9H_{11})_2$] (solution 1). Amphetamine sulfate was dissolved in water and with the minimum quantity of H_2SO_4 1M to prepare 0.05 M acidic solution (solution 2). Next, 20 mL of solution 1 and 20 mL of solution 2 were mixed and after stirring a yellow precipitate was obtained. This was filtered off, washed with H_2SO_4 0.1 M and dried under vacuum.

Amphetamine presenting a protonable primary amine and being slightly soluble in water, S = 1.7 mg/ml, is a good candidate to be isolated with cobalt bis(dicarbollide) anion, [3,3'-Co(1,2-*closo*-$C_2B_9H_{11})_2]^-$ as ion-par complex, $[C_9H_{13}NH]^+$[3,3'-Co(1,2-$C_2B_9H_{11})_2]^-$ (see **Fig. 20**). When amphetamonium cation (-NH_3^+) is formed in acidic aqueous media and put in contact with [3,3'-Co(1,2-*closo*-$C_2B_9H_{11})_2]^-$ anion, a highly hydrophobic precipitated is formed immediately. The characteristic strength of this association comes from the fact that the -NH_3^+ is associated to the cobalt bis(dicarbollide) anion through electrostatic interaction and the alkylic chain through lipophilic interaction resulting in a highly hydrophobic product. Thus, the resulting ion-pair complex is presented as an excellent charged amphetamine-ionophore to be used in lipophilic membranes due to its high hydrophobicity.

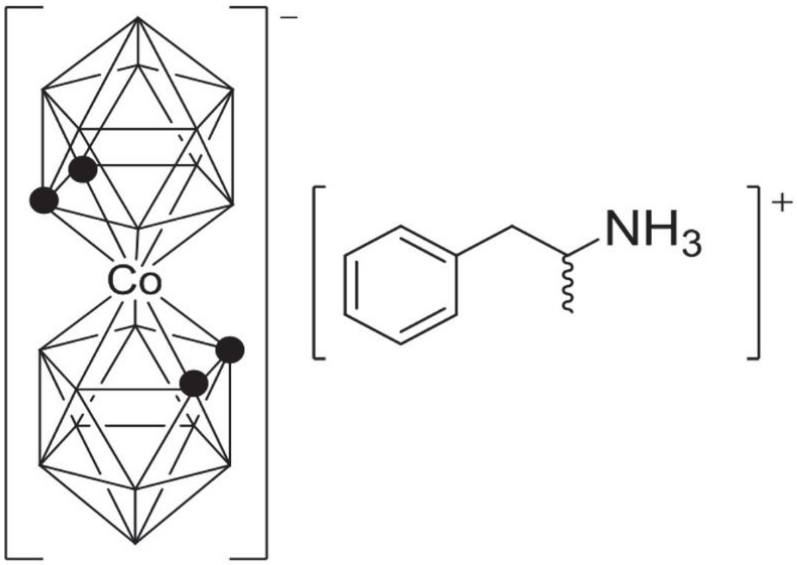

Figure 20. Chemical structure of the $[C_9H_{13}NH]^+$ [3,3'-Co(1,2-$C_2B_9H_{11})_2]^-$ ion-pair complex synthetized. Black spots represent the carbon atoms.

The chemical composition of the isolated ion-pair complex obtained was characterized by FT-IR, ^{1}H-NMR, ^{11}B-NMR, ^{13}C-NMR spectroscopies and MALDI-TOF spectrometry. IR spectra were obtained on PerkinElmer® Universal ATR Accessory spectrophotometer. The ^{1}H- and ^{1}H{^{11}B}-NMR (300.13 MHz), ^{13}C{^{1}H}-NMR (75.47 MHz) and ^{11}B- and ^{11}B{^{1}H}-NMR (96.29 MHz) spectra were recorded on a Bruker ARX 300 instrument equipped with the appropriate decoupling accessories. All NMR spectra were performed in acetone deuterated solvent at 22 ˚C. The ^{11}B- and ^{11}B{^{1}H}-NMR shifts were referenced to external BF_3•OEt_2, while the ^{1}H, ^{1}H{^{11}B}, and ^{13}C{^{1}H}-NMR shifts were referenced to $SiMe_4$. Chemical shifts are reported in units of parts per million downfield from reference, and all coupling constants in Hz. The mass spectra were recorded in the negative ion mode using a Bruker Biflex MALDI-TOF- MS [N_2 laser; λ exc 337 nm (0.5 ns pulses); voltage ion source 20.00 kV (Uis1) and 17.50 kV (Uis2)]. As a result, the compound $[C_9H_{13}NH]^{+}[3,3'\text{-}Co(1,2\text{-}C_2B_9H_{11})_2]^{-}$ was identified.

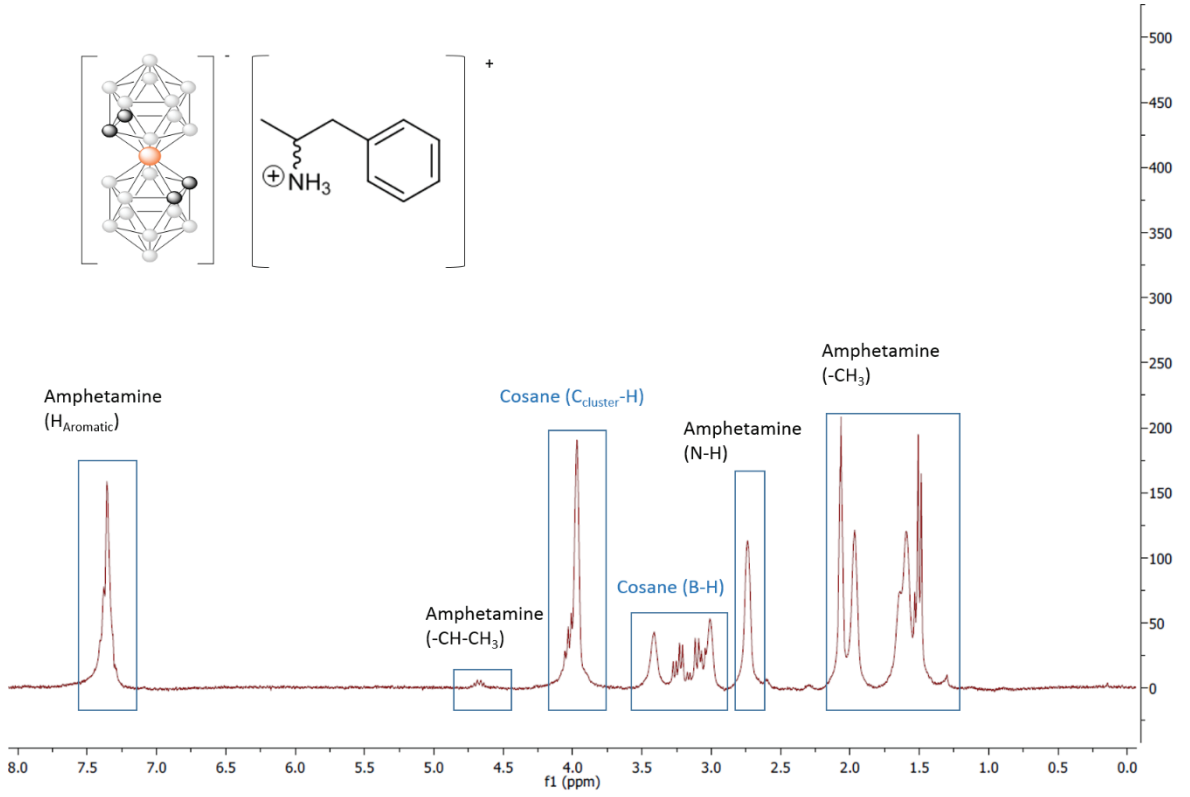

Figure 21. ^{1}H-NMR spectrum of the ion pair complex.

In the ^{1}H-NMR spectrum obtained the following bands were identified:

- Multiplet at 7.36 ppm (m, 5H, C_6H_5) corresponding to the 5 aromatic protons.
- Multiplet at 4.66 ppm (m, 1H, CH-CH_3) corresponding to the proton of the stereocenter.
- Singlet at 3.97 ppm (br s, 4H, C_c-H) corresponding to the four protons of the $C_{cluster}$ in the metallocarborane.

- Multiple signal at 3.21 ppm (dd, $^{3}J(H,H) = 7$ Hz, 1H, CH_2-CH) corresponding to the B-H protons and hydrophobic interaction with amphetamine.
- Singlet at 2.72 ppm (s, 3H, -N-H) corresponding to the amine protons.
- Double doublet at 1.49 ppm (dd, $^{3}J(H,H) = 6$ Hz, 3H, CH_3) corresponding to the methyl terminal group of amphetamine.

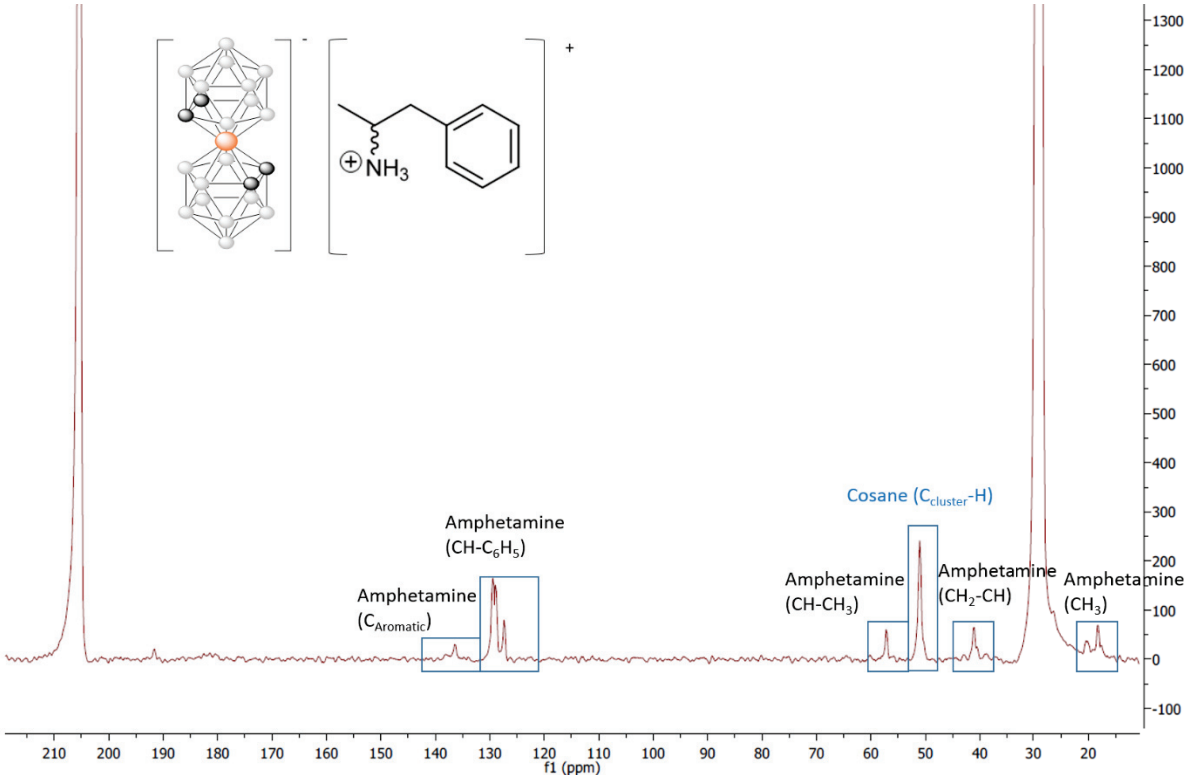

Figure 22. ^{13}C-NMR spectrum of the ion pair complex.

In the ^{13}C-NMR spectrum obtained the following bands were identified:

- Singlet at 136.37 ppm (s, C_6H_5) corresponding to the aromatic carbons.
- Three singlet at 129.43, 128.89 and 127.32 ppm (s, CH-C_6H_5) corresponding to the carbon CH-C_6H_6.
- Singlet at 57.13 ppm (s, CH-CH_3) corresponding to the carbon CH-CH_3 stereocenter.
- Singlet at 51.01 ppm (s, C_c-H) corresponding to the $C_{cluster}$ in the metallocarborane.
- Singlet at 41.10 (s, CH_2-CH)
- Singlet at 18.21 ppm (s, CH_3) corresponding to the methyl terminal group

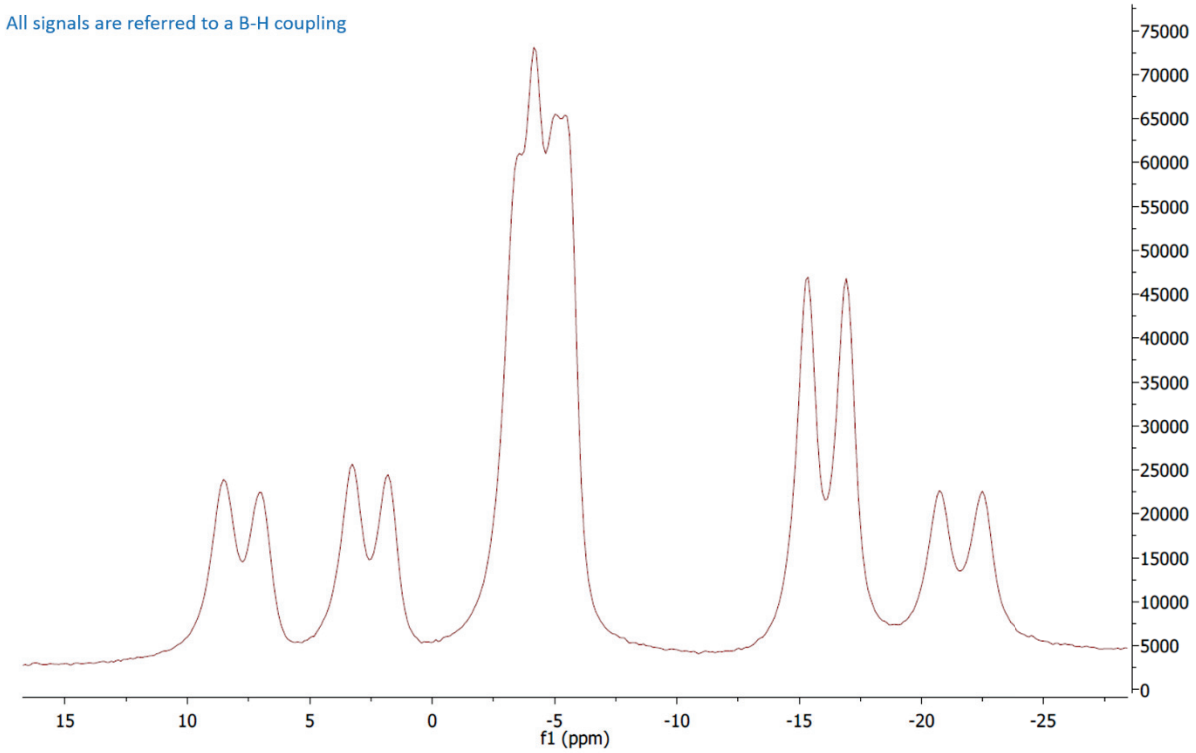

Figure 23. ^{11}B-NMR spectrum of the Amphetamine-Cosane ion pair complex.

All bands correspond to B-H interaction (overlapped) both in the cluster and with amphetamine.

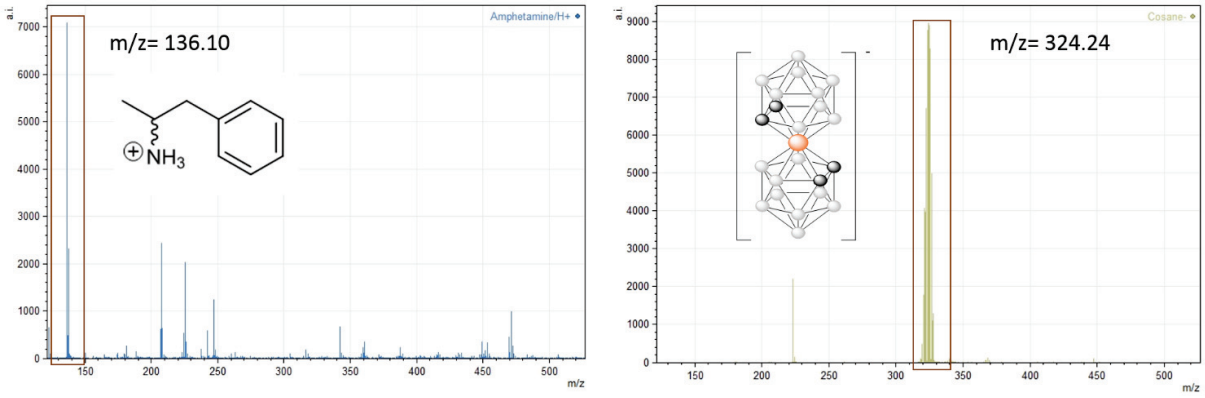

Figure 24. MALDI-TOF spectra of the ion pair complex.

The m/z calculated for $[C_9H_{14}N]^+$ was136.21. The peak found was 136.10.

The m/z calculated for $[Co(C_2B_9H_{11})_2]^-$ was 324.76. The peak found was 324.24.

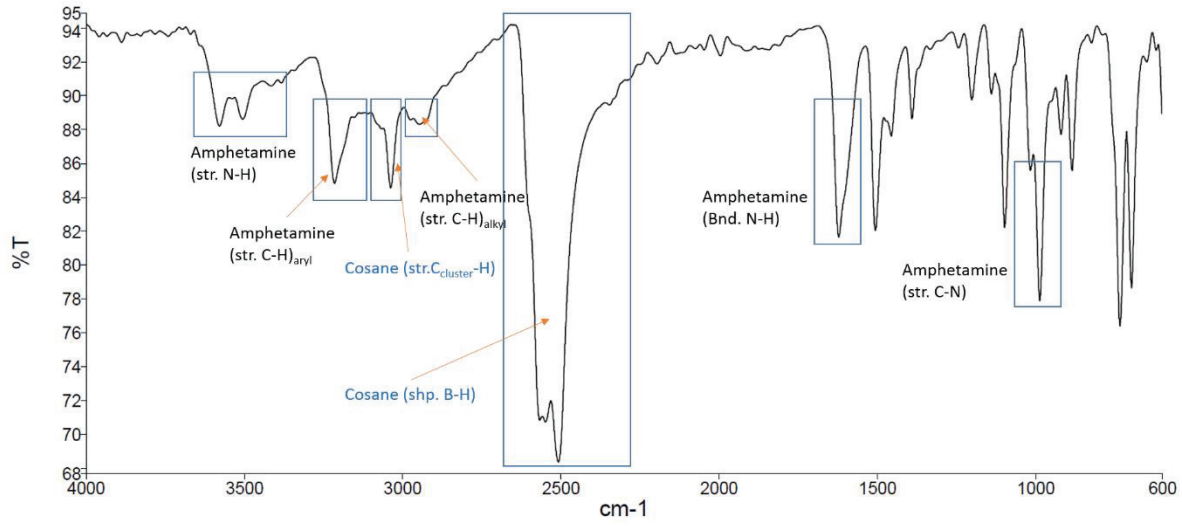

Figure 25. FTIR spectra of the ion pair complex.

In the IR spectrum the following bands were identified.

- Two bands were observed at ν = 3582 and 3504 cm^{-1} corresponding to the N-H.
- At 3215 cm^{-1} a band that correspond to the C-H_{aryl} resonance appeared.
- A band appeared at 3037 cm^{-1} corresponding to C_c-H
- A band at 2948 cm^{-1} corresponding to C-H_{alkyl} appeared
- Two strong bands overlapped at 2549, 2509 cm^{-1} appeared corresponding to B-H.
- Two strong bonds appeared at 1619 and 1096 cm^{-1} corresponding to NH bending and C-N respectively.

4.6. The sensitive membrane.

Four poly (vinyl chloride)-type membranes were prepared using four different plasticizers; di-butyl phthalate (DBP), di-octyl phthalate (DOP), di-octyl sebacate (DOS) and o-nitrophenyloctyl ether (o-NPOE) as solvent, PVC as polymeric matrix and the electroactive ion-pair complex synthetized as charged amphetamine-ionophore. The compositions of the four ASEs prepared are summarized in **Table 5.**

Table 5. Membrane composition of different ion-pair based amphetamine-selective electrodes (ASEs) prepared expressed in wt.%.

ASE	Polymeric membrane (31%)	Plasticizer (65%)	Ion-pair complex (4%)
1	Poly (vinyl chloride)	Di-buty phthalate	$[C_9H_{13}NH]^+[3,3'\text{-}Co(1,2\text{-}C_2B_9H_{11})_2]^-$

2	Poly (vinyl chloride)	Di-octyl phthalate	$[C_9H_{13}NH]^+[3,3'\text{-}Co(1,2\text{-}C_2B_9H_{11})_2]^-$
3	Poly (vinyl chloride)	Di-octyl sebacete	$[C_9H_{13}NH]^+[3,3'\text{-}Co(1,2\text{-}C_2B_9H_{11})_2]^-$
4	Poly (vinyl chloride)	o-nitrophenyloctyl ether	$[C_9H_{13}NH]^+[3,3'\text{-}Co(1,2\text{-}C_2B_9H_{11})_2]^-$

The mixtures were dissolved in 1.5 ml of THF. Afterwards, the polymeric membrane was drop-cast onto the PPyCOSANE-modified gold WEs. Then the device was left overnight for total solvent evaporation. **Fig 26** shows micrographs of the three steps involved in the preparation of the amphetamine-selective microelectrode.

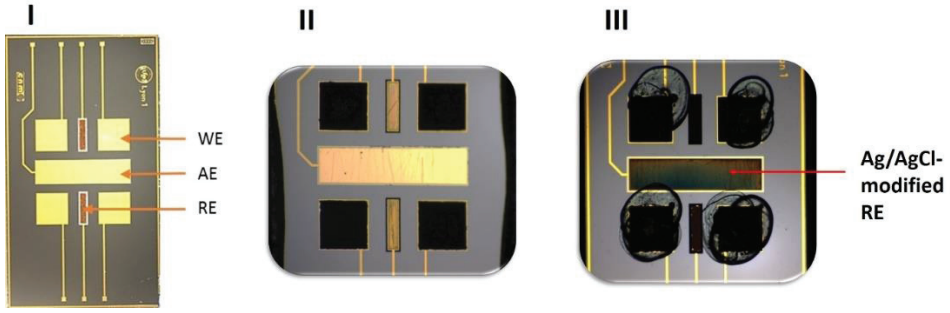

Figure 26. Micrographs of **I**, transducer holding four bare gold WEs, one gold CE and two Ag/AgCl REs. **II**, PPyCOSANE-modified gold WEs and **III**, microelectrodes coated with one of the amphetamine-sensitive membranes.

The addition of the ion-exchanger Na-TPB to the ASE first version described in the previous section was mandatory. The ionophore DB18C6 being neutral ionophore needed the support of an anionic additive to prevent anion co-extration from the aqueous solution. However, the addition of the ion-pair complex to the membrane plays the role of both ionophore and ion-exchanger what is one of the reasons of its good performance.

Due to the great hydrophobicity of the ion-pair complex, it gets highly dissociated into $[C_9H_{13}NH]^+$ and $[3,3'\text{-}Co(1,2\text{-}C_2B_9H_{11})_2]^-$ in the membrane phase. Moreover, the remaining impurities from the synthesis that are in the form $H[3,3'\text{-}Co(1,2\text{-}C_2B_9H_{11})_2]$ are also spread in the lipophilic membrane. As a result, the former dissociation pair serves as amphetamine-ionophore when a gradient of concentration at the interface membrane/solution is created. The later dissociation pair plays the role of ion-exchanger (bulky anion) preventing the anions to interact with the membrane and supporting the ionic flux through the interface membrane/solution and across the lipophilic membrane what enhance the performance of the sensor and also increases its lifetime.

4.7. Potentiometric measurements and sensor calibration.

All measurements were carried out at room temperature using a multichannel homemade-data-acquisition system setup with four microelectrodes connected at the same time and controlled by a personal computer. Measurements were made relative to an Ag/AgCl reference microelectrode integrated in the transducer (see micrelectrodes array in **Fig. 26** (**III**)) and under magnetic stirring. The transformation of CE into Ag/AgCl pseudo-RE was performed in-situ through electrochemical reduction of a solution made of $NaNO_3$ 1M + $AgNO_3$ 25mM at pH = 1 by CV. The potential was scanned from -0.5 and 0.3 V at scan rate of 50 mV/s for 16 s. Afterwards, the microelectrode was chlorined through chronoamperometry of a solution of KCl saturated at a potential, E = -1.8 V for 30 s. Since potentiometric measurements are commonly carried out under the zero current conditions, there is no need to connect the counter electrode. For this reason, it was functionalized as RE enabling therefore, to measure simultaneously four WEs using only one RE. The performances of the ASEs were determined following the generalized standard addition method (GSAM) by titration of amphetamine sulfate solutions from 10^{-7} to 10^{-3} M in 25 ml of deionized water. Variations in emf were recorded after signal stabilization and the value was plotted as a function of the logarithm of the amphetamine activity. The pH working range was also measured by increasing the pH of a 1mM acidic solution of amphetamine sulfate at pH = 1.5 with small amounts of NaOH 1M in order to obtain approximately an emf reading per unit of pH from 1.50 to 12.5 (pH-meter: Mettler Toledo FE20/EL20). Five-microelectrode electrochemical cell was used based on Ag/AgCl pseudo-reference microelectrode and four working microelectrodes (four ASEs) that can measure simultaneously using a single device (see **Fig. 27**). This configuration is very useful not only for multi-detection applications but also to obtain fast statistical data.

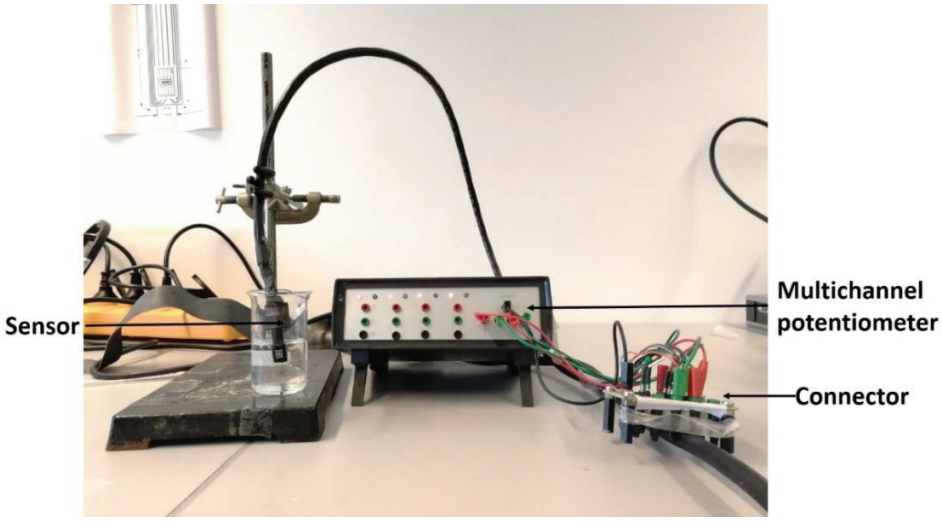

Figure 27. The image shows a single-device electrochemical cell operating simultaneously with four WEs enabling to perform electrochemical measurements in small volumes. The device is controlled through a multichannel potentiometer.

The calibration results of the four ASEs prepared are summarized in **Table 6** and their characteristic response curves are shown in **Fig 28.**

Table 6. Comparison of the characteristic responses of different ASEs developed

Parameter	ASE1	ASE2	ASE3	ASE4
Slope (mV/decade)	60	42	53	45
Lower limit of detection (M)	$1 \cdot 10^{-5}$	$8 \cdot 10^{-6}$	$4 \cdot 10^{-5}$	$2 \cdot 10^{-5}$
Useful pH range	1.5-8.5	NA[1]	NA	NA
Time of response (s)	< 10	< 10	< 10	< 10

[1]Not Available

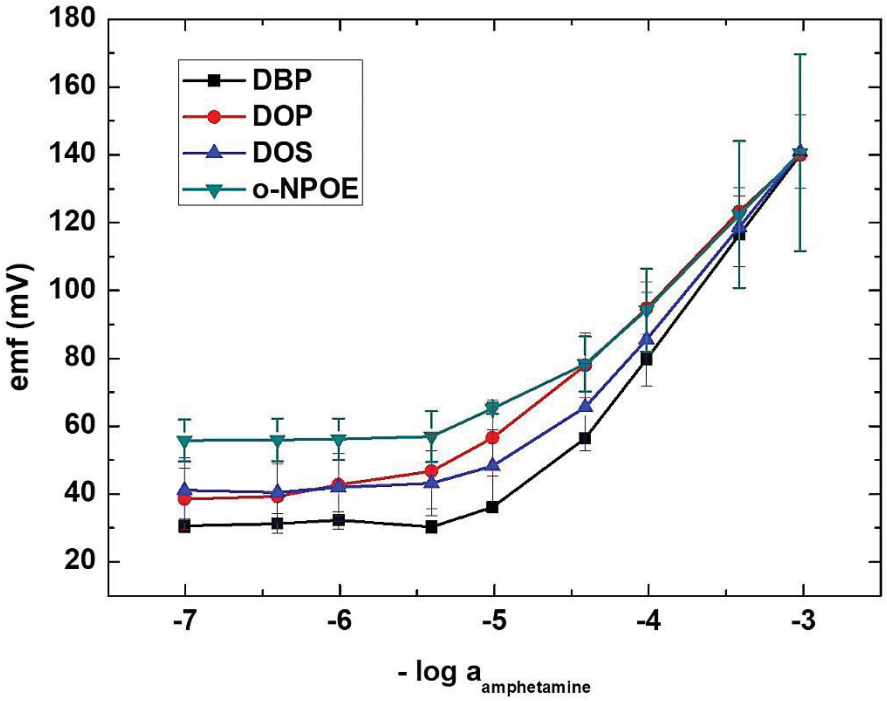

Figure 28. Potentiometric response of amphetamine-selective microelectrodes prepared with different plasticizers. Calibration obtained by titration of standard amphetamine sulfate solutions in 25 ml of deionized water.

ASE2 and ASE4 provided similar sub-Nernstian response in which the slope varies from 42 to 45 mV/decade of concentration of amphetamine. Once again, the limit of detection was calculated as the crossing point between the two linear segments forming the calibration curves. Membranes of ASE2 in which the plasticizers used was DOP, showed the lowest limit of detection around $8 \cdot 10^{-6}$ M concentration of amphetamine. ASE3 in which DOS was used as plasticizer showed near-Nernstian response with a slope of 53 mV/decade and a limit of detection about $4 \cdot 10^{-5}$ M (about eight times higher comparing to sensor ASE4).

Once again DBP plasticizer (used in ASE1) appeared to be the best one for the amphetamine-selective electrodes as it has shown the best sensitivity. A perfect Nernstian response was obtained, 60 mV/decade and a limit of detection of $1 \cdot 10^{-5}$ M. The time of response, $t_{95,}$ was calculated for ASE1 (see **Fig 29)** and it was found to be very fast. The 95% of the total response was reached in less than 10 s.

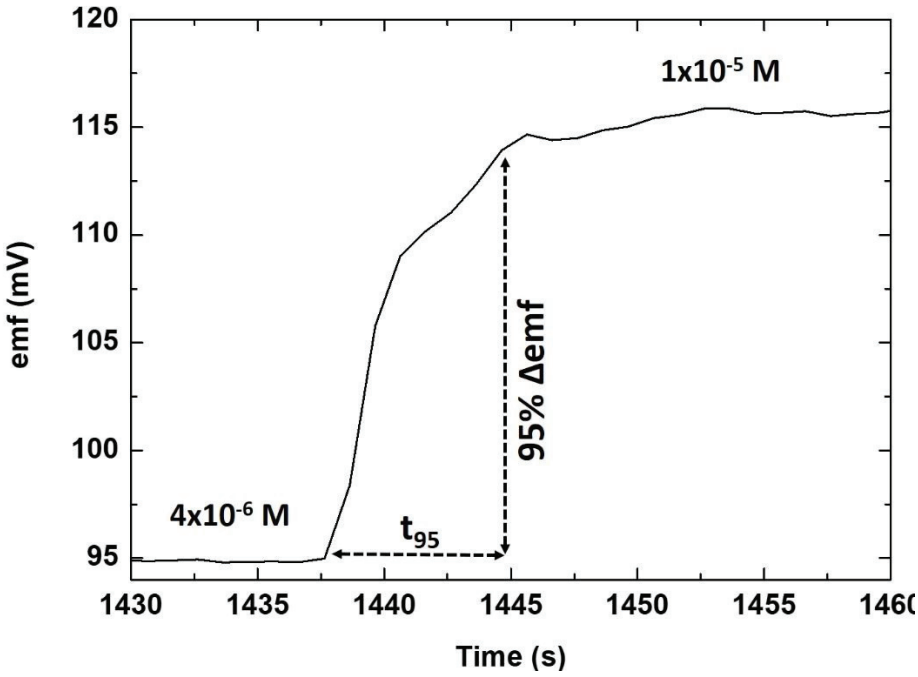

Figure 29. Time of response, t_{95}, obtained in the linear range during the calibration of ASE1.

Table 7 presents a comparison of the amphetamine-selective microelectrodes reported in the literature. ASE1 presents the best sensitivity (60 mV/decade of amphetamine concentration) when compared to the amphetamine sensors found in literature. The limit of detection was found to be slightly higher when compared to the liquid-membrane based amphetamine sensor previously reported by Hassan et *al*. who used the ionophore dibenzo-18-crown 6-ether as active site for amphetamine recognition in 1,2-dichloroethane liquid membrane. Nevertheless, it was still lower than the rest of amphetamine sensors reported previously. Moreover, the time of response was much faster as well as the useful pH range was wider. These features together with the miniature size and all-solid-state make this sensor to be very useful for real-time and on-site applications.

Table 7. Characteristic response of the ion-pair complex-based amphetamine selective microsensor compared to other amphetamine sensors reported in literature.

Para meter	Ion-Pair Complex-Based Amphetamine-Selective Microsensor (ASE1)	αCyclodextrins-based amphetamine sensor[22]	Dibenzo-18-crown 6-ether amphetamine sensor (liquid membrane macrosensor) [13]	Dibenzo-24-crown 8-ether amphetamine sensor (liquid membrane macrosensor) [13]	Dibenzo-18-crown 6-ether-based Amphetamine microsensor[3]
Slope (mV/decade)	60.1	50	58	55	53
Lower limit of detection (M)	$1.0 \cdot 10^{-5}$	$2.5 \cdot 10^{-4}$	$8.0 \cdot 10^{-6}$	$3.0 \cdot 10^{-5}$	$4.0 \cdot 10^{-5}$
Useful pH range	1.5 to 8.5	NA[1]	3.0 to 7.0	3.5 to 6.5	1.5 to 8.5
Time of full response (s)	<10	NA	30-60	30-60	12-16

[1]Not Available

4.8. Cross-selectivity study

ASE1 was used to perform the selectivity study as it showed the best performance among the four ASEs evaluated. The study of sensor's selectivity was followed using the fixed interference method in the presence of some amine/amide compounds presented in **Fig 30** (see Section 3.7 for details on the experimental procedure). Potentiometric coefficients of selectivity, $Log\ K_{IJ}^{Pot}$, were obtained after titration of amphetamine sulfate standard solutions from 10^{-7} to 10^{-3} M in 25 ml of 1mM solution of N-formyl amphetamine, methylbenzylamine and phenylalanine respectively.

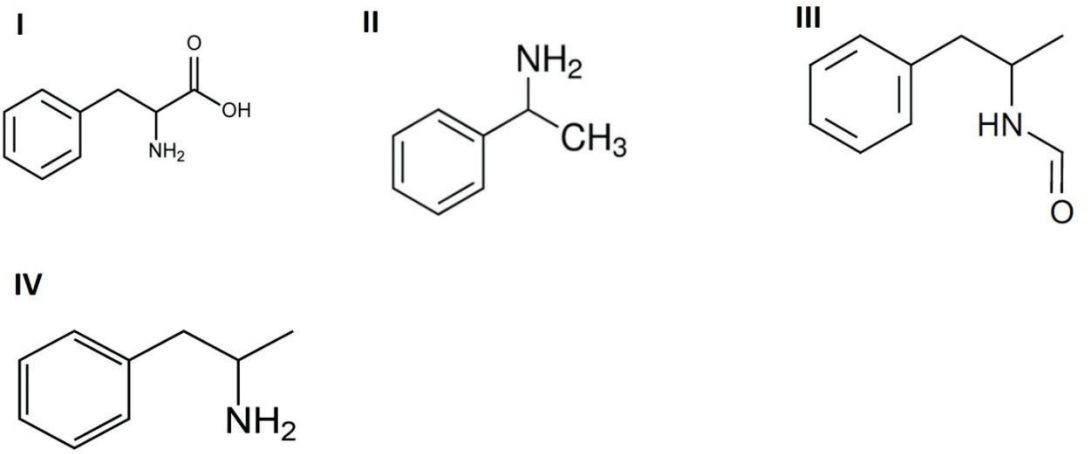

Figure 30. Chemical structures of **I**, phenylalanine, **II**, methylbenzylamine, **III**, N-formyl amphetamine and **IV**, amphetamine.

When performing μISEs selectivity studies, most inorganic cations such as K^+, Na^+ or Ca^{2+} are used as interferences since they are ionic species that potentially interact with conventional membranes containing neutral ionophores. Nevertheless, it has been reported previously that ion-pair complexes, when used as electroactive component for potentiometric sensors, can be selective so much as to distinguish between enantiomers [27]. In our case, no difference was found between D- and L-amphetamine as a racemic mixture of DL-amphetamine sulphate was used for both the preparation of the ion-pair complex and potentiometric analysis. Moreover, as a narcotic, amphetamine does not present differences between enantiomers from a biological point of view so far. Thus, for the cross-selectivity study three structurally similar molecules were studied as possible interferences. N-formyl amphetamine is an intermediary compound formed during the Leuckart synthesis [28] whose presence in wastewater can only be attributed to nearby illicit amphetamine laboratories. On the other hand, methylbenzylamine and phenylalanine where also used to explore the sensor's selectivity toward compounds whose chemical structure was very similar to amphetamine. A titration of amphetamine sulfate standard solutions was carried out from 10^{-7} to 10^{-3} M in 25 ml of 1mM solution of N-formyl amphetamine, methylbenzylamine or phenylalanine respectively. Results are summarized in **Table 8**.

Table 8. Selectivity coefficient of the amphetamine-selective microsensor, ASE1.

Interference	$-\log K_{IJ}^{Pot}$
N-formyl amphetamine	-2.15
Methylbenzylamine	-2.09
Phenylalanine	-2.09

The results obtained confirm the high selectivity of the amphetamine-selective microsensor ASE1. The $Log\ K_{IJ}^{Pot}$ values show that the response toward amphetamine is hundred times more selective when compared to those amine/amide compounds that are structurally similar to amphetamine.

Although plasticizers play an important role concerning the life-time, sensitivity and selectivity of ISE, introducing the target molecule into the polymeric membrane through the ion-pair complex $[C_9H_{13}NH]^+[3,3'\text{-}Co(1,2\text{-}C_2B_9H_{11})_2]^-$ is crucial to achieve those values of selectivity since a specific gradient of amphetamine concentration is created at the interface solution/ISE.

4.9. Sensor lifetime.

The ASE1 sensor's response was followed during a period of five months. For the first month period, the ASE1 was daily used for several hours and exposed to extreme pH conditions. For the next four

months the sensor was used weekly. As it can be observed from **Fig 31**, after five months, slight changes were observed in the performance of working electrodes.

Commonly, a decrease of the sensor's sensitivity which is directly correlated to its lifetime is associated to the lixiviation of common ionophore from the polymeric membrane as we have experienced in the first generation of amphetamine-selective microelectrode reported in the previous section. The more the ionophore is chemically stable inside the membrane, the less the ionophore bleeds from its exterior. In our case, where the ionophore has been replaced by the electroactive ion-pair complex, the anion [3,3'-$Co(1,2\text{-}C_2B_9H_{11})_2]^-$ chosen presents high lipophilicity, low charge density, ability to produce $C_{cluster}$-H···H-B dihydrogen bonds and to be non-covalently bonded to the plasticizer through $C_{cluster}$-H···O hydrogen bond providing high stability of the active component in the polymeric membrane. Furthermore, it produces weak B-H···H-N dihydrogen bonds with the protonated amphetamine cation, as observed from the spectroscopy data, enhancing the membrane stability. All this features, explained the long lifetime of the amphetamine sensor second generation as well as its excellent performance.

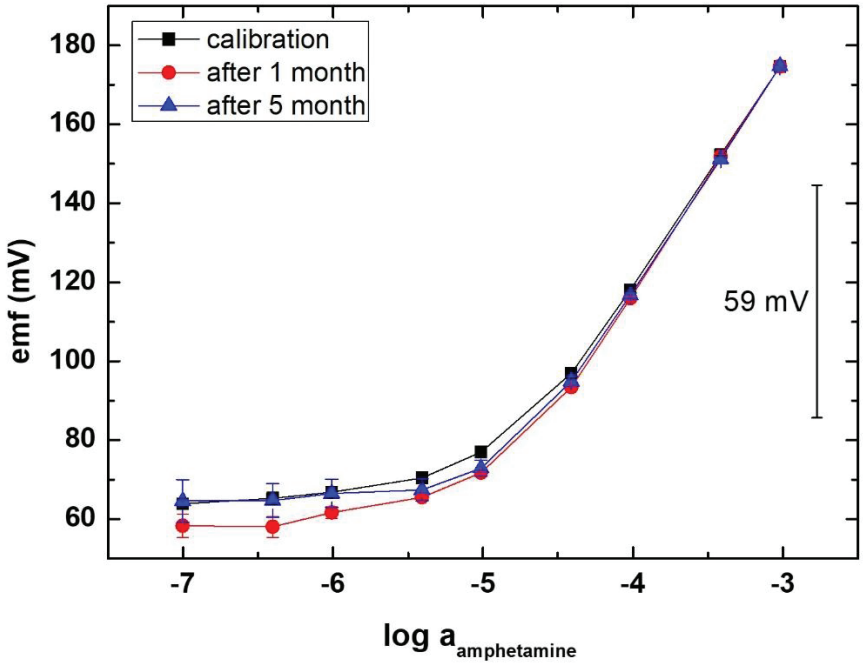

Figure 31. Potentiometric response of the amphetamine-selective microsensor over a period of five months.

4.10. Influence of pH on the sensor's response.

The pH range at which the sensor provided stable response was also evaluated following the emf variation over a pH range between 1.50 and 12.5 in 25 ml of a 1 mM acidic solution of amphetamine sulfate as it was previously described in Section 3.9. The pH of the solution was increased by small additions of NaOH 1 M solution. The emf observed remains constant for a pH between 1.50 and 8.50 as the potential at the working microelectrode varies approximately 30 mV for seven decade of H^+

concentration as shown in **Fig. 32**. This is negligible when compared to the 60mV variation per decade of amphetamine concentration in the sensor's linear range. Contrarily, beyond pH = 8.5 the amphetamonium cation starts deprotonating and so the emf changes drastically as the concentration of amphetamine in the neutral form increases.

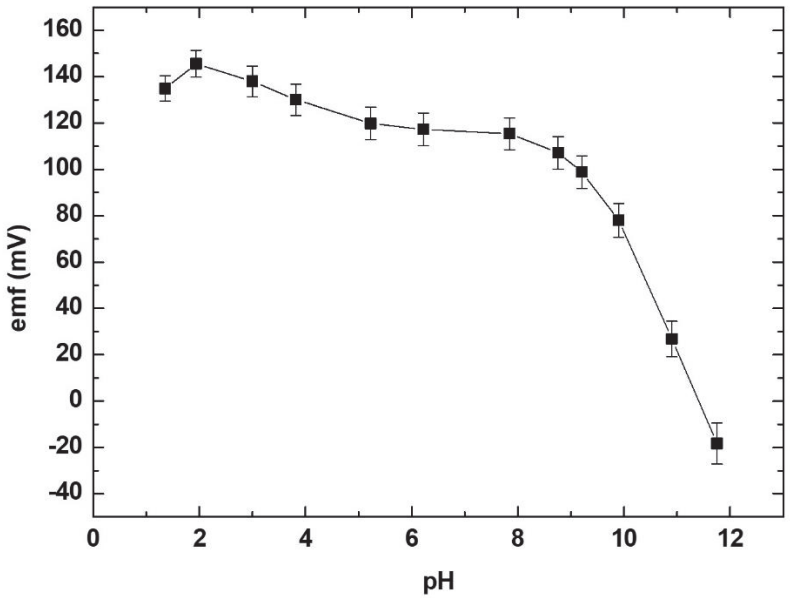

Figure 32. Reilley diagram showing the effect of pH on the emf of the amphetamine-selective microsensor. The pH working range is measured increasing the pH of a 1mM solution of amphetamine sulfate by titration of small aliquots of NaOH 1M solution.

5. Conclusions.

In this chapter, two generations of amphetamine-selective microelectrodes have been reported. To the best of our knowledge, these are the first all-solid-state potentiometric microsensors described in the literature for the quantification of amphetamine.

Regarding the first amphetamine sensor described, five ASEs were developed using two concentrations of DB18C6 as ionophore and four plasticizers. Good sensitivity to amphetamine, 53 mV/decade, and low limit of detection, 4.10^{-5} M, were achieved when the sensitive membrane was made of dibutyl phthalate and 5% (w/w) of DB18C6. The selectivity toward amphetamine when compared to some amine/amide compounds and common inorganic cations was demonstrated to be also good. The ASE5 developed showed a time of response 15s approx. and the working pH was found to be between 1.5 and 8.5.

The ASE second generation described in this chapter proved to be more performant when compared to the previously developed amphetamine sensors. The ion-pair complex, $[3,3'\text{-}Co(1,2\text{-}C_2B_9H_{11})_2]^-$

$[C_9H_{13}NH]^+$, was successfully synthetized as it was confirmed by spectroscopic and spectrometric analysis. Its incorporation to the sensitive polymeric membrane as active site for amphetamine recognition was proven to be useful, specially to increase the sensor's selectivity which was enhanced by an order of magnitude approximatively when compared to the first ASE generation reported in this chapter. The sensor showed Nernstian response with a slope of 60 mV/decade within the concentration range of 10^{-5} M to 10^{-3} M of amphetamine, a limit of detection of 12 µM and a time of response less than 10 s. Moreover, the sensor lifetime was also enhanced as the ion-pair complex being very stable in the polymeric membrane prevents its co-extraction. All these characteristics make the final ASE suitable as an end product for rapid and real-time detection of amphetamine in-situ.

6. References.

[1] United Nations Office of Drugs and Crime. Vienna, Recommended methods for the identification and analysis if Amphentamine, Methamphetamine and their ring-substituted analogues in seized materials., 2006.

[2] S.S.M.H. J, E.M. Elnemma, H. Saad S M, E. Eman M, Amphetamine Selective Electrodes Based on Dibenzo- 18-crown-6 and Dibenzo-24-crown-8 Liquid Membranes, Anal. Chem. (1989) 2189–2192.

[3] J. Gallardo-González, A. Baraket, A. Bonhomme, N. Zine, M. Sigaud, J. Bausells, A. Errachid, Sensitive Potentiometric Determination of Amphetamine with an All-Solid-state Micro Ion-Selective-electrode, Anal. Lett. 58 (2018) 348–358. doi:10.1080/00032719.2017.1326053.

[4] K.N. Mikhelson, Lecture Notes in Chemistry 81. Ion-Selective Electrodes, 2013. doi:10.1007/978-3-319-10410-2.

[5] A. Saini, J. Gallardo-Gonzalez, A. Baraket, I. Fuentes, C. Viñas, N. Zine, J. Bausells, F. Teixidor, A. Errachid, A novel potentiometric microsensor for real-time detection of Irgarol using the ion-pair complex [Irgarol-H]+[Co(C2B9H11)2]−, Sensors Actuators, B Chem. 268 (2018) 164–169. doi:10.1016/j.snb.2018.04.070.

[6] R. Matesic-Puac, M. Sak-Bosnar, M. Bilic, B.S. Grabaric, Potentiometric determination of anionic surfactants using a new ion-pair-based all-solid-state surfactant sensitive electrode, Sensors Actuators, B Chem. 106 (2005) 221–228. doi:10.1016/j.snb.2004.08.001.

[7] I.A. Marques de Oliveira, M. Pla-Roca, L. Escriche, J. Casabó, N. Zine, J. Bausells, F. Teixidor, E. Crespo, A. Errachid, J. Samitier, Novel all-solid-state copper(II) microelectrode based on a dithiomacrocycle as a neutral carrier, Electrochim. Acta. 51 (2006) 5070–5074.

[8] O.A. Biloivan, S.V. Verevka, S.V. Dzyadevych, N. Zine, J. Bausells, J. Samitier, A. Errachid, Protein detection based on microelectrodes with the PPy[3,3-Co(1,2-C2B9H11)]2 solid contact and immobilized proteinases: Preliminary investigations, Mater. Sci. Eng. C. 26 (2006) 574–577.

[9] N. Zine, J. Bausells, F. Vocanson, R. Lamartine, Z. Asfari, F. Teixidor, E. Crespo, I.A.M. de Oliveira, J. Samitier, A. Errachid, Potassium-ion selective solid contact microelectrode based on a novel 1,3-(di-4-oxabutanol)-calix[4]arene-crown-5 neutral carrier, Electrochim. Acta. 51 (2006) 5075–5079.

[10] N. Zine, J. Bausells, A. Ivorra, J. Aguiló, M. Zabala, F. Teixidor, C. Masalles, C. Viñas, A. Errachid, Hydrogen-selective microelectrodes based on silicon needles, Sensors Actuators B Chem. 91 (2003) 76–82.

[11] I.A. Marques de Oliveira, D. Risco, F. Vocanson, E. Crespo, F. Teixidor, N. Zine, J. Bausells, J. Samitier, A. Errachid, Sodium ion sensitive microelectrode based on a p-tert-butylcalix[4]arene ethyl ester, Sensors Actuators B Chem. 130 (2008) 295–299.

[12] M. C., B. S., V. C., T. F., Are Low-Coordinating Anions of Interest as Doping Agents in Organic Conducting Polymers?, Adv. Mater. 12 (2000) 1199–1202. doi:10.1002/1521-4095(200008)12:16<1199::AID-ADMA1199>3.0.CO;2-W.

[13] J. Gallardo-González, A. Baraket, S. Boudjaoui, A. Streklas, F. Teixidor, N. Zine, J. Bausells, A. Errachid, A Highly Sensitive Potentiometric Amphetamine Microsensor Based on All-Solid-State Membrane Using a New Ion-Par Complex , Proc. Eurosensors Conf. Paris 2017. 1 (2017) 2–5. doi:10.3390/proceedings1040481.

[14] A.J. Heeger, S. Kivelson, J.R. Schrieffer, W.P. Su, Solitons in conducting polymers, Rev. Mod. Phys. 60 (1988) 781–850.

[15] H. Freiser, Ion-selective electrodes in analytical chemistry, Springer Science & Business Media, 2012.

[16] G. Dimeski, T. Badrick, A.S. John, Ion Selective Electrodes (ISEs) and interferences-A review, Anal. Lett. 411 (2010) 309–317. doi:10.1016/j.cca.2009.12.005.

[17] E. Bakker, P. Bühlmann, E. Pretsch, Carrier-Based Ion-Selective Electrodes and Bulk Optodes. 1. General Characteristics, Chem. Rev. 97 (1997) 3083–3132.

[18] J.L.F.C. Lima, A. a. S.C. Machado, Procedure for the construction of all-solid-state PVC membrane electrodes, Analyst. 111 (1986) 799–802. doi:10.1039/an9861100799.

[19] G. Baum, M. Lynn, Polymer membrane electrodes: Part II. A potassium ion-selective membrane electrode, Anal. Chim. Acta. 65 (1973) 393–403. doi:https://doi.org/10.1016/S0003-2670(01)82506-X.

[20] M. De los A. Arada Pérez, L. Marín Pérez, J. Calvo Quintana, M. Yazdani-Pedram, Influence of different plasticizers on the response of chemical sensors based on polymeric membranes for nitrate ion determination, Sensors Actuators B Chem. 89 (2003) 262–268.

[21] B.E.H. Saxberg, B.R. Kowalski, Generalized standard addition method, Anal. Chem. 51 (1979) 1031–1038. doi:10.1021/ac50043a059.

[22] R. Kataky, D. Parker, P.M. Kelly, Potentiometric, enantioselective sensors for alkyl and aryl ammonium ions of pharmaceutical significance, based on lipophilic cyclodextrins, Scand. J. Clin. Lab. Invest. 55 (1995) 409–419. doi:10.3109/00365519509104980.

[23] E. Bakker, E. Pretsch, P. Bühlmann, Selectivity of Potentiometric Ion Sensors, Anal. Chem. 72 (2000) 1127–1133.

[24] P. Bühlmann, E. Pretsch, E. Bakker, Carrier-based ion-selective electrodes and bulk optodes. 2. Ionophores for potentiometric and optical sensors, Chem. Rev. 98 (1998) 1593–1688. doi:cr970113+ [pii].

[25] P.D.J. Grootenhuis, P.A. Kollman, Molecular mechanics and dynamics studies of crown ether - cation interactions: free energy calculations on the cation selectivity of dibenzo-18-crown-6 and dibenzo-30-crown-10, J. Am. Chem. Soc. 111 (1989) 2152–2158.

[26] S. Schneider, F. Meis, Analysis of illicit cocaine and heroin samples seized in Luxembourg from 2005 – 2010, Forensic Sci. Int. 212 (2011) 242–246.

[27] A.-I. Stoica, C. Vinas, F. Teixidor, Cobaltabisdicarbollide anion receptor for enantiomer-selective membrane electrodes, Chem. Commun. (2009) 4988–4990. doi:10.1039/B910645F.

[28] K. Graniczkowska, M. Pütz, F.M. Hauser, S. De Saeger, N. V Beloglazova, Capacitive sensing of N-formylamphetamine based on immobilized molecular imprinted polymers, Biosens. Bioelectron. 92 (2016) 741–747. doi:http://dx.doi.org/10.1016/j.bios.2016.09.083.

Chapter 3

A fully integrated passive microfluidic Lab-on-a-Chip (LOC) for real-time potentiometric detection of ammonium in sewage applications

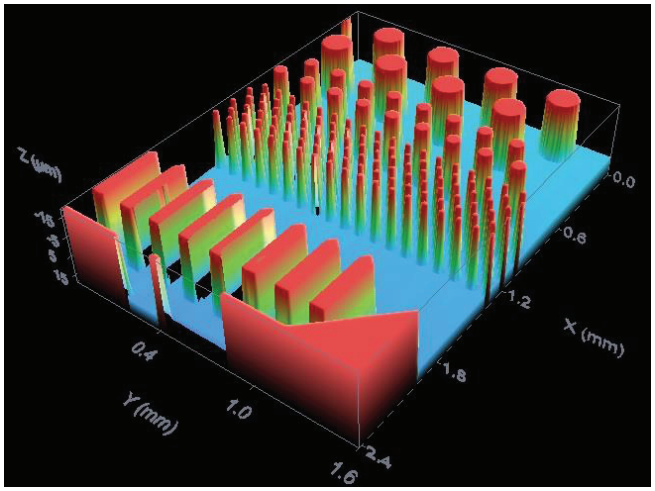

1. Objectives.

The aim of this chapter was to develop a first generation of Lab-on-a-chip (LOC) to perform in-situ and real-time potentiometric measurements in a water flow. The device consisted of two differentiated parts: a poly (dimethylsiloxane) (PDMS) microfluidic structure obtained by soft litography and a fully integrated chemical sensing platform including four working microelectrodes, two reference microelectrodes and one counter microelectrode for the detection of ammonium in real conditions. Consequently, as the main objective of the MicroMole project is to develop an automated chemical sensing device that enables to continuously monitor wastewater for tracking illicit drugs laboratories, the development of the microfluidic LOC reported here contributes to the progress on real time monitoring of sewage.

2. Introduction

Since the worldwide population and global economy grow, waste discharges from industrial, agriculture, animal and human activities are constantly increasing [1]. In this context, wastewater quality assessment has become an indispensable tool for environmental analysis on the last decades. Yet, sewage monitoring is not only helpful to improve wastewater quality from an environmental point of view, but also to perform epidemiology studies in communities.

Sewage epidemiology has also surged as an essential tool for profiling drug uses in communities since all we consume ends up in the sewer network. However, most of extended analytical techniques reported to analyze wastewater are sample-based studies like spectroscopic measurements and especially capillary electrophoresis and chromatographic analyses coupled with mass spectrometry techniques (HPLC and GC/GC-MS) [2–9].

The aim of the MicroMole project was to develop an autarkic device that can track the activities of clandestine laboratories of amphetamines through the monitoring of sewage. However, as the main objective was to work on the field, strategies used commonly in sewage epidemiology, i.e. to perform sampling campaigns and further analysis in external laboratories, cannot be applied. On the contrary, it is a priority to use devices whose characteristics are: compactness, low sample consumption, low-cost production, better overall process control, real-time analysis and fast response. All-solid-state ISEs, fulfil most of those requirement. However, their lifetime is very limited when working in such a harsh environment as sewage. To minimize the contact of the sensor itself to the sewage, we report in this chapter on the development of a Lab-on-a-Chip (LOC) made of two differentiated units: an ammonium-selective microelectrode for potentiometric measurements linked to a PDMS microfluidic structure that reduce the exposure of the sensor to the wastewater (see **Fig. 1**).

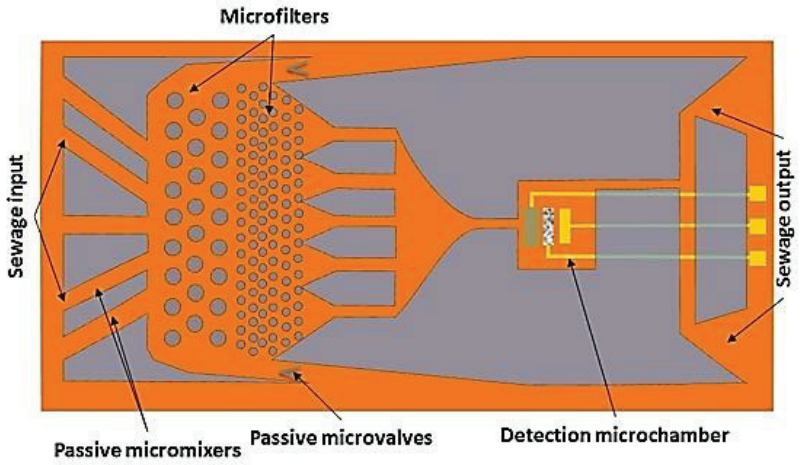

Figure 1. Illustration showing the configuration of the microfluidic LOC

3. A fully integrated passive microfluidic Lab-on-a-Chip for real-time potentiometric detection of ammonium: sewage applications.

3.1. Microelectrodes fabrication and characterization.

An upgraded version of the transducers presented in Chapter 2 was fabricated at the Centro Nacional de Microelectrónica, IMB-CNM (CSIC), Spain. The transducer configuration that included four gold working microelectrodes was chosen again (see **Fig. 2**). However, in the upgraded version the auxiliary microelectrode was fabricated in platinum as it was observed that it provided more stable signal for electrochemical measurements (see Chapter 2 Section 4.2 for the fabrication process).

Transducers were made-up in silicon-substrate wafers of 100 mm diameter which contain 230 devices. The final device size is 4 x 7 mm and it integrates four gold working electrodes (WEs), two Ag/AgCl reference electrodes (REs) and one platinum auxiliary electrode (AE) as shown in **Fig. 2**.

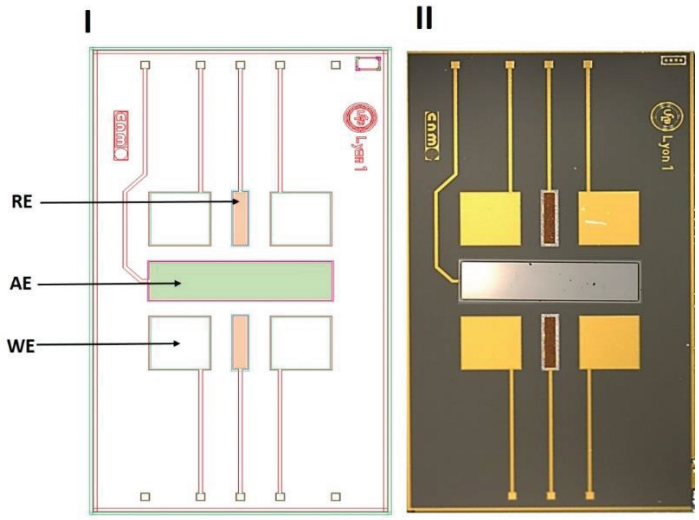

Figure 2. In (**I**), transducer layout. In (**II**), a micrograph of the transducer manufactured.

In order to validate the microelectrodes manufacturing process, gold WEs were characterized by cyclic voltammetry (CV). Measurements were made in redox probe $K_3[Fe(CN)_6]/K_4[Fe(CN)_6]$ (5 mM) in phosphate buffer saline (PBS, pH 7.4). The potential was scanned from -0.2 to 0.6 V vs Ag/AgCl internal reference microelectrode at scan rate of 100 mV/s. Cyclic voltammograms were recorded simultaneously for each WE as shown in **Fig. 3**. The redox peaks observed at E= 0.12 V and 0.27 V as well as the symmetry of the intensity current peaks recorded at I = ± 8 µA are uniform and stable over the four microelectrodes. This confirmed the normal behaviour of the redox reaction; $Fe^{2+} \leftrightarrow Fe^{3+} + e^-$, at the gold interface which validates the good microelectrodes manufacturing process.

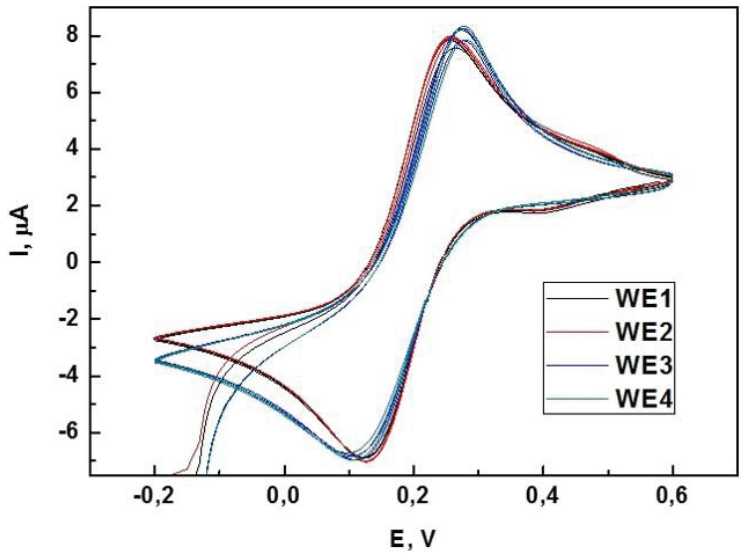

Figure 3. Cyclic voltammogram of four gold microelectrodes in redox probe $K_3[Fe(CN)_6]/K_4[Fe(CN)_6]$ 5mM in phosphate buffer solution using a single-device electrochemical cell.

3.2. Silicon molds fabrication.

A batch of negative-shaped silicon molds was fabricated at the IMB-CNM (CSIC), using four design that included microstructures such as microfilters, passive micromixers and microchannels (see **Fig. 4**).

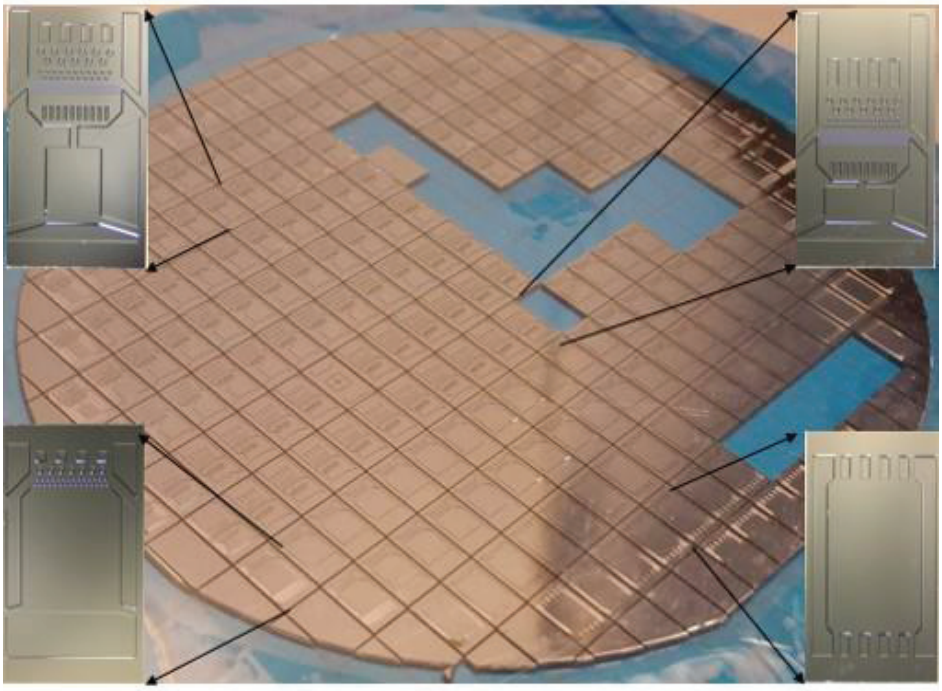

Figure 4. Image of the wafer as received and optical micrographs of different microfluidic designs manufactured.

The heights of the structures were etched to a depth of 100 µm. The microstructures were defined in the silicon surface to produce PDMS microfluidic systems with positive-shaped superficial structures by

replica molding technique. Silicon molds were fabricated by patterning the surface with a photoresist resin using established photolithography techniques. Then, the silicon wafer with <100> orientation was etched to a depth of 100 µm using deep reactive ion etching (601 DRIE, Alcatel, France). This method provided good definition of the side walls to depths of hundreds of nanometers. After wafer dicing, the individual masters were treated with Octadecyltrichlorosilane (OTS) to prevent irreversible bonding between silicon surface and PDMS structure. An OTS monolayer was formed on the surface of the silicon master, by immersion for 10 min in OTS (5µM) and carbon tetrachloride (0.4 mM) in heptane. After this time, the silicon masters were then rinsed with heptane and placed into the oven for 1 hour. At this point, the silicon molds were silanized and ready for replica molding.

Four different designs were developed so that the microfluidic structures were adapted to the four transducers configurations fabricated and described in Chapter 2, section 4.2. **Fig. 5**, shows the layout and the Si molds fabricated.

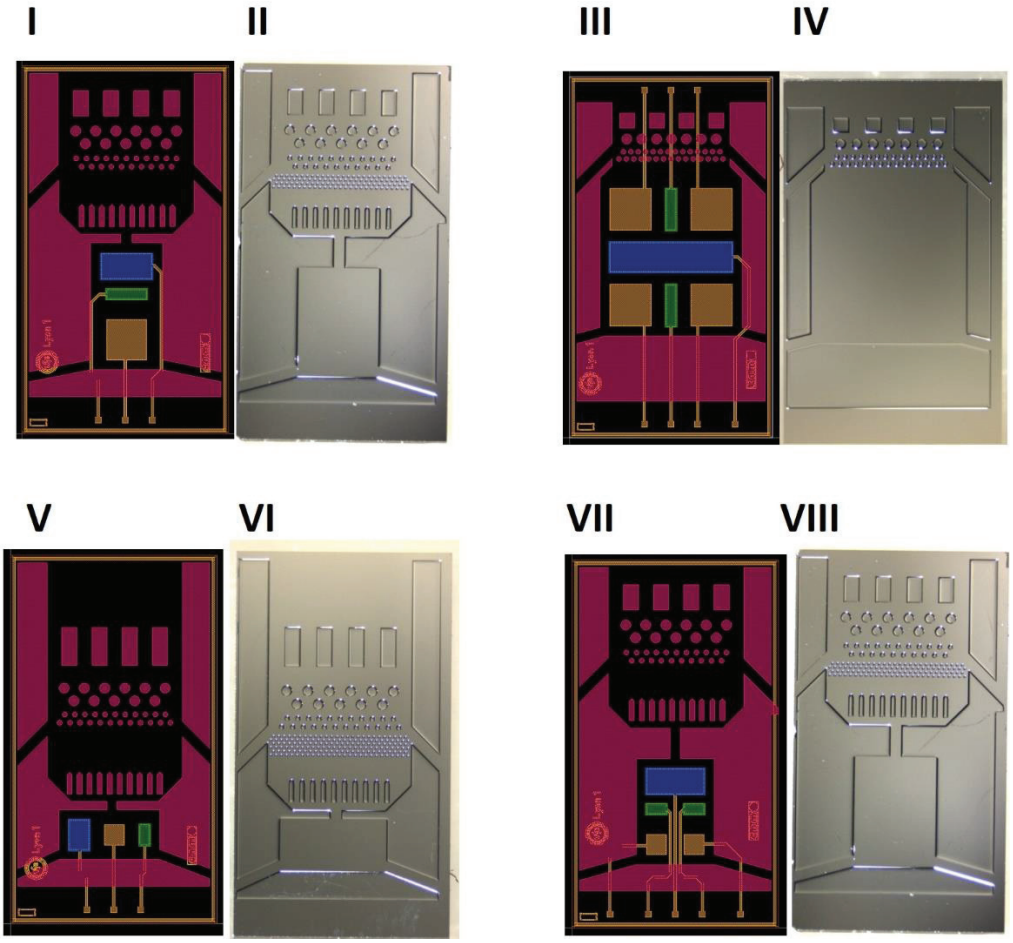

Figure 5. Layouts and Si molds fabricated.

As it can be observed from **Fig. 5** where the pink-colored parts represent the microfluidic system, all the conformations contained the shape adapted to each transducer configuration and presented the microfluidic elements desired: micromixers, microfilters, microchannels and windows of analysis.

In our application, the design **IV** was chosen among the four configurations manufactured as the microfluidic system incorporated to the LOC developed, since it was adapted to the shape of transducer chosen (see **Fig. 2**) to perform the potentiometric measurements. The rest of the microfluidic structure are currently under evaluation and therefore, will not be discussed in this manuscript.

3.3. Ammonium-selective microelectrode.

All-solid-state ammonium-selective microelectrodes (ASE) were prepared using an optimized membrane composition that has been reported previously for ammonium detection using ISEs [15][16]. Consequently, the sensitive membrane prepared was made from a combination of 33 wt% of PVC-COOH, 66 wt% DOS and 2 wt% of nonactine as ammonium ionophore. Although the objective of the project was to use amphetamine-selective electrodes as the potentiometric sensors in the LOC, two reason drove us to choose ammonium instead of amphetamine. In one hand, amphetamine is expensive and it is also more difficult to obtain in big amounts due to the legal restrictions. Moreover, it represents a source of pollution to the environment so we must avoid its use as much as we can. On the other hand, high concentration of ammonium is expected to be found in the sewage nearby clandestine laboratories since it represents one of the most found components of the amphetamine synthesis' wastes.

To validate the correct functioning of the microfluidic LOC fabricated its time of responses was compared to that of a commercial electrical-conductivity (EC) sensor used as reference sensor for the detection of ammonium-containing samples.

The fabrication process started by growing a solid contact layer of conductive polymer polypyrrole[3,3'-$Co(1,2\text{-}C_2B_9H_{11})_2$], by electrochemical polymerization onto gold microelectrodes using cyclic voltammetry as we have reported previously in Chapter 2 Section 3.3. This step serves to enhance the adhesion between the gold substrate and the polymeric membrane. After that, the sensitive membrane described above was dissolved in 1.5 mL of THF. Afterwards, 2 µL of the mixture were drop-cast on top of each WE already modified with the PpyCOSANE layer. The device was then left at room temperature overnight for total solvent evaporation. At this stage, the chemical sensor was ready to be joined to the microfluidic system. **Fig. 6** shows the steps involved in the ASEs preparation.

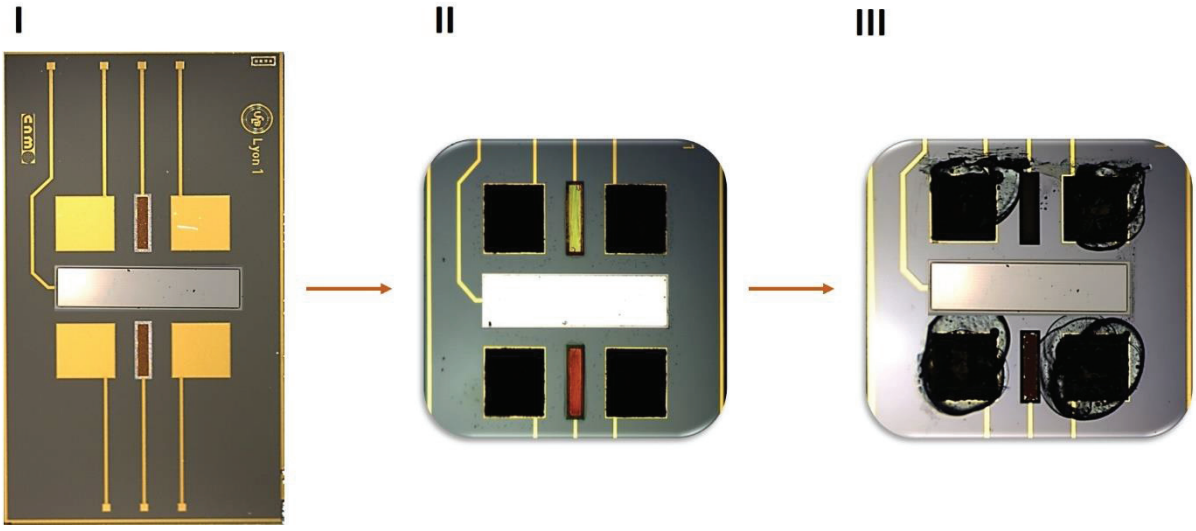

Figure 6. Micrographs of (**I**) transducer with bare electrodes. In (**II**) PpyCOSANE modified working microelectrodes In (**III**), final ammonium-selective microelectrode.

3.4. PDMS-microfluidic system. Replica molding.

The microfluidic systems based on PDMS were manufactured by replica molding soft-lithography. As indicated by its name, this method enables to obtain a replicate polymeric structure from the Si mold. Prior to replica molding, the Si molds were silianized using OTS. For this purpose, they were immersed in piranha (H_2SO_4/H_2O_2 ratio 2:1) solution for 2h. Thus, Si-OH groups are formed on the Si surface. Subsequently, the activated surface is put in contact with a solution of OTS (5µM) and carbon tetrachloride (0.4 mM) in heptane creating therefore, an octadecyl silane monolayer at the Si surface through nucleophilic reaction between Cl groups from OTS and Si-OH. Afterwards, a pre-polymer (PDMS) was mixed with the curing agent at the ratio of 10:3. The PDMS pre-polymer mixture was degassed in order to remove all air bubbles trapped in the polymer mixture. This step is very important to prevent mechanical defects in the microfluidic system. The mixture was then casted onto the silicon mold and the ensemble mold/PDMS was left in the oven at 90°C for 1 hour. After PDMS curing, the elastomeric microfluidic system was peeled off from the silicon master bearing the microstructures on its surface.

Fig 7 shows the positive-shaped microfluidic structure obtained by replica molding of the Si master bearing the desire microstructures.

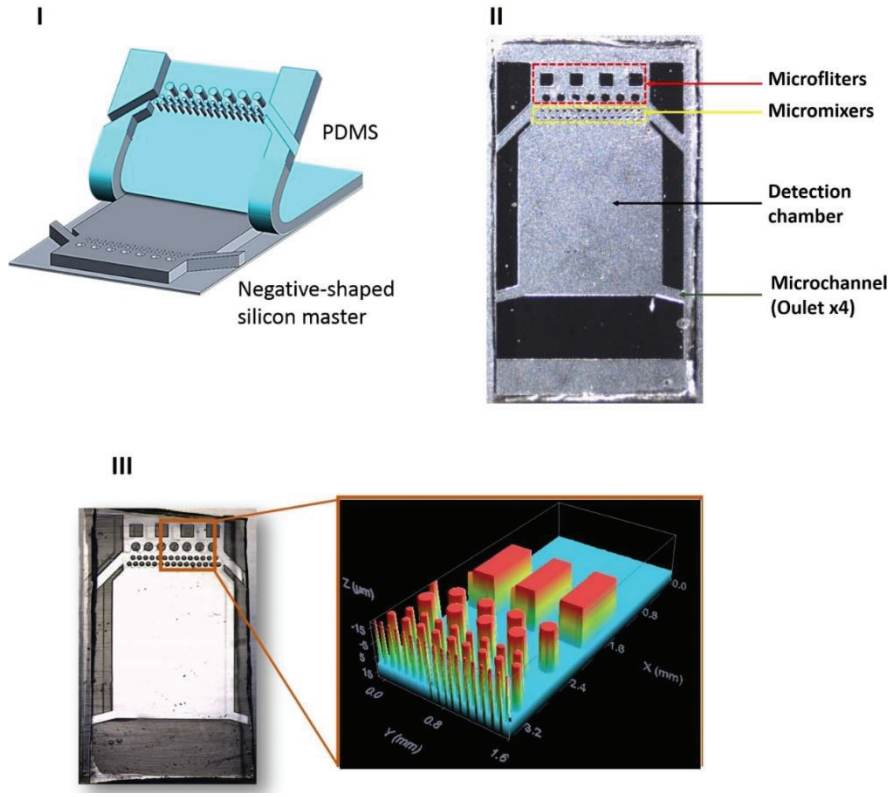

Figure 7. In (**I**), replica molding illustration. In (**II**) PDMS microfluidic structure obtained by replica molding of Si mold. In (**III**), Interferometry image of a part of the PDMS microfluidic structure.

The covalent bonding between the silicon-based transducer and PDMS microfluidic structure was made through O-Si-O bond formation between Me_2SiO_2 group from PDMS and SiO_2 from the silicon transducer as described previously [10–14]. For this purpose, oxygen plasma was applied at 100 mTorr of pressure and 0.4 W/cm^2 during 30 seconds for PDMS and 2 min for silicon transducer. An inert and opaque mask was manufactured in epoxy resin to protect the microelectrodes area from the plasma source. Immediately after the activation process, both subunits (PDMS/transducer) were placed in a conformal contact and immediately an irreversible bonding O-Si-O was formed providing the sealing of the final microfluidic device. At this point the LOC was ready. The microfluidic system has been designed to present a depth of 100 µm when assembled with the potentiometric sensor. Therefore, the liquid sample reaches the detection microchamber through capillarity and then diffuses through the microfluidic system.

In a first stage, the microfluidic LOC fabrication process was evaluated after covalent bonding of PDMS microfluidic structure with a bare transducer. For this purpose, a blue ink was placed at the inlet of the microfluidic system and was let to flow into the LOC through capillary forces. **Fig. 8**, shows a time line at different points where the fluid enters the microfluidic LOC. As a result, no leakage from the microfluidic system was observed. Over a matter of seconds, the droplet was driven by capillarity

throughout the microfilters, and micromixer, reaching the window of electrochemical analyses. This homogenous passive flow of the ink has filled completely the window of analyses which is very important for potentiometric measurements. It was also demonstrated that the microfluidic system was perfectly aligned to the transducer so that the electrodes were inside the chamber of analyses.

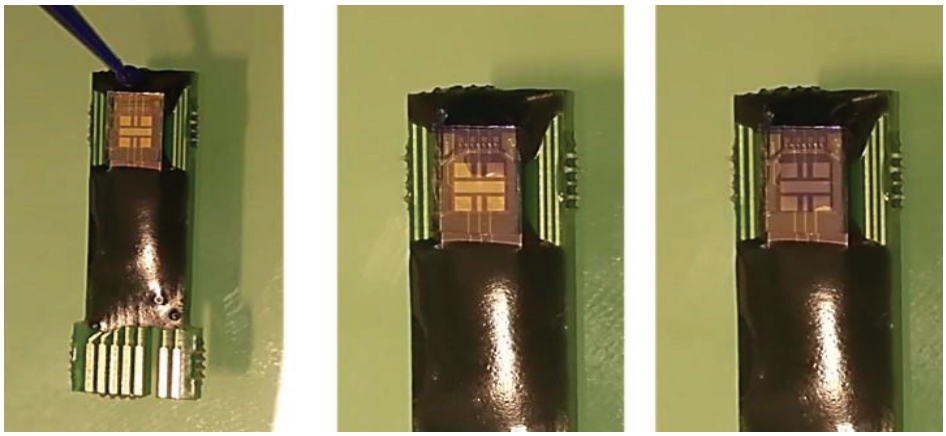

Figure 8. Blue ink flowing by capillarity through the microfluidic LOC at three different times. The device was filled in several seconds.

3.5. Lab-on-a-chip assembly.

The microfluidic LOC assembly was carried out as described in section 2.4. For this purpose, the PDMS microfluidic structure and the Si transducer (holding four ASEs) were irreversibly bonded after surface activation using O_2 plasma. As it can be seen from **Fig. 9**, the PDMS microfluidic structure was designed in such a way to protect the sensitive part of the sensor from harsh environment. For this interest, the inlet of the microfluidic system was placed in the front side and it forms a combination of pillars with different sizes and geometries acting as microfilters and passive micromixers.

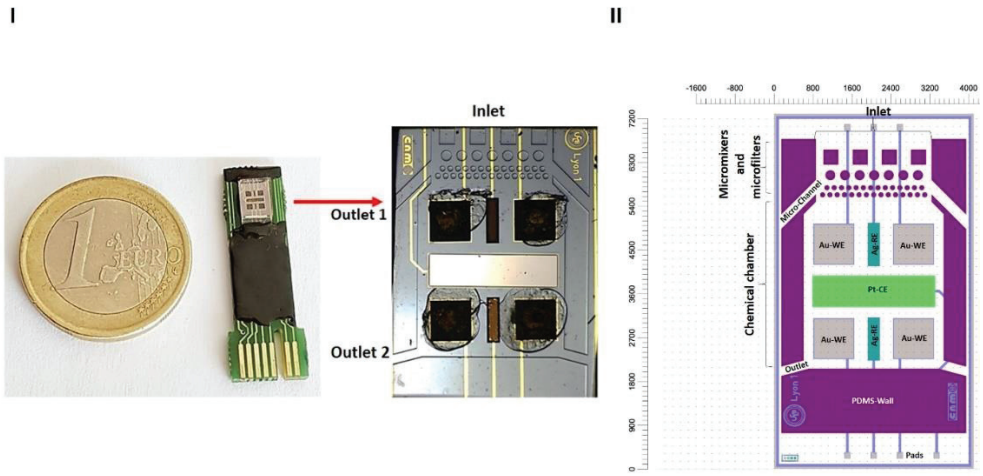

Figure 9. Final microfluidic LOC (**I**) and layout (**II**) of LOC assembly.

3.6. Potentiometric measurements.

3.6.1. Microfluidic LOC calibration.

Once the LOC was assembled, the calibration of the sensing device was performed in laboratory by titration of standard solutions of ammonium chloride from 10^{-8} M up to 1 M in 25 mL of deionized water at pH = 6.1 using the generalized standard addition method (GSAM) [17]. A solution of $(NH_4)_2CO_3$ 2M (denoted as ammonium solution from now) was used for control tests at technical scale with a commercial EC sensor used as time-of-response-reference sensor.

As it has been described in Chapter 1, for any ISE the most sought parameters are the slope, the limit of detection (LOD), the selectivity in the presence of a complex matrix and the time of response. The slope provides information about the electrical-charge interaction between target-compound and membrane. Thus, in the case of a monovalent cation such as ammonium, the ideal value should be close to 59 mV/decade of ammonium concentration according to the Nernst equation (see Chapter 1 Section 4.2). As the ratio NH_3/NH_4^+ strongly depends on the pH value, all measurements were made at constant pH and the sensor's responses were referred to the total ammonium concentration (TAC) as an aqueous equilibrium NH_3/NH_4^+. The ISE's sensitivity is given by the LOD and the time of response (t_{95}) is defined as the time needed by the sensor to achieve the 95 % of the response expected when a detection event occurred. **Fig 10** present the dynamic response of potentiometric measurements carried out using the LOC for ammonium detection following the GSAM. For this purpose, potentiometric measurements were carried out in laboratory using a single-device electrochemical cell following the GSAM. The initial volume was V_0= 25ml of deionized water at pH = 6.1.

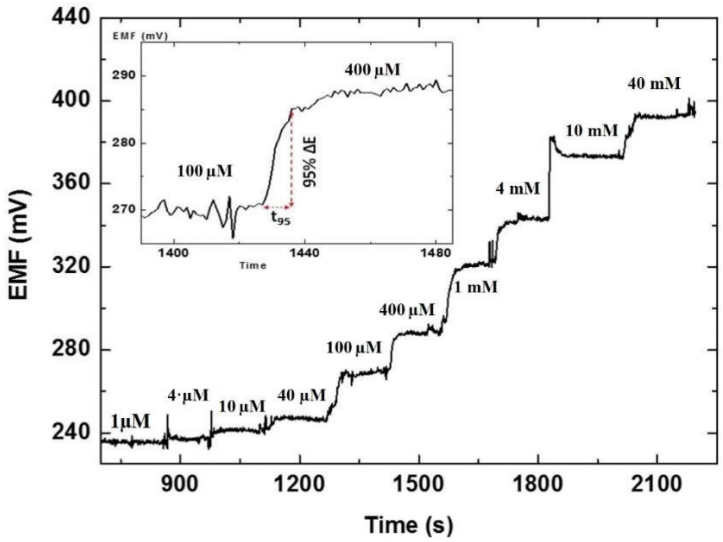

Figure 10. Dynamic response of one of the ASEs included in the microfluidic LOC for step changes in the concentration of NH_4Cl from 1 µM to 40 mM.

The results (see **Table 1**) confirmed that the presence of the microfluidic PDMS structure does not affect the sensor's response so far.

Table 1. Potentiometric characteristic response of the ASEs included in the LOC. Calibration carried out at initial volume, V_0 = 25 mL of deionized water pH = 6.1.

Parameter	ASE
Slope (mV/decade)	55
Lower limit of detection (M)	$4 \cdot 10^{-5}$
Lower limit of linear range (M)	$1.0 \cdot 10^{-4}$
Time of full response (s)	10-12

3.6.2. Evaluation under real conditions.

One of the key factors for a microfluidic LOC that is able to perform continuous and in-situ analysis is the time of response. To evaluate this, the LOC time of response was compared to that of a commercial EC sensor used as reference sensor during the analysis of ammonium-containing samples. In this context, both devices (LOC and EC sensor) were placed in a beaker that contained 200 mL of tap water under stirring and the baselines were recorded until signal stabilization was reached. Afterwards, 20 mL of ammonium solution were added at t = 10 seconds. The LOC time of response was delayed by 15 seconds when compared to the EC sensor response as seen in **Fig. 11**. Subsequently, a second addition of 20 mL of ammonium solution were added once the sensors signals were stable again (at t =130 seconds). Again, the LOC response time was delayed by 15 seconds when compared to the EC sensor response.

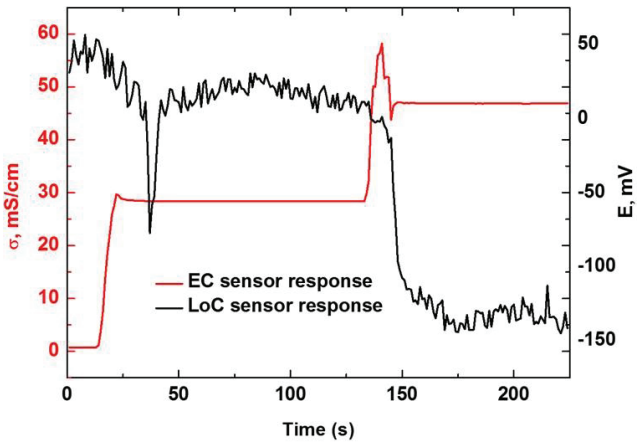

Figure 11. LOC and EC sensor's responses to ammonium containing samples. Initial volume, V_0 = 200ml of tap water.

Afterwards, in order to simulate the laminar flow of sewage, a testbed made of roof gutter (pipe diameter of 75 mm; length: 2 m; slope ~ 2 %) with a partly dammed outlet and supplied with flowing tap water was set up. The flow-rate was set at 2L/min using a peristaltic pump. After reaching stable conditions with tap water, 500 mL of the ammonium solution were pumped into the testbed. The experimental set-up is shown in **Fig. 12.**

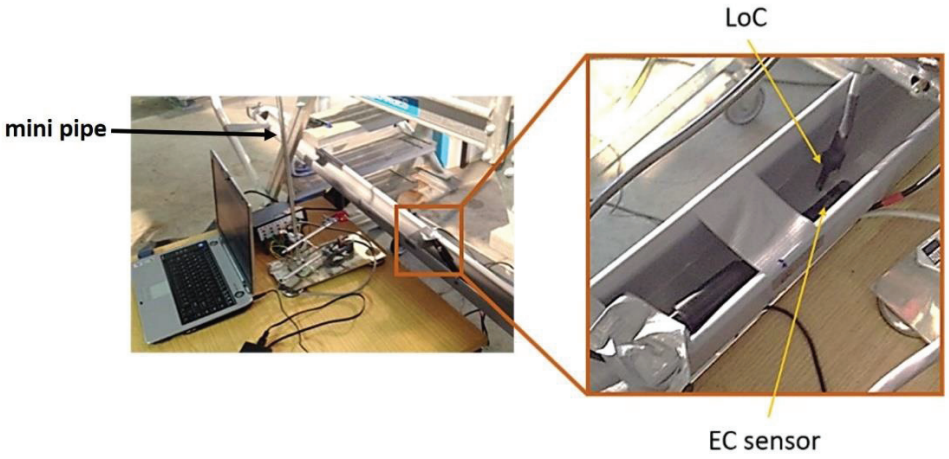

Figure 12. Experimental test-bed set up. LOC and commercial EC-sensor are placed side-by-side in the pipe. The water flow-rate is controlled by a peristaltic pump at 2L/min.

In this case, no delay was observed when the time of response of both the LOC and EC sensor was compared. Since the microfluidic-system's inlet was oriented to the laminar flow applied in the pipe, liquid diffusion is favored and therefore, the sample reaches the LOC's detection chamber faster when compared to the previous test performed in a beaker. Moreover, as the LOC's signal returns to the baseline right after the peak related to the ammonium detection (see **Fig. 13**), it was confirmed that the liquid flows ceaselessly through the microfluidic system creating a continuous stream. The results suggest that in a first stage, the LOC is filled with the sample through capillarity when it was immersed in the liquid medium. Subsequently, as the device is oriented to a laminar flow, diffusion governs the dynamic flow created throughout the microfluidic system.

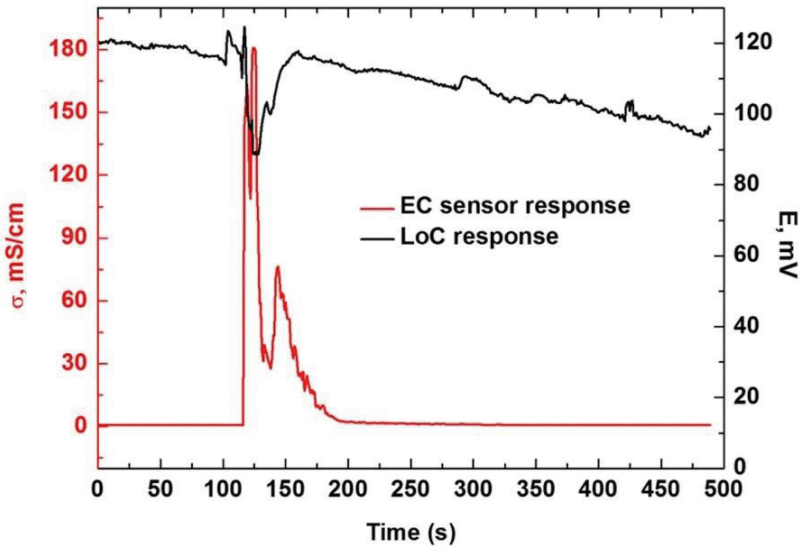

Figure 13. LOC's and EC sensor's responses recorded when 500 ml of ammonium solution were pumped into the testbed. No delay is observed when both the LoC and EC sensor responses were compared.

To finish the evaluation of the device, the microfluidic LOC was immersed in a real municipal sewage pipe at a test-facility in Berlin, Germany, in order to test the robustness of the LOC. The wastewater used in the test facility was pumped from a combined sewer of the Berlin sewer-network into a storage tank which was placed before the testbed (pipe-diameter of 350 mm) at a higher elevation. A flow of wastewater up to 10 L/s could be provided continuously. The respective velocity in the pipe ranged from 0 – 0.6 m/s (and max. 0.8 m/s at 15 L/s). The test-facility is frequently used within the MicroMole project for real-condition tests and it is intended to be used for experiments of the following types:

- short and long term exposure of sensors or parts of sensors to flowing real wastewater in a controlled environment with less strict safety regulations and easy access;
- tests on sedimentation processes to assess clogging phenomena and counter measures;
- re-mobilization of sediments and self-cleaning of sensors due to flushing events in the sewer;
- experiments on dispersion of substances in wastewater in short distances.

In this context, two exposure times were conducted to evaluate the robustness of the LOC when it was immersed in a real wastewater stream. The LOC was set in a plastic module especially designed for sewage application (see **Fig 14** (**II**) and (**III**)) and the ensemble was immersed in the sewage for 15 and 60 min respectively.

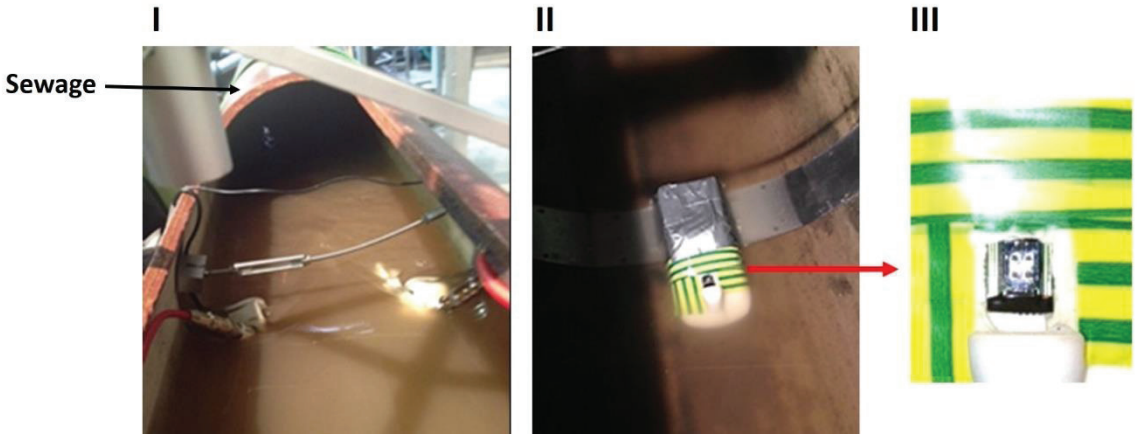

Figure 14. (**I**) Wastewater flowing through the testbed where the LOC was immersed. (**II**) and (**III**) LOC set up in a plastic module designed for sewage applications within the EU-project MicroMole.

Immediately after the microfluidic LOC was removed from the pipe, it was immersed into a beaker with 200 ml of tap water under stirring together with the commercial EC sensor. The objective was to check again the LOC time of response but this time after being submerged into the wastewater stream for 15 min. Firstly, the sensors baselines were recorded. Once LOC and EC sensor reached stable conditions (at t =125 seconds) 20 mL of ammonium solution were added. Here both EC and LOC had the same response time. Subsequently, once the LOC and EC sensor signals were stable again, a second addition of 20 mL of the ammonium solution was added at t = 300 seconds. Once again, it was observed that the response time seen for both the LOC and EC sensors was the same. **Fig. 15** shows the LOC and EC sensor responses to ammonium after being immersed in the wastewater stream for 15 minutes. For both injections, the LOC time of response remains in the same order when compared to the EC sensor's response. This confirmed that the LOC was still functional after 15 minutes immersion in sewage and therefore no clogging phenomenon was observed.

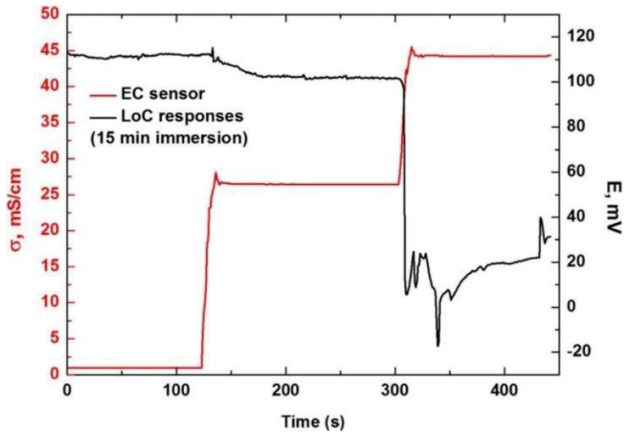

Figure 15. LOC and EC sensor's responses to two additions of 20 mL of ammonium solution after LOC immersion in flowing wastewater for 15 min.

The same previous experience was repeated with 60 min immersion of the LOC in sewage. In this case, the LOC only responded to the second addition of 20 mL of the ammonium solution (see **Fig. 16**) which might be a sign of partial clogging. Moreover, the time of response of the LOC to the second injection was about 20 second delayed, when compared to the previous test where the response was immediate. Therefore, even if the LOC was still functional, the results confirmed the partial clogging at the inlet of the LOC when it was immersed in the wastewater for 60 min. Consequently, a decrease of the flow-rate inside the microfluidic system occurred as the sample start to diffuse more slowly through the LOC and therefore the response time increased.

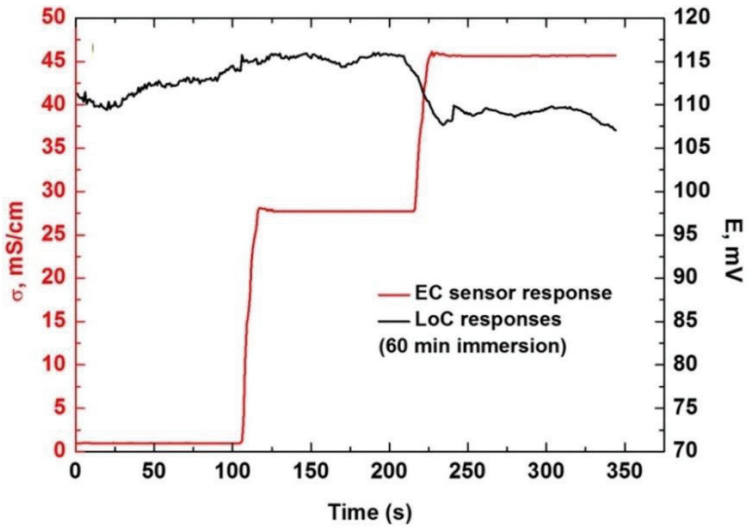

Figure 16. LOC and EC sensor's responses to two additions of 20 mL of ammonium solution after LOC immersion in flowing wastewater for 60 min.

4. Conclusions

A microfluidic Lab-on-a-Chip for real-time electrochemical measurements in wastewater for short periods of time has been developed. The device was manufactured by covalent bonding of two subunits: a PDMS-flexible passive microfluidic structure and a transducer holding an array of four gold working microelectrodes, two Ag/AgCl reference microelectrodes and one Pt auxiliary microelectrode. The LOC was chemically functionalized to incorporate four ammonium-selective microelectrodes and therefore, ammonium-containing samples were analyzed in continuous water-flow successfully. As a result, it was demonstrated that a continuous water stream is created through the microfluidic LOC when it was immersed in a laminar flow of water. Moreover, it was confirmed that the time of response was still comparable to the response of a commercial EC sensor when detecting ammonium-containing samples after being immersed in sewage for at least 15 minutes. Therefore, the low-cost, easy-to-operate and miniaturized LOC developed can be used for in-situ and real-time analysis during short periods of time.

Future work will contribute to develop a waterproof instrumentation that enable chemical analysis directly in wastewater and to improve the microfluidic shape that will highly minimize clogging events when longer exposure times than 15 minutes are required. Nevertheless, even if it is in its early stages of development, the microfluidic LOC reported here suppose a step further in the field of real-time and in-situ sewage monitoring.

5. References.

[1] H. Wang, D.W. Juma, H. Wang, F. Li, Impacts of population growth and economic development on water quality of a lake : Case study of Lake Victoria Kenya water., Environ. Sci. Pollut. Res. 21 (2014) 5737–5746. doi:10.1007/s11356-014-2524-5.

[2] L. Rizzo, C. Manaia, C. Merlin, T. Schwartz, C. Dagot, M.C. Ploy, I. Michael, D. Fatta-kassinos, Urban wastewater treatment plants as hotspots for antibiotic resistant bacteria and genes spread into the environment : A review, Sci. Total Environ. 447 (2013) 345–360. doi:10.1016/j.scitotenv.2013.01.032.

[3] B. Petrie, R. Barden, B. Kasprzyk-hordern, A review on emerging contaminants in wastewaters and the environment : Current knowledge , understudied areas and recommendations for future monitoring, Water Res. 72 (2015) 3–27. doi:10.1016/j.watres.2014.08.053.

[4] L. He, G. Ying, Y. Liu, H. Su, J. Chen, S. Liu, J. Zhao, Discharge of swine wastes risks water quality and food safety : Antibiotics and antibiotic resistance genes from swine sources to the receiving environments, Environ. Int. 92–93 (2016) 210–219. doi:10.1016/j.envint.2016.03.023.

[5] B.P. Bougnom, L.J. V Piddock, Wastewater for Urban Agriculture: A Significant Factor in Dissemination of Antibiotic Resistance, Environ. Sci. Technol. 51 (2017) 5863–5864.

[6] A.K. Awasthi, X. Zeng, J. Li, Environmental pollution of electronic waste recycling in India : A critical review, Environ. Pollut. 211 (2016) 259–270. doi:10.1016/j.envpol.2015.11.027.

[7] S. Castiglioni, K. V Thomas, B. Kasprzyk-hordern, L. Vandam, P. Grif, Testing wastewater to detect illicit drugs :, Sci. Total Environ. 487 (2014) 613–620. doi:10.1016/j.scitotenv.2013.10.034.

[8] Z. Xu, P. Du, K. Li, T. Gao, Z. Wang, X. Fu, X. Li, Tracing methamphetamine and amphetamine sources in wastewater and receiving waters via concentration and enantiomeric profiling, Sci. Total Environ. 601–602 (2017) 159–166. doi:https://doi.org/10.1016/j.scitotenv.2017.05.045.

[9] E. Zuccato, E. Gracia-Lor, N.I. Rousis, A. Parabiaghi, I. Senta, F. Riva, S. Castiglioni, Illicit

drug consumption in school populations measured by wastewater analysis, Drug Alcohol Depend. 178 (2017) 285–290. doi:https://doi.org/10.1016/j.drugalcdep.2017.05.030.

[10] A. Baraket, M. Lee, N. Zine, N. Yaakoubi, J. Bausells, A. Errachid, A flexible electrochemical micro lab-on-chip : application to the detection of interleukin-10, Microchim. Acta. 183 (2016) 2155–2162. doi:10.1007/s00604-016-1847-y.

[11] L. Tang, N.Y. Lee, A facile route for irreversible bonding of plastic-PDMS hybrid microdevices at room temperature., Lab Chip. 10 (2010) 1274–1280. doi:10.1039/b924753j.

[12] A. Baraket, N. Zine, M. Lee, J. Bausells, N. Jaffrezic-renault, F. Bessueille, N. Yaakoubi, A. Errachid, Development of a flexible microfluidic system based on a simple and reproducible sealing process between polymers and poly (dimethylsiloxane), Microelectron. Eng. 111 (2013) 332–338. doi:10.1016/j.mee.2013.02.059.

[13] G.M. Whitesides, E. Ostuni, X. Jiang, D.E. Ingber, Soft Lithography in Biology and Biochemistry., Annu. Rev. Biomed. Eng. 3 (2001) 335–73. doi:10.1146/annurev.bioeng.3.1.335.

[14] Y. Xia, G.M. Whitesides, Soft Lithography, Angew. Chemie Int. Ed. 37 (1998) 550–575. doi:10.1002/(SICI)1521-3773(19980316)37:5<550::AID-ANIE550>3.0.CO;2-G.

[15] M.S. Ghauri, J.D.R. Thomas, Evaluation of an ammonium ionophore for use in poly(vinyl chloride) membrane ion-selective electrodes: solvent mediator effects, Analyst. 119 (1994) 2323. doi:10.1039/an9941902323.

[16] O. Davies, G. Moody, J. Thomas, Optimisation of poly (vinyl chloride) matrix membrane ion-selective electrodes for ammonium ions, Analyst. 113 (1988) 497–500. doi:10.1039/AN9881300497.

[17] B.E.H. Saxberg, B.R. Kowalski, Generalized standard addition method, Anal. Chem. 51 (1979) 1031–1038. doi:10.1021/ac50043a059.

Chapter 4

The Sample Storage Unit

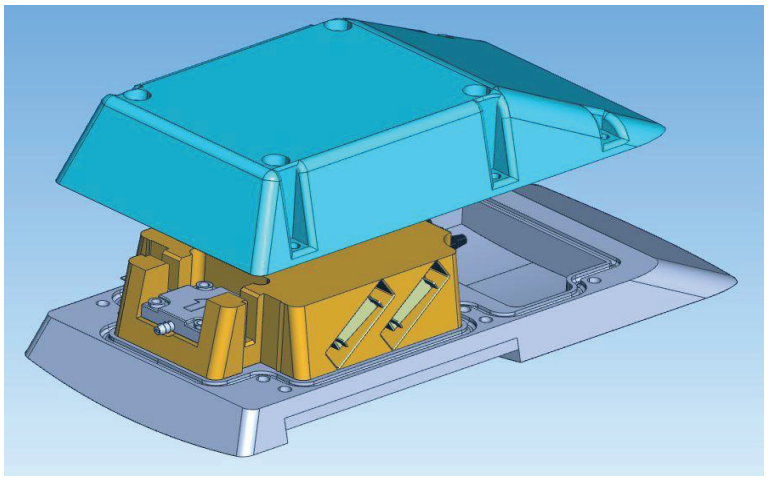

1. Objectives

The aim of this chapter is to present the development of a miniaturized automated sampler, called Sample Storage Unit (SSU). The SSU was fabricated as a single device that contained two manifolds manufactured through 3D printing tecnhology. The main body represents a microfluidic manifold with three independent microchannels that are either opened or closed through the activation of three miniature electrovalves. The manifold includes also a piezoelectric micropump at its inlet that enables to intake the sample. The second manifold was also 3D-printed in a single block of polymer and contained three independent reservoirs whose inlet are connected to the outlets of the previous manifold The SSU purpose was to collect samples from the sewage that ultimately serve as evidences for the forensic police on their investigations related to clandestine laboratories activities. In this context, the automated sampler will be installed in the sewage and will be controlled by serial periphery interface (SPI) communication. The device was powered by an energy harvesting module located at the same place as the automated sampler in the sewage. The SSU was placed several meters behind physical and chemical sensors that continuously analyse the wastewater searching for illicit substances from the Leuckart synthesis (see Chapter 1, Section 3), namely, benzyl methyl ketone (BMK), amphetamine (AMP) and N-formyl amphetamine (NFA). Accordingly, the SSU who initially is on standby mode, is triggered automatically when the sensors have detected an anomaly in the wastewater baseline, commonly extreme pH, electrical conductivity (EC) or the presence of BMK, AMP and NFA. Afterwards, the device stores a sample and then comes back to the standby mode until a new signal is sent by the sensors.

2. A miniature and automated Sample Storage Unit for in-situ collection of forensic evidences in the sewer network.

2.1. Introduction.

Sewage epidemiology has been proven to be a powerful tool to profile a community's behaviour both in large and small areas [1]. The approach is based on the fact that traces of almost everything we consume are released unchanged or as a mixture of metabolites in our daily wastes and ultimately end up in the sewer network [2][3]. Moreover, the vast amount of residues originated nowadays coming from the industrial, municipal or agricultural activities among others, aggravate the quality of wastewater as they present a constant source of traditional and emerging contaminants [4–9]. Accordingly, wastewater quality assessment has become an essential means for environmental monitoring on the last decades. In this context, the sampling strategy is presented as a key factor since the chemical analysis accuracy of wastewater relies directly on the quality and representation of the sample collected [10]. Commonly, the objectives in collecting samples for analysis is to obtain a small but representative portion of the population or the area under study [11]. Such is the case of profiling illicit drug intake by population. Collecting information concerning illicit-drug uses plays a vital role in not only helping law enforcement agencies in prevention and fight against criminal organizations, but also to estimate illegal stimulating substances production and consumption [12,13]. A wide variety of studies have been reported concerning drug abuse in which the sampling strategy varies depending on the goals sought. Thus, the analysis can focus on small areas such as cities [14], middle areas such us a country [14,15] or big areas such as a continent [16,17]. Likewise, the time-frame of sampling differs from one strategy to another as samples can be collected over the course of several days, weeks or months and so the results obtained are representatives of community's behaviour for a short period of time, a spontaneous event or even a habit [11]. Usually, representative samples are the most sought in sewage epidemiology as they adequately reflect the properties of interest of the population being sampled. However, sometimes targeted, or non-representative sample are needed. Frequently, these analyses are collected by the scientific police and used later during trial to help court to render a judgment. An example might be a particular site near an industrial outfall suspected of polluting a river [18]. In such a case, police technicians collect the samples needed at the correct site and time that ultimately will confirm or deny the industry's illegal activities. Conventional wastewater analysis is based on manually taken samples [19-22], subsequent transport to a specialised laboratory and further analysis within a certain period of time. However, due to the high logistic efforts, sampling intervals are usually rather long and can hardly be carried out spontaneously or out of a well-planned sampling campaign as in the case of the MicroMole where the opportunity of collecting a sample will be very limited. Therefore, we report on an automated sampling devices that can be placed on-site in a single

operation and be in standby mode during long periods of times waiting to be triggered by a predefined sampling protocol.

2.2. Automated sampling in sewage epidemiology. The state-of-the-art.

In 2012, A. O. Maldaner et al. [15] published the first study reported until then that estimated the occurrence of cocaine and benzoylecgonine residues in six samples collected from different wastewater treatment plants (WTP) located in the Brazilian Federal District by sewage analysis. In their work, they used an automatic water/wastewater sampler, ISCO-6712, (Teledyne Isco, Lincoln, NE) that was located at the inlet of each WTP where the samples were collected. They used concentrations of benzoylecgonine in the influent sewage to calculate cocaine consumption (kg/ year per 1000 inhabitants) for each region attended by the WTP from two sampling campaigns (March and June, 2010). As a result, they found from 3866 to 2477 ng L^{-1} of benzoylecgonine and 805 to 579 ng L^{-1} of cocaine depending on the region, what supposed an average of more than 13 doses per inhabitant per year in several cases. Likewise, the estimation of amphetamine and methamphetamine uses in Beijing through sewage-based analysis was reported [23]. Here, the same autosampler mentioned previously, the ISCO-6712 from Teledyne Isco, NE (USA) was used together with another automatic sampling system with similar characteristics, FC-9624 from GRASP Science& Technology Co., Ltd., Beijing (China) (see **Fig. 1**). Authors collected influent and effluent samples from all the thirteen sewage treatment plants (STPs) in the urban area during two sampling campaigns. They found methamphetamine concentrations in influents to range from several tens to several hundred ng L^{-1}, whereas amphetamine concentrations ranged from several to several tens ng L^{-1}. They also found that the highest methamphetamine loads were observed in the centre part of the urban area in Beijing, indicating a strong correlation between methamphetamine use and economic level and entertainment activities. Recently, N. Mastroianni et al. [24] published a long term study based on five year monitoring of nineteen illicit and legal substances of abuse at the inlet of a wastewater treatment plant in Barcelona. For this purpose, they used the automated sampler ISCO-6712 that was programed to collect 50 mL every 10 min in the time of the year corresponding with the low season for tourism. Analysis of the selected drugs and metabolites in the wastewater samples was performed by means of two methodologies based on liquid chromatography-tandem mass spectrometry. As a result, the authors concluded that alcohol followed by cannabis, cocaine, amphetamine-like compounds, and methadone were the most consumed drugs. Alcohol, cannabis, and cocaine consumption were on average 18 mL (14 g)/day/inhabitant (>15), 38 g/day/1000 inhabitants aging 15–64, and 2.4 g/day/1000 inhabitants aging 15–64, respectively. As for drug use trends, consumption increased over the 5 years monitored for all drugs, but for heroin and diazepam.

Local tobacco consumption was also assessed by sewage analysis [25]. Authors followed the concentration of cotinine, trans-3′-hydroxycotinine, cotinine-N-β-glucuronide and trans-3′-hydroxycotinine-O-β-glucuronide which are product excreted in urine following the intake of nicotine. In their sampling strategy, they used two automated sampler systems; Liquiport 200 from Endress Hauser, Weil am Rhein, (Germany) and Sigma SD900 from Hach−Lange, Derio, (Spain). Composite sewage samples were collected during 1 week in three different years in Santiago de Compostela (Galicia, Spain). They found that cotinine and trans-3′-hydroxycotinine concentrations of 0.3−1.9 μg L^{-1} and 1.0−3.3 μg L^{-1}, respectively to be the more present biomarkers. Thereby, the average nicotine consumption derived was in the 1.7−1.9 mg/day/person range, being comparable to those derived from tobacco sales statistics.

Figure 1. Commercially available automated samplers reported in the scientific community for sewage epidemiology: (**I**) ISCO-6712 from Teledyne Isco, NE, (USA), (**II**) FC-9624 from GRASP Science & Technology Co., Ltd., Beijing (China), (**III**) SD900 from Hach−Lange, Derio, (Spain) and (**IV**) Liquiport 200 from Endress Hauser, Weil am Rhein, (Germany).

2.3. Sample Storage Unit fabrication.

For the fabrication of the SSU, a deep research on the best active fluidic (pumps and valves) components that are commercially available has been done firstly. Here, some criteria were applied such as: high miniaturization, low power consumption and robustness. Those requirements are mandatory as we aimed to implement the SSU in such a harsh and inaccessible environment as sewage. Secondly, two manifolds were developed as the main part of the automated sampler: one microfluidic manifolds that served as support for the micropumps and electrovalves and another that contained three reservoirs for sample storage.

2.4. Active fluidic components.

In this section, the active fluidic components chosen for the SSU are described. An extensive market research has been performed in order to find the best components that can work reliably in sewage and are adapted to the specifications reported within the MicroMole project. To fulfil such specifications, they have to be as much miniaturized as possible but should work under harsh conditions and provide enough power and robustness to be in contact with sewage water. In addition, low power consumption is required as the entire system must be operational using a 3200 mA/h Li-ion battery. In this way, only two piezoelectric micropumps from two companies, Dolomite Microfluidics and Bartel's Mikrotechnik and one electrovalve from Takasago INC, were found that initially fulfilled the criteria mentioned. Therefore, they were purchased and tested.

2.4.1. Stainless steel piezoelectric micropump..

Dolomite microfluidics manufactures a miniature stainless-steel-based (SS) piezo-electric micropump suitable for small volumes of fluid within microfluidic applications with low power consumption (see **Table 1** for the specifications).

Table 1. Specifications of Dolomite's SS-piezoelectric micropump

SS piezoelectric micropump	
Maximum flow rate	3.5 ml/min
Maximum pump pressure	90 kPa
Applied voltage range	0 – 120 Vpp
Applied frequency range	1 – 200 Hz
Power consumption	7.5 mW

Operating temperature	5 – 50°C
Wetted materials	Stainless steel
Body Dimensions	7 x 7 x 2 mm
Connection (mm)	Gasket to custom interface (manifold mounting)
Weight	0.38g

The piezo-electric micropump was manufactured together with a control board (driver) and a software.

The driver enables to deliver a maximum voltage up to 120 Vpp to the micropump. **Table 2** shows the driver specifications.

Table 2 Control board specifications.

Control Board (provided by Dolomite)

Input Voltage	5V (USB bus power)
Output Frequency	1-350 Hz
Output Voltage	±10V - ± 80 V (1V resolution)
Drive mode	Continuous and intermittent (variable duty cycle)
Power consumption	85 mW
Operating temperature	0 – 50 °C
Dimensions	20 x 20 x 7 mm
Weight	3.3g
Software	Provided by Dolomite-microlfuidics

As it can be seen from **Fig. 2**, the size of this micropump is one of the greatest advantages, as the ensemble micropump and control board is highly miniaturized (7x7x2 mm for the micropump + 20x20x7 mm for the control board). Moreover, it is low power consumption (7.5 + 85 mW), the flow

rate is reasonably high (3.5 ml/min max.), it is lightweight (0.38g + 3.3g) and offers excellent chemical resistance as the wetted parts are made of stainless steel.

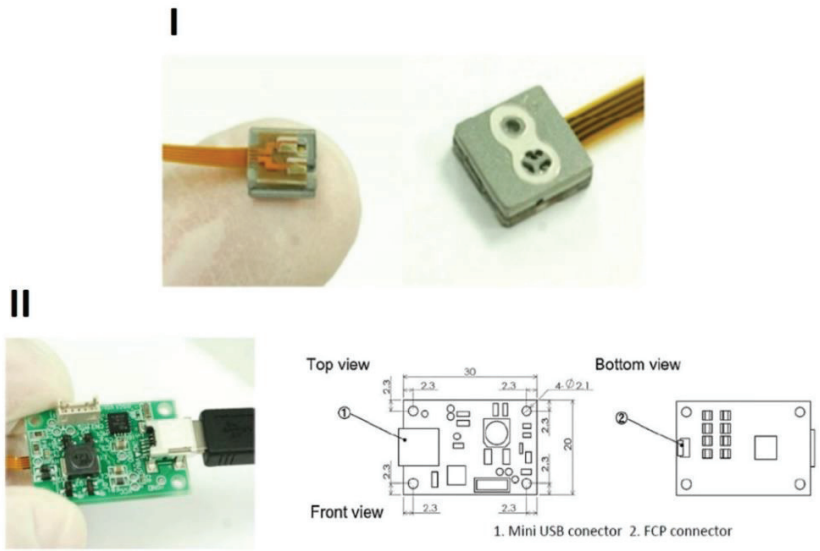

Figure 2. In (I) SS-piezoelectric micropump purchased from Dolomites. In (**II**) the control board provided with the micropump.

The components were purchased and tested in the laboratory. For this purpose, a manifold adapted to the SS piezoelectric micropump was designed and produced in polymethylmetacrilate (PMMA) material as shown in **Fig 3**.

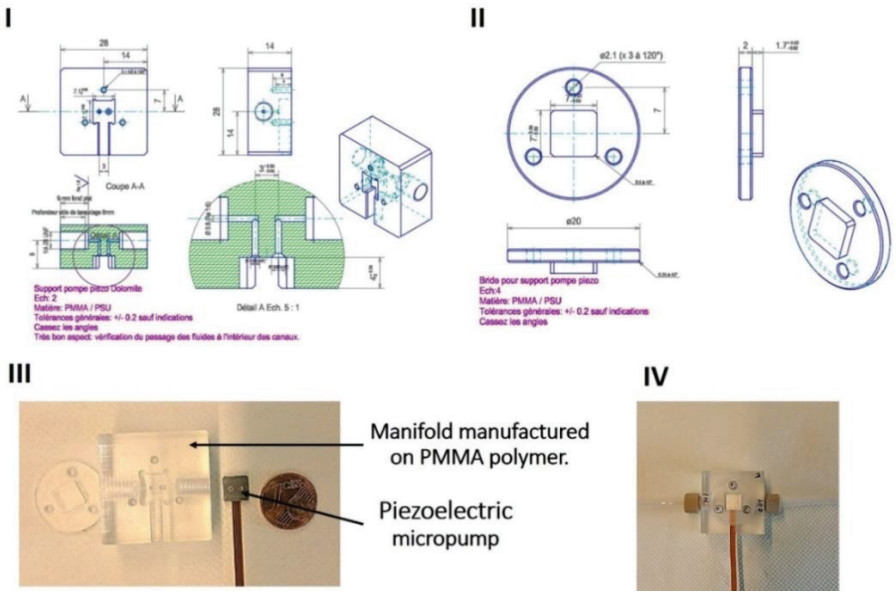

Figure 3. (**I**) CAD 3D of the manifold designed to host the Dolomite's SS piezoelectric micropump**.** (**II**) CAD 3D of the lid designed to seal the manifold**.** (**III**) Manifold and lid manufactured in PMMA polymer and SS piezoelectric micropump**.** (**IV**) Manifold and SS piezoelectric micropump final assembly**.**

The performance of the piezoelectric micropump was evaluated in laboratory using deionized water first, then tap water and finally wastewater. The best flow rate reached in the first two cases (deionized and tap water) was 2 mL/min approx. when operating at 120 Vpp and 100 Hz. Secondly, a test was performed using pre-filtered wastewater. However, the SS piezoelectric micropump presents a major drawback as it can be damaged if foreign particles of greater than 10 µm enter inside. Thus a pre-filter of 8 µm was used. As a result, the micropump was not powerful enough to overcome the pressure created when such a small pore-sized filter was used. Therefore, this component was discarded for the final application.

2.4.2. Piezoelectric diaphragm micropump, mp5.

To remediate those drawbacks, another piezoelectric micropump that was slightly bigger and more robust was purchased from Bartels Mikrotechnik. They manufacture a range of micropumps that are small in size and low in weight, with good particle tolerance, temperature resistance and low power consumption. In this case, the mp5 micropump was chosen. It contained a piezo ceramic that is mounted on a coated brass membrane (diaphragm). The diaphragm is deformed when voltage is applied and thus the fluid is pumped through the vibration of the diaphragm. The specifications are shown in **Table 3.**

Table 3. mp5 piezoelectric micropump specification.

mp5 diaphragm piezoelectric micropump	
Maximum flow rate	5 mL/min
Maximum pump pressure	250 mbar
Applied voltage range	0 – 250 Vpp
Applied frequency range	1 – 100 Hz
Power consumption	<200 mW
Operating temperature	5 – 70 °C
Wetted materials	Polyphenylsulfone (PPSU), polyimide (PI) and nitrile butadiene rubber (NBR)
Body Dimensions	14 x 14 x 3.5 mm
Connection (mm)	Barbed tube clip, (outer diameter 2mm, length 3mm)
Weight	0.8g

A driver can be purchased from Bartels Mikrotechnikand to control the piezoelectric micropump (see **Fig 4**). The mp6-OEM controller drives the pump at adjustable performance in a package similar to an

integrated circuit. The advantage of this component is that not external software is required. The mp6-OEM driver is powered using an external power supply (battery) what makes the ensemble suitable for the MicroMole application.

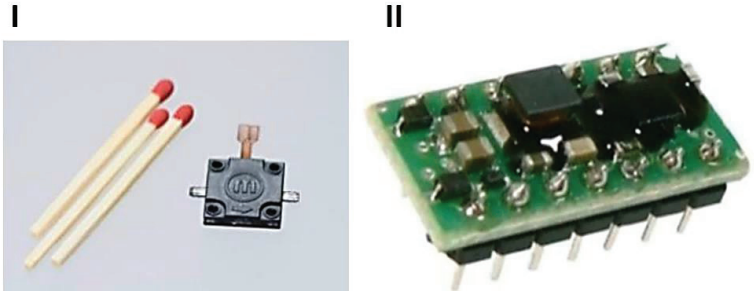

Figure 4. (**I**) Diaphragm piezoelectric micropump purchased from Bartels Mikrotechnik. (**II**) mp6-OEM driver.

The performance of the micropump was tested in laboratory using distilled water first, then tap water and filtered wastewater finally. For this purpose, the miniature control board mp6-OEM driver (see **Fig. 4** (**II**)) was purchased from the same company to actuate the pump. All test were carried out using an external power supply connected directly to the driver. As a result, the mp5 micropump showed to be much more robust when compare to the SS-pizeoelectric micropump purchased from Dolomite. It was able to pump from wastewater for long periods of time using a 250 µm pore-size filter.

A calibration was carried out to evaluate the flow rate dependency with regards to the frequency applied to the piezoelectric. Moreover, it has served as well to evaluate the impact of the power consumption at the different flow-rates applied. The calibration was carried out using tap water and the corresponding plot is shown in **Fig. 5**.

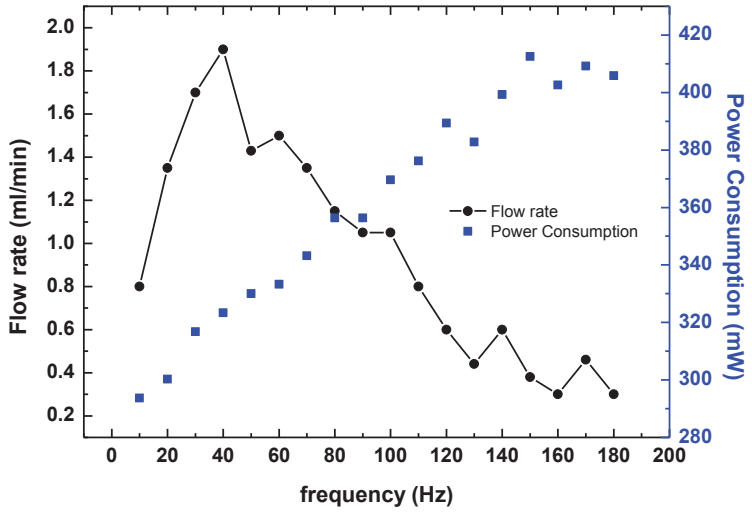

Figure 5. Calibration curve showing the flow rate and power consumption dependency with the frequency applied to the piezoelectric actuator.

In one hand, the results indicated that the flow rate increases with the frequency to a maximum of 40 Hz (2 mL/min) then it decreases drastically when higher frequencies than 40 Hz are applied. The piezoelectric works as a diaphragm that opens and closes periodically and whose rate depends directly on the frequency applied. Thus, higher frequencies, implies that the diaphragm opens/closes so fast that liquid do not have enough time to enter the piezoelectric and therefore, the flow rate decreases as only a few open/close cycles are effective in pumping the liquid. It was also found that the flow rate is highly affected by the fluid viscosity. When the frequency is decreased to 40 Hz the open/close timing is synchronized with the highest volume that fits the diaphragm so that the flow rate increases. On the other hand, the power consumption rises linearly with the frequency applied to the piezoelectric micropump.

In conclusion, and based on the resulted obtained, the mp5 micropump was chosen for our application as it is still highly miniaturized, needs of low power to actuate and is much more robust when compared to the SS-piezoelectric micropump from Dolomite.

2.4.3. Miniature electrovalve, SMV.

Complementarily to the micropump, a market research on the best electrovalves was carried out. The electrovalves have served to open/close the microchannels that connect the inlet of the SSU to the reservoirs where the samples will be stored. The shape-memory-alloy electrovalves from the serie SMV-2R-BN1F (see **Fig. 6**) were purchased from Takasago Electric, INC. Japan. Three electrovalves in the normally closed (NC) mode were installed in the microfluidic manifold to create three independent microchannels that ended up in three reservoirs. The electrovalves specifications are shown in **Table 4**.

Table 4. SMV-2R-BN1F electrovalve specifications.

Shape-memory-alloy electrovalve SMV-2R-BN1F (Takasago Electric, INC)

Type	2-way (NC)
Orifice diameter	0.4 mm
Operating pressure IN	0 – 80 kPa
Operating pressure OUT	1 – 30 kPa
Temp. range	5-40 °C
Current	250 mA
Voltage	3.1 V
Wetted materials	Perfluoroelastomer

Body Dimensions	4 x 16 x 16.5 mm

The Takasago valve uses a shape-memory alloy actuator which resistor drops by -25% during the mechanical change of state. This drop occurs after 450 ms in the 250 mA constant-current test setup, and it might be possible to observe the state of the actuator via this drop in resistance. It implies that the valve must be supplied with 250 mA to be open but it can be kept open at 150 mA reducing therefore, the power consumption.

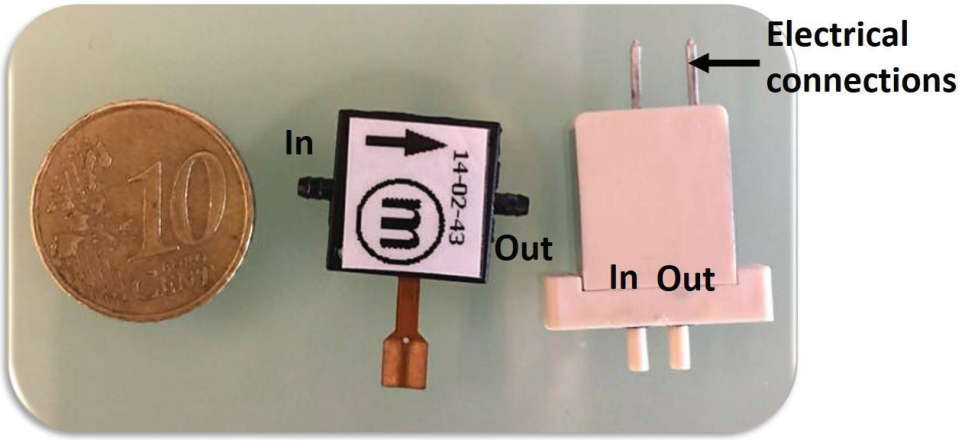

Figure 6. Image of mp5 piezoelectric micropump (in the middle) and SMV-2R-BNF1 electrovalve (right).

2.5. Sample Storage Unit first prototype.

A first prototype was built up to validate the principle-of-proof of the SSU as well as to evaluate the performance of the fluidic components chosen during some tests in real conditions. For this purpose, the mp5 micropump, the mp6-OEM driver and three electrovalves similar to the series SMV-2R-BNF1 were mounted in a platform that contained a microfluidic manifold made in polysulfonate polymer (PSU) and consisted of several independent microchannels as it can be seen in **Fig 7**.

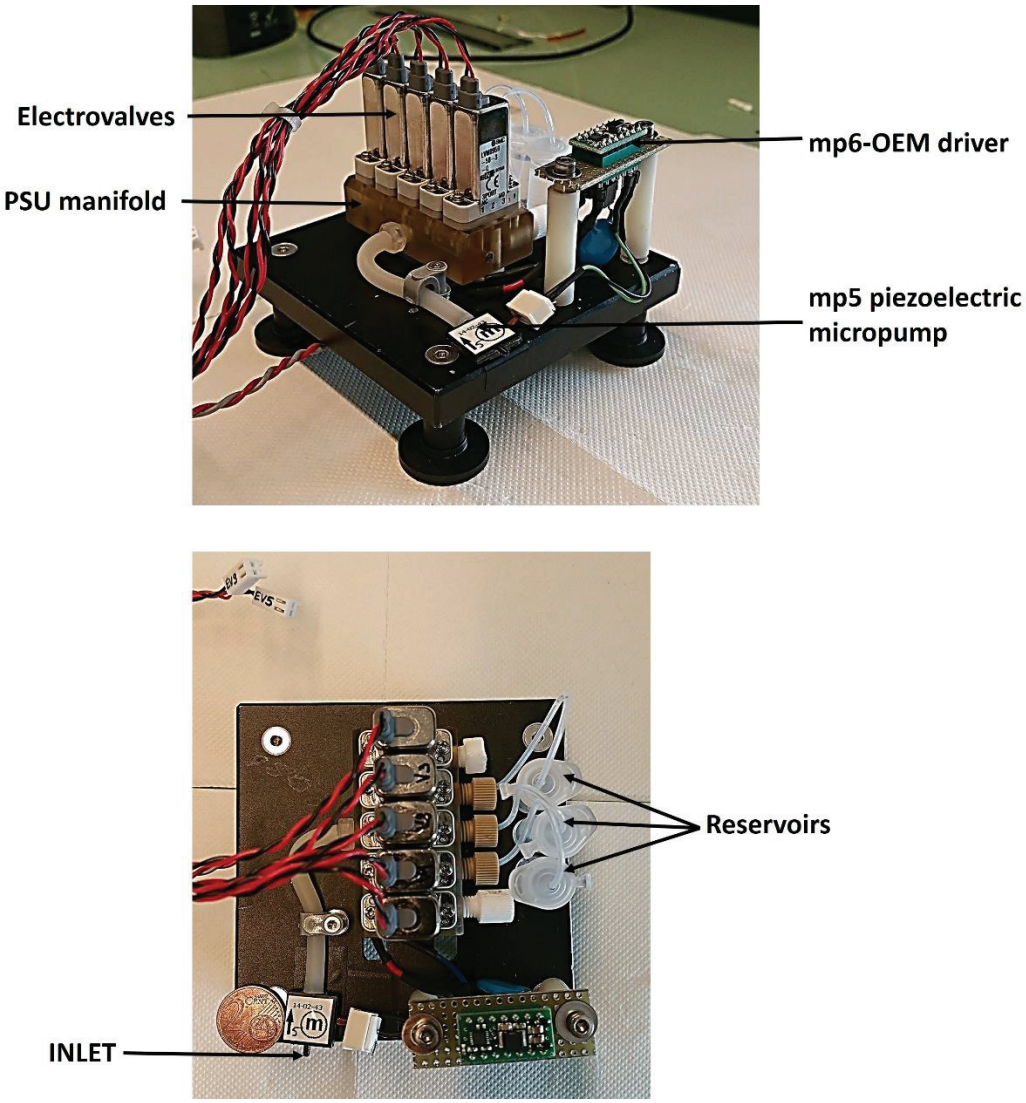

Figure 7. Sampling unit first prototype including one mp5 micropump, mp6-OEM driver, five electrovalves from which three were connected to three reservoirs and microfluidic manifold mounted in a platform

The system was controlled using an external flow-controller provided by the company BioTray, France, the FlowTest™ , and a personal computer. The first prototype was tested in laboratory using tap water and filtered wastewater as follow. A capillary was adapted to the inlet of the mp5 micropump in one extremity and was immersed into a beaker at the other extremity. An external power supply was connected to the system enabling to actuate the piezoelectric micropump. The electrovalves were connected to the FlowTest™. At this point, the system started pumping and the sample was collected from the beaker passing through the micropump, one of the electrovalves and the microfluidic manifold to end up into one of the three Eppendorf provided. Results confirmed that the system was able to store up to three independent samples of 1.5 mL successfully in 60 s approx.

Afterwards, the system was evaluated under real conditions. For this purpose, a test campaign was carried out at the Berlin Center of Competence for Water (KWB) facilities in Berlin, Germany. The setup consisted of a long capillary installed in a housing module specially designed for the MicroMole project and fixed into a sewer pipe. A 250 µm filter was set at the inlet of the capillary to protect the system from big particles. The outlet of the capillary was connected to the mp5 piezoelectric micropump mounted in the platform who intakes the sample and drive it through the manifold up to one of the three reservoirs (see **Fig. 8**).

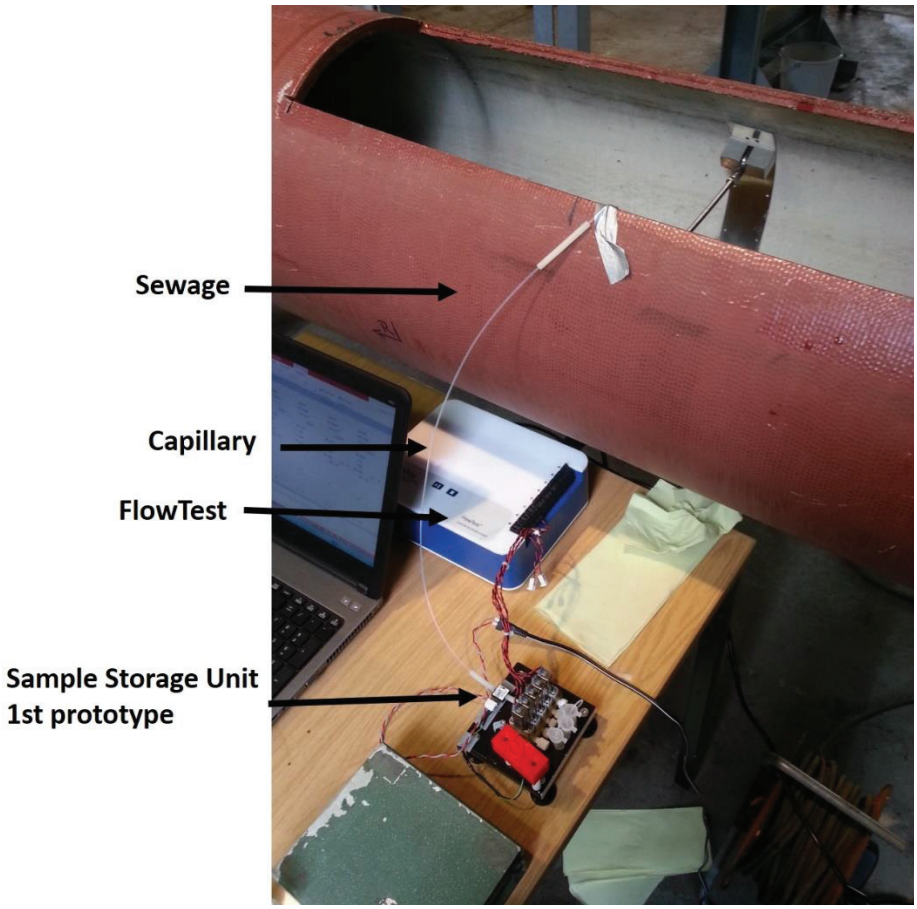

Figure 8. Experimental setup to evaluate the performance of the sample storage unit first prototype under real conditions.

During the tests campaign, the principle-of-proof was validated as the system was able to store samples for a whole week with good repeatability. The microfluidic device's inlet with the filter were immersed in the pipe for several days to evaluate possible clogging. It did not appear to affect the device as it was still operational after exposure to the sewage for longtime.

2.6. Microfluidic manifold.

The microfluidic manifold and the reservoirs were designed using SolidWorks 3D modeling software and were printed using a Projet MJP 3600 Max 3D printer from 3D Systems France, SARL. The automated sampling device's main body was divided into two manifolds whose CAD 3D are shown in **Fig. 9**. A first microfluidic manifold was designed to contain three microchannels with an internal diameter of 1 mm. They meet at the inlet of the fluidic path where the mp5 micropump is located. Afterwards, they are separated into three independent microchannels by means of three SMV-2R-BNF1 electrovalves. Thus, the sample is driven through one of the three possible fluidic ways when the micropump and one of the three electrovalves are switched-on at the same time. A second manifold was designed as a single piece to store up to three samples of 2.3 mL capacity. Both manifolds were designed so that the inlet of the three tanks meets with one of the microchannel's outlet as it is shown in **Fig. 9** (**III**).

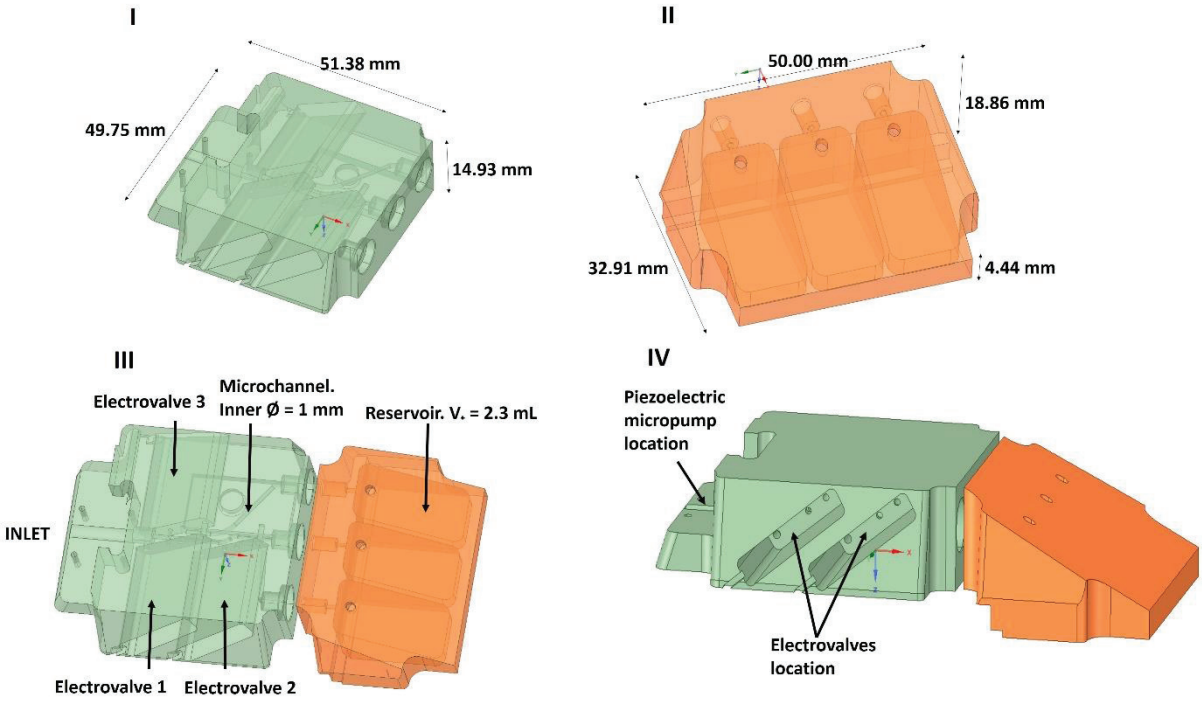

Figure 9. (**I**) CAD 3D of the microfluidic manifold. It contains three independent microchannels with an internal diameter, $Ø_{inner}$ = 1 mm and the locations for three electrovalves and one mp5 micropump. (**II**) CAD 3D of the manifold containing three reservoirs to store the samples collected. Each reservoir has a capacity of 2.3 mL and they are connected to the three outlet of the microfluidic manifold. Once the samples were collected, the reservoirs can be removed for further analysis and be replaced by a new manifold. (**III**) and (**IV**) show the assembled CAD 3D of the two manifolds that form the main body of the automated sampling device.

The manifolds were manufactured into two single blocks of polymers by means of a high resolution 3D printer that uses multijet printing (polyjet) as printing process. The Visijet M3 Crystal was the material used in this case. It was chosen as it presents good transparency as well as very good chemical resistance which are essential features for microfluidic applications. The Polyjet technology is based on micro-droplets of the liquid material that are deposited on the working platform to partially soften the previous layer of material and solidify as one piece during the material jetting process. When all the layers are deposited as one part, the object is removed from the building platform to remove the support material. This phase-change methodology enables to achieve a maximum resolution of 16 µm between the layers that are deposited. As it can be observed from **Fig 10** the printing process was successfully accomplished giving as results two block of transparent polymer in which the features are highly defined.

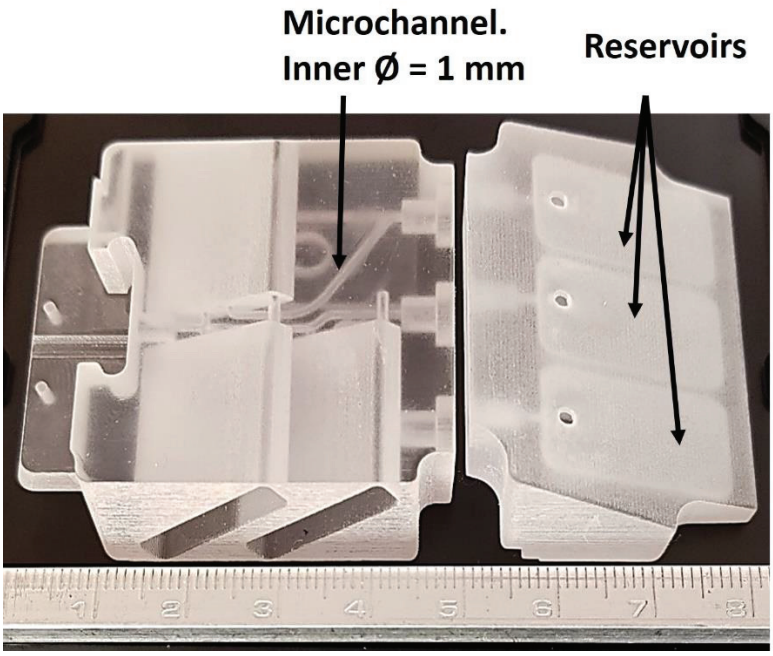

Figure 10. Image of transparent manifolds manufactured using the Projet MJP 3600 Max 3D printer.

2.7. Customized control board.

A customized printed circuit board (PCB) (see **Fig. 11**) has been designed to control the automated sampling system. Its main element is the microcontroller MKL03Z32VFK4 with Cortex-M0+ core (U1), purchased from NXP Semiconductors. Additionally, the mp6-OEM driver to operate the piezoelectric micropump, mp5, was integrated into the mainboard. The electronic circuit was designed in such a way that it fulfilled not only the basic requirements for switching on and off the mircopump and the electrovalves when needed, but also to provide additional capabilities in order to increase its versatility and energy efficiency. The microcontroller controls the amplitude and frequency of the supplied voltage

needed to actuate the piezoelectric micropump so that the flow rate can be adjusted. For this purpose, the appropriate input pins of mp6-OEM circuit (CLK, AMP) are connected to the microcontroller pins.

The three SMV-2R-BN1F electrovalves are current-driven. AOZ1083 was used as a high frequency switching current source in buck topology. In this application the AOZ1083 was chosen mainly because of the very low current feedback voltage (280 mV), which minimizes the power dissipation of the external sense resistor, and therefore, increasing its efficiency. In order to adjust the provided current, a current-sense circuit consisting of two resistors (R2 and R3) and one transistor (Q5) is included in the design. In the first phase, to open the valve, the transistor is turned on. The resultant resistance in the current sense-circuit is low, so current flowing through the valve coil is high (250 mA). Afterwards, when only a holding current is needed, the transistor is turned off what increases the value of the resultant resistance of the current-sense resistor and reduces the valve driving current to about 180 mA. Selecting the valve which should be open is achieved by switching on individual transistors Q1-Q4. Gates of every transistors and the EN input (enable) pin of the AOZ1083 are connected to the microcontroller pins. Thus, the entire valves-driving process is controlled by microcontroller.

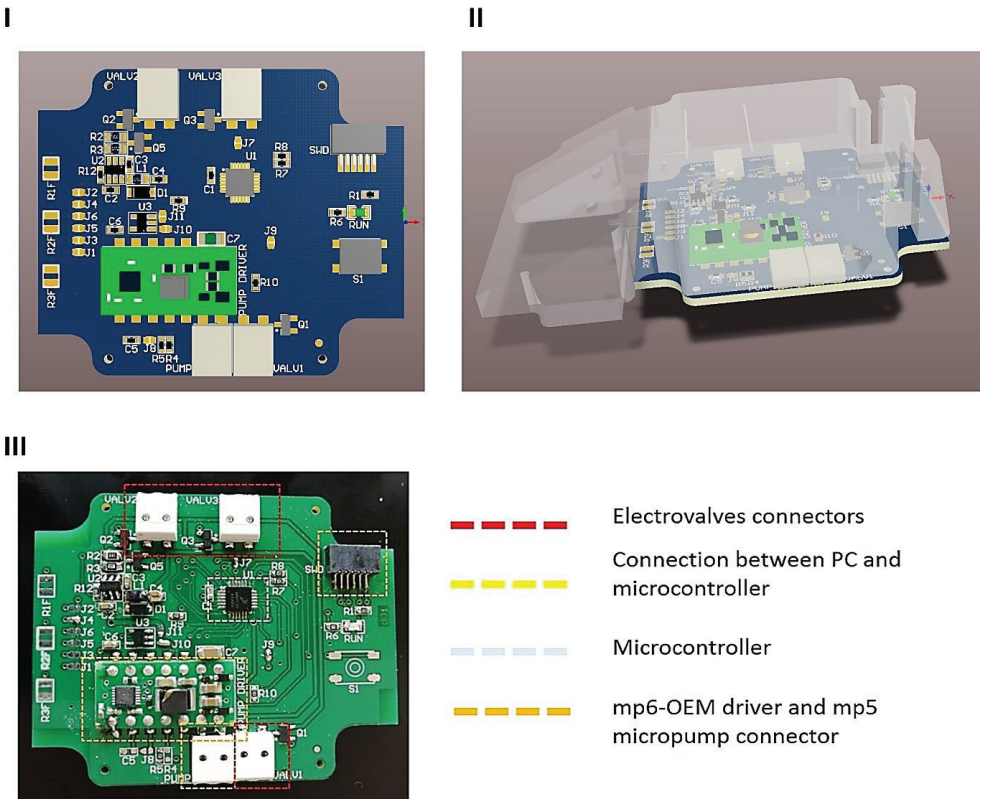

Figure 11. 3D CAD of (**I**) electronic board and (**II**) automated sampling unit and PCB assembly. In (**III**) a picture of the PCB fabricated is shown.

2.8. Evaluation of the Sample Storage Unit final device.

The performance of the final automated sampling device has been evaluated by collecting samples both in static and flowing conditions for the detection of chemical markets related to illegal amphetamine synthesis that were ultimately analysed by GC-MS chromatography at the Central Laboratories of Forensic Police (CFLP) in Warsaw, Poland. For this purpose, the manifold previously manufactured was assembled with the corresponding mp5 micropump, the three electrovalves and the homemade control board as seen in **Fig. 12**. Additionally, a metallic filter with a pore size of 250 µm was located at the inlet of the automated sampler to protect the microfluidic system from big particles.

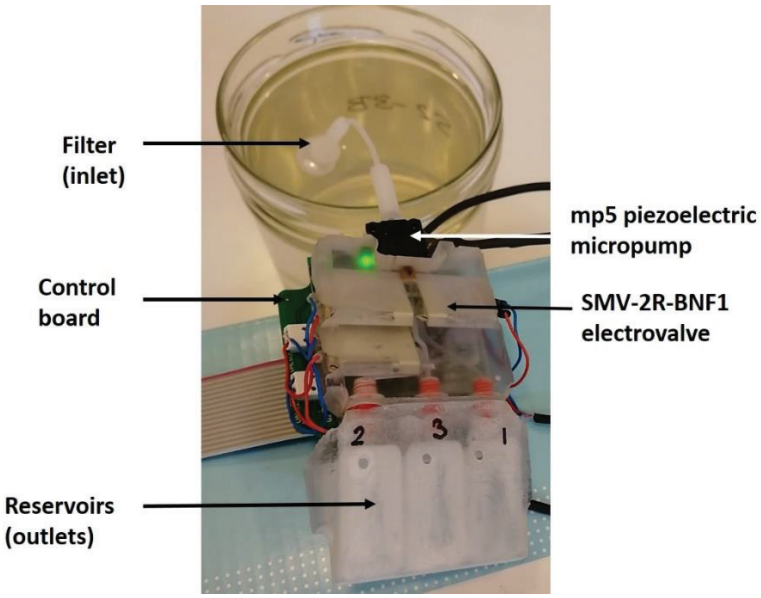

Figure 12. Image of the Sample Storage Unit during a laboratory test.

Since the aim of the Sample Storage Unit is to store samples that can serve as evidence for the forensic police investigations related to illicit drugs laboratories locations, some parameters such as sampling time, cross-contamination of taken samples and stability of samples stored in tanks for long periods of time were evaluated at the CFLP facilities.

The sampling time has been established as one of the key parameters when evaluating the device's performance. This is due to the dilution effect of markers of interests flowing from a discharge point through the sewer. Therefore, as the automated sampler is triggered by physical and chemical sensors located several meters before it in the sewer, when a discharge event occurs it needs to intake the sample quick enough so that it is representative from what the previous sensors responded to. For example, in the case that sampling time is too long the collected sample might be diluted enough so that the concentration of the marker would not be detectable using the GC-MS.

Cross-contamination was also evaluated. It represents an important parameter as the three reservoirs share the same inlet. Therefore, contamination can occur if the dead volume of liquid stored in the microchannels and the filter is important. However, the microfluidic design has been made so that dead volume represents less than 2% of the total sample stored.

Finally, the stability of samples stored for long time was also studied. It can happen that an interval of several days pass between two samples were stored. Therefore, the chemical stability of both the sample and the container must be evaluated so that it can be estimated the time of residence of a sample once it has been stored.

2.8.1. Static conditions.

In a first stage, the automated sampling was evaluated in static conditions. Here, the objective was to evaluate the repeatability and the time needed for sampling as well as the volume collected. For this purpose, several solutions containing benzyl methyl ketone (BMK), amphetamine (AMP) and N-formyl amphetamine (NFA) were prepared which are the markers that are expected to be found in the wastewater matrix near clandestine laboratories. All samples were collected in static condition. Therefore, the SSU was placed near to a beaker that contained 800 mL of any substance. The device was started pumping at the highest flow rate (frequency, f = 40 Hz), and the first sample was collected until one reservoir was filled. Subsequently, the same procedure was repeated to fill the other two reservoirs and once the three tanks were full, the manifold was removed, the samples were transferred to glass tube for further GC-MS analysis, they were cleaned with tap water and were placed again in SSU to continue the experiments. **Table 5** summarizes the solutions prepared and the results obtained.

Table 5. Characteristics of samples collected in static mode**.**

Type of substance (carrier/marker)	**Concentration of marker [µM]**	**Volume [ml]**	**solution pH**	**EC of solution (mS)**	**Time of sample collection**	**Volume of collected sample [ml]**
Pure water	-	800	7,91	0,193	53 s, 49 s, 54 s	1.9; 2.0; 2.1
Water/BMK	300	800	8,14	0,192	43 s	2.0
Water/AMP	300	800	8,98	0,182	47 s	2.0

Water/NFA	300	800	8,14	0,185	53 s	2.0
Water/BMK	1875	800	8,04	0,193	61 s	2.2
Water/AMP	1875	800	9,87	0,192	58 s	2.1
Water/NFA	1875	800	8,17	0,193	61 s	2.2
Water/BMK	3750	800	8,01	0,192	66 s	2.2
Water/AMP	3750	800	10,22	0,191	78 s	2.2
Water/NFA	3750	800	8,14	0,192	80 s	2.2
Sewage /BMK	300	800	7,73	0,144	41 s	2.0
Sewage /AMP	300	800	7,82	0,146	32 s	2.0
Sewage /NFA	300	800	7,74	0,144	33 s	2.0
Water/NaOH	300 BMK/AMP /NFA	800	11,94	1,046	50 s	2.0
Water/HCl	300 BMK/AMP /NFA	800	2,25	0,154	68 s	2.1

Results indicated that all samples were collected satisfactorily. In most cases the sampling time was less than 60 s and only for samples with the highest concentration of markers this time was longer probably because of high viscosity of BMK and NFA and AMP at high concentration. During around 60 s of sampling about 2 ml of sample were collected in every case and this volume was found to be representative enough when it was analysed by GC-MS in forensic laboratory according to police officers.

2.8.2. Dynamic conditions.

Results reported in section 2.61 were confirmed by evaluation of the SSU under dynamic conditions. In order to perform the experiments with flowing water, a testbed made of roof gutter was setup as shown in **Fig. 13**. Different solutions were prepared to be discharged in flowing water as reported in **Table 6**.

The moment of sampling was triggered manually following the signal of commercial pH and conductivity sensors located before the sampling module in the pipe so that real situation was simulated. As the pH and EC sensors were measuring in continuous the tap-water background, a peak of pH and conductivity is observed after every discharge. Therefore, that was the signal that triggered the SSU. Moreover, solutions were colored using commercial pigments to make visible the dispersion effect and to know the best time for collecting the samples.

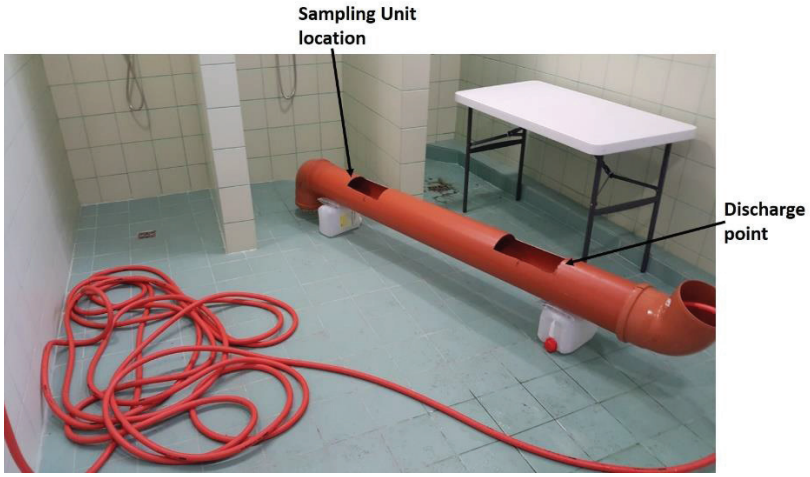

Figure 13. Testbed setup for experiment in flowing water.

The sampling experimental procedure was the same as described in section 2.4.1 (see Table 2 for the description of samples collected in dynamic mode). Additional samples were collected directly from water stream using plastic syringes next to the sampling module location in the pipe. All samples taken were analyzed using GC-MS to check the presence of markers and their concentration.

Tableau 6. Characteristics of samples collected in dynamic mode

Type of substance (carrier/marker)	**Concentration of marker [µM]**	**Time of discharge [s]**	**Volume [l]**	**pH**	**EC** [mS]	**Time of sample collection**	**Volume of collected sample [ml]**
Water/BMK	300	26	10	7,97	0,499	51 s	2,0
Water/AMP	300	29	10	9,24	0,503	52 s	2,0
Water/NFA	300	29	10	8,09	0,493	48 s	2,0

Water/BMK	300	7	10	8,10	0,352	45 s	2,1
Water/AMP	300	10	10	9,07	0,347	49 s	2,1
Water/NFA	300	9	10	8,18	0,347	48 s	2,1
Water/BMK	1875	29	10	7,90	0,363	53 s	2,4
Water/AMP	1875	31	10	9,81	0,367	56 s	2,1
Water/NFA	1875	28	10	8,28	0,352	54 s	2,1
Water/BMK	3750	29	10	7,64	0,350	61 s	2,2
Water/AMP	3750	27	10	9,92	0,374	70 s	2,1
Water/NFA	3750	29	10	8,14	0,345	68 s	2,1
Water/CA	20 g Citric acid	27	10	3,05	1,19	65 s	2,0
Water/PC	30 ml Pipe cleaner	28	10	12,41	22,1	42 s	2,0
Water/CA	40 g Citric acid	28	10	2,71	1,15	43 s	2,0
Water/synt. Waste*	350 ml	23	7	2,13	13,5	47 s	2,0
Water/synt. Waste*	500 ml	27	10	12,05	21,8	59 s	2,1
Water/synt. Waste*	700 ml	21	7	8,45	0,336	48 s	2,0

* Samples corresponding to diluted wastes obtained from Leuckart synthesis (see Chapter 1, Section 3 for more information concerning the Leuckart synthesis)

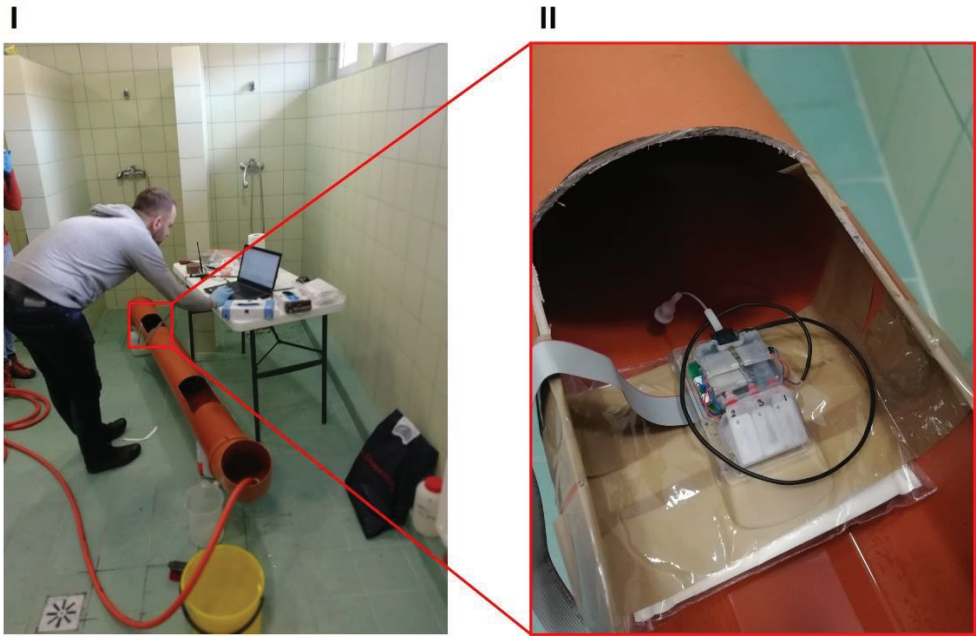

Figure 14. (**I**) image showing the testbed facilities where the evaluation campaign was carried out. (**II**) shows the automated sampler installed inside the pipe.

A platform was installed inside the pipe in order to place the Sample Storage Unit the closest to the water stream. The experimental setup is shown in **Fig. 14**. A constant flow of tap water was supplied at 3 L/ min approximately. Afterwards, the solutions were discharged and the SSU was triggered manually once the EC and pH sensor gave an alarm. Every three collected samples, the reservoirs manifold was removed from the Sample Storage Unit and the three samples were transferred to a flask for later GC-MS analysis in the laboratory. The manifold was flashed with tap water and installed again for subsequent sampling.

Once again, the results indicated that samples about 2 mL can be collected in less than 60 s even in a flowing stream.

GC-MS analysis of samples taken were carried out to measure the concentration of marker and compare it with initial concentration in the solution discharged. Thus, one can estimate the impact of the dilution effect and the possibility of further determination of specific substances related to the amphetamine synthesis (BMK, NFA or AMP). Moreover, the cross-contamination was evaluated.

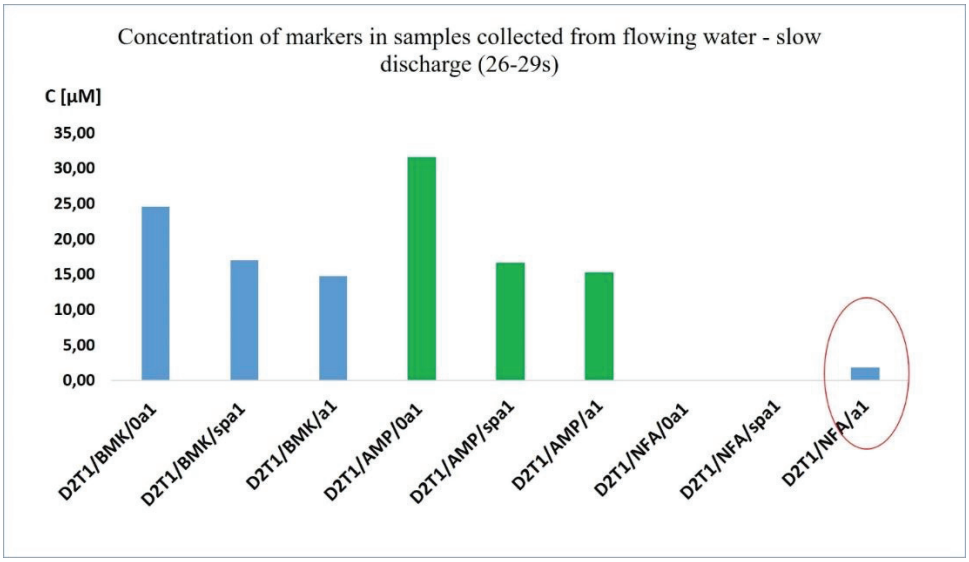

Figure 15. Concentration determined by GC-MS for samples collected using the Sample Storage Unit for slow discharges of 30 s of BMK, AMP and NFA. **D2T1/MARKER/0a1** – Initial concentration of marker. Solution discharged. **D2T1/MARKER/spa1** – Sample taken manually from the pipe next to the automated sampler. **D2T1/MARKER/a1** – Sample collected by the Sample Storage Unit.

As it can be seen from **Fig. 15**, a dilution between 25-30 % may be expected when collecting samples during slow discharges of approximately 30 s. However, the concentration remains great enough regarding the sensitivity of the GC-MS. Therefore, the dilution effect was found to be negligible. Moreover, it has also been demonstrated that the samples taken manually using a syringe contained the same amount of marker than the samples collected using the Sample Storage Unit. However, cross-contamination was found when the sample that theoretically only contained NFA (D2T1/NFA/a1) was analysed. Traces of BMK (1.16 µM) were found in the sample. It may be explained as BMK being the most viscous and oil-like compound remained inside the inlet of the microfluidic manifold. It was furthermore confirmed as in a second test, BMK was also found at concentration between 0.4 and 1.1 µM in D2T1/AMP/a2 where only AMP was expected. Nevertheless, as BMK can only be related to the Leukart synthesis, its presence in any sample taken from the sewage will indicate that an illicit laboratory is nearby what would not mask the analysis of other markers but would confirm instead.

2.9. Tests under real condition. The sewer network of Berlin.

Finally, the SSU was assembled with the housing module as shown in **Fig. 16** and its performance was evaluated in real conditions at the KWB facilities in Berlin. For this purpose, the SSU final device was set in a metallic ring and installed in a sewer pipe (see **Fig. 16** (**III**)). The housing module hosts the microfluidic manifolds as well as the fluidic components and the electronic board providing the waterproofness needed so that the automated sampler can be immerse in water. The wastewater flow

was set at 10 L/s and subsequently, three samples were stored. First sample contained only wastewater, second and third samples contained real waste obtained from the Leuckart synthesis that was discharged into the pipe 3 meters away from the Sample Storage Unit location, simulating thus, a real event. The device was controlled using a personal computer located out of the pipe and it was triggered manually. For every sample, the system was set to pump at 100 Hz during 60 s, so we ensure to collect a representative sample from the discharge. The procedure was repeated to store three samples and subsequently, the SSU was removed from the pipe and the samples were transferred to glass tubes for further analysis. Results confirmed that the device was able to store three samples of 1 mL each in 60 s. In this case, the flow rate observed was decreased by 50% when compared to the flow rate average obtained using tap water. It can be explained as the viscosity and the presence of particles in wastewater is very high and therefore, the fluidic resistance is greater so that the pumping system needs more time to fill the tanks. Thus, the volume of the samples stored during 60 s was 1 mL. Nevertheless, that volume was enough to analyse the sample through GC-MS where a few microliters are needed. The chemical analysis was further performed at the German Forensic Police Laboratories, (BKA), and as a results, the markers of interest (BMK, NFA and AMPH) were identified satisfactorily in the second and third reservoirs where no contamination was observed. Moreover, it was confirmed that placing the inlet at the housing module's backside, clogging phenomena was highly minimized as the it was oriented to the same direction as wastewater flow.

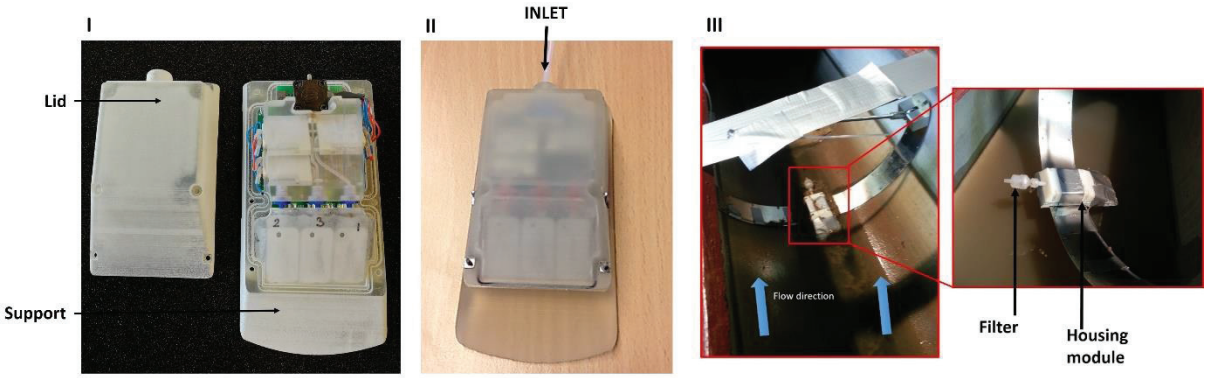

Figure 16. In (**I**), Sample Storage Unit together with support and lid that integrate the housing module. In (**II**), Sample Storage Unit final device. In (**III**), the SSU set in the sewer network ready for sampling.

3. Conclusions.

An automated sampler, the Sample Storage Unit, has been developed to store up to three independent samples of 2 mL each. The aim of this device was to help the Forensic Police to collect evidences when investigating illicit drug clandestine laboratories without the need of being "in the field". For this purpose, the system was made of two manifolds: the main body containing the pumping system that is

fixed and the second manifold connected to the main body and containing three reservoirs that can be easily replaced for further analysis when they are filled. The Sample Storage Unit presented in this chapter was fabricated in a very inexpensive way as it contained the rigid body manufactured through 3D-printing techniques and fluidic components that are commercially available such as the micropump and microvalves. Moreover, a homemade electronic board has been fabricated and validated. It enabled to actuate the system that was in standby mode until it was triggered by a predefined alarm. Its performance was evaluated in static and dynamic mode using both tap water and real wastewater. As a result, the system demonstrated to be able to store samples at 2 mL/min in the case of tap water and 1 mL/min in the case of real wastewater. The robustness was also evaluated by immersion of the Sample Storage Unit for long periods of time (several days) in the sewage. It was confirmed that not clogging phenomena was observed as the system was still operational and worked in a repeatable manner after being exposed to the wastewater for longtime. Moreover, it was confirmed that no cross-contamination is observed when the reservoirs are used for only one time. Therefore, the automated sampler presented here, can be adapted to store samples in the sewer network, can be wireless controlled and demonstrated to be reliable when collecting evidences for spontaneous events. In addition, it has been miniaturized and is cost-effective.

4. References.

[1] S. Nurani, H. Abdul, W. Lau, Detection of contaminants in water supply : A review on state-of-the-art monitoring technologies and their applications, Sensors Actuators B. Chem. 255 (2017) 2657–2689. doi:10.1016/j.snb.2017.09.078.

[2] S. Castiglioni, K. V Thomas, B. Kasprzyk-hordern, L. Vandam, P. Grif, Science of the Total Environment Testing wastewater to detect illicit drugs : State of the art , potential and research needs, 487 (2014) 613–620. doi:10.1016/j.scitotenv.2013.10.034.

[3] S.D. Melvin, F.D.L. Leusch, Removal of trace organic contaminants from domestic wastewater: A meta-analysis comparison of sewage treatment technologies, Environ. Int. 92–93 (2016) 183–188. doi:10.1016/j.envint.2016.03.031.

[4] S. Gaw, C.N. Glover, A case of contagious toxicity ? Isoprostanes as potential emerging contaminants of concern, Sci. Total Environ. 560–561 (2016) 295–298. doi:10.1016/j.scitotenv.2016.04.005.

[5] J.W. Zabinski, K.J. Pieper, J.M. Gibson, A Bayesian Belief Network Model Assessing the Risk to Wastewater Workers of Contracting Ebola Virus Disease During an Outbreak, Risk Anal. 38 (2017) 376–391. doi:10.1111/risa.12827.

[6] B. Petrie, R. Barden, B. Kasprzyk-hordern, A review on emerging contaminants in wastewaters and the environment : Current knowledge , understudied areas and recommendations for future monitoring, Water Res. 72 (2015) 3–27. doi:10.1016/j.watres.2014.08.053.

[7] L. Rizzo, C. Manaia, C. Merlin, T. Schwartz, C. Dagot, M.C. Ploy, I. Michael, D. Fatta-kassinos, Urban wastewater treatment plants as hotspots for antibiotic resistant bacteria and genes spread into the environment : A review, Sci. Total Environ. 447 (2013) 345–360. doi:10.1016/j.scitotenv.2013.01.032.

[8] L. He, G. Ying, Y. Liu, H. Su, J. Chen, S. Liu, J. Zhao, Discharge of swine wastes risks water quality and food safety : Antibiotics and antibiotic resistance genes from swine sources to the receiving environments, Environ. Int. 92–93 (2016) 210–219. doi:10.1016/j.envint.2016.03.023.

[9] A.K. Awasthi, X. Zeng, J. Li, Environmental pollution of electronic waste recycling in India : A critical review, Environ. Pollut. 211 (2016) 259–270. doi:10.1016/j.envpol.2015.11.027.

[10] L.M. Keith, Environmental sampling and analysis: a practical guide, 1991. http://scholar.google.com/scholar?hl=en&as_sdt=0,5&as_ylo=1991&q=Environmental+sampling+and+analysis%3A+a+practical+guide+author%3Akeith.

[11] L.H. Keith, Environmental sampling: A summary, Environ. Sci. Technol. 24 (1990) 610–617. doi:10.1021/es00075a003.

[12] T.H. Boles, M.J.M. Wells, Analysis of amphetamine and methamphetamine in municipal wastewater influent and effluent using weak cation-exchange SPE and LC-MS/MS, Electrophoresis. 37 (2016) 3101–3108. doi:10.1002/elps.201600271.

[13] European Monitoring Centre for Drugs and Drug Addiction, Assesing ilicit drugs in wastewater: advances in wastwater-based drug epidemiology, Publication Office of the European Union, Luxembourg, 2016. doi:10.2810/017397.

[14] M. Östman, J. Fick, E. Näsström, R.H. Lindberg, A snapshot of illicit drug use in Sweden acquired through sewage water analysis, Sci. Total Environ. 472 (2014) 862–871. doi:10.1016/j.scitotenv.2013.11.081.

[15] A.O. Maldaner, L.L. Schmidt, M.A.F. Locatelli, W.F. Jardim, F.F. Sodré, F. V. Almeida, C.E.B. Pereira, C.M. Silva, Estimating cocaine consumption in the brazilian federal district (FD) by sewage analysis, J. Braz. Chem. Soc. 23 (2012) 861–867. doi:10.1590/S0103-50532012000500011.

[16] K. V. Thomas, L. Bijlsma, S. Castiglioni, A. Covaci, E. Emke, R. Grabic, F. Hernández, S. Karolak, B. Kasprzyk-Hordern, R.H. Lindberg, M. Lopez de Alda, A. Meierjohann, C. Ort, Y. Pico, J.B. Quintana, M. Reid, J. Rieckermann, S. Terzic, A.L.N. van Nuijs, P. de Voogt, Comparing illicit drug use in 19 European cities through sewage analysis, Sci. Total Environ. 432 (2012) 432–439. doi:10.1016/j.scitotenv.2012.06.069.

[17] C. Ort, A.L.N. van Nuijs, J.D. Berset, L. Bijlsma, S. Castiglioni, A. Covaci, P. de Voogt, E. Emke, D. Fatta-Kassinos, P. Griffiths, F. Hernández, I. González-Mariño, R. Grabic, B. Kasprzyk-Hordern, N. Mastroianni, A. Meierjohann, T. Nefau, M. Östman, Y. Pico, I. Racamonde, M. Reid, J. Slobodnik, S. Terzic, N. Thomaidis, K. V. Thomas, Spatial differences and temporal changes in illicit drug use in Europe quantified by wastewater analysis, Addiction. 109 (2014) 1338–1352. doi:10.1111/add.12570.

[18] A. Assaad, S. Pontvianne, M.N. Pons, Assessment of organic pollution of an industrial river by synchronous fluorescence and UV–vis spectroscopy: the Fensch River (NE France), Environ. Monit. Assess. 189 (2017). doi:10.1007/s10661-017-5933-3.

[19] M.J. Reid, L. Derry, K. V. Thomas, Analysis of new classes of recreational drugs in sewage: Synthetic cannabinoids and amphetamine-like substances, Drug Test. Anal. 6 (2014) 72–79. doi:10.1002/dta.1461.

[20] M.C. Gavin, J.N. Solomon, S.G. Blank, Measuring and monitoring illegal use of natural resources, Conserv. Biol. 24 (2010) 89–100. doi:10.1111/j.1523-1739.2009.01387.x.

[21] X. Shen, H. Chang, D. Sun, L. Wang, F. Wu, Trace analysis of 61 natural and synthetic progestins in river water and sewage effluents by ultra-high performance liquid chromatography–tandem mass spectrometry, Water Res. 133 (2018) 142–152. doi:10.1016/j.watres.2018.01.030.

[22] D.W. Lachenmeier, J. Rehm, Comparative risk assessment of alcohol, tobacco, cannabis and other illicit drugs using the margin of exposure approach, Sci. Rep. 5 (2015) 1–7. doi:10.1038/srep08126.

[23] J. Li, L. Hou, P. Du, J. Yang, K. Li, Z. Xu, C. Wang, H. Zhang, X. Li, Estimation of amphetamine and methamphetamine uses in Beijing through sewage-based analysis, Sci. Total Environ. 490 (2014) 724–732. doi:10.1016/j.scitotenv.2014.05.042.

[24] N. Mastroianni, E. López-García, C. Postigo, D. Barceló, M. López de Alda, Five-year monitoring of 19 illicit and legal substances of abuse at the inlet of a wastewater treatment plant in Barcelona (NE Spain) and estimation of drug consumption patterns and trends, Sci. Total

Environ. 609 (2017) 916–926. doi:10.1016/j.scitotenv.2017.07.126.

[25] T. Rodríguez-Álvarez, R. Rodil, M. Rico, R. Cela, J.B. Quintana, Assessment of local tobacco consumption by liquid chromatography-tandem mass spectrometry sewage analysis of nicotine and its metabolites, cotinine and trans-3′-hydroxycotinine, after enzymatic deconjugation, Anal. Chem. 86 (2014) 10274–10281. doi:10.1021/ac503330c.

General Conclusions

The principle objective of this thesis was to develop a total analysis system for the monitoring of amphetamines and the derivatives of its illegal synthesis in wastewater. In a first stage, two potentiometric amphetamine sensor were developed that enabled the real-time detection of amphetamine in liquid samples. Subsequently, a passive microfluidic system was fabricated to protect the sensor from harsh environment. Finally, an automated sample-storage unit was made-up to store evidences of clandestine laboratories activities by collecting wastewater samples directly from the sewer network.

Two all-solid-state amphetamine-selective electrodes have been developed. In a first stage, the previously reported amphetamine ionophore, dibenzo-18-crown-6 ether, was used as the sensitive part for amphetamine recognition. Five PVC-type amphetamine-selective electrodes were fabricated using four plasticizers and two concentrations of ionophore. The polymeric membranes prepared were drop-cast onto a PpyCOSANE-modified platinum electrode. The PpyCOSANE layer demonstrated to enhance the electrical properties of the transducer as well as to serve as porous layer that improved the contact between the polymeric membrane and platinum substrate. Among the five amphetamine sensor fabricated, the combination of 26 wt.% PVC, 63 wt.% DBP, 5 wt.% DB18C6 and 6 wt.% Na-TPB provided the best results. In this case, good sensitivity, 53 mV/decade, and low limit of detection, 4.10^{-5} M, were achieved as well as good selectivity toward amphetamine when compared to some amine/amide compounds and common inorganic cations. Moreover, the sensor developed showed a time of response 15s approx. and the working pH was found to be between 1.5 and 8.5.

For the amphetamine-selective electrode second version, the ion-pair complex, $[3,3'\text{-}Co(1,2\text{-}C_2B_9H_{11})_2]^-[C_9H_{13}NH]^+$ was used as active site for amphetamine detection. It was successfully synthetized through ion-exchange using the metallocarborane in the cesium salt form, $Cs[3,3'\text{-}Co(1,2\text{-}C_2B_9H_{11})_2]$, and amphetamine sulfate. The product obtained was characterized by NMR (^1H, $^1H\{^{11}B\}$, ^{11}B, $^{11}B\{^1H\}$ $^{13}C\{^1H\}$), FTIR spectroscopies and MALDI-TOF-MS. As a result, the isolated compound $[C_9H_{13}NH]^+[3,3'\text{-}Co(1,2\text{-}C_2B_9H_{11})_2]^-$ could be identified. The ion-pair complex was incorporated to PVC-type polymeric membranes using different plasticizers. Among those tested, the combination of 31 wt.% of PVC, 65 wt.% of DBP and 4 wt.% of $[C_9H_{13}NH]^+[3,3\text{-}Co(1,2\text{-}C_2B_9H_{11})_2]^-$ ion-pair complex provided the best response. The microsensor showed Nernstian response with a slope of 60.1 mV/decade within the concentration range 10^{-5} M to 10^{-3} M of amphetamine, limit of detection of 12 µM and a time of response less than 10 s. The sensor's selectivity was evaluated in the presence of N-formyl amphetamine, phenylalanine and methylbenzylamine, three compounds with very similar chemical structure and it was confirmed that the sensor was highly selective toward amphetamine. Therefore, it was demonstrated that introducing the target molecule, amphetamine, to the sensitive membrane in the

form of ion-pair complex is crucial to achieve high values of selectivity since a specific gradient of amphetamine concentration is created at the interface solution/membrane. In addition, the high lipophilic character of the ion-pair complex enhanced the membrane stability and therefore, the sensor's lifetime.

In parallel, a microfluidic LOC for real-time electrochemical measurements in flowing water was succesfully developed. The device was manufactured by covalent bonding of two subunits: a PDMS-flexible microfluidic structure and a transducer holding an array of four gold working microelectrodes, two Ag/AgCl reference microelectrodes and one Pt auxiliary microelectrode. The PDMS microfluidic structure was designed in such a way so it contained passive microfilters, micromixers and microchannels that protect the sensitive part of the sensor from the water-flow strength as well as from impacts of eventual particles. The LOC was chemically functionalized to incorporate four ammonium-selective electrodes and therefore, ammonium-containing samples were analysed in continuous flowing water successfully. As a result, it was demonstrated that a continuous water stream is spontaneously created through the microfluidic LOC when it was immersed in a laminar flow of water. At the beginning, the water reaches the LOC by capillary and afterwards the continuous flow is created by diffusion as the device is oriented to the laminar flow of water. The LOC performance was assessed by comparing its time of response to that of a commercial conductivity sensor when measuring ammonium discharges both in static and flowing water. Results confirmed that both sensors responded at the same time proving therefore, the good functioning of the LOC in tap water. Its robustness was also evaluated by immersion of the LOC into the sewer network in a testbed facility in Berlin, Germany for 15 and 60 minutes respectively. The LOC did not appear to be affected after 15 minutes immersed in wastewater as its time of response was comparable to that obtained during the experiments with tap water. However, after 60 minutes immersion, the time of response was delayed by more than 1 minute what indicated that the inlet of the microfluidic system was clogged and therefore the wastewater diffused slowly throughout the LOC. Nonetheless, the low-cost, easy-to-operate and miniaturized LOC developed can be used for in-situ and real-time analysis in flowing water what suppose a step further in the field of wastewater monitoring. Future work will contribute to develop a waterproof instrumentation that enable chemical analysis directly in wastewater and to improve the LOC's microfluidic shape that will highly minimize clogging events when longer exposure times than 15 minutes are required.

Finally, an automated sample-storage unit was fabricated as a complementary device in the context of wastewater monitoring. The system was conceived to for sporadic sampling. Therefore, the device was on standby mode until it is triggered by an external alarm sent when the chemical and physical sensors detect an anomaly in the wastewater background. It was designed in such a way so it was as miniaturized as possible and enabled to store up to three independent samples of 2 mL each. It was made of two manifold manufactured by 3D printing technology. The main body contained the active components:

three electrovalves and one piezoelectric micropump that enabled to pump the sample through the system. The sample, ended up in one of the three reservoirs provided in the second manifold. The ensemble was integrated in a housing module that provided the water tightness so that it was protected from the water. The aim of this device was to help the LEA to collect evidences when investigating illicit drug clandestine laboratories without the need of being "in the field" for sampling. The system was controlled successfully using a homemade electronic board and its performance was evaluated in static and dynamic mode using both tap water and real wastewater. As a result, the system demonstrated to be able to store representative samples at 2 mL/min in the case of tap water and 1 mL/min in the case of real wastewater. The robustness was also evaluated by immersion of the sample storage unit for long periods of time (several days) in the sewage. It was confirmed that not clogging phenomena was observed as the system was still operational and worked in a repeatable manner after being exposed to the wastewater for longtime. Moreover, it was confirmed that no cross-contamination is observed when the reservoirs are used for only one time. Therefore, the automated sampler presented, can be adapted to store samples in the sewer network, can be wireless controlled and demonstrated to be reliable when collecting evidences for sporadic events.

Future perspectives of this work will be to take advantage of the lessons learned during this three years working in such as harsh environment as wastewater to improve the LOC performance so that clogging is minimized, as well as to include the amphetamine-selective sensor second generation to the LOC to analyze amphetamine in wastewater in a real situation. Furthermore, we are currently working on the development of an active microfluidic system for chemical sensing. It will be analogue to the sample storage unit and will include the place for an electrochemical sensor for the multidetection of amphetamine, NFA and BMK. The system will help to control the flow of sample that reaches the sensor so that it will highly minimize its exposure to the wastewater and will increase therefore, the device's lifetime and its overall performance.

Publications

[1] J. Gallardo-González, A. Baraket, A. Bonhomme, N. Zine, M. Sigaud, J. Bausells, A. Errachid, Sensitive Potentiometric Determination of Amphetamine with an All-Solid-state Micro Ion-Selective-electrode, Anal. Lett. 58 (2018) 348–358. doi:10.1080/00032719.2017.1326053.

[2] J. Gallardo-Gonzalez, A. Saini, A. Baraket, S. Boudjaoui, A. Alcácer, A. Streklas, F. Teixidor, N. Zine, J. Bausells, A. Errachid, A highly selective potentiometric amphetamine microsensor based on all-solid-state membrane using a new ion-pair complex, [3,3″-Co(1,2-closo-C2B9H11)2]−[C9H13NH]+, Sensors Actuators, B Chem. 266 (2018) 823–829. doi:10.1016/j.snb.2018.04.001.

[3] A. Saini, J. Gallardo-Gonzalez, A. Baraket, I. Fuentes, C. Viñas, N. Zine, J. Bausells, F. Teixidor, A. Errachid, A novel potentiometric microsensor for real-time detection of Irgarol using the ion-pair complex [Irgarol-H]+[Co(C2B9H11)2]−, Sensors Actuators, B Chem. 268 (2018) 164–169. doi:10.1016/j.snb.2018.04.070.

[4] J. Gallardo-González, A. Baraket, S. Boudjaoui, A. Streklas, F. Teixidor, N. Zine, J. Bausells, A. Errachid, A Highly Sensitive Potentiometric Amphetamine Microsensor Based on All-Solid-State Membrane Using a New Ion-Par Complex , Proc. Eurosensors Conf. Paris 2017. 1 (2017) 2–5. doi:10.3390/proceedings1040481.

Under review/preparation

J. Gallardo-Gonzalez, A. Baraket S. Boudjaoui, Y. Clément, N. Zine, M. Sigaud, A. Alcacer, A. Streklas, J. Bausells and A. Errachid, Novel impedimetric amphetamine-selective microsensor based on the electrochemical grafting of in-situ generated diazoted amphetamine ionophore. **(Submited to ChemComm. July 2018).**

J. Gallardo-Gonzalez, A. Baraket, S. Boudjaoui, T. Metzner, F. Hauser, T. Rößler S. Krause, N. Zine, A. Streklas, A. Alcácer, J. Bausells- and A. Errachid, A Fully Integrated Passive Microfluidic Lab-on-a-Chip for Real-Time Electrochemical Detection of Ammonium: Sewage Applications. **(Submited to Science of the Total Environment. July 2018)**

J. Gallardo-Gonzalez, A. Baraket, S. Boudjaoui, F. Palacio, F. Solano, K. Pachowicz., A. Tynda, N. Zine, D. Bouraya, R. Anasthase, J. Bausells and A. Errachid. A miniature and autarkic Sample Storage Unit for the in-situ collection of forensic evidences in the sewer network, 2018 (**Under preparation**)

Conferences

J. Gallardo-Gonzalez, A. Baraket, Anne Bonhomme, N. Zine, M. Sigaud, J. Bausells and A. Errachid. *Highly sensitive potentiometric µISE for amphetamine detection using dibenzo-18-crown-6 as charge carrier.* Oral presentation at « 10èmes JOURNEES MAGHREB-EUROPE. Les Materieux et leurs applications aux dispositif capteurs », MADICA 2016. Septembre 2016, Mahdia, Tunisia.

J. Gallardo-Gonzalez, A. Baraket, S. Boudjaoui, Y. Clément, A. Alcácer, A. Streklas, F. Teixidor, N. Zine, J. Bausells and A. Errachid. *A highly selective potentiometric amphetamine microsensor based on all-solid-state membrane using a new ion-pair complex* $[C_9H_{13}NH]^+[3,3\text{-}Co(1,2\text{-}closo\text{-}C_2B_9H_{11})_2]^-$. Poster presentation at "Eurosensors Conference 2017". 31st Edition. Septembre 2017, Paris, France.

J. Gallardo-Gonzalez, A. Baraket, S. Boudjaoui, Y. Clément, A. Alcácer, A. Streklas, F. Teixidor, N. Zine, J. Bausells and A. Errachid. *Highly Sensitive Impedimetric Ion Selective µElectrode for Amphetamine Detection.* Oral presentation at "10th International Workshop on Impedance Spectroscopy", IWIS 2017. Septembre 2017, Chemnitz, Germany.

J. Gallardo-Gonzalez, S. Boudjaoui, A. Baraket, Y. Cément, N. Zine, J. Bausells and A. Errachid. *PDMS-based Microfluidic Lab-on-a-Chip for Real Time Electrochemical Measurements in Sewage applications* Poster presentation at "International Conference on Micro and Nano Engineering 2017". MNE 2017, October 2017, Braga, Portugal.

S. Boudjaoui, J. Gallardo-Gonzalez A. Baraket, Y. Cément, N. Zine, J. Bausells and A. Errachid *Acetone sensor based on electro-addresing chitosan/zeolites Ag-ZSM5 onto gold µIDEs: Application to diagnostic of heart failure* Poster presentation at "International Conference on Micro and Nano Engineering 2017". MNE 2017, October 2017, Braga, Portugal.

J. Gallardo-Gonzalez, A. Baraket, S. Boudjaoui Y. Clément, N. Zine, M. Sigaud, A. Alcacer, A. Streklas, J. Bausells and A. Errachid. *Novel Amphetamine-Selective Microsensor Based on the Electrochemical Grafting of In-Situ Generated Amphetamine Diazoted-Ionophore.* Poster presentation at "28th Anniversary World Congress of Biosensors". BIOS 2018. June 2018, Miami, USA

S. Boudjaoui, J. Gallardo-Gonzalez, A. Baraket, Y. Clément, N. Zine, M. Sigaud, A. Alcacer, A. Streklas, J. Bausells and A. Errachid. *Multiple breath biomarkers detection by a novel conductometric sensor based on combination of nanomaterials : application to heart failure..* Poster presentation at "28th Anniversary World Congress of Biosensors". BIOS 2018. June 2018, Miami, USA

A. Sonu, A. Baraket, S. Boudjaoui, J. Gallardo-Gonzalez, N. Zine, M. Sigaud, M. Hangouet, A. Alcacer, A. Streklas, J. Bausells and A. Errachid. "*Solid State Gas Sensor based on Polyaniline doped with [3,3-Co(1,2-closo-$C_2B_9H_{11})_2$] for the detection of Acetone*: *Diagnostic to Heart Failure disease"*. Poster presentation at "Eurosensors Conference 2018". 32nd Edition. Septembre 2018, Graz, Austria.

Z. Ayroud, J. Gallardo-Gonzalez, A. Baraket, M. Hangouet, A. Alcácer, A. Streklas, J. Bausells, A. Errachid and N. Zine. "*A highly sensitive impedimetric metamitron microsensor based on all-solid-state membrane using a new Ion-Pair Complex, [3,3'-Co(1,2-closo-$C_2B_9H_{11})_2]^-[C_{10}H_{11}ON_4]^+$"*. Poster presentation at "Eurosensors Conference 2018". 32nd Edition. Septembre 2018, Graz, Austria.

Angelos Streklas, Albert Alcacer, Abdoullatif Baraket, Nadia Zine, Nadia Alami, Juan Gallardo-Gonzalez, Abdelhamid Errachid, Joan Bausells. "*Pocket-sized potentiostat for non-invasive detection of heart failure related TNF-α biomarker"*. Oral presentation at 12th Spanish Conference on Electronic Devices. CDE 2108. November 2018, Salamanca, Spain.

TITRE en français : **Développent d'un laboratoire sur puce pour la détection des amphétamines dans les égouts.**

Ce travail de thèse est consacré au développement d'un dispositif autarcique pour le contrôle des amphétamines dans les égouts. Il a été conçu dans le cadre du projet européen MicroMole pour aider la police scientifique à résoudre des scènes concernant la localisation des laboratoires clandestins d'amphétamines et produits dérivés. Il est composé de trois volets : le premier volet est dédié au développement de deux générations de capteurs potentiométriques sélectifs à l'amphétamine en utilisant le ionophore commercial dibenzo-18-crown-6 éther dans un premier temps puis le ion-pair complexe [amphetamine-H]$^{+}$[3,3'-Co(1,2-$C_2B_9H_{11}$)$_2$]$^{-}$ synthétisé comme sites actifs pour la reconnaissance sélective d'amphétamine. Le deuxième volet est consacré au développement d'un système microfluidique passif permettant de contrôler le flux d'échantillon arrivant à la partie sensible du capteur en utilisant des micro-filtres et micro-mélangeurs. Le troisième et dernier volet est dédié à la conception et fabrication d'un système autonome d'échantillonnage miniaturisé pour le stockage des échantillons dans les égouts lors des enquêtes menées par la police scientifique correspondant à la localisation de laboratoires clandestins d'amphétamines.

TITRE en anglais : **Development of a fully integrated Lab-o-a-Chip for amphetamine detection in sewage.**

The work in this thesis is devoted to the development of an autarkic device for real-time monitoring of amphetamines in sewage. It has been developed within the EU project Micromole to help Law Enforcement Agents (LEA) to solve forensic scenarios related to the production of amphetamines and amphetamines-type stimulants (ATS). It is composed of three main sections. The first section is devoted to the development of two generation of potentiometric sensors for the detection of amphetamines using first, the commercial ionophore dibenzo-18-crown-6 ether, then the synthetized ion-pair complex [amphetamine-H]$^{+}$[3,3'-Co(1,2-$C_2B_9H_{11}$)$_2$]$^{-}$ as active sites for amphetamine recognition. The second section is dedicated to the fabrication of a passive microfluidic system integrated into a Lab-on-a-Chip to protect the sensor from harsh environment through the control of the sample amount reaching the sensor. For this purpose, the microfluidic system formed a combination of passive micromixers, microfilters and microchannels. The final section was devoted to the development of an autarkic sample storage unit to help LEA to store spontaneous samples during forensic investigations related to the clandestine production of amphetamines in illegal laboratories.

DISCIPLINE: **Electroanalytical chemistry and micro-nanotechnology**

MOTS-CLES en français: **Laboratoire sur puce ; µISE ; amphétamine ; potentiométrie ; spectroscopie d'impédance ; analyse des égouts.**

MOTS-CLES en anglais : **Lab-on-a-Chip**, **µISE ; amphetamine ; potentiometry ; electrochemical impedance spectroscopy ; sewage analysis.**

INTITULE ET ADRESSE DE L'U.F.R. OU DU LABORATOIRE : **ISA- Institut des Sciences analytiques. Département LSA-Laboratoire des Sciences Analytiques. Université Claude Bernard Lyon 1, 5 Rue de la Doua, 69100, Villeurbanne, CEDEX, France.**